UNIVERSIDADE ESTADUAL PAULISTA
"JÚLIO DE MESQUITA FILHO"
INSTITUTO DE BIOCIÊNCIAS – RIO CLARO

PROGRAMA DE PÓS-GRADUAÇÃO EM CIÊNCIAS BIOLÓGICAS
(ZOOLOGIA)

REVISÃO TAXONÔMICA E ESTUDO FILOGENÉTICO DA SÉRIE DE *ISCHNOCNEMA GUENTHERI* (ANURA: BRACHYCEPHALIDAE)

PEDRO PAULO GOULART TAUCCE

RIO CLARO – SP

2018

PEDRO PAULO GOULART TAUCCE

REVISÃO TAXONÔMICA E ESTUDO FILOGENÉTICO DA SÉRIE DE *ISCHNOCNEMA GUENTHERI* (ANURA: BRACHYCEPHALIDAE)

Tese apresentada ao Instituto de Biociências do Câmpus de Rio Claro, Universidade Estadual Paulista, como parte dos requisitos para obtenção do título de Doutor em Ciências Biológicas (área de concentração Zoologia).

Orientador: Dr. Célio F. B. Haddad
Co-orientadora: Dra. Clarissa C. Canedo

RIO CLARO – SP

2018

597.8 Taucce, Pedro Paulo Goulart
T224r Revisão taxonômica e estudo filogenético da série de Ischnocnema guentheri / Pedro Paulo Goulart Taucce. - Rio Claro, 2018
249 f. : il., figs., gráfs., tabs., mapas

Tese (doutorado) - Universidade Estadual Paulista, Instituto de Biociências de Rio Claro
Orientador: Célio Fernando Baptista Haddad
Coorientadora: Clarissa Coimbra Canedo

1. Anuro. 2. Bioacústica. 3. Brachycephaloidea. 4. Sistemática. 5. Taxonomia. 6. Terrarana. I. Título.

Ficha Catalográfica elaborada pela STATI - Biblioteca da UNESP
Campus de Rio Claro/SP - Ana Paula S. C. de Medeiros / CRB 8/7336

unesp

UNIVERSIDADE ESTADUAL PAULISTA

Câmpus de Rio Claro

CERTIFICADO DE APROVAÇÃO

TÍTULO DA TESE: Revisão taxônomica e Estudo Filogenético da série de Ischnocnema guentheri (Anura: Brachycephalidae)

AUTOR: PEDRO PAULO GOULART TAUCCE
ORIENTADOR: CELIO FERNANDO BAPTISTA HADDAD
COORIENTADORA: CLARISSA COIMBRA CANEDO

Aprovado como parte das exigências para obtenção do Título de Doutor em CIÊNCIAS BIOLÓGICAS (ZOOLOGIA), pela Comissão Examinadora:

Prof. Dr. CELIO FERNANDO BAPTISTA HADDAD
Departamento de Zoologia / UNESP - Instituto de Biociências de Rio Claro - SP

Profa. Dra. LUCIANA BOLSONI LOURENÇO
Departamento de Biologia Celular / UNIVERSIDADE ESTADUAL DE CAMPINAS

Profª. Drª. MARIANE TARGINO ROCHA
Departamento de Zoologia / UNIVERSIDADE DE SÃO PAULO

Prof. Dr. DÉLIO PONTES BAÊTA DA COSTA
Departamento de Zoologia / Unesp/ Câmpus de Rio Claro

Prof. Dr. BORIS LEONARDO BLOTTO ACUNA
Departamento de Zoologia / Instituto de Biociências, Universidade de São Paulo, São Paulo/SP

Rio Claro, 18 de maio de 2018

AVISO DE RESPONSABILIDADE NOMENCLATURAL

As alterações taxonômicas apresentadas neste documento, incluindo novos taxa, combinações e sinonímia, são rejeitadas como atos nomenclaturais e não estão disponíveis, de acordo com o Artigo 8.3 do Código Internacional de Nomenclatura Zoológica.

NOMENCLATURAL DISCLAIMER

The taxonomic changes presented herein, including new taxa, combinations, and synonymy, are disclaimed as nomenclatural acts and are not available, in accordance with Article 8.3 of the International Code of Zoological Nomenclature.

Dedico esta tese aos meus familiares, professores, amigos, e aos sapos, todos partes importantes de mim e partes essenciais na confecção deste trabalho.

AGRADECIMENTOS

Ao meu orientador, Prof. Célio F. B. Haddad, pelos seus ensinamentos, pelas saudáveis conversas acerca da tese, por ter aberto as portas do seu laboratório e por ter atendido tão prontamente às minhas necessidades acadêmicas ao longo desses mais de quatro anos. Obrigado também pela confiança depositada, pelos momentos de descontração e pelo exemplo.

À minha co-orientedora, Profa. Clarissa Canedo, pelos ensinamentos, pelas conversas e pelos conselhos (talvez ela não saiba que foi graças a um desses conselhos que eu resolvi pedir uma bolsa para sair do país). Também por ter confiado a mim a responsabilidade de defender uma tese com um tema que eu sei que ela tanto gosta. Obrigado por ter sido presente, mesmo com todos os problemas que um cenário político como o atual acarreta para as universidades e o claro impacto desse cenário na sua instituição, a UERJ. **#UERJresiste!**

Ao Prof. Michael J. Hickerson, por ter me recebido em seu laboratório na City College of New York, Nova Iorque, NY, USA de portas abertas e ter me proporcionado o conhecimento e a estrutura necessários para que eu pudesse lidar com um problema tão novo na minha vida acadêmica. Agradeço também pelos inúmeros *Happy Hours* e por ter me apresentado um pouco da música folclórica estadunidense e de várias outras partes do globo.

Aos funcionários da UNESP, principalmente os da Seção Técnica de Pós-Graduação, sem os quais seguramente esta tese não poderia ter sido concluída.

Às agências de fomento que me proporcionaram a bolsa de doutorado e auxílios financeiros para pesquisa. No primeiro ano minha bolsa foi concedida pelo Conselho Nacional de Desenvolvimento Científico e Tecnológico (CNPq) processo **165852/2013-5** e no restante do doutorado pela Fundação de Amparo à pesquisa do Estado de São Paulo (FAPESP) em convênio com a Coordenação de Aperfeiçoamento de Pessoal de Nível Superior (CAPES) processos **FAPESP 2014/05772-4** e **FAPESP (BEPE) 2016/22450-6**. Outros auxílios foram proporcionados pelo projeto temático **FAPESP 2013/50741-7**, ao qual meu projeto de doutorado é vinculado.

Ao Instituto Chico Mendes de Conservação da Biodiversidade (ICMBio), pelas licenças de coleta concedidas.

Aos curadores e técnicos por terem me recebido sempre de portas abertas nas coleções as quais são os responsáveis e por terem fornecido a ajuda e a estrutura necessárias para que eu pudesse trabalhar. Também aos amigos que ajudaram nas saídas de campo e com as

análises. Existe um agradecimento individualizado a cada um de vocês em cada capítulo da tese.

Um agradecimento especial a Mariana Lyra, que desde o princípio me ajudou com a parte molecular deste trabalho, e me ensinou um montão! Fico feliz que essa parceria vai resultar em alguns trabalhos. Muito obrigado! Aproveito para agradecer ao centro de Estudos de Insetos Sociais (CEIS, UNESP) por permitir o uso de suas dependências para as reações moleculares necessárias para a confecção desta tese e à Macrogen pelas reações de sequenciamento.

Ao Núcleo de Computação Científica (NCC/GridUNESP) da Universidade Estadual Paulista (UNESP) e ao CIPRES Science Gateway (www.phylo.org) pelos recursos computacionais disponibilizados para as análises moleculares. Sem este apoio seguramente esta tese demoraria muito mais pra ficar pronta.

Aos colegas do Laboratório de Herpetologia da UNESP pela amizade, pelos momentos de descontração, por terem ouvido meus lamentos e por sempre estarem dispostos a ajudar. Infelizmente a maioria das pessoas está apenas de passagem por este laboratório, assim como eu, mas ficam em nossas lembranças os bons momentos, as parcerias e a saudade!

Aos colegas do Hickerlab, do Departamento de Biologia da CCNY e do American Museum of Natural History, pelos momentos agradáveis, os passeios, as reuniões semanais, as conversas e por me apresentarem um mundo onde eu nunca havia estado. No começo foi muito difícil, mas vocês tornaram essa jornada muito mais simples e agradável. Obrigado!

A todos os amigos que moraram comigo por terem me aguentado por tanto tempo, alguns por anos até! Desculpa qualquer coisa! Obrigado também aos amigos que fiz nessa Rio Claro e aos que tenho carregado ao longo destes anos! A vida é muito melhor com vocês!

Aos meus pais, Pedro Paulo e Zezé, meu irmão, João e minha cunhada, Mirella: obrigado pelo amor, pela dedicação e pelos excelentes momentos que temos passado ao longo de todos esses anos.

“A saudade é uma estrada longa
Nem é boa e nem é ruim
Vou seguindo sempre adiante
Nunca volto,
Eu sou mesmo assim”.

(Almir Sater e Paulo Simões)

RESUMO

O gênero *Ischnocnema* compreende 33 espécies divididas em quatro séries. Dentre elas, a série de *I. guentheri* conta com 10 espécies que se distribuem principalmente pela Mata Atlântica brasileira. Dentro desta série, algumas espécies têm status taxonômico bastante complexo e sua posição filogenética, mesmo tendo sido testada de maneira robusta, tem se mostrado bastante instável. Assim, o presente trabalho faz uma revisão taxonômica dos membros da série de *I. guentheri* baseando-se em dados bioacústicos, morfológicos e moleculares, além de testar o monofiletismo da série de *I.guentheri* como hoje é conhecida. Como resultado, são descritas duas espécies relacionadas a *I. oea* dos estados de Minas Gerais e Espírito Santo e duas espécies relacionadas a *I. venancioi* e *I. hoehnei* dos estados do Espírito Santo e Rio de Janeiro com base em dados morfológicos, bioacústicos e moleculares. O posicionamento filogenético dessas espécies também é inferido utilizando-se marcadores moleculares, e um novo arranjo de séries dentro do gênero é proposto. Além disso, dados de sequenciamento de alto rendimento aliados a dados bioacústicos revelam que, como suspeitado anteriormente, há pelo menos seis espécies diferentes sendo tratadas sob o nome de *I. guentheri* ou *I. henselii*. Estas espécies, apesar de serem morfologicamente indistinguíveis entre si, são linhagens que possuem fluxo gênico nulo ou muito pequeno. Por fim, o genoma mitocondrial de cinco espécies de *Ischnocnema* da série de *I. guentheri* é construído utilizando-se os dados crus do sequenciamento de alto rendimento.

Palavras-chave: Bioacústica, Brachycephaloidea, Sistemática, Taxonomia, Terrarana.

ABSTRACT

The *Ischnocnema* genus comprises 33 species divided into four series. Among them, the *I. guentheri* series houses 10 species distributed mainly through the Brazilian Atlantic Forest. This phylogenetic position of this species series, even though it has been robustly tested, has been shown to be quite unstable and some of its species have a very complex taxonomic status. Thus, in the present thesis we make a careful taxonomic review of the members of the *I. guentheri* series based on bioacoustic, morphological and molecular data, and to test its monophyly as it is known today. We describe two species related to *I. oea* from the states of Minas Gerais and Espírito Santo and two species related to *I. venancioi* and *I. hoehnei* from the states of Espírito Santo and Rio de Janeiro based on morphological, bioacoustic, and molecular data. We also propose a new phylogenetic hypothesis for *Ischnocnema* using molecular markers, and based on this hypothesis we propose a new arrangement of species series. In addition, high-throughput sequencing coupled with bioacoustic data reveal that, as previously suspected, there are at least six different species being treated under the names *I. guentheri* or *I. henselii*. These species, although morphologically indistinguishable from each other, are lineages that show no or very little gene flow. Finally, we construct the mitochondrial genome of five *Ischnocnema* species from the *I. guentheri* series using raw high-throughput sequencing data.

Keywords: Bioacoustics, Brachycephaloidea, Sistematics, Taxonomy, Terrarana.

SUMÁRIO

Introdução Geral 13

Histórico Taxonômico 13
Literatura citada 17

Two New Species of *Ischnocnema* Reinhardt & Lütken, 1862 (Anura: Brachycephalidae) from Southeastern Brazil and their Phylogenetic Position within the *I. guentheri* Series 20

Material and Methods 24
Taxon and Gene Sampling 24
Laboratory Procedures 24
Alignment, Partition Schemes, and Nucleotide Substitution Model Selection 25
Genetic Distance and Phylogenetic Analyses 25
Morphological Analyses 26
Call Analyses 27
Results 28
Alignment, Partition Schemes, and Nucleotide Substitution Model Selection 28
Genetic Distance and Phylogenetic Analyses 29
Morphological Analyses 29
Call Analyses 30
Species Accounts 30
Discussion 48
Tree Topology and Genetic Distance 49
The *Ischnocnema guentheri* Series 50
Literature Cited 53
Appendix I 62
Appendix II 64
Appendix III 65
Appendix IV 67

Molecular phylogeny of *Ischnocnema* (Anura: Brachycephalidae) with the redefinition of its series and the description of two new species 84

Introduction 86
Material and Methods 90
Taxon and Gene Sampling 90
Laboratory procedures 91
Molecular analyses 91
Morphological analyses 93

Call analyses....94
Results....95
Molecular analyses....95
Morphological analyses....97
Call analyses....98
Taxonomic accounts....99
Discussion....132
Phylogenetic relationships....132
Systematics within *Ischnocnema*....134
The nuptial pad....135
Conclusions....137
References....139
Appendix A....170
Appendix B....173
Appendix C....176
Species limits within the *Ischnocnema guentheri* species complex (Anura: Brachycephalidae) revealed by an integrative approach using high-throughput sequencing....178
Introduction....182
Material and Methods....184
Taxon sampling, species hypothesis, and species recognition....184
Laboratory procedures....185
Phylogenetic analyses....185
Gene Flow Inference....187
Phenotypic analyses....188
Results....191
Species Tree Analyses....191
Gene Flow Inference....192
Phenotypic analyses....193
Discussion....195
Tree topologies....195
Species limits within the *Ischnocnema guentheri* complex....196
Comments about the taxonomic status of *Elosia divisa* Wandolleck, 1907 and *Hylodes nasutus* Lutz, 1925....198
Conclusions....200
References....202
Appendix A....228
Appendix B....233
Appendix C....235

The mitochondrial genomes of five frog species of the Neotropical genus *Ischnocnema* (Anura: Brachycephaloidea: Brachycephalidae) 237
References 241
Suplemental Online Material 246
Conclusões Gerais 248

INTRODUÇÃO GERAL

A superfamília Brachycephaloidea Günther, 1858 compreende mais de 1000 espécies (FROST, 2018) de anfíbios anuros neotropicais de desenvolvimento direto e representa boa parte da diversidade dos anfíbios atuais. A taxonomia desta superfamília tem sido bastante discutida nos últimos anos e seu conteúdo pode variar de três (PADIAL; GRANT; FROST, 2014) a cinco famílias (HEINICKE *et al.*, 2018) dependendo do autor. Apesar das diferentes classificações, a validade da família Brachycephalidae Günther, 1858 é senso comum entre os autores e inclui os gêneros *Brachycephalus* Fitzinger, 1826 e *Ischnocnema* Reinhardt e Lütken, 1862.

O gênero *Ischnocnema* atualmente compreende 33 espécies divididas nas séries de *I. guentheri*, *I. lactea*, *I. parva* e *I. verrucosa* (CANEDO; HADDAD, 2012; PADIAL; GRANT; FROST, 2014). Dentre estas, a série de *I. guentheri* contém 10 espécies: *I. epipeda* (Heyer, 1984), *I. erythromera*, (Heyer, 1984), *I. gualteri* (B. Lutz, 1974), *I. guentheri* (Steindachner, 1864), *I. henselii* (Peters, 1870), *I. hoehnei* (B. Lutz, 1958), *I. izecksohni* (Caramaschi e Kisteumacher, 1989), *I. nasuta* (A. Lutz, 1925), *I. oea* (Heyer, 1984) e *I. venancioi* (B. Lutz, 1958). As espécies da série de *I. guentheri* se distribuem pela Mata Atlântica brasileira, sendo que *I. henselii* chega até a província de Misiones, na Argentina (GEHARA *et al.*, 2013; HEDGES; DUELLMAN; HEINICKE, 2008). Até pouco tempo, *Ischnocnema* era sinônimo júnior do gênero *Eleutherodactylus* Duméril e Bibron, 1841 (CARAMASCHI; CANEDO, 2006) e muito tem se discutido sobre a taxonomia e sobre a posição filogenética do gênero, bem como da série de *I. guentheri* e seus membros nos últimos anos.

HISTÓRICO TAXONÔMICO

Os *Eleutherodactylus* da Mata Atlântica brasileira (hoje pertencentes a três gêneros, incluindo *Ischnocnema*) eram divididos em quatro grupos taxonômicos baseandos na morfologia dos dedos e na pele do ventre (LYNCH, 1976). Dentre estes grupos, o de *E. binotatus* continha seis espécies (três delas na atual série de *I. guentheri*): *E. binotatus* (Spix, 1824), *E. gualteri*, *E. guentheri*, *E. nasutus*, *E. octavioi* Bokermann, 1965 e *E. plicifer* (Boulenger, 1888).

Alguns anos mais tarde, o grupo de *E. guentheri* foi criado (no original em inglês foi chamado de "cluster" de *E. guentheri*) para alocar uma parte dos membros do grupo de *E.*

binotatus (HEYER, 1984). Apesar desta hipótese não ter sido testada, o grupo foi considerado como sendo um arranjo natural dentro do grupo de *E. binotatus*. O grupo de *E. guentheri* continha seis espécies, todas na atual série de *I. guentheri*: *E. epipedus*, *E. erythromerus*, *E. gualteri*, *E. guentheri*, *E. nasutus* e *E. oeus*.

Depois de algum tempo foi criado o subgênero *Eleutherodactylus*, que foi dividido em cinco séries de espécies (LYNCH; DUELLMAN, 1997). Uma destas séries era a de *E. binotatus*, que continha o grupo de *E. binotatus* (*sensu* HEYER, 1984) e outros três grupos, totalizando 19 espécies, a maioria da Mata Atlântica brasileira. Ao grupo de *E. binotatus* ainda foram adicionados *E. heterodactylus* (Miranda-Ribeiro, 1937), *E. hoehnei*, *E. izecksohni* (Caramaschi e Kisteumacher, 1989) e *E. juipoca* (Sazima e Cardoso, 1978).

Até recentemente, o gênero *Ischnocnema* possuía apenas uma espécie na Mata Atlântica, *I. verrucosa* (Reinhardt e Lütken, 1862), e as outras cinco espécies do gênero habitavam os Andes e regiões vizinhas (PADIAL *et al.*, 2005). Porém, características osteológicas presentes em *I. verrucosa,* espécie tipo do gênero, fizeram com que o gênero *Ischnocnema* fosse colocado na sinonímia de *Eleutherodactylus* (onde a maioria dos Brachycephaloidea se encontrava na época) e o gênero *Oreobates* Jiménez-de-la-Espada, 1872 fosse revalidado para alocar as outras cinco espécies andinas. Porém, logo um estudo filogenético incluindo diversas espécies de *Eleutherodactylus* (HEINICKE; DUELLMAN; HEDGES, 2007) foi realizado, e o gênero *Ischnocnema* foi revalidado para alocar a maioria das espécies de *Eleutherodactylus* da Mata Atlântica brasileira.

Posteriormente foi feita uma nova classificação baseada em um extensivo estudo filogenético abrangendo inúmeras espécies de anuros do novo mundo que possuíam desenvolvimento direto (atualmente Brachycephaloidea) e *Ischnocnema* foi dividido em cinco séries de espécies, uma delas sendo a série de *I. guentheri* (HEDGES; DUELLMAN; HEINICKE, 2008). Este táxon continha 11 espécies, muitas delas presentes no grupo de *E. guentheri* de classificações anteriores, porém com algumas novidades. São elas: *I. epipeda, I. erythromera, I. gualteri, I. guentheri, I. henselii* (que havia sido recentemente retirada da sinonímia de *I. guentheri*; KWET; SOLÉ, 2005), *I. hoehnei*, *I. izecksohni*, *I. nasuta, I. octavioi, I. oea* e *I. vinhai.* Porém, logo em seguida, *I. octavioi* foi retirada da série de *I. guentheri* e realocada para a série de *I. verrucosa*, com base em características morfológicas (CANEDO *et al.*, 2010).

Uma nova hipótese filogenética, abrangendo diversas espécies de Brachycephaloidea e contando com a maioria das espécies de *Ischnocnema* descritas até então (aproximadamente 80 %), foi realizada e a série de *I. guentheri* sofreu algumas modificações (CANEDO;

HADDAD, 2012). Com base nos resultados da filogenia, *I. vinhai* foi realocada para o gênero *Pristimantis* Jiménez-de-la-Espada, 1870 e *I. venancioi*, anteriormente na série de *I. lactea* (HEDGES; DUELLMAN; HEINICKE, 2008), se tornou parte da série de *I. guentheri*. *Ischnocnema epipeda* e *I. gualteri* não foram testadas, mas com base em similaridades morfológicas foram mantidas na série de *I. guentheri*.

Além da intensa discussão acerca da posição filogenética e da taxonomia da série de *Ischnocnema guentheri* como um todo, o *status* taxonômico de algumas espécies dentro da série tem se mostrado complexo e isso gerou discussão na literatura. *Ischnocnema guentheri* foi considerada durante muito tempo uma espécie de ampla distribuição ao longo da Mata Atlântica (GEHARA *et al.*, 2013; HEYER, 1984). Sua localidade tipo é a Floresta da Tijuca, dentro da cidade do Rio de Janeiro, (HÄUPL; TIEDEMAN; GRILLITSH, 1994) e a espécie era considerada presente em mais seis estados brasileiros (HEYER, 1984): Espírito Santo, Minas Gerais, Paraná, Rio Grande do Sul, Santa Catarina e São Paulo. A morfologia da espécie é similar ao longo de toda esta distribuição, mas *I. henselii* foi retirada da sinonímia de *I. guentheri* (KWET; SOLÉ, 2005) com base em bioacústica, posição em que havia sido colocada por estudos anteriores baseados em morfologia (COCHRAN, 1955; HEYER, 1984). Os cantos analisados no estudo que revalidou *I. henselii* eram oriundos dos estados de Santa Catarina, norte do Rio Grande do Sul e província de Misiones, Argentina, o que levou os autores a concluir que esta era a distribuição de *I. henselii*. No mesmo trabalho, também foram comparados cantos de populações de localidades distintas atribuídas a *I. guentheri*. Devido à grande variação nesses cantos, os autores chegaram à conclusão de que *I. guentheri* era provavelmente um complexo de espécies. Mais tarde, um estudo utilizando dados moleculares e bioacústicos e envolvendo inúmeras populações de atribuídas a *I. guentheri* e *I. henselii* dentro da distribuição conhecida dessas espécies, concluiu algo um tanto surpreendente. *Ischnocnema guentheri*, uma espécie até então de distribuição bastante ampla, constituía uma única linhagem que estava restrita à Floresta da Tijuca, um fragmento de mata urbano com cerca de 12.500 ha (GEHARA *et al.*, 2013). Este mesmo estudo também concluiu que, além das duas espécies já descritas, o complexo de *I. guentheri* possuía pelo menos mais quatro espécies, sendo várias delas sintópicas, e que a distribuição de *I. henselii* se estende por pelo menos 600 km ao norte da distribuição até então conhecida para a espécie (chegando até o estado de São Paulo). Entretanto, o trabalho é concluído indicando a necessidade de uma revisão taxonômica e uma avaliação mais detalhada das espécies aparentemente novas para a ciência.

Ischnocnema izecksohni era considerada endêmica do Quadrilátero Ferrífero, porção sul da Cadeia do Espinhaço, no estado de Minas Gerais (LEITE; JUNCÁ; ETEROVICK, 2008). A espécie, descrita da cidade de Belo Horizonte, tem como espécie mais próxima *I. nasuta* (CARAMASCHI; KISTEUMACHER, 1989) e teve o canto descrito recentemente (TAUCCE *et al.*, 2012). Além disso, com base em morfologia e bioacústica, sua distribuição foi estendida para várias outras localidades no estado de Minas Gerais, todas na Serra da Mantiqueira. Devido às diferenças morfológicas subjetivas entre *I. izecksohni* e *I. nasuta,* também foi constatado que estas espécies poderiam ser sinônimos e mais dados deveriam ser levantados, principalmente com relação a *I. nasuta* em sua localidade tipo, Nova Friburgo, região serrana do estado do Rio de Janeiro (A. LUTZ, 1925), para que o *status* taxonômico dessas duas espécies fosse confirmado (TAUCCE *et al.*, 2012). Na árvore resultante do trabalho de Canedo e Haddad (2012), *I. nasuta* se mostrou parafilética com relação a *I. izecksohni*, porém não foi analisado material de Nova Friburgo, apenas de Minas Gerais e Espírito Santo. Além de toda informação presente na literatura, saídas de campo e visitas às coleções taxonômicas também revelaram espécies ainda não descritas pela ciência (P.P.G. Taucce, dados não publicados).

Tendo tudo isto em vista, o presente trabalho teve como objetivo testar o monofiletismo da série de *Ischnocnema guentheri* como hoje é conhecida, bem como seu relacionamento dentro do gênero *Ischnocnema*. Também se objetivou realizar uma cuidadosa revisão taxonômica dos membros da série de *I. guentheri*, utilizando três fontes de evidência principais: molecular, bioacústica e morfológica. Para isto, esta tese se divide em quatro capítulos. O primeiro deles trata de *I. oea* e duas novas espécies proximamente relacionadas a ela, e do posicionamento filogenético deste clado dentro da série de *I. guentheri*. O segundo capítulo engloba uma filogenia para o gênero *Ischnocnema*, com a redefinição de suas séries de espécies e a descrição de duas novas espécies relacionadas a *I. hoehnei* e *I. venancioi*. O terceiro capítulo trata de *I. guentheri* e *I. henselii*, utilizando quase 400 marcadores moleculares oriundos de sequenciamento de alto rendimento, aliados a dados bioacústicos e morfológicos, para corroborar a suspeita de que na verdade estas duas espécies são um complexo de espécies morfologicamente crípticas. Este capítulo também trata da série tipo de *I. nasuta* e de *Elosia divisa* Wandolleck, 1907, um nome atualmente sob a sinonímia de *I. guentheri* (COCHRAN, 1955; HEYER, 1984; KWET; SOLÉ, 2005) e que pode ser revalidado. Por último, o quarto capítulo usa técnicas de bioinformática para construir os genomas mitocondriais de cinco espécies da série de *I. guentheri*, utilizando os dados crus do

sequenciamento de alto rendimento utilizado no capítulo anterior. Os capítulos foram formatados segundo modelo dos periódicos científicos os quais foram ou serão submetidos.

LITERATURA CITADA

BOKERMANN, W. C. A. A new *Eleutherodactylus* from Southeastern Brazil. *Copeia*, v. 1965, n. 4, p. 440–441, 1965.

BOULENGER, G. A. V. On some reptiles and batrachians from Iguarasse, Pernambuco. *Journal of Natural History Series 6*, v. 2, n. 7, p. 40–43, 1888.

CANEDO, C. *et al.* New species of *Ischnocnema* (Anura: Brachycephalidae) from the state of Minas Gerais, Southeastern Brazil, with comments on the *I. verrucosa* species series. *Copeia*, v. 2010, n. 4, p. 629–634, 2010.

CANEDO, C.; HADDAD, C. F. B. Phylogenetic relationships within anuran clade Terrarana, with emphasis on the placement of Brazilian Atlantic rainforest frog genus *Ischnocnema* (Anura: Brachycephalidae). *Molecular Phylogenetics and Evolution*, v. 65, n. 2, p. 610–620, 2012.

CARAMASCHI, U.; CANEDO, C. Reassessment of the taxonomic status of the genera *Ischnocnema* Reinhardt and Lütken, 1862 and *Oreobates* Jiménez-de-la-Espada, 1872, with notes on the synonymy of *Leiuperus verrucosus* Reinhardt and Lütken, 1862 (Anura: Leptodactylidae). *Zootaxa*, v. 1116, p. 43–54, 2006.

CARAMASCHI, U.; KISTEUMACHER, G. A new species of *Eleutherodactylus* (Anura : Leptodactylidae) from Minas Gerais , Southeastern Brazil. *Herpetologica*, v. 44, n. 4, p. 423–426, 1989.

COCHRAN, D. M. Frogs of Southeastern Brazil. *Bulletin of the U.S. National Museum*, v. 206, p. 1–406, 1955.

DUMERIL, A. M. C.; BIBRON, G. *Erpétologie générale ou histoire naturelle complète des reptiles. Tome Huitième*. Paris: Librarie Enclyclopedique de Roret, 1841.

FITZINGER, L. J. F. J. *Neue classification der reptilien nach ihren natürlichen verwandtschaften : nebst einer verwandtschafts-tafel und einem verzeichnisse der reptilien-sammlung des K. K. zoologischen museum's zu Wien*. Wien : J. G. Heubner, 1826.

FROST, D. R. *Amphibian species of the world: an online reference*. Disponível em: <http://research.amnh.org/herpetology/amphibia/index.html>. Acesso em: 8 mar. 2018.

GEHARA, M. *et al.* From widespread to microendemic: Molecular and acoustic analyses show that *Ischnocnema guentheri* (Amphibia: Brachycephalidae) is endemic to Rio de Janeiro, Brazil. *Conservation Genetics*, v. 14, n. 5, p. 973–982, 2013.

GÜNTHER, A. On the systematic arrangement of the tailless batrachians and the structure of *Rhinophrynus dorsalis*. *Proceedings of the Zoological Society of London*, v. 26, n. 1, p. 339–352, 1858.

HÄUPL, M; TIEDEMAN, F; GRILLITSH, H. Katalog der Typen der Herpetologischen Sammlung nach dem Stand vom 1. Jänner 1994. Teil I: Amphibia. *Kataloge der Wissenschaftlichen Sammlungen des Naturhistorischen Museums in Wien*, v. 9, p. 1–42, 1994.

HEDGES, S. B.; DUELLMAN, W. E.; HEINICKE, M. P. New World direct-developing frogs (Anura: Terrarana): molecular phylogeny, classification, biogeography, and conservation. *Zootaxa*, v. 1737, p. 1–182, 2008.

HEINICKE, M. P. *et al.* Phylogenomic support for evolutionary relationships of New World direct-developing frogs (Anura: Terraranae). *Molecular Phylogenetics and Evolution*, v. 118,, p. 145–155, 2018.

HEINICKE, M. P.; DUELLMAN, W. E.; HEDGES, S. B. Major Caribbean and Central American frog faunas originated by ancient oceanic dispersal. *Proceedings of the National Academy of Sciences of the United States of America*, v. 104, n. 24, p. 10092–10097, 2007.

HEYER, W. R. Variation, systematics, and zoogeography of *Eleutherodactylus guentheri* and closely related species (Amphibia: Anura: Leptodactylidae). *Smithonian Contributions to Zoology*, v. 402, p. 1–42, 1984.

JIMÉNEZ-DE-LA-ESPADA, M. Fauna neotropicalis species quaedam nondum cognitae. *Jornal de Sciências, Mathemáticas, Physicas e Naturaes*, v. 3, p. 57–65, 1870.
JIMÉNEZ-DE-LA-ESPADA, M. Nuevos Batrácios Americanos. *Anales de la Sociedad Española de Historia Natural*, v. 1, p. 84–88, 1872.

KWET, A.; SOLÉ, M. Validation of *Hylodes henselii* Peters, 1870, from Southern Brazil and description of acoustic variation in *Eleutherodactylus guentheri* (Anura: Leptodactylidae). *Journal of Herpetology*, v. 39, n. 4, p. 521–532, 2005.

LEITE, F. S. F.; JUNCÁ, F. A.; ETEROVICK, P. C. Status do conhecimento, endemismo e conservação de anfíbios anuros da Cadeia do Espinhaço, Brasil. *Megadiversidade*, v. 4, p. 158–176, 2008.

LUTZ, A. Batraciens du Brésil. *Comptes Rendus et Mémoires Hebdomadaires des Séances de la Société de Biologie et des ses Filiales*, v. 22, p. 211–214, 1925.

LUTZ, B. Anfíbios novos e raros das Serras Costeiras do Brasil: *Eleutherodactylus venancioi* n. sp., *E. hoehnei* n. sp., *Holoaden bradei* n. sp. e *H. lüderwaldti* Mir. Rib., 1920. *Memórias do Instituto Oswaldo Cruz*, v. 56, n. 2, p. 372–389, 1958.

LUTZ, B. *Eleutherodactylus gualteri*, a new species from the Organ Mountains of Brazil. *Journal of Herpetology*, v. 8, n. 4, p. 293–295, 1974.

LYNCH, J. D. The species groups of South American frogs of the genus *Eleutherodactylus* (Leptodactylidae). *Occasional papers of the Museum of Natural History of the University of Kansas*, v. 61, p. 1–24, 1976.

LYNCH, J. D.; DUELLMAN, W. E. Frogs of the genus *Eleutherodactylus* in western Ecuador biogeography. *Special Publication of the Natural History Museum, The University of Kansas*, v. 23, p. 1–236, 1997.

MIRANDA-RIBEIRO, A. Alguns batrachios novos das colleçcões do Museo Nacional. *O Campo*, v. 8, p. 66–69, 1937.

PADIAL, J. M. *et al.* New species of *Ischnocnema* (Anura: Leptodactylidae) from the Andes of Bolivia. *Journal of Herpetology*, v. 39, n. 2, p. 186–191, 2005.

PADIAL, J. M.; GRANT, T.; FROST, D. R. Molecular systematics of terraranas (Anura: Brachycephaloidea) with an assessment of the effects of alignment and optimality criteria. *Zootaxa*, v. 3825, n. 1, p. 1, 26 jun. 2014.

PETERS, W. C. H. Über neue Amphien (*Hemidactylus*, *Urosaura*, *Tropdolepisma, Geophis, Uriechis, Scaphiophis, Hoplocephalus, Rana, Entomoglossus, Cystignathus, Hylodes, Arthroleptis, Phyllobates, Cophomantis*) des Königlich Zoologisch Museum. *Monatsberichte der Königlichen Preussische Akademie des Wissenschaften zu Berlin*, v. 1870, p. 641–652, 1870.

REINHARDT, J. T.; LÜTKEN, C. F. Bidrag til Kundskab om Brasiliens Padder og Krybdyr. Förste Afdeling: Padderne og Öglerne. *Videnskabelige Meddelelser fra Dansk Naturhistorisk Forening i Kjøbenhavn*, v. 2, n. 3, p. 143–242, 1862.

SAZIMA, I.; CARDOSO, A. J. Uma espécie nova de *Eleutherodactylus* do sudeste Brasileiro (Amphibia, Anura, Leptodactylidae). *Revista Brasileira Biologia*, v. 38, p. 921–925, 1978.

SPIX, J. B. von. *Animalia nova sive Species novae Testudinum et Ranarum quas in itinere per Brasiliam annis MDCCCXVII–MDCCCXX jussu et auspiciis Maximiliani Josephi I.* München: F. S. Hübschmann, 1824.

STEINDACHNER, F. Batrachologische Mittheilungen. *Verhandlungen des Zoologisch-Botanischen Vereins in Wien*, v. 14, p. 239–288, 1864.

TAUCCE, P. P. G. *et al.* The advertisement call, color patterns and distribution of *Ischnocnema izecksohni* (Caramaschi and Kisteumacher, 1989) (Anura, Brachycephalidae). *Papéis Avulsos de Zoologia*, v. 52, n. 9, 2012.

WANDOLLECK, B. Einige neue und weniger bekannte Batrachier von Brazilien. *Abhandlungen und Berichte des Zoologischen und Anthropologisch-Ethnographischen Museums zu Dresden*, v. 11, p. 1–15, 1907.

Two New Species of *Ischnocnema* Reinhardt & Lütken, 1862 (Anura: Brachycephalidae) from Southeastern Brazil and their Phylogenetic Position within the *I. guentheri* Series*

PEDRO P. G. TAUCCE[1,4], CLARISSA CANEDO[2, 3], AND CÉLIO F. B. HADDAD[1]

[1] Instituto de Biociências, UNESP – Univ Estadual Paulista, Câmpus Rio Claro, Departamento de Zoologia, Laboratório de Herpetologia, Cx. Postal 199, 13506-569, Rio Claro, São Paulo, Brazil

[2] Instituto de Biologia Roberto Alcântara Gomes, UERJ – Universidade do Estado do Rio de Janeiro, Departamento de Zoologia, Rua São Francisco Xavier, 524, Maracanã, 20550-013, Rio de Janeiro, Rio de Janeiro, Brazil

[3] Museu Nacional, UFRJ – Universidade Federal do Rio de Janeiro, Departamento de Vertebrados, Setor de Herpetologia, Quinta da Boa Vista, 20940-040, Rio de Janeiro, Rio de Janeiro, Brazil

[4] Correspondence: e-mail, pedrotaucce@gmail.com

*Capítulo aceito para publicação no periódico *Herpetological Monographs*

ABSTRACT: We describe two new species of *Ischnocnema* from the states of Minas Gerais and Espírito Santo, southeastern Brazil, based on morphological, bioacoustical, and molecular data. We use three mitochondrial and two nuclear genes in Bayesian inference and maximum likelihood analyses to assess their phylogenetic placement within the *I. guentheri* series. The two new species group with *I. oea* in a well-supported clade in both analyses and have a calcar tubercle that is at least as long as wide. This type of tubercle seems to be a putative synapomorphy for the clade. We provide a revised diagnosis for the *I. guentheri* series, with characters shared by all its members, and discuss the close relationship between the *I. parva* and the *I. guentheri* series.

Key words: Advertisement call; External morphology; Integrative taxonomy; *Ischnocnema* ***feioi*** sp. nov.; *Ischnocnema* ***garciai*** sp. nov.; *Ischnocnema oea*; Molecular phylogeny

THE GENUS *Ischnocnema* Reinhardt & Lütken, 1862 "1861"comprises 33 species (Frost 2016) and it is currently divided into four series: *I. guentheri, I. lactea, I. parva,* and *I. verrucosa* (Canedo and Haddad 2012, Padial et al. 2014). Ten species are currently recognized in the *I. guentheri* series: *I. epipeda* (Heyer 1984), *I. erythromera* (Heyer 1984), *I. gualteri* (B. Lutz 1974), *I. guentheri* (Steindachner 1867), *I. henselii* (Peters 1870), *I. hoehnei* (B. Lutz 1958), *I. izecksohni* (Caramaschi and Kisteumacher 1989 "1988"), *I. nasuta* (A. Lutz 1925), *I. oea* (Heyer 1984), and *I. venancioi* (B. Lutz 1958). The series occurs throughout the Atlantic Forest in southeastern and southern Brazil and adjacent northern Argentina (Frost 2016). The systematics of the *I. guentheri* series has experienced many changes over the past few decades.

Lynch (1976) divided the former *Eleutherodactylus* Duméril and Bibron 1841 from the Brazilian Atlantic Forest into four species groups based on finger morphology and venter skin texture: the *E. binotatus*, *E. lacteus*, *E. parvus,* and *E. ramagii* groups. The *E. binotatus* (currently *Haddadus binotatus* [Spix, 1824]) group contained six species, three of them in the current *I. guentheri* series: *I. gualteri, I. guentheri*, and *I. nasuta*. *Ischnocnema henselii* and *I. hoehnei* were not assigned to this group due to lack of data and *I. venancioi* was placed into the *E. lacteus* group. Heyer (1984) studied the variation, systematics, and zoogeography of the former *E. guentheri* (= *I. guentheri*) and created what he called the "*E. guentheri* cluster," based on external morphology. His grouping was a part of the *E. binotatus* group (sensu Lynch, 1976), and included *I. gualteri*, *I. guentheri*, *I. nasuta*, and three new species he described at the time: *I. epipeda, I. erythromera,* and *I. oea.* Just over a decade later, Lynch and Duellman (1997) created the *E. binotatus* series to allocate all the Atlantic Forest *Eleutherodactylus* species, including the *E. binotatus*, *E. lacteus*, *E. parvus*, and *E. ramagii* groups (sensu Lynch, 1976). Their *E. binotatus* group included the members of the *E. binotatus* group proposed by Lynch (1976), the members of the *E. guentheri* cluster proposed

by Heyer (1984), *I. hoehnei*, *I. izecksohni*, and two other species. *Ischnocnema venancioi* was placed in the *E. binotatus* series but was unassigned to any goup. Heinicke et al. (2007), in a molecular study assessing several *Eleutherodactylus* from all over the American continent, reallocated most of the *Eleutherodactylus* from the Brazilian Atlantic Forest to the genus *Ischnocnema*, and Hedges et al. (2008) divided the genus into five series. They placed *I. venancioi* in the *I. lactea* series, and their *I. guentheri* series included 11 species: all the members from the former *E. guentheri* cluster (Heyer 1984) plus *I. henselii, I. hoehnei, I. izecksohni, I. octavioi* (Bokermann 1965), and *I. vinhai* (Bokermann 1975" 1974"). Shortly thereafter, Canedo et al. (2010) examined the external morphology of *I. octavioi* and based on these observations reallocated the species to the *I. verrucosa* series. Canedo and Haddad (2012) made the first phylogenetic study encompassing most species of *Ischnocnema* (more than 80% of the described species at the time), and transferred *I. vinhai* to the genus *Pristimantis* Jiménez de la Espada 1870. They also included *I. venancioi* in the *I. guentheri* series based on its phylogenetic placement. Gehara et al. (2013) did the first attempt in assessing the taxonomy of the *I. guentheri* series using molecular and acoustic data together. Authough they did not make any taxonomic decision, they found four candidate species related to *I. guentheri* and *I. henselii*, showing that the species richness in the *I. guentheri* series is probably underestimated.

Recent field work in the state of Minas Gerais and museum visits resulted in the discovery of two unnamed species of the *I. guentheri* series with overall morphology similar to *I. oea*, from the localities of Serra do Brigadeiro, municipalities of Ervália and Muriaé, and Usina da Fumaça, municipality of Muriaé. The aims of this paper are primarily to: (1) describe the two new species using morphological, bioacoustical, and molecular data; (2) evaluate the phylogenetic position of the two new species within the *I. guentheri* series; and (3) reevaluate the diagnostic characters proposed in recent literature for the *I. guentheri* series.

MATERIAL AND METHODS

Taxon and Gene Sampling

Aiming to assess the phylogenetic position of the two new species we compiled a molecular dataset with all nominal species of *Ischnocnema* available in GenBank (all terminals and respective Genbank accession numbers are listed in Appendix I) and also the four unnamed candidate species related to *I. guentheri* from the Gehara et al. (2013) study. Outgroup selection was based on previous phylogenetic studies (Canedo and Haddad 2012; Padial et al. 2014) and included members of the superfamily Brachycephaloidea Günther 1858: *Barycholos* Heyer 1969, *Brachycephalus* Fitzinger 1826, *Craugastor* Cope 1862, *Eleutherodactylus*, *Haddadus* Hedges et al. 2008, *Hypodactylus* Hedges et al. 2008, *Lynchius* Hedges et al. 2008, *Pristimantis*, and *Yunganastes* Padial et al. 2007. We selected the mitochondrial 12S rRNA, tRNAVal, and partial sequence 16S rRNA genes, and partial sequences of the nuclear tyrosinase precursor (Tyr) and recombination activating gene 1 (RAG1) genes because they were available for most *Ischnocnema* species.

Laboratory Procedures

We extracted whole cellular DNA from 100% ethanol-preserved muscle tissues using the Standard Ammonium Precipitation Method (Maniatis et al. 1982). PCR amplifications were carried out using Taq DNA Polymerase Master Mix (Ampliqon S/A, Denmark) and Axygen Maxygene thermocyclers. The standard PCR program consisted of a 3 min initial denaturing step at 95ºC, followed by 35–36 (nuclear 40–42) cycles of 20 s at 95ºC, 20 s at 45–

60ºC, and 45 or 80 s at 68 or 72ºC, followed by a final extension step of 5 min at 68 or 72ºC. We carried out PCR product cleaning using enzymatic purifications (Shrimp Alkaline Phosphatase and Exonuclease I, Werle et al. 1994). Purified PCR products were sent to Macrogen Inc. (South Korea) where they conducted sequencing in an ABI 3730XL sequencer. Primer pairs are detailed in Table 1 and Genbank accession numbers are given in Appendix II.

Alignment, Partition Schemes, and Nucleotide Substitution Model Selection

We performed alignment using MAFFT v. 7.273 (Katoh and Standley 2013). For the nuclear gene fragments we used the FFT-NS-2 algorithm and for the 12S-tVal-16S concatenated fragment we used the E-INS-i algorithm, which is adapted for sequences with conserved domains and variable regions rich in gaps.

We conducted a search for the best partition scheme and best fitting nuclear models with PartitionFinder v. 1.1.1 (Lanfear et al. 2012) using the Corrected Akaike Information Criterion (AICc; Hurvich and Tsai 1989) and considering each gene and each codon as separate partitions.

Genetic Distance and Phylogenetic Analyses

We computed uncorrected pairwise distances using R version 3.2.4 (R Core Team 2016) with the packages APE version 3.4 (Paradis et al. 2004) and SPIDER version 1.3-0 (Brown et al. 2012). The fragment of the 16S rDNA employed in the genetic distance calculation was the one delimited by the primers 16S AR–BR (ca. 600 bp; Palumbi et al. 1991).

We conducted tree searches using both maximum likelihood and Bayesian inference optimality criterions. We computed maximum likelihood analysis in RAxML v. 8.2.2 (Stamatakis 2014), searching the most likely tree 100 times and conducting 1000 non-parametric bootstrap replicates. We computed Bayesian inference analysis in MrBayes 3.2.6 (Ronquist et al. 2012) using two independent runs of 1.0×10^7 generations, starting with random trees and four Markov chains (one cold), sampled every 1000 generations. We discarded 25% of generations and trees as burnin and performed the run with unlinked character state frequencies, substitution rates of GTR model, gamma shape parameters, and proportion of invariable sites between partitions. We used standard deviation of split frequencies (< 0.01), Estimated Sample Size (ESS > 100), and Potential Scale Reduction Factor (PSRF; Gelman and Rubin 1992; should approach 1.0 as runs converge) to assess run convergence. We used *Eleutherodactylus* as root for both analyses, and we draw phylogenetic trees using FigTree 1.4.2 (Rambaut 2014).

Morphological Analyses

The following measurements were taken to the nearest 0.1 mm with a Mitutoyo® digital caliper under a stereomicroscope: snout-vent length (SVL), head length (from the tip of the snout to the angle of the jaw), head width (between the angles of the jaws), forearm length (from the elbow to the wrist), hand length (from the wrist to the tip of the third finger), thigh length (from the middle of the cloacal opening to the outer edge of the knee), tibia length (from the outer edge of the knee to the outer edge of the heel), tarsal length (from the outer edge of the heel to the inner metatarsal tubercle), and foot length (from the proximal border of the inner metatarsal tubercle to the tip of the fourth toe). Eye diameter (between anterior and posterior margins of the eye), tympanum diameter (between anterior and

posterior margins of the tympanum), eye to nostril distance (from the anterior margin of the eye to the posterior margin of the nostril), internarial distance (between the two medial margins of the nostrils), eye to eye distance (between the anterior margins of the eyes), third finger disk length (maximum width of disk on third finger), and fourth toe disk length (maximum width of disk on fourth toe) were taken with an ocular micrometer coupled to a stereomicroscope. Sex was determined by the observation of nuptial pads and vocal slits in males and gonads of females. Morphological nomenclature follows previous literature on Brachycephaloidea (Heyer 1984; Heyer et al. 1990; Hedges et al. 2008; Duellman and Lehr 2009). Museum acronyms follow Sabaj (2016) and a full list of specimens examined is given in Appendix III.

Call Analyses

We recorded advertisement calls from both of the new species using a Marantz PMD 660, PMD 661 or a Tascam DR-40, coupled to a Sennheiser K6/ME66 unidirectional microphone. Recordings were carried out at 44.1 kHz on a 16 bit sampling size. To analyze the recordings we used the software Raven pro 1.4 (Bioacoustics Research Program 2011). Spectrograms were produced using window size of 512 samples, 75% overlap, hop size of 128 samples, Discrete Fourier Transform (DFT) of 1024 samples, and window type Hann. Resolution, contrast, and brightness were program default. We obtained spectrogram and oscillogram figures using tuneR version 1.0 (Ligges et al. 2013) and seewave version 2.0.2 (Sueur et al. 2008) packages of R platform version 3.2.4 (R Core Team 2016). Spectrogram figures were produced with window length of 512 samples, 75% overlap, hop size of 128 samples, and window name Hanning. Call recordings of Pedro P. G. Taucce (PPGT 001–008) are deposited in the CFBH collection and remaining analyzed call recordings are deposited in

188 the Bioacoustics Collection of the Universidade Federal de Minas Gerais, Belo Horizonte,
189 Minas Gerais, Brazil (CBUFMG 916–917) and in the voice collection of the Museu Nacional,
190 Rio de Janeiro, Rio de Janeiro, Brazil (MNVOC 043:1–3). Voucher specimens are housed at
191 CFBH, MZUFV, and UFMG. Full information for the recordings is listed in Appendix IV.
192 The following acoustic parameters were taken: call duration (= call length from
193 Cocroft and Ryan 1995), call rise time (Hepp and Canedo 2013), dominant frequency
194 (Cocroft and Ryan 1995), notes per call, note repetition rate (Gehara et al. 2013), and note
195 repetition rate acceleration (Gehara et al. 2013). *Ischnocnema oea* recently had its
196 advertisement call described (Hepp and Canedo 2013). Although we did not reanalyse the
197 recordings used in this description, we measured note repetition rate acceleration for the sake
198 of comparison with our recordings, since this parameter was not used by Hepp and Canedo
199 (2013).
200
201 ## RESULTS
202
203 ### Alignment, Partition Schemes, and Nucleotide Substitution Model Selection
204
205 We obtained a final alignment of 3585 base pairs divided in three mitochondrial and
206 two nuclear genes, respectively: 12S rRNA (1016 bp), tRNAVal (75 bp), partial 16S rRNA
207 (1533 bp), partial RAG1 (417 bp), and partial Tyr (531 bp). The best-fit partition scheme
208 comprised seven partitions, which are shown with respective substitution models used in the
209 Bayesian inference analysis in Table 2. For the maximum likelihood analysis we used the
210 General Time Reversible model with γ-distribution for all the partitions because RAxML does
211 not support estimating different models for different partitions.
212

Genetic Distance and Phylogenetic Analyses

The uncorrected pairwise distance of partial 16S rRNA between *Ischnocnema oea* and *I. garciai* was 10.4 to 10.7% and between *I. oea* and *I. feioi* was 9.9%. The genetic distance between *I. feioi* and *I. garciai* was 7.0 to 7.8%. Distances among these species and other closely related species within the *I. guentheri* series are summarized in Table 3.

The Bayesian inference and the maximum likelihood analyses resulted in the same topology. Mostly with high support, we recovered all currently recognized *Ischnocnema* series as reciprocally monophyletic groups, as well as the same relationships among series as those recovered by Canedo and Haddad (2012, Fig. 1). However, we recovered the *I. guentheri* and the *I. parva* series with low support (61% of posterior probability and 55% of maximum likelihood bootstrap, 91% of posterior probability and 62% of maximum likelihood bootstrap, respectively). Within the *I. guentheri* series, results were mostly consistent with previous hypotheses (Canedo and Haddad 2012; Gehara et al. 2013). *Ischnocnema oea* clustered with *I. garciai* and *I. feioi* in a well-supported clade (100% of posterior probability and maximum likelihood bootstrap) and was the sister species of *I. garciai*.

Morphological Analyses

Morphological characteristics allowed us to distinguish the three new species within the *Ischnocnema oea* cluster from all other members from the *I. guentheri* series. The main character states distinguishing the three species are the calcar tubercle being at least as long as wide in adult males (absent or less long than wide in other species; Fig. 2) and smaller SVL. Among the three species, *I. oea* is morphologically indistinguishable from *I. garciai*, but *I.*

237 *feioi* has a larger SVL (Table 4) and a straight *canthus rostralis* in dorsal view (concave in the
238 other two species).
239
240 Call Analyses
241
242 We analyzed 52 advertisement calls from 12 individuals, and all of them showed the
243 same basic structure: groups of short notes emitted sporadically, with irregular intervals
244 between calls. The advertisement calls begin with low energy notes, increasing in energy
245 gradually until a peak is reached, which is accordant with the other known calls of the
246 *Ischnocnema guentheri* series. Despite having great genetic distance and being
247 morphologically distinguishable (see above), *I. oea* and *I. feioi* have similar advertisement
248 calls, exhibiting some degree of overlap in all analyzed parameters (Fig. 3A, 3B; Table 5).
249 However, *I. garciai* has a notably distinct advertisement call (Fig. 3C; Table 5).
250 Based on the molecular, bioacoustical, and morphological data presented here we
251 consider the three species within the *Ischnocnema oea* cluster as distinct evolving lineages.
252 Here we redescribe *I. oea* and describe the other two new species.
253
254 Species Accounts
255
256 *Ischnocnema oea* (Heyer 1984)
257 Figs. 4A, 5
258
259 *Eleutherodactylus oeus* Heyer 1984: Heyer (1984:iii, 22 [his table 20], 23, 26, 27 [his fig.
260 21], 31–33 [his fig. 26], 40), species description.

Eleutherodactylus (Eleutherodactylus) oeus: Lynch and Duellman (1997:229 [their appendix III]).

Ischnocnema oea: Heinicke et al. (2007: by implication); Hedges et al. (2008:25, 27, 151 [their appendix I]); Canedo et al. (2010: 632–633); Canedo and Haddad (2012: 611, 619 [their table 3]), Padial et al. (2014:122 [their appendix II]).

Holotype.— MNRJ 1244, adult male. Municipality of Santa Teresa, state of Espírito Santo, Brazil. Collected by Augusto Ruschi in December 1942.

Paratypes.— USNM 235612, MZUSP 59684 (not examined).

Diagnosis.— In the *Ischnocnema guentheri* series by phylogenetic placement (Canedo and Haddad 2012, Fig. 1) and the following combination of characters: (1) long legs, tibia length > 60% of SVL; (2) one large, conspicuous, glandular appearing nuptial pad on Finger I; (3) dorsum smooth. *Ischnocnema oea* is distinguished from all other species of the *I. guentheri* series by the following combination of characters: (1) calcar tubercle at least as long as wide in adult specimens; (2) small size (SVL in males 13.5–17.8 mm, n = 13; females 24.7–25.0, n = 2); (3) posterior face of the thigh uniform or mottled; (4) canthus rostralis concave in dorsal view; (5) Finger I approximately the same size as Finger II; (6) advertisement call duration 4.56–8.49 s; (7) dominant frequency 3.09–4.13 kHz; (8) 25–41 notes per call; (9) note repetition rate 4.80–5.70 notes/s; (10) note repetition rate acceleration -9–61%.

Redescription of the holotype.— Small size (SVL 17.1 mm). Head longer than wide; head length 44% of SVL, head width 33% of SVL; snout rounded in dorsal and lateral views; nostrils rounded; oriented laterally, located near the tip of the snout; canthus rostralis moderately distinct, curved; loreal region slightly concave; eyes protuberant and laterally oriented, eye diameter 30% of head length; tympanum distinct, rounded, tympanic membrane

indifferentiated, annulus present, visible externally, tympanum diameter 38% of eye diameter; supratympanic fold absent; vocal slits present; vocal sac single, subgular, slightly expanded externally, with a fold of skin on the right side; tongue large, elliptical, posterior notch absent; choanae rounded; dentigerous processes of the vomer located posteromedially to choanae, triangle-shaped, medially separated by a gap approximately the width of one dentigerous process, teeth present, barely distinct.

Forelimbs slender; fingers slender, bearing discrete fringes, with small discs on fingers I and II, larger discs on fingers III and IV with a V-shaped median slit in dorsal view; finger lengths I ≈ II < IV < III; palmar tubercle barely distinct; thenar tubercle elliptical, barely distinct; single nuptial pad apparently glandular, with the same color as the hand, extending dorsaly from the distal to the proximal portion of the metacarpus on Finger I, divided ventraly on the distal margin of the thenar tubercle, extending all over its caudal third; palm smooth with one barely distinguishible supernumerary tubercle; single subarticular tubercles prominent, rounded, and large.

Hind limbs slender; shank longer than thigh, tibia length 67% of SVL, thigh length 60% of SVL; calcar tubercle well-developed, cone-shaped, as long as wide; knees with two pointed tubercles; tarsal fold absent; toes long, slender, fringed, with large discs on toes II–V, which have a V-shaped median slit in dorsal view; small disc on Toe I; toe lengths I < II < III < V < IV; inner metatarsal tubercle elliptical, much larger than the rounded outer metatarsal tubercle; sole of the foot smooth, with one supernumerary tubercle; single large, prominent, and rounded subarticular tubercles.

Dorsal skin smooth, with a few sparse tubercles; dorsal surface of the snout and upper eyelid with some barely distinguishible, pointed tubercles; venter smooth, with no tubercles; discoidal and thoracic folds present.

Coloration of the holotype in preservative.— The specimen is somewhat faded. Background yellowish-brown; dorsum completely variegated; head with cream-colored interorbital bar; brown lateral strip from right below eyes to upper lip; canthus rostralis with brown blotch near nostrils; brown supratympanic stripe starting in tympanum, contouring arm, and reaching abdomen at mid-body; inguinal region with brown spot; dorsal portion of forelimbs yellowish-brown with transversal brown stripes; ventral portion of forelimbs yellowish-brown; hidden portion of thigh yellowish-brown; external portion of tibia with brown longitudinal bar; venter yellowish-brown; gular region yellowish-brown with some irregularly spaced brown blotches; margins of jaw brown.

Measurements of holotype (in millimeters).— SVL 17.1, head length 7.4, head width 5.6, eye diameter 2.2, tympanum diameter 0.8, eye–nostril distance 2.2, internarial distance 1.6, eye to eye distance 3.3, forearm length 3.7, hand length 3.8, third finger disk length 0.5, thigh length 10.3, tibia length 11.4, tarsal length 5.8, foot length 9.9, fourth toe disk length 0.6.

Variation.— Additional referred specimens are listed in Appendix III. Some specimens have a sub-elliptical snout in dorsal view. We found great variation in the shape of the nostrils, which may be triangular, elliptical, and ovoid. The supratympanic stripe may be just a blotch in the upper tympanic region or may reach the mid-body without going down to the abdominal region. The shapes of the tongue and choanae openings are highly variable. Some individuals have the tongue and choanae openings rounded, ovoid, and elliptical. Upper eyelid tubercles and finger fringes are absent in some specimens, and postrictal tubercles are present in some. Females were markedly larger than males (SVL in females 24.7–25 mm, n = 2; males 13.5–17.8 mm, n = 13). In juveniles, the calcar tubercle may be as long as wide, shorter than wide, or absent. Variation in measurements and body proportions are given in Table 4.

335 **Advertisement call.—** The advertisement call is described in detail by Hepp and
336 Canedo (2013).
337 **Comparisons with other species.—** The long legs (tibia length/SVL = 66–74%)
338 distinguish *I. oea* from the species of the *I. lactea* (tibia length/SVL usually < 50%, Hedges et
339 al. 2008), *I. parva* (tibia length/SVL < 60%; Hedges et al. 2008; Brusquetti et al. 2013), and *I.*
340 *verrucosa* (tibia length/SVL < 55%; Hedges et al. 2008; Canedo et al. 2010, 2012) series, and
341 from *I. sambaqui* (Castanho and Haddad 2000) (currently unassigned to any series; tibia
342 length/SVL < 55%; Castanho and Haddad 2000). The large and conspicuous, glandular-
343 appearing nuptial pad on Finger I distinguishes *I. oea* from the species of the *I. lactea* (minute
344 nuptial pad in *I. randorum* [Heyer 1985]*;* translucent in *I. nigriventris* [A. Lutz 1925] and *I.*
345 *vizottoi* Martins and Haddad 2010; reduced to some white granules in *I. holti* [Cochran 1948];
346 absent in *I. melanopygia* Targino, Costa and Carvalho-e-Silva 2009 and *I. spanios* [Heyer
347 1985]; unknown in other species; Heyer 1985; Hedges et al. 2008; Targino and Carvalho-e-
348 Silva 2008; Berneck et al. 2013) and *I. verrucosa* series (except for *I. surda* Canedo et al.
349 2010, in which the nuptial pad is also large, conspicuous, and glandular-appearing; faint,
350 translucent nuptial pad in *I. karst* Canedo et al. 2012; absent in other species; Hedges et al.
351 2008; Canedo et al. 2010, 2012) and from *I. manezinho* (Garcia 1996) (currently unassigned
352 to any series) and *I. sambaqui* (absent in these last two species; Garcia 1996; Castanho and
353 Haddad 2000). The smooth dorsum distinguishes *I. oea* from the species of the *I. verrucosa*
354 series (dorsum tuberculate in these species; Hedges et al. 2008; Canedo et al. 2010, 2012),
355 from *I. manezinho* (finelly tuberculate; Garcia 1996), and from *I. sambaqui* (slightly rugose to
356 rugose; Castanho and Haddad 2000).
357 *Ischnocnema oea* differs from all species of the *I. guentheri* series by having a calcar
358 tubercle that is at least as long as it is wide in adult specimens (calcar tubercle absent or not as
359 long as wide in other species).

By its smaller body size, *I. oea* (SVL in males 13.5–17.8 mm; females 24.7–25 mm) differs from *I. erythromera* (SVL in males 22.3–24.4 mm; females 24.3–35.3 mm; Heyer 1984), *I. gualteri* (SVL in males 21.3–34.1 mm; females 33.6–45.7 mm; Heyer 1984), *I. henselii* (SVL in males 21.0–27.5 mm; females 28.4–38.4 mm; Kwet and Solé 2005), *I. izecksohni* (SVL in male 32.4 mm; females 43.5–49.0 mm; Caramaschi and Kisteumacher 1989 "1988"), and *I. nasuta* (SVL in males 24.7–41.5 mm; females 36.1–53.9 mm; Heyer 1984).

By the uniform or mottled posterior surface of its thighs, *I. oea* is distinguished from *I. erythromera* (*I. erythromera* with a light area on the posterior surface of the thigh in fixed specimens and red in life; Heyer 1984) and from *I. venancioi* (*I. venancioi* with clear spots surrounded by a dark background in fixed specimens and spots orange or yellow in life; B. Lutz 1958). Finger I approximately the same size as Finger II also distinguishes *I. oea* from *I. venancioi* (Finger I smaller than Finger II in *I. venancioi*). The concave *canthus rostralis* in dorsal view distinguishes *I. oea* from *I. hoehnei, I. izecksohni*, *I. nasuta*, and *I. venancioi* (canthus rostralis straight in dorsal view in these species).

Advertisement call duration (4.56–8.49 s; Hepp and Canedo 2013) distinguishes *I. oea* from *I. gualteri* (1.50–1.90 s; Heyer 1984), *I. guentheri* (26.30–41.90 s; Gehara et al. 2013), *I. henselii* (10.00–23.00 s; Gehara et al. 2013), *I. izecksohni* (1.03–2.15 s; Taucce et al. 2012), and *I. nasuta* (1.15–1.50 s; Heyer 1984). *Ischnocnema oea* emits more notes per call (25–41; Hepp and Canedo 2013) than *I. gualteri* (4–9; Heyer 1984) and fewer notes per call than *I. henselii* (86–170; Gehara et al. 2013). The higher dominant frequency (3.09–4.10 kHz; Hepp and Canedo 2013) distinguishes *I. oea* from *I. gualteri* (2.10–2.70 kHz; Heyer 1984), *I. henselii* (2.10–3.10 kHz; Gehara et al. 2013), *I. izecksohni* (2.25–2.63 kHz; Taucce et al. 2012), and *I. nasuta* (2.10–2.60 kHz; Heyer 1984). Note repetition rate distinguishes *I. oea* (4.80–5.70 notes/s; Hepp and Canedo 2013) from *I. henselii* (6.60–7.10 notes/s; Gehara et al.

2013) and *I. izecksohni* (29.91–31.10 notes/s; Taucce et al. 2012), and note repetition rate acceleration distinguishes *I. oea* (-9–61%) from *I. henselii* (107–125%; Gehara et al. 2013).

Geographic distribution.— *Ischnocnema oea* is currently known only from the state of Espírito Santo, southeastern Brazil, from the municipalities of Cariacica, Santa Teresa, and Vargem Alta (Fig. 6).

Remarks.— Silva-Soares et al. (2009) expanded the known distribution of *I. oea* to Macaé de Cima, municipality of Nova Friburgo, state of Rio de Janeiro. We examined the referred specimen MBML 212 and concluded that it is probably a juvenile *I. nasuta*. Almeida-Gomes et al. (2010) cited *I. oea* from the municipality of Cambuci, state of Rio de Janeiro. We examined the referred specimens (MNRJ 49504–49506) and they are indeed morphologically similar to *I. oea*. But since we are not aware of any morphological differences between *I. oea* and *I.* garciai, and we have no additional data to compare the population from Cambuci with specimens surely belonging to each of these species, the identity of these specimens will remain undetermined.

Ischnocnema ***feioi*** sp. nov.

Figs. 4B, 7

Ischnocnema sp. (aff. *guentheri*): Moura et al. (2012:214 [their Table 2], 216 [their Fig. 2d], 233 [their Appendix 1]), in part; [misidentification]).

Holotype.— CFBH 35994, adult male. Lar dos Muriquis, Serra do Brigadeiro, municipality of Muriaé, state of Minas Gerais, Brazil (20º53’34.7” S, 42º32’48.6” W, 1297 m above sea level), collected by Taucce, P. P. G., Lacerda, J. V., Guimarães, C. S., Moreira, L. S., and Feio, R. N. on 23 January 2014.

Paratypes.— All adult males. MZUFV 15712, Careço, municipality of Ervália, state of Minas Gerais, Brazil, collected by Taucce, P. P. G., Lisboa, B., and Guimarães, C. S. on 3 December 2014. UFMG 3285, Parque Estadual da Serra do Brigadeiro, municipality of Araponga, state of Minas Gerais, Brazil, collected by Garcia, P. C. A., Santos, P. S., and Taucce, P. P. G. in December 2009. UFMG 17078, Parque Nacional do Caparaó, municipality of Santa Marta, state of Espírito Santo, Brazil (20º29'25.2" S, 41º44'23.15" W, 1128 m above sea level), collected by Garcia, P. C. A. on 29 November 2014.

Referred specimens.— MZUFV 15575, juvenile, Trilha do Cruzeiro, Parque Estadual do Brigadeiro, Careço, municipality of Ervália, state of Minas Gerais, Brazil, collected by Feio, R. N., Assis, C. L., and Guimarães, C. S. on 18 September 2014.

Diagnosis.— In the *Ischnocnema guentheri* series by phylogenetic placement (Canedo and Haddad 2012, Fig. 1) and the following combination of characters: (1) long legs, tibia length > 60% of SVL; (2) one large, conspicuous, glandular appearing nuptial pad on Finger I; (3) dorsum smooth. *Ischnocnema feioi* is distinguished from all other species of the *I. guentheri* series by the following combination of characters: (1) calcar tubercle at least as long as wide in adult specimens; (2) medium size (SVL in males 20.7–23.6 mm, n = 4); (3) posterior surface of the thigh mottled; (4) canthus rostralis straight in dorsal view; (5) Finger I approximately the same size as Finger II; (6) advertisement call duration 1.54–5.51 s; (7) dominant frequency 2.53–3.23 kHz; (8) 10–27 notes per call; (9) note repetition rate of 4.13–6.19 notes/second; (10) note repetition rate acceleration of -26–21%.

Description of the holotype.— Medium size (SVL = 20.0 mm). Head longer than wide; head length 42% of SVL, head width 33% of SVL; snout sub-elliptical in dorsal view, rounded in lateral view; nostrils triangular, oriented laterally, located near the tip of the snout; canthus rostralis distinct, straight; loreal region slightly concave; postrictal tubercle present, v-shaped; eyes protuberant, oriented laterally; eye diameter 28% of head length; tympanum

distinct, rounded, tympanic membrane indifferentiated, annulus present, visible externally, tympanum diameter 40% of eye diameter; supratympanic fold absent; vocal slits present; vocal sac single, subgular, slightly expanded externally, with two oblique folds of skin on each margin of the throat; tongue large, heart-shaped, posterior notch absent; choanae rounded; dentigerous processes of the vomer located posteromedially to choanae, triangle shaped, medially separated by a gap approximately the width of one dentigerous process, teeth present, six on the right and five on the left dentigerous process.

Forelimbs slender; fingers slender, bearing discrete fringes, with small discs on fingers I and II, larger discs on fingers III and IV with a V-shaped median slit in dorsal view; Finger I approximately the same size as Finger II; finger lengths I ≈ II < IV < III; palmar tubercle heart-shaped, its diameter approximately equal to the diameter of the thenar tubercle; thenar tubercle elliptic; single nuptial pad apparently glandular, whitish, extending dorsaly from the distal to the proximal portion of the metacarpus on Finger I, divided ventraly on the distal margin of the thenar tubercle, extending all over its caudal third; palm smooth, with one barely distinguishible supernumerary tubercle towards Finger III; single subarticular tubercles prominent, rounded, and large.

Hind limbs slender; shank longer than thigh, tibia length 73% of SVL, thigh length 66% of SVL; calcar tubercle well-developed, cone-shaped, as long as wide on left leg, on right leg smashed against the heel; tarsal fold absent; toes long, slender, fringed, with large discs on toes II–V, which have a V-shaped median slit in dorsal view; small disc on Toe I; toe lengths I < II < III < V < IV; inner metatarsal tubercle elliptical, much larger than rounded outer metatarsal tubercle; sole of foot smooth; single large, prominent, and rounded subarticular tubercles.

458 Dorsal skin smooth, with a few sparse tubercles; upper eyelid with a few small, barely
459 distinguishible tubercles, one larger distinct tubercle on each side of the eyelids, positioned
460 medially; venter smooth; discoidal fold present; thoracic fold absent.
461 **Coloration of the holotype in preservative.—** Background grayish-white; dorsum
462 with medial clear whitish pinstripe from tip of snout to vent over two dark-brown spots, one
463 between eyes and other on the posterior fifth of snout, brown x-shaped mark on its second
464 third; yellowish-brown longitudinal mid-dorsal band from posterior fifth of snout to vent,
465 with four grayish-white blotches along it; head with dark-brown loreal stripe from tip of snout
466 to eyes, bordering canthus rostralis; lateral strip from right below eyes to upper lip; dark-
467 brown supratympanic stripe starting attympanum, contouring arm, and reaching abdomen at
468 mid-body; inguinal region with dark-brown spot; forelimbs variegated yellowish-brown to
469 brown with three dark brown blotches dorsally; palm of the hand cream with brown blotches;
470 dorsal portion of hind limbs variegated yellowish-brown to brown and feet with four dark-
471 brown blotches; sole of feet brown with cream blotches; ventral portion of forelimbs cream,
472 with some dark brown dots mainly on its posterior margin; hidden portion of thigh cream-
473 colored, mottled dark-brown; external portion of tibia with dark-brown longitudinal bar;
474 venter cream-colored; gular region cream-colored, with dark-brown margins and some small
475 dark-brown dot aggregations, and clear cream-colored stripe from tip of snout to end of
476 throat.
477 **Measurements of the holotype (in millimeters).—** SVL 22.0, head length 9.2, head
478 width 7.3, eye diameter 2.5, tympanum diameter 1.0, eye-nostril distance 2.6, internarial
479 distance 2.0, eye to eye distance 3.9, forearm length 4.6, hand length 6.9, third finger disk
480 length 0.9, thighlength 14.5, tibia length 16.1, tarsal length 7.5, foot length 15.6, fourth toe
481 disk length 0.9.

Variation.— One paratype had an ovoid tympanum. The supratympanic stripe does not reach the abdomen at mid-body in some specimens. The postrictal tubercle is elongated or absent in some specimens. Variation of measurements and body proportions are given in Table 4.

Etymology.— The specific epithet honors the Brazilian herpetologist Dr. Renato Neves Feio (Museu de Zoologia João Moojen de Oliveira, Universidade Federal de Viçosa, Minas Gerais, Brazil) for his substantial contributions to the study of the amphibians from Minas Gerais and to the conservation of the "Serra do Brigadeiro" [Brigadeiro Mountain Range] as well as his pleasant company during field work.

Advertisement call.— The advertisement call of *Ischnocnema feioi* (*n* = 31 calls of six males; Table 6; Fig. 3B) was composed of 10 to 27 notes ($\overline{X}$ = 19.06 ± 5.09), emitted sequentially, with the energy increasing in each note throughout the call, until reaching a peak near the end of the call. Call duration ranged from 1.54 to 5.51 s ($\overline{X}$ = 3.64 ± 1.24) and call rise time ranged from 79 to 100% ($\overline{X}$ = 97 ± 5) of the call. Note repetition rate was 4.13–6.19 notes/s ($\overline{X}$ = 5.20 ± 0.48) and note repetition rate acceleration ranged -26–21% ($\overline{X}$ = -3 ± 14). Dominant frequency was 2.53–3.23 kHz ($\overline{X}$ = 2.94 ± 0.20).

Comparison with other species.— The long legs (tibia length/SVL = 69–79%) distinguishes *I. feioi* from the species of the *I. lactea* (tibia length/SVL usually < 50%; Hedges et al. 2008), *I. parva* (tibia length/SVL < 60%; Hedges et al. 2008; Brusquetti et al. 2013), and *I. verrucosa* (tibia length/SVL < 55%; Hedges et al. 2008; Canedo et al. 2010, 2012) series and from *I. sambaqui* (tibia length/SVL < 55%; Castanho and Haddad 2000). The large and conspicuous, glandular-appearing nuptial pad on Finger I distinguishes *I. feioi* from the species of the *I. lactea* (minute nuptial pad in *I. randorum;* translucent in *I.* nigriventris and *I. vizottoi*; reduced to some white granules in *I. holti*; absent in *I. melanopygia* and *I. spanios*; unknown in other species; Heyer 1985; Hedges et al. 2008;

Targino and Carvalho-e-Silva 2008; Berneck et al. 2013) and *I. verrucosa* series (except for *I. surda*; faint, translucent nuptial pad in *I. karst*; absent in other species; Hedges et al. 2008; Canedo et al. 2010, 2012) and from *I. manezinho* and *I. sambaqui* (absent in these species; Garcia 1996; Castanho and Haddad 2000). The smooth dorsum differentiates *I. feioi* from the species of the *I. verrucosa* series (dorsum tuberculate in these species; Hedges et al. 2008; Canedo et al. 2010, 2012), *I. manezinho* (finelly tuberculate; Garcia 1996), and *I. sambaqui* (slightly rugose to rugose; Castanho and Haddad 2000).

Ischnocnema feioi differs from all species of the *I. guentheri* series, except for *I. oea* by having a calcar tubercle that is at least as long as it is wide in adult specimens (absent or not as long as wide in other species).

By its smaller body size, *I. feioi* (SVL in males 20.7–23.6 mm) differs from *I. izecksohni* (SVL in male 32.4 mm; Caramaschi and Kisteumacher 1989 "1988") and *I. nasuta* (SVL in males 24.7–41.5 mm; Heyer 1984). By its larger body size, *I. feioi* differs from *I. oea* (SVL in males 13.5–17.8 mm).

By the mottled posterior surface of the thighs *I. feioi* is distinguished from *I. erythromera* (*I. erythromera* with a light area on the posterior surface of the thigh in fixed specimens and red in life; Heyer 1984) and from *I. venancioi* (*I. venancioi* with clear spots surrounded by a dark background in fixed specimens and spots orange or yellow in life; B. Lutz 1958). Finger I being approximately the same size as Finger II also distinguishes *I. feioi* from *I. venancioi* (Finger I about half of the size of Finger II in *I. venancioi*). The straight *canthus rostralis* in dorsal view distinguishes *I. feioi* from *I. oea* (canthus rostralis curved in dorsal view in this species).

Advertisement call duration (1.54–5.51 s) distinguishes *I. feioi* from *I. guentheri* (26.30–41.90 s; Gehara et al. 2013), *I. henselii* (10.00–23.00 s; Gehara et al. 2013), and *I. nasuta* (1.15–1.50 s; Heyer 1984). *Ischnocnema feioi* emits more notes per call (10–27) than *I.*

gualteri (4–9; Heyer 1984) and less notes per call than *I. guentheri* (71–146; Gehara et al. 2013), *I. henselii* (86–170; Gehara et al. 2013), *I. izecksohni* (34–60; Taucce et al. 2012), and *I. nasuta* (34–43, Heyer 1984). Note repetition rate distinguishes *I. feioi* (4.13–6.19 notes/s) from *I. guentheri* (2.20–3.50 notes/s; Gehara et al. 2013), *I. henselii* (6.60–7.10 notes/s; Gehara et al. 2013), and *I. izecksohni* (29.91–31.10 notes/s; Taucce et al. 2012) and note repetition rate acceleration distinguishes *I. feioi* (-26–21%) from *I. guentheri* (31–121%; Gehara et al. 2013) and *I. henselii* (107–125%; Gehara et al. 2013).

Geographic distribution.— *Ischnocnema feioi* is known only from the Serra do Brigadeiro, in the municipalities of Araponga, Muriaé, and Ervália, state of Minas Gerais, Brazil, and from the Caparaó National Park, municipality of Santa Marta, state of Espírito Santo, Brazil (Fig. 6), at elevations over 1000 m above sea level.

Remarks.— Figure 2d from Moura et al. (2012) corresponds to paratype UFMG 3285 of *Ischnocnema feioi*, although the specimen is not in their examined material list. All examined specimens have a clear cream-colored ventral stripe from the tip of the snout to the end of the throat on a dark brown background. Although it is not a common trait in the *I. guentheri* series, we did not use it as a diagnostic character because some *I. oea* and *I. izecksohni* exemplars possess the same pattern.

Ischnocnema ***garciai*** sp. nov.

Figs. 4C, 8

Ischnocnema sp.: (Santana et al. 2010: 2 [their Table 1], 3 [their Fig. 2C], 4, 10 [their Appendix 1]).

Ischnocnema oea (Heyer 1984): Mângia et al. (2011:164 [their Fig. 1], 165), [misidentification]).

Holotype.— CFBH 39028, adult male. Usina da Fumaça, municipality of Muriaé, state of Minas Gerais, Brazil (21°0'57.6" S, 42°26'36.6 W, 430 m above sea level), collected by Taucce, P. P. G. and Lisboa, B. on 30 November 2014.

Paratopotypes.— CFBH 39026–39027, 39029–39033, MNRJ 90703–90704 (adult males), all collected with the holotype. UFMG 18889 (adult male), collected by Taucce, P. P. G., Pezzini, F. F., Hatori, E. K. O., and Neves, D. M. on 18 January 2014. UFMG 18890 (adult male), collected by Taucce, P. P. G. and Lisboa, B. on 29 November 2014. MZUFV 8894–8895 (adult females) and MZUFV 8896–8899 (adult males) collected by Santana, D. J. and Silva, E. T. on 13 September 2008.

Referred specimens.— MZUFV 8900, juvenile, Usina da Fumaça, municipality of Muriaé, state of Minas Gerais, Brazil, collected by Santana, D. J. and Silva, E. T. on 13 September 2008.

Diagnosis.— In the *Ischnocnema guentheri* series by phylogenetic placement (Canedo and Haddad 2012, Fig. 1) and the following combination of characters: (1) long legs, tibia length > 60% of SVL; (2) one large, conspicuous, glandular appearing nuptial pad on Finger I; (3) dorsum smooth. *Ischnocnema garciai* is distinguished from all other species of the *I. guentheri* series by the following combination of characters: (1) calcar tubercle at least as long as wide in adult specimens; (2) small size (SVL in males 13.3–18.5 mm, n = 16; SVL in females 21.9–24.7 mm, n = 2); (3) posterior surface of thigh mottled; (4) canthus rostralis concave in dorsal view; (5) Finger I approximately the same size as Finger II; (6) advertisement call duration 14.84–29.11 s; (7) dominant frequency 3.27–3.88 kHz; (8) 57–96 notes per call; (9) note repetition rate of 3.27–4.47 notes/s; (10) note repetition rate acceleration of 5–198%.

Description of the holotype.— Small size (SVL = 17.1 mm). Head longer than wide; head length 43% of SVL, head width 37% of SVL; snout rounded in dorsal and lateral views; nostrils rounded, oriented laterally, located near the tip of the snout; canthus rostralis moderately distinct, curved; loreal region slightly concave; postrictal tubercle present, slightly distinct; eyes protuberant and laterally oriented, eye diameter 28% of head length; tympanum distinct, rounded, tympanic membrane indifferentiated, annulus present, visible externally, tympanum diameter 48% of eye diameter; supratympanic fold absent; vocal slits present; vocal sac single, subgular, slightly expanded externally, with a longitudinal fold of skin from the posterior part to half of the throat, on both sides; tongue large, heart-shaped, posterior notch absent; choanae elliptical; dentigerous processes of the vomer located posteromedially to choanae, triangle shaped, medially separated by a gap approximately the width of one dentigerous process, teeth present, six on the right an seven on the left dentigerous process.

Forelimbs slender; fingers slender, bearing discrete fringes, with small discs on fingers I and II, larger discs on fingers III and IV with a V-shaped median slit in dorsal view; finger lengths I ≈ II < IV < III; palmar tubercle heart-shaped, its diameter approximately equal to thenar tubercle; thenar tubercle elliptic; single nuptial pad apparently glandular, conspicuous, extending dorsaly from the distal to the proximal portion of the metacarpus on Finger I, divided ventraly on the distal margin of the thenar tubercle, extending all over its caudal third; palm smooth, with one barely distinguishible supernumerary tubercle; single subarticular tubercles prominent, rounded, and large.

Hind limbs slender; shank longer than thigh, tibia length 70% of the SVL, thigh length 60% of SVL; calcar tubercle well-developed, cone-shaped, as long as wide; tarsal fold absent; toes long, slender, fringed, with large discs on toes II–V, which have a V-shaped median slit in dorsal view; small disc on toe I; toe lengths I < II < III = V < IV; inner metatarsal tubercle

elliptical, much larger than the rounded outer metatarsal tubercle; sole of the foot smooth, with one supernumerary tubercle; single large, prominent, and rounded subarticular tubercles.

Dorsal skin smooth; upper eyelid with a few barely distinguishible pointed tubercles and one distinct tubercle on each eyelid margin, positioned medially; venter smooth, with no tubercles; discoidal fold present; thoracic fold absent.

Coloration of the holotype in preservative.— Background variegated, predominantly light-brown, with brown and grayish-white details; dorsum with medial clear whitish pinstripe from tip of snout to vent, with barely distinguishible x-shaped brown mark on itssecond third; head brown with light-brown interocular bar and light-brown spot bordered by two dark-brown spots on tip of snout; dark-brown loreal stripe from tip of snout to eyes, bordering *canthus rostralis*; dark-brown lateral strip from right below eyes to upper lip; dark-brown supratympanic stripe starting at tympanum, contouring arm, and reaching abdomen at mid-body; inguinal region with dark-brown spot; forelimbs variegated of brown with light-brown with two dark-brown blotches dorsally; palm of the hand brown and cream-colored; dorsal portion of hind limbs striped with brown and light-brown alternately; dorsal surface of feet with three dark-brown blotches; sole of feet brown; ventral portion of forelimbs cream-colored, with some dark brown dots mainly on posterior margin; hidden portion of the thigh cream-colored, mottled dark-brown; external portion of tibia with dark-brown longitudinal bar; venter cream-colored with some aggregations of brown dots on thorax; gular region cream-colored with brown dots spread throughout.

Measurements of the holotype (in millimeters).— SVL 17.1, head length 7.4, head width 6.3, eye diameter 2.0, tympanum diameter 1.0, eye–nostril distance 1.7, internarial distance 1.6, eye to eye distance 3.2, forearm length 3.7, hand length 5.0, third finger disk length 0.4 , thigh length 10.3, tibia length 12.0, tarsal length 5.6, foot length 10.7, fourth toe disk length 0.7.

630 **Variation.—** One male specimen and the two female specimens had a sub-elliptical
631 snout in dorsal view. Nostril shape was also triangular, elliptical, and ovoid. Tympanum was
632 elliptic in two specimens and the postrictal tubercle could also be absent. The supratympanic
633 stripe does not reach the abdomen at mid-body in some specimens. Shape of the choanae
634 varied between rounded and elliptical. Toe III could be slightly smaller or slightly larger than
635 Toe V. Female specimens (SVL 21.9–24.7 mm, *n* = 2) were considerably larger than male
636 specimens (SVL 13.3–18.5 mm, *n* = 16). Variation of measurements and body proportions
637 are given in Table 4.
638 **Etymology.—** The specific epithet honors the Brazilian herpetologist Dr. Paulo C. A.
639 Garcia (Laboratório de Herpetologia, Departamento de Zoologia, Universidade Federal de
640 Minas Gerais, Belo Horizonte, Minas Gerais, Brazil) for his important contributions to the
641 knowledge of the genus *Ischnocnema* and the amphibians of the Atlantic Forest and in
642 gratitude for his substantial contribution to the academic education of the first author of this
643 paper.
644 **Advertisement call.—** The advertisement call of *Ischnocnema garciai* (*n* = 12 calls of
645 four males; Table 7; Fig. 3C) is composed of 57 to 96 notes ($\overline{X}$ = 79.25 ± 9.09), emitted
646 sequentially, with the the energy increasing in each note throughout the call, until reaching a
647 peak typically at the beginning of the last third of the call. Most calls (ca. 80%) gradually
648 decreased the energy until the end of the call after reaching the peak. Call duration ranged
649 from 14.84 to 29.11 s ($\overline{X}$ = 19.50 ± 3.47) and call rise time ranged from 45 to 92% ($\overline{X}$ = 71 ±
650 14) of the call. Note repetition rate was 3.27–4.47 notes/s ($\overline{X}$ = 4.06 ± 0.35) and note
651 repetition rate acceleration ranged 5–198% ($\overline{X}$ = 75 ± 51). Dominant frequency was 3.27–
652 3.88 kHz ($\overline{X}$ = 3.40 ± 0.16).
653 **Comparison with other species.—** The long legs (tibia length/SVL = 64–72%)
654 distinguish *I. garciai* from the species of the *I. lactea* (tibia length/SVL usually < 50%;

Hedges et al. 2008), *I. parva* (tibia length/SVL < 60%; Hedges et al. 2008; Brusquetti et al. 2013), and *I. verrucosa* (tibia length/SVL < 55%; Hedges et al. 2008; Canedo et al. 2010, 2012) series and from *I. sambaqui* (tibia length/SVL < 55%; Castanho and Haddad 2000). The large and conspicuous, glandular-appearing nuptial pad on Finger I distinguishes *I. feioi* from the species of the *I. lactea* (minute nuptial pad in *I. randorum;* translucent in *I.* nigriventris and *I. vizottoi*; reduced to some white granules in *I. holti*; absent in *I. melanopygia* and *I. spanios*; unknown in other species; Heyer 1985; Hedges et al. 2008; Targino and Carvalho-e-Silva 2008; Berneck et al. 2013) and *I. verrucosa* series (except for *I. surda*; faint, translucent nuptial pad in *I. karst*; absent in other species; Hedges et al. 2008; Canedo et al. 2010, 2012) and from *I. manezinho* and *I. sambaqui* (absent in these species; Garcia 1996; Castanho and Haddad 2000). The smooth dorsum distinguishes *I. garciai* from the species of the *I. verrucosa* series (dorsum tuberculate in these species; Hedges et al. 2008; Canedo et al. 2010, 2012), *I. manezinho* (finelly tuberculate; Garcia 1996), and *I. sambaqui* (slightly rugose to rugose; Castanho and Haddad 2000).

Ischnocnema garciai differs from all species of the *I. guentheri* series, except for *I. oea* and *I. feioi*, by its calcar tubercle being at least as long as it is wide in adult specimens (absent or not as long as wide in other species).

By its smaller body size, *I. garciai* (SVL in males 13.3–18.5 mm; females 21.9–24.7 mm) differs from *I. erythromera* (SVL in males 22.3–24.4 mm; females 24.3–35.3 mm; Heyer 1984), *I. feioi* (SVL in males 20.7–23.6 mm), *I. gualteri* (SVL in males 21.3–34.1 mm; females 33.6–45.7 mm; Heyer 1984), *I. henselii* (SVL in males 21.0–27.5 mm; females 28.4–38.4 mm; Kwet and Solé 2005), *I. izecksohni* (SVL in male 32.4 mm; females 43.5–49.0 mm; Caramaschi and Kisteumacher 1989 “1988”) and *I. nasuta* (SVL in males 24.7–41.5 mm; females 36.1–53.9 mm; Heyer 1984).

By the mottled posterior surface of the thighs *I. garciai* is distinguished from *I. erythromera* (*I. erythromera* with a light area on the posterior surface of the thigh in fixed specimens and red in life; Heyer 1984) and from *I. venancioi* (*I. venancioi* with clear spots surrounded by a dark background in fixed specimens and spots orange or yellow in life; B. Lutz 1958). Finger I being approximately the same size as Finger II also distinguishes *I. garciai* from *I. venancioi* (Finger I smaller than Finger II in *I. venancioi*). The concave *canthus rostralis* in dorsal view distinguishes *I. garciai* from *I. feioi*, *I. hoehnei, I. izecksohni*, *I. nasuta*, and *I. venancioi* (canthus rostralis straight in dorsal view in these species).

Advertisement call duration (14.84–29.11 s) distinguishes *I. garciai* from *I. feioi* (1.54–5.51 s), *I. izecksohni* (1.03–2.15 s; Taucce et al. 2012), *I. nasuta* (1.15–1.50 s; Heyer 1984), and *I. oea* (4.56–8.49 s; Hepp and Canedo 2013). *Ischnocnema garciai* emits more notes per call (57–96) than *I. feioi* (10–27), *I. gualteri* (4–9; Heyer 1984), *I. oea* (25–42; Hepp and Canedo 2013), and *I. nasuta* (34–43; Heyer 1984). The higher dominant frequency (3.27–3.88 kHz) distinguishes *I. garciai* from *I. feioi* (2.53–3.23 kHz), *I. gualteri* (2.10–2.70 kHz; Heyer 1984), *I. henselii* (2.10–3.10 kHz; Gehara et al. 2013), *I. izecksohni* (2.25–2.63 kHz; Taucce et al. 2012), and *I. nasuta* (2.10–2.60 kHz; Heyer 1984). Note repetition rate distinguishes *I. garciai* (3.27–4.47 notes/s) from *I. henselii* (6.60–7.10 notes/s; Gehara et al. 2013), *I. izecksohni* (29.91–31.10 notes/s; Taucce et al. 2012), and *I. oea* (4.80–5.70 notes/s; Hepp and Canedo 2013).

Geographic distribution.— *Ischnocnema garciai* is known only from the type locality at Usina da Fumaça, municipality of Muriaé, state of Minas Gerais, Brazil (Fig. 6).

Remarks.— Except for advertisement call characters, we are not aware of any phenotypic~~al~~ difference between *Ischnocnema garciai* and *I. oea*, its sister species.

DISCUSSION

Tree Topology and Genetic Distance

Unlike Canedo and Haddad (2012), we recovered the *Ischnocnema guentheri* series as poorly supported (61% of posterior probability and 55% of maximum likelihood bootstrap). This may be a result of the addition of *I. nanahallux* Brusquetti et al. 2013, because the two terminals representing this species in our tree had only the final portion of the 16S r RNA (600 bp) available, which represented only 16.7% of our final alignment. On the other hand, other *Ischnocnema* series and their phylogenetic relationships were recovered with high support, including the *I. guentheri* + *I. parva* series (100% of posterior probability and 93% of maximum likelihood bootstrap).

Fouquet et al. (2007) suggested a mean distance of 3% for 16S rDNA to identify Neotropical anuran species. Our results show a genetic distance well above this threshold among almost all examined specimens, including those of *Ischnocnema oea, I. feioi*, and *I. garciai* (Table 3). The only exception is low distance between *I. nasuta* and *I. izecksohni* (1.2–1.9%). Although some authors have discussed the difficulties associated with using genetic distance thresholds to identify species (Padial et al. 2009), arguing that in some cases two distinct species may have a genetic distance as low as 0.0% in partial 16S rDNA (Blotto et al. 2013), the status of *I. nasuta* and *I. izecksohni* is remarkable, because the distance between them is less than the distance within *I. nasuta* itself. Since there are no known morphological characters distinguishing *I. izecksohni* and *I. nasuta* (Taucce et al. 2012), they may indeed be a single species. However, a study taking into account molecular and bioacoustical data from the type locality of *I. nasuta* (in Nova Friburgo, state of Rio de Janeiro, Brazil; A. Lutz 1925) and from throughout a greater part of the known distribution of the two species is necessary to make any taxonomic decision about their validity.

729

730 The *Ischnocnema guentheri* Series

731

732 Heyer (1984) proposed some diagnostic characters for what he called the *Ischnocnema*
733 *guentheri* cluster, including a smooth dorsum, white glandular-appearing nuptial pads and a
734 noticeable calcar tubercle. Hedges et al. (2008) excluded the presence of a calcar tubercle and
735 the nuptial pads, which they said were absent from *I. hoehnei* and unknown in other species of
736 the *I. guentheri* series, and proposed a few other characters, such as an acuminate snout in
737 dorsal view and Finger I approximately the same length as Finger II. Canedo et al. (2010)
738 maintained this diagnosis and reincluded the presence of a nuptial pad. Canedo and Haddad
739 (2012) excluded *I. vinhai* (= *Pristimantis vinhai*) and included *I. venancioi* in the *I. guentheri*
740 series, and even with the inclusion of the latter (which was in the *I. lactea* series) they
741 retained the character of having long legs (tibia length > 60%). Herein, we reformulate the
742 diagnosis to include only characters shared by all members of the current *I. guentheri* series,
743 including *I. epipeda*, *I. erythromera, I. feioi, I. garciai, I. gualteri, I. guentheri, I. henselii, I.*
744 *hoehnei, I. izecksohni, I. nasuta, I. oea,* and *I. venancioi*: (1) long legs, tibia length > 60% of
745 SVL; (2) large, whitish, glandular appearing, nuptial pads; and (3) dorsum smooth.
746 Heyer (1984) was the first to propose a group including the former *Eleutherodactylus*
747 *guentheri* (= *I. guentheri*) similar to the current *I. guentheri* series (see Introduction). Among
748 the characters shared by all species in his cluster was a calcar tubercle on the heel and white
749 glandular-appearing nuptial pads. At the time, Heyer (1984) considered only
750 presence/absence character states, and although we have not noticed any remarkable
751 difference in the nuptial pads of members of the *I. guentheri* series, we have found that the
752 calcar tubercle is more developed in the clade containing *I. oea, I. feioi,* and *I. garciai*. Thus,
753 we consider the character of having a calcar tubercle that is at least as long as it is wide a

putative synapomorphy for this clade. Even though the development of the calcar tubercle is somewhat variable within the other species of the series, we also noted it is variable among species (Fig. 2), and is worthy of further investigation among members of the *I. guentheri* series. The only species lacking the calcar tubercle is *I. venancioi*.

In agreement with previous phylogenetic studies (Hedges et al. 2008; Canedo and Haddad 2012; Padial et al. 2014 [except by the tree-alignment + parsimony tree]), we recovered a clade including the *Ischnocnema guentheri* and the *I. parva* series. Despite important differences between the two series (see results); there are a few important morphological features they share that may reinforce their close relationship.

Brusquetti et al. (2013) noted a well-developed calcar tubercle in *I. nanahallux,* and stated that this feature is absent in *I. pusilla* and may be present or absent in *I. parva.* With exception of *I. venancioi*, all other members of the *I. guentheri* series possess the calcar tubercle. Also, *I. parva* and *I. pusilla* possess a large, whitish glandular-appearing nuptial pad, just like that of the members of the *I. guentheri* series. Nuptial pads are also present in *I. surda* (Canedo et al. 2010) and *I. karst* (faint, translucent in this species; Canedo et al. 2012) from the *I. verrucosa* series and in *I. randorum* (minute in this species; Hedges et al. 2008) from the *I. lactea* series. Further study of the morphology and the evolution of these characters within *Ischnocnema* is necessary in order to evaluate the homology of these characters between the *I. guentheri* and the *I. parva* series.

As a result of the present work, we have raised the number of species of the *I. guentheri* series to 12. Although *I. feioi* is easily distinguishable from all other closely related species, *I. garciai* and *I. oea* seem to be morphologically cryptic species (see Bickford et al. 2007 for a cryptic species concept). The last *Ischnocnema* from the *I. guentheri* series described based only on morphological characters was *I. izecksohni* (Caramaschi and Kisteumacher 1989 “1988”). A few years later, Kwet and Solé (2005) resurrected *I. henselii*

779 from the synonym of *I. guentheri*, based mainly on bioacoustical characters, and later on
780 some species had their advertisement calls described (Taucce et al. 2012; Gehara et al. 2013;
781 Hepp and Canedo 2013). Gehara et al. (2013) also assessed molecular data throughout the
782 geographic distribution of *I. guentheri* and *I. henselii* and concluded that *I. guentheri* is a
783 species complex. In agreement with these recent studies involving the *I. guentheri* series, our
784 results show that integrating different datasets is of paramount importance for evaluating the
785 species limits within the series.

786 **Acknowledgments.—** We thank H. Q. Boudet (MBML), R. N. Feio (MZUFV), P. C.
787 A. Garcia (UFMG), J. P. Pombal Jr (MNRJ), and K. de Queiroz (USNM) for making
788 available material under their care. For support at the MNRJ we thank P. Pinna and M. W.
789 Cardoso, at UFMG we thank S. Velasquez, and at USNM we thank A. Wynn. M. L. Lyra
790 helped with laboratory procedures. M. T. T. Santos took pictures of some specimens. E. R.
791 Wild made English review. We are grateful to Centro de Estudos de Insetos Sociais (CEIS;
792 São Paulo State University [UNESP]) for allowing us the use of the molecular laboratory. D.
793 M. Neves, F. F. Pezzini, E. K. O. Hatori, B. Lisboa, A. C. Sant'Anna, C. S. Guimarães, J. V.
794 Lacerda, R. N. Feio, P. S. Santos, and L. S. Moreira gave field assistance. D. J. Santana gave
795 some GPS coordinates of the species locations and R. Collins helped with package SPIDER.
796 This research was supported by resources supplied by the Center for Scientific Computing
797 (NCC/GridUNESP) of the UNESP and Cyberinfrastructure for Phylogenetic Research
798 (CIPRES). R. N. Feio and L. S. Moreira allowed collecting on their private properties. CNPq
799 proc#14/2013 financed the stereomicroscope used for the photos of the *I. oea* holotype. P. P.
800 G. T. thanks São Paulo Research Foundation (FAPESP), grant #2014/05772-4, Conselho
801 Nacional de Desenvolvimento Científico e Tecnológico (CNPq), and Coordenação de
802 Aperfeiçoamento de Pessoal de Nível Superior (CAPES) for the PhD fellowship and financial
803 support and Instituto Chico Mendes de Conservação da Biodiversidade (ICMBio) for

collection permits (#42108). C. C. thanks Fundação Carlos Chagas Filho de Amparo à Pesquisa do Estado do Rio de Janeiro (FAPERJ), grant E-26/102.818/2011, for financial support. C. F. B. H. thanks FAPESP grant #2013/50741-7 and CNPq for financial support.

LITERATURE CITED

Almeida-Gomes, M., M. Almeida-Santos, P. Goyannes-Araújo, ... C.F.D. Rocha. 2010. Anurofauna of an Atlantic Rainforest fragment and its surroundings in Northern Rio de Janeiro State, Brazil. Brazilian Journal of Biology 70:871–877.

Berneck, B.M., M. Targino and P.C.A. Garcia. 2013. Rediscovery and re-description of *Ischnocnema nigriventris* (Lutz, 1925) (Anura: Terrarana: Brachycephalidae). Zootaxa 3692:131–142.

Bickford, D., D.J. Lohman, N.S. Sodhi, P.K.L Ng, R. Meier, K. Winker, K.K. Ingram and I. Das. 2007. Cryptic species as a window on diversity and conservation. Trends in Ecology and Evolution 22:148–155.

Bioacoustics Research Program. 2011. Raven Pro: Interactive Sound Analysis Software. Ithaca, NY: The Cornell Lab of Ornithology. http://www.birds.cornell.edu/raven

Blotto, B. L., J.J. Nuñez, N.G. Basso, C.A. Úbeda, W.C. Wheeler and J. Faivovich. 2013. Phylogenetic relationships of a Patagonian frog radiation, the *Alsodes* + *Eupsophus* clade (Anura: Alsodidae), with comments on the supposed paraphyly of *Eupsophus*. Cladistics 29:113–131.

Bokermann, W.C.A. 1965. A new *Eleutherodactylus* from Southeastern Brazil. Copeia 1965:440–441.

Bokermann, W.C.A. 1975 “1974”. Três espécies novas de *Eleutherodactylus* do sudeste da Bahia, Brasil (Anura, Leptodactylidae). Revista Brasileira de Biologia 34:11–18.

829 Bossuyt, F., and M.C. Milinkovitch. 2000. Convergent adaptive radiations in Madagascan and
830 Asian ranid frogs reveal covariation between larval and adult traits. Proceedings of the
831 National Academy of Sciences of the United States of America 97:6585–6590.

832 Brown, S.D.J., R.A. Collins, S. Boyer, M.C. Lefort, J. Malumbres-Olarte, C. Vink, and R.H.
833 Cruickshank. 2012. Spider: An R package for the analysis of species identity and
834 evolution, with particular reference to DNA barcoding. Molecular Ecology Resources
835 12:562–565.

836 Brusquetti, F., M.T.C. Thomé, C. Canedo, T.H. Condez and C.F.B. Haddad. 2013. A new
837 species of *Ischnocnema parva* species series (Anura, Brachycephalidae) from Northern
838 State of Rio De Janeiro, Brazil. Herpetologica 69: 175–185.

839 Canedo, C., and C.F.B. Haddad. 2012. Phylogenetic relationships within anuran clade
840 Terrarana, with emphasis on the placement of Brazilian Atlantic rainforest frogs genus
841 *Ischnocnema* (Anura: Brachycephalidae). Molecular Phylogenetics and Evolution
842 65:610–620.

843 Canedo, C., B.V.S Pimenta, F.S.F. Leite and U. Caramaschi,.2010. New species of
844 *Ischnocnema* (Anura: Brachycephalidae) from the State of Minas Gerais, Southeastern
845 Brazil, with comments on the *I. verrucosa* species series. Copeia 2010:629–634.

846 Canedo, C., M. Targino, F.S.F. Leite and C.F.B. Haddad. 2012. A new species of
847 *Ischnocnema* (Anura) from the São Francisco basin Karst Region, Brazil. Herpetologica
848 68:393–400.

849 Caramaschi, U., and G. Kisteumacher. 1989 “1988”. A new species of *Eleutherodactylus*
850 (Anura : Leptodactylidae) from Minas Gerais , Southeastern Brazil. Herpetologica
851 44:423–426.

852 Castanho, L.M., and C.F.B. Haddad. 2000. New species of *Eleutherodactylus* (Amphibia :
853 Leptodactylidae) from Guaraqueçaba, Atlantic Forest of Brazil. Copeia 2000:777–781.

854 Cochran, D.M. 1948. A new subspecies of frog from Itatiaya, Brazil. American Museum
855 Novitates 1375:1–3.
856 Cocroft, R., and M.J. Ryan. 1995. Patterns of advertisement call evolution in toads and chorus
857 frogs. Animal Behaviour 49:283–303.
858 Cope, E.D. 1862. On some new and little known American Anura. Proceedings of the
859 Academy of Natural Sciences of Philadelphia 14:151–159.
860 Duellman, W.E., and E. Lehr. 2009. Terrestrial-Breeding Frogs (Strabomantidae) in Peru.
861 Natur und Tier - Verlag GmbH, Germany.
862 Dumeril, A.M.C., and G. Bibron. 1841. Erpétologie Générale ou Histoire Naturelle Complète
863 des Reptiles. Tome Huitième. Librarie Enclyclopedique de Roret, France.
864 Feller, A.E., and S.B. Hedges. 1998. Molecular evidence for the early history of living
865 amphibians. Molecular Phylogenetics and Evolution 9:509–516.
866 Fitzinger, L.J.F.J. 1826. Neue Classification der Reptilien Nach Ihren Natürlichen
867 Verwandtschaften : Nebst Einer Verwandtschafts-Tafel und Einem Verzeichnisse der
868 Reptilien-Sammlung des K. K. Zoologischen Museum's zu Wien. Isis Von Oken. J. G.
869 Heubner, Austria.
870 Fouquet, A., A. Gilles, M. Vences, C. Marty, M. Blanc and N.J. Gemmell. 2007.
871 Underestimation of species richness in neotropical frogs revealed by mtDNA analyses.
872 PLoS ONE 2: e1109.
873 Frost, D.R. 2016. Amphibian Species of the World: an Online Reference. American Museum
874 of Natural History, USA. Available at
875 http://research.amnh.org/herpetology/amphibia/index.html. Archived by WebCite at
876 http://www.webcitation.org/6mBxOq4NO on 21 November 2016.
877 Garcia, P.C.A. 1996. Nova espécie de *Eleutherodactylus* Duméril & Bibron, 1891 (Amphibia,
878 Anura, Leptodactylidae) do estado de Santa Catarina, Brasil. Biociências 4:57–68.

879 Gehara, M., C. Canedo, C.F.B. Haddad and M. Vences. 2013. From widespread to
880 microendemic: Molecular and acoustic analyses show that *Ischnocnema guentheri*
881 (Amphibia: Brachycephalidae) is endemic to Rio de Janeiro, Brazil. Conservation
882 Genetics 14:973–982.
883 Gelman, A., and D.B. Rubin. 1992. Inference from iterative simulation using multiple
884 sequences. Statistical Science 7:457–472.
885 Goebel, A.M., J.M. Donnelly and M.E. Atz, M. E. 1999. PCR primers and amplification
886 methods for 12S ribosomal DNA, the control region, cytochrome oxidase I, and
887 cytochrome b in bufonids and other frogs, and an overview of PCR primers which have
888 amplified DNA in amphibians successfully. Molecular Phylogenetics and Evolution
889 11:163–199.
890 Graybeal, A. 1997. Phylogenetic relationships of bufonid frogs and tests of alternate
891 macroevolutionary hypotheses characterizing their radiation. Zoological Journal of the
892 Linnean Society 119:297–338.
893 Günther, A. 1858. On the systematic arrangement of the tailless batrachians and the structure
894 of *Rhinophrynus dorsalis*. Proceedings of the Zoological Society of London 26:339–
895 352.
896 Hedges, S.B. 1994. Molecular evidence for the origin of birds. Proceedings of the National
897 Academy of Sciences of the United States of America 91:2621–2624.
898 Hedges, S.B., W.E. Duellman and M.P. Heinicke. 2008. New World direct-developing frogs
899 (Anura: Terrarana): Molecular phylogeny, classification, biogeography, and
900 conservation. Zootaxa 1737:1–182.
901 Heinicke, M. P., W.E. Duellman and S.B. Hedges. 2007. Major Caribbean and Central
902 American frog faunas originated by ancient oceanic dispersal. Proceedings of the
903 National Academy of Sciences of the United States of America 104:10092–10097.

Hepp, F., and C. Canedo. 2013. Advertisement and aggressive calls of *Ischnocnema oea* (Heyer, 1984) (Anura, Brachycephalidae). Zootaxa 3710:197–199. DOI: http://dx.doi.org/10.11646/zootaxa.3710.2.6

Heyer, W.R. 1969. Studies on the genus *Leptodactylus* (Amphibia, Leptodactyldae) III. A redefinition of the genus *Leptodactylus* and a description of a new genus of Leptodactylid frogs. Los Angeles County Museum Contributions in Science 155:1–14.

Heyer, W.R. 1984. Variation, systematics, and zoogeography of *Eleutherodactylus guentheri* and closely related species (Amphibia: Anura: Leptodactylidae). Smithsonian Contributions to Zoology 40:21−42.

Heyer, W.R. 1985. New species of frogs from Boracéia, São Paulo, Brazil. Proceedings of the Biological Society of Washington 98:657–671.

Heyer, W.R., A.S. Rand, C.A.G. Cruz, O.L. Peixoto and C.E. Nelson. 1990. Frogs of Boraceia. Arquivos de Zoologia 31:235–410.

Hurvich, C., and C. Tsai. 1989. Regression and time series model selection in small samples. Biometrika 76:297–307.

Jiménez de la Espada, M. 1870. Fauna neotropicalis species quaedam nondum cognitae. Jornal de Sciências, Mathemáticas, Physicas e Naturaes 3:57–65.

Katoh, K., and D.M. Standley. 2013. MAFFT multiple sequence alignment software version 7: Improvements in performance and usability. Molecular Biology and Evolution 30:772–780.

Kwet, A., and M. Solé. 2005. Validation of *Hylodes henselii* Peters, 1870, from Southern Brazil and Description of Acoustic Variation in *Eleutherodactylus guentheri* (Anura: Leptodactylidae). Journal of Herpetology 39:521–532.

Lanfear, R., B. Calcott, S.Y.W. Ho and S. Guindon. 2012. PartitionFinder: Combined selection of partitioning schemes and substitution models for phylogenetic analyses.

929 Molecular Biology and Evolution 29:1695–1701.
930 Ligges, U., S. Krey, O. Mersman, and S. Schnackenberg. 2013. tuneR: Analysis of music.
931 URL: http://r-forge.r-project.org/projects/tuner/
932 Lutz, A. 1925. Batraciens du Brésil. Comptes Rendus et Mémoires Hebdomadaires des
933 Séances de la Société de Biologie et des ses Filiales 22:211–214.
934 Lutz, B. 1958. Anfíbios novos e raros das Serras Costeiras do Brasil: *Eleutherodactylus*
935 *venancioi* n.sp., *E. hoehnei* n.sp., *Holoaden bradei* n.sp. e *H. lüderwaldti* Mir. Rib.,
936 1920. Memórias do Instituto Oswaldo Cruz 56:372–389.
937 Lutz, B. 1974. *Eleutherodactylus gualteri*, a new species from the Organ Mountains of Brazil.
938 Journal of Herpetology 8:293–295.
939 Lynch, J.D. 1976. The species groups of South American frogs of the genus
940 *Eleutherodactylus* (Leptodactylidae). Occasional papers of the Museum of Natural
941 History of the University of Kansas 61:1–24.
942 Lynch, J.D., and W.E. Duellman. 1997. Frogs of the genus *Eleutherodactylus* in Western
943 Ecuador biogeography. Special Publication of the Natural History Museum, The
944 University of Kansas 23:1–236.
945 Mângia, S., E.T. da Silva, A.C. Sant'Anna, and D.J. Santana. 2011. Amphibia, Anura,
946 Brachycephalidae, *Ischnocnema oea* (Heyer, 1984): Distribution extension, new state
947 record and geographic distribution map. Checklist 7:164–165. DOI:
948 https://doi.org/10.15560/7.2.164
949 Maniatis, T., E.F. Fritsch and J. Sambrook .1982. Molecular Cloning: A Laboratory Manual.
950 Cold Spring Harbour Laboratory, USA.
951 Martins, I.A., and C.F.B. Haddad. 2010. A new species of *Ischnocnema* from highlands of the
952 Atlantic Forest, Southeastern Brazil (Terrarana, Brachycephalidae). Zootaxa 2617:55–
953 65.

954 Moura, M.R., A.P. Motta, V.D. Fernandes and R.N. Feio. 2012. Herpetofauna da Serra do
955 Brigadeiro, um remanescente de Mata Atlântica em Minas Gerais, sudeste do Brasil.
956 Biota Neotropica 12:209–235.
957 Padial, J.M., S. Castroviejo-Fisher, J. Köhler, E. Domic and I. De la Riva .2007. Systematics
958 of the *Eleutherodactylus fraudator* species group (Anura: Brachycephalidae).
959 Herpetological Monographs 21:213–240.
960 Padial, J.M., S. Castroviejo-Fisher, J. Köhler, C. Vilà, J.C. Chaparro and I. De La Riva. 2009.
961 Deciphering the products of evolution at the species level: The need for an integrative
962 taxonomy. Zoologica Scripta 38:431–447.
963 Padial, J. M., T. Grant and D.R. Frost. 2014. Molecular systematics of terraranas (Anura:
964 Brachycephaloidea) with an assessment of the effects of alignment and optimality
965 criteria. Zootaxa 3825:1–132. DOI: http://dx.doi.org/10.11646/zootaxa.3825.1.1
966 Palumbi, S. R., A.P. Martin, B.D. Kessing and W.O. McMillan. 1991. Detecting population
967 structure using mitochondrial DNA. Pp. 271–278 in Genetic Ecology of Whales and
968 Dolphins (A.R. Hoelzel ed.), International Whaling Comission, UK.
969 Paradis, E., J. Claude and K. Strimmer. 2004. APE: Analyses of phylogenetics and evolution
970 in R language. Bioinformatics 20:289–290.
971 Peters, W.C.H. 1870. Über neue Amphien (*Hemidactylus*, *Urosaura*, *Tropdolepisma,*
972 *Geophis, Uriechis, Scaphiophis, Hoplocephalus, Rana, Entomoglossus, Cystignathus,*
973 *Hylodes, Arthroleptis, Phyllobates, Cophomantis*) des Königlich Zoologisch Museum.
974 Monatsberichte der Königlichen Preussische Akademie des Wissenschaften zu Berlin,
975 1870:641–652.
976 R Core Team. (2016). R: A language and environment for statistical computing. R Foundation
977 for Statistical Computing, Austria. URL: https://www.r-project.org/
978 Rambaut, A. (2014). FigTree. URL: http://tree.bio.ed.ac.uk/software/figtree/

979 Reinhardt, J.T., and C.F. Lütken. 1862. Bidrag til Kundskab om Brasiliens Padder og
980 Krybdyr. Förste Afdeling: Padderne og Öglerne. Videnskabelige Meddelelser fra
981 Dansk Naturhistorisk Forening i Kjøbenhavn 2:143–242.
982 Ronquist, F., M. Teslenko, P. van der Mark, D.L. Ayres, A. Darling, S. Höhna, B. Larget, L.
983 Liu, M.A. Suchard and J.P. Huelsenbeck. 2012. Mrbayes 3.2: Efficient bayesian
984 phylogenetic inference and model choice across a large model space. Systematic
985 Biology 61:539–542.
986 Sabaj, M.H. 2016. Standard symbolic codes for institutional resource collections in
987 herpetology and ichthyology: an Online Reference. Version 6.5 (16 August 2016).
988 American Society of Ichthyologists and Herpetologists, USA. Available at
989 http://www.asih.org/. Archived by WebCite at
990 http://www.webcitation.org/6mDRaPxHw on 22 November 2016.
991 Santana, D.J., V.A. São Pedro, P.S. Hote, H.M. Roberti, A.C. Sant'Anna, C.A. Figueiredo-de-
992 Andrade and R.N. Feio. 2010. Anurans in the region of the High Muriaé River, State of
993 Minas Gerais, Brazil. Herpetology Notes 3:1–10.
994 Silva-Soares, T., R.B. Ferreira and P.N. da Costa. 2009. Geographic distribution:
995 *Ischnocnema oea*. Herpetological Review 40:109.
996 Spix, J.B. von. 1824. Animalia nova sive Species novae Testudinum et Ranarum quas in
997 itinere per Brasiliam annis MDCCCXVII–MDCCCXX jussu et auspiciis Maximiliani
998 Josephi I. Bavariae Regis. F.S. Hübschmann, Germany.
999 Stamatakis, A. 2014. RAxML version 8: a tool for phylogenetic analysis and post-analysis of
1000 large phylogenies. Bioinformatics 30:1312–1313.
1001 Steindachner, F. 1867. Reise der österreichischen Fregatte Novara um die Erde in den Jahren
1002 1857, 1858, 1859 unter den Bafehlen des Commodore B. von Wüllerstorf-Urbair.
1003 Zologischer Theil. 1. Amphibien. K. K. Hof- und Staatsdruckerei, Austria.

1004 Sueur, J., T. Aubin and C. Simonis. 2008. Seewave , a free modular tool for sound analysis
1005 and synthesis. Bioacoustics 18:213–226.
1006 Targino, M., and S.P. de Carvalho-e-Silva. 2008. Redescrição de *Ischnocnema holti*
1007 (Amphibia:Anura:Brachycephalidae). Revista Brasileira de Zoologia 25:716–723.
1008 Targino, M., P.N. da Costa and S.P. de Carvalho-e-Silva. 2009. Two new species of the
1009 *Ischnocnema lactea* species series from Itatiaia highlands, southeastern Brazil
1010 (Amphibia, Anura, Brachycephalidae). South American Journal of Herpetology 4:139–
1011 150.
1012 Taucce, P.P.G., F.S.F. Leite, P.S. Santos, R.N. Feio and P.C.A. Garcia. 2012. The
1013 advertisement call, color patterns and distribuition of *Ischnocnema izecksohni*
1014 (Caramaschi and Kisteumacher, 1989) (Anura, Brachycephalidae). Papéis Avulsos de
1015 Zoologia 52:111–119.
1016 Titus, T.A., and A. Larson. 1996. Molecular phylogenetics of Desmognathine salamanders
1017 (Caudata:Plethodontidae): a reevaluation of evolution in ecology, life history, and
1018 morphology. Systematic Biology 45:451–472.
1019 Werle, E., C. Schneider, M. Renner, M. Völker and W. Fiehn. 1994. Convenient single-step,
1020 one tube purification of PCR products for direct sequencing. Nucleic Acids Research
1021 22:4354–4355.
1022
1023 **ZooBank.org** registration LSID: 8FD6BCC9-B930-4F5B-9445-B3955DB7A82E
1024 **Published on** XX Month 2018
1025

1026 APPENDIX I

1027 List of terminals and accession numbers of sequences taken from Genbank. Species names

1028 followed by an asterisk are re-identified taxa.

Species	RAG1 Genbank ID	Tyrosinase Genbank ID	12S–tVal–16S Genbank ID
Barycholos ternetzi	JX267543	JX267680	JX267466
Brachycephalus cf. *didactylus*	JX267544	JX267681	JX267389, JX267467
Brachycephalus ephippium	EU186761	----	AF375484
Craugastor daryi	EF493452	EF493480	EF493531
Eleutherodactylus cooki	EF493413	EF493455	EF493539
Haddadus binotatus	JX267548	JX267685	JX267391, JX267469
Hypodactylus dolops	EF493414	EF493483	EF493394
Ischnocnema abdita	JX267551	JX267687	JX267326, JX267472
Ischnocnema aff. *holti*	JX267554	JX267690	JX267336, JX267475
Ischnocnema bolbodactyla	JX267557	JX267692	JX267327, JX267476
*Ischnocnema henselii**	JX267563	JX267698	JX267328, JX267478
*Ischnocnema henselii**	JX267599	JX267734	JX267303
Ischnocnema cf. holti	JX267564	JX267699	JX267329, JX267479
Ischnocnema cf. *manezinho*	JX267566	JX267701	JX267335, JX267481
Ischnocnema cf. *nigriventris*	JX267568	JX267704	JX267398, JX267483
Ischnocnema cf. *penaxavantinho*	JX267574	JX267708	JX267298
Ischnocnema cf. *randorum*	JX267578	JX267799	JX267401, JX267361
Ischnocnema cf. spanios	JX267665	JX267805	JX267453, JX267536
Ischnocnema concolor	JX267594	JX267727	JX267413, JX267366
Ischnocnema concolor	JX267595	JX267728	JX267414, JX267493
Ischnocnema erythromera	----	JX267729	JX267340
Ischnocnema erythromera	JX267596	JX267730	JX267341
Ischnocnema aff. *guentheri**	JX267597	JX267731	JX267339, JX267494
Ischnocnema aff. *guentheri**	JX267602	JX267737	JX267417, JX267368
Ischnocnema aff. *guentheri**	JX267605	JX267740	JX267420, JX267370
Ischnocnema aff. *guentheri**	JX267606	JX267741	JX267421, JX267371
Ischnocnema guentheri	JX267611	JX267746	JX267331, JX267501, JX267502
Ischnocnema guentheri	JX267612	JX267747	JX267332, JX267503
Ischnocnema hoehnei	----	JX267749	JX267347
Ischnocnema hoehnei	JX267614	JX267750	JX267372
Ischnocnema hoehnei	JX267615	JX267751	JX267506
Ischnocnema hoehnei	JX267616	JX267752	JX267345, JX267507
Ischnocnema holti	JX267617	JX267754	JX267306
Ischnocnema izecksohni	JX267618	JX267755	JX267307
*Ischnocnema izecksohni**	JX267636	JX267774	JX267433, JX267375
Ischnocnema juipoca	JX267620	JX267757	JX267349
Ischnocnema lactea	JX267632	JX267769	JX267310, JX267518
Ischnocnema melanopygia	JX267634	JX267771	JX267431, JX267292

1029 APPENDIX I
1030 Continued.

Species	RAG1 Genbank ID	Tyrosinase Genbank ID	12S–tVal–16S Genbank ID
Ischnocnema nasuta	----	JX267772	JX267311
Ischnocnema nasuta	JX267637	JX267775	JX267434, JX267291, JX267520
Ischnocnema nanahallux	----	----	KC569985
Ischnocnema nanahallux	----	----	KC569986
Ischnocnema octavioi	JX267639	JX267777	JX267334, JX267521
Ischnocnema oea	JX267640	JX267778	JX267338
Ischnocnema oea	JX267641	JX267779	JX267313
Ischnocnema parva	JX267645	JX267783	JX267317
Ischnocnema parva	JX267646	JX267784	JX267435, JX267376
Ischnocnema parva	JX267649	JX267787	JX267438, JX267379
Ischnocnema parva	JX267650	JX267788	JX267439, JX267523
Ischnocnema parva	JX267653	JX267790	JX267442, JX267526
Ischnocnema parva	JX267656	JX267795	JX267445, JX267529
Ischnocnema parva	JX267657	JX267796	JX267446, JX267344, JX267530
Ischnocnema sambaqui	JX267661	JX267801	JX267449, JX267531
Ischnocnema spanios	JX267584	JX267717	JX267407, JX267490
Ischnocnema venancioi	JX267666	JX267806	JX267321
Ischnocnema venancioi	JX267667	JX267807	JX267454, JX267382
Ischnocnema verrucosa	JX267670	JX267810	JX267457, JX267538
Ischnocnema vizottoi	JX267672	JX267812	JX267350
Lynchius flavomaculatus	EU186745	EU186766	EU186667
Pristimantis ramagii	JX267658	JX267797	JX267318
Yunganastes mercedesae	----	----	FJ539071, FJ539066

1031

APPENDIX II

List of terminals and GenBank accession numbers for sequences generated in this study. Museum acronyms follow Sabaj (2016).

Species	Voucher#	RAG1 Genbank ID	Tyrosinase Genbank ID	12S–tVal–16S Genbank ID
Ischnocnema feioi (holotype)	CFBH 35994	MF957146	MF957157	MF957167
Ischnocnema feioi	UFMG 17078	MF957147	MF957156	MF957165
Ischnocnema feioi	MZUFV 15712	MF957150	MF957160	MF957166
Ischnocnema garciai (holotype)	CFBH 39028	MF957148	MF957158	MF957170
Ischnocnema garciai	CFBH 39029	MF957149	MF957159	MF952878, MF957163
Ischnocnema garciai	UFMG 18889	----	----	MF957168
Ischnocnema garciai	UFMG 18890	----	----	MF957169
Ischnocnema aff. *guentheri*	UFMG 13906	MF957144	MF957154	MF952879, MF952883
Ischnocnema aff. *guentheri*	UFMG 13908	MF957145	MF957155	MF952880, MF952884
Ischnocnema aff. *guentheri*	CFBH 41853	MF957141	MF957151	MF957164
Ischnocnema aff. *guentheri*	CFBH 39282	MF957143	MF957153	MF952877, MF957162, MF952881
Ischnocnema oea	CFBH 12394	MF957142	MF957152	MF952876, MF957161, MF952882

APPENDIX III

Specimens examined.

Ischnocnema epipeda.—BRAZIL: ESPÍRITO SANTO: Santa Teresa (MNRJ 1874 *Eleutherodactylus epipedus* paratype).

Ischnocnema erythromera.—BRAZIL: RIO DE JANEIRO: Santa Maria Magdalena: Parque Estadual do Desengano (CFBH 28111–28115); Teresópolis (CFBH 27349, 40985).

Ischnocnema guentheri.—BRAZIL: RIO DE JANEIRO: Rio de Janeiro: Floresta da Tijuca (CFBH 26989–26994, 27440, 27442–27444, MNRJ 31666, 36483, 87540–87541, 87544–87545, 87548).

Ischnocnema henselii.—BRAZIL: PARANÁ: Arianópolis (CFBH 27470–27471); Piraquara (CFBH 11039–11040). SANTA CATARINA: Anitápolis (CFBH 9367–9368); São Bonifácio (CFBH 27549–27554). SÃO PAULO: São Bernardo do Campo (CFBH 12298); Tapiraí (CFBH 23298).

Ischnocnema hoehnei.—BRAZIL: SÃO PAULO: Pilar do Sul (CFBH 8336); Santo André: Paranapiacaba (CFBH 29043).

Ischnocnema izecksohni.—BRAZIL: MINAS GERAIS: Aiuruoca (CFBH 36919–36920); Alto Caparaó: Parque Nacional do Caparaó (CFBH 40977–40980); Belo Horizonte (MNRJ 4217 *Eleutherodactylus izecksohni* holotype, MNRJ 4218–4219 *Eleutherodactylus izecksohni* paratypes); Conceição do Ouro (CFBH 39908–39910); Muriaé (CFBH 35990–35991, 39016, 39020–39021, 39039); Ouro Preto: Rodrigo Silva (CFBH 35793, 35796–35799).

Ischnocnema nasuta.—BRAZIL: RIO DE JANEIRO: Nova Friburgo (CFBH 40981–40984); Macaé de Cima (MBML 212).

Ischnocnema oea.—BRAZIL: ESPÍRITO SANTO: Cariacica: Reserva Biológica de Duas Bocas (CFBH 22517–22518, 22520); Santa Teresa (MNRJ 1244 *Eleutherodactylus oeus* holotype, UFMG 13735–13738, USNM 235612 *Eleutherodactylus oeus* paratype); Santa

Teresa: Reserva Biológica Augusto Ruschi (CFBH 24778–24779, 30732, 40987); Santa Teresa: São Lourenço (CFBH 10815–10816, 10876–10877, 27090–27091, 37242); Vargem Alta (CFBH 25050, 27013).

Ischnocnema cf. *oea*.—BRAZIL: Rio de Janeiro: Cambuci (MNRJ 49504–49506).

Ischnocnema venancioi.—BRAZIL: Rio de Janeiro: Nova Friburgo (CFBH 27435); Teresópolis (CFBH 40986).

APPENDIX IV

Call records analyzed.

Call ID	Voucher	Species	Locality	Recorder
PPGT 001	CFBH 35994	*Ischnocnema feioi*	Lar dos Muriquis, Muriaé, Minas Gerais, Brazil	Marantz PMD-661
PPGT 002	CFBH 35994	*I. feioi*	Lar dos Muriquis, Muriaé, Minas Gerais, Brazil	Marantz PMD-661
PPGT 003	MZUFV 15712	*I. feioi*	Careço, Ervália, Minas Gerais, Brazil	Marantz PMD-660
PPGT 004	unvouchered	*I. feioi*	Careço, Ervália, Minas Gerais, Brazil	Marantz PMD-660
CBUFMG 916	UFMG 3285	*I. feioi*	Parque Estadual da Serra do Brigadeiro, Araponga, Minas Gerais, Brazil	Marantz PMD-660
CBUFMG 917	UFMG 17028	*I. feioi*	Parque Nacional do Caparaó, Santa Marta, Espírito Santo, Brazil	Tascam DR-40
PPGT 005	CFBH 39028	*I. garciai*	Usina da Fumaça, Muriaé, Minas Gerais, Brazil	Marantz PMD-660
PPGT 006	CFBH 39029	*I. garciai*	Usina da Fumaça, Muriaé, Minas Gerais, Brazil	Marantz PMD-661
PPGT 007	unvouchered	*I. garciai*	Usina da Fumaça, Muriaé, Minas Gerais, Brazil	Marantz PMD-661
PPGT 008	CFBH 39031	*I. garciai*	Usina da Fumaça, Muriaé, Minas Gerais, Brazil	Marantz PMD-661
MNVOC 043:1	unvouchered	*I. oea*	Reserva Biológica Augusto Ruschi, Santa Teresa, Espírito Santo, Brazil	Marantz PMD-660
MNVOC 043:2	CFBH 24778	*I. oea*	Reserva Biológica Augusto Ruschi, Santa Teresa, Espírito Santo, Brazil	Marantz PMD-660
MNVOC 043:3	unvouchered	*I. oea*	Reserva Biológica Augusto Ruschi, Santa Teresa, Espírito Santo, Brazil	Marantz PMD-660

1069 TABLE 1.— Primers used in this study.

Primer		Gene	Sequence	Reference
MVZ59	F	12S	ATAGCACGTAAAAYGCTDAGATG	Graybeal (1997)
tRNAphe-L	F	tRNA-F–12S	AAAGCATAACACTGAAGATGTTAAGATG	Goebel et al. (1999)
12S F-H	R	12S	CTTGGCTCGTAGTTCCCTGGCG	Goebel et al. (1999)
12S A-L	F	12S–tRNA-V	AAACTGGGATTAGATACCCCACTAT	Goebel et al. (1999)
tRNAval-H	R	12S–tRNA-V	GGTGTAAGCGARAGGCTTTKGTTAAG	Goebel et al. (1999)
12SL13	F	tRNA-V–16S	TTAGAAGAGGCAAGTCGTAACATGGTA	Feller and Hedges (1998)
16STitus_1	R	tRNA-V–16S	GGTGGCTGCTTTTAGGCC	Titus and Larson (1996)
16SL2A	F	16S	CCAAACGAGCCTAGTGATAGCTGGTT	Hedges (1994)
16S-H10	R	16S	TGCTTACGCTACCTTTGCACGGT	Hedges (1994)
16SAR	F	16S	CGCCTGTTTATCAAAAACAT	Palumbi et al. (1991)
16SBR	R	16S	GACCTGGATTACTCCGGTCTGA	Palumbi et al. (1991)
Tyr1B	F	Tyrosinase	AGGTCCTCYTRAGGAAGGAATG	Bossuyt and Milinkovitch (2000)
Tyr1E	R	Tyrosinase	GAGAAGAAAGAWGCTGGGCTGAG	Bossuyt and Milinkovitch (2000)
Tyr1C	F	Tyrosinase	GGCAGAGGAWCRTGCCAAGATGT	Bossuyt and Milinkovitch (2000)
Tyr1G	R	Tyrosinase	TGCTGGGCRTCTCTCCARTCCCA	Bossuyt and Milinkovitch (2000)
R182	F	RAG1	GCCATAACTGCTGGAGCATYAT	Heinicke et al. (2007)
R270	R	RAG1	AGYAGATGTTGCCTGGGTCTTC	Heinicke et al. (2007)
RAG1FF2	F	RAG1	ATGCATCRAAAATTCARCAAT	Heinicke et al. (2007)
RAG1FR2	R	RAG1	CCYCCTTTRTTGATAKGGWCATA	Heinicke et al. (2007)

1070

1071 TABLE 2.— Best partition scheme and respective best fitting molecular models.

Partition	Model
12S	GTR + Γ + I
tVal	GTR + Γ
16S	GTR + Γ + I
RAG1 1st and 2nd positions	HKY + Γ
RAG 1 3rd position	K80 + Γ
Tyr 1st and 2nd positions	GTR + Γ + I
Tyr 3rd position	GTR + Γ

1072

TABLE 3.— Uncorrected pairwise genetic distances within and between members of the *Ischnocnema guentheri* series closely related to *I. oea.* Within species distances are highlighted in gray. Data are shown as range (mean) where appropriate.

	Uncorrected pairwise distance between species							
	I. feioi	*I. garciai*	*I. oea*	*I. guentheri*	*I. henselii*	*I. izecksohni*	*I. nasuta*	*I. erythromera*
I. feioi	0.0–1.5 (0.9, *n* = 3)							
I. garciai	7.0–7.8 (7.5)	0.0 (*n* = 4)						
I. oea	9.9	10.4–10.7 (10.6)	0.0 (*n* = 2)					
I. guentheri	9.7–10.7 (10.3)	13.1–13.6 (13.3)	14.0–14.3 (14.1)	0.0–0.5 (0.1, *n* = 11)				
I. henselii	10.2–12.1 (11.3)	12.8–14.3 (13.7)	13.6–14.8 (13.9)	7.5–9.0 (8.2)	0.0–3.6 (1.8, *n* = 57)			
I. izecksohni	10.7–11.9 (11.1)	13.6–13.8 (13.7)	13.6	12.8–13.1 (13.1)	13.6–14.5 (13.8)	0.0 (*n* = 2)		
I. nasuta	10.9–12.8 (11.7)	13.8–14.8 (14.3)	13.3–14.0 (13.6)	12.3–13.1 (12.8)	13.6–14.8 (13.9)	1.2–1.9 (1.8)	0.0–3.2 (2.3, *n* = 4)	
I. erythromera	9.4–10.7 (9.9)	11.6–11.9 (11.8)	13.1–13.6 (13.3)	11.1–11.6 (11.5)	12.4–13.8 (13.1)	12.1–12.6 (12.4)	11.9–12.6 (12.2)	1.0 (*n* = 2)

TABLE 4.— Snout-vent length (SVL) and body proportions of *Ischnocnema oea, I. feioi*, and *I. garciai*. Data are given as range (mean ± standard deviation) where appropriate.

Character	Adult males			Adult females	
	Ischnocnema oea (*n* = 13)	*Ischnocnema feioi* (*n* = 4)	*Ischnocnema garciai* (*n* = 16)	*Ischnocnema oea* (*n* = 2)	*Ischnocnema garciai* (*n* = 2)
SVL (mm)	13.5–17.8 (16.0 ± 1.3)	20.7–23.6 (22.1 ± 1.2)	13.3–18.5 (16.8 ± 1.2)	24.7–25.0	21.9–24.7
Head length/SVL	0.44–0.52 (0.48 ± 0.03)	0.40–0.44 (0.42 ± 0.02)	0.39–0.47 (0.43 ± 0.02)	0.42–0.42	0.40–0.41
Head width/SVL	0.33–0.40 (0.38 ± 0.02)	0.32–0.34 (0.33 ± 0.01)	0.33–0.39 (0.36 ± 0.01)	0.36–0.38	0.34–0.36
Eye diameter/head length	0.20–0.30 (0.26 ± 0.03)	0.25–0.28 (0.26 ± 0.01)	0.26–0.32 (0.29 ± 0.02)	0.26–0.28	0.28–0.30
Tympanum diameter/eye diameter	0.27–0.66 (0.45 ± 0.12)	0.40–0.53 (0.46 ± 0.07)	0.41–0.55 (0.47 ± 0.04)	0.45–0.55	0.45–0.47
Tibia length/SVL	0.67–0.74 (0.70 ± 0.02)	0.69–0.79 (0.73 ± 0.04)	0.64–0.72 (0.69 ± 0.03)	0.66–0.69	0.66–0.72
Thigh length/SVL	0.57–0.69 (0.64 ± 0.04)	0.61–0.66 (0.63 ± 0.02)	0.56–0.66 (0.61 ± 0.03)	0.60–0.61	0.57–0.64

1080 TABLE 5.—Advertisement call parameters comparing the members of the *Ischnocnema guentheri*

1081 series. Data are given as ranges.

Species	Call duration (s)	Call rise time (%)	Dominant Frequency (kHz)	Notes per call	Note rate (notes/s)	Note repetition rate acceleration (%)	Source
Ischnocnema feioi	1.54–5.51	79–100	2.53–3.23	10–27	4.13–6.19	-26–21	this study
Ischnocnema garciai	14.84–29.11	45–92	3.27–3.88	57–96	3.27–4.47	5–198	this study
Ischnocnema oea	4.56–8.49	90–99	3.09–4.13	25–41	4.80–5.70	-9–61	Hepp and Canedo (2013), this study
Ischnocnema gualteri	1.50–1.90	—	2.10–2.70	4–9	—	—	Heyer (1984)
Ischnocnema guentheri	26.30–41.90	—	2.81–3.28	71–146	2.20–3.50	31–121	Gehara et al. (2013)
Ischnocnema henselii	10.00–23.00	—	2.10–3.10	86–170	6.60–7.10	107–125	Kwet and Solé (2005), Gehara et al. (2013)
Ischnocnema izecksohni	1.03–2.15	—	2.25–2.63	34–60	26.91–32.10	—	Taucce et al. (2012)
Ischnocnema nasuta	1.15–1.50	—	2.10–2.60	34–43	—	—	Heyer (1984)

1082

1083 TABLE 6.—Advertisement call parameters of five recorded males of *Ischnocnema feioi*. Data are

1084 given as min–max (mean ± standard deviation) where appropriate.

Call recording	PPGT 001	PPGT 002	PPGT 003	PPGT 004	CBUFMG 916	CBUFMG 917
Number of analyzed calls	2	6	3	4	10	6
Call duration (s)	4.94–5.51	3.70–5.34 (4.84 ± 0.62)	5.07–5.14 (5.12 ± 0.04)	4.18–4.43 (4.28 ± 0.12)	2.49–3.09 (2.82 ± 0.20)	1.54–2.56 (2.11 ± 0.37)
Call rise time (%)	96–99	99–100 (99 ± 0)	98–99 (99 ± 0)	79–100 (91 ± 9)	91–99 (96 ± 4)	91–100 (98 ± 4)
Dominant Frequency (kHz)	2.89–2.93	2.71–2.97 (2.90 ± 0.09)	3.06–3.10 (3.09 ± 0.03)	2.76–2.76 (2.76 ± 0)	3.09–3.23 (3.16 ± 0.05)	2.53–2.76 (2.68 ± 0.09)
Notes per call	25.00–27.00	19.00–27.00 (25.00 ± 3.16)	22.00–22.00 (22.00 ± 0)	21.00–22.00 (21.50 ± 0.58)	14.00–18.00 (16.20 ± 1.14)	10.00–15.00 (12.50 ± 1.76)
Note rate (notes/s)	4.90–4.94	4.88–5.10 (4.99 ± 0.08)	4.13–4.18 (4.15 ± 0.03)	4.80–6.19 (5.32 ± 0.62)	5.21–5.82 (5.44 ± 0.21)	5.27–5.90 (5.52 ± 0.22)
Note repetition rate acceleration (%)	2–19	-14–7 (1 ± 9)	4–5 (4 ± 1)	18–21 (19 ± 1)	-26–-9) (-20 ± 5)	-8–2 (-3 ± 3)

1085

TABLE 7.—Advertisement call parameters of four recorded males of *Ischnocnema garciai*. Data are given as min–max (mean ± standard deviation) where appropriate.

Call recording	PPGT 005	PPGT 006	PPGT 007	PPGT 008
Number of analyzed calls	1	1	5	5
Call duration (s)	29.11	20.89	14.84–19.14 (17.60 ± 1.64)	16.90–20.80 (19.20 ± 1.49)
Call rise time (%)	69	81	45–74 (61 ± 13)	62–92 (80 ± 12)
Dominant Frequency (kHz)	3.88	3.45	3.27–3.36 (3.29 ± 0.04)	3.36–3.40 (3.396 ± 0.02)
Notes per call	96.00	79.00	57.00–83.00 (76.60 ± 11.08)	71.00–84.00 (78.60 ± 4.98)
Note rate (notes/s)	3.27	3.74	3.79–4.47 (4.29 ± 0.29)	3.90–4.15 (4.05 ± 0.10)
Note repetition rate acceleration (%)	108	19	85–198 (114 ± 47)	5–61 (40 ± 22)

FIG. 1.— The 50% majority rule consensus tree from Bayesian inference analysis of concatenated mitochondrial 12S rRNA, tVal rRNA, 16S rRNA, and nuclear Recombination Activating Gene 1 (RAG1) and tyrosinase precursor (Tyr), showing Bayesian posterior probabilities (above branches) and maximum likelihood non-parametric bootstrap values (below) values. Asterisks (*) indicate 100% values.

FIG. 2.— Calcar tubercles of members of the *Ischnocnema guentheri* series: (A) *I. feioi* (UFMG 3285), (B) *I. garciai* (CFBH 39029), (C) *I. oea* (CFBH 24778), (D) *I. guentheri* (CFBH 27443), (E) *I. hoehnei* (CFBH 8336), and (F) *I. izecksohni* (CFBH 35793). Scale bars = 1 mm.

FIG. 3.— Advertisement call of three species of the *Ischnocnema guentheri* series. Oscillogram (below) and spectrogram (above) of (A) *I. oea* (recording MNVOC 043:2), (B) *I. feioi* (recording PPGT 004), and (C) *I. garciai* (recording PPGT 007).

FIG. 4.— Dorsal (left) and ventral (right) views of (A) *Ischnocnema oea* (CFBH 30732), (B) *I. feioi* (CFBH 35994, holotype), and (C) *I. garciai* (CFBH 39028, holotype). Scale bar = 5 mm.

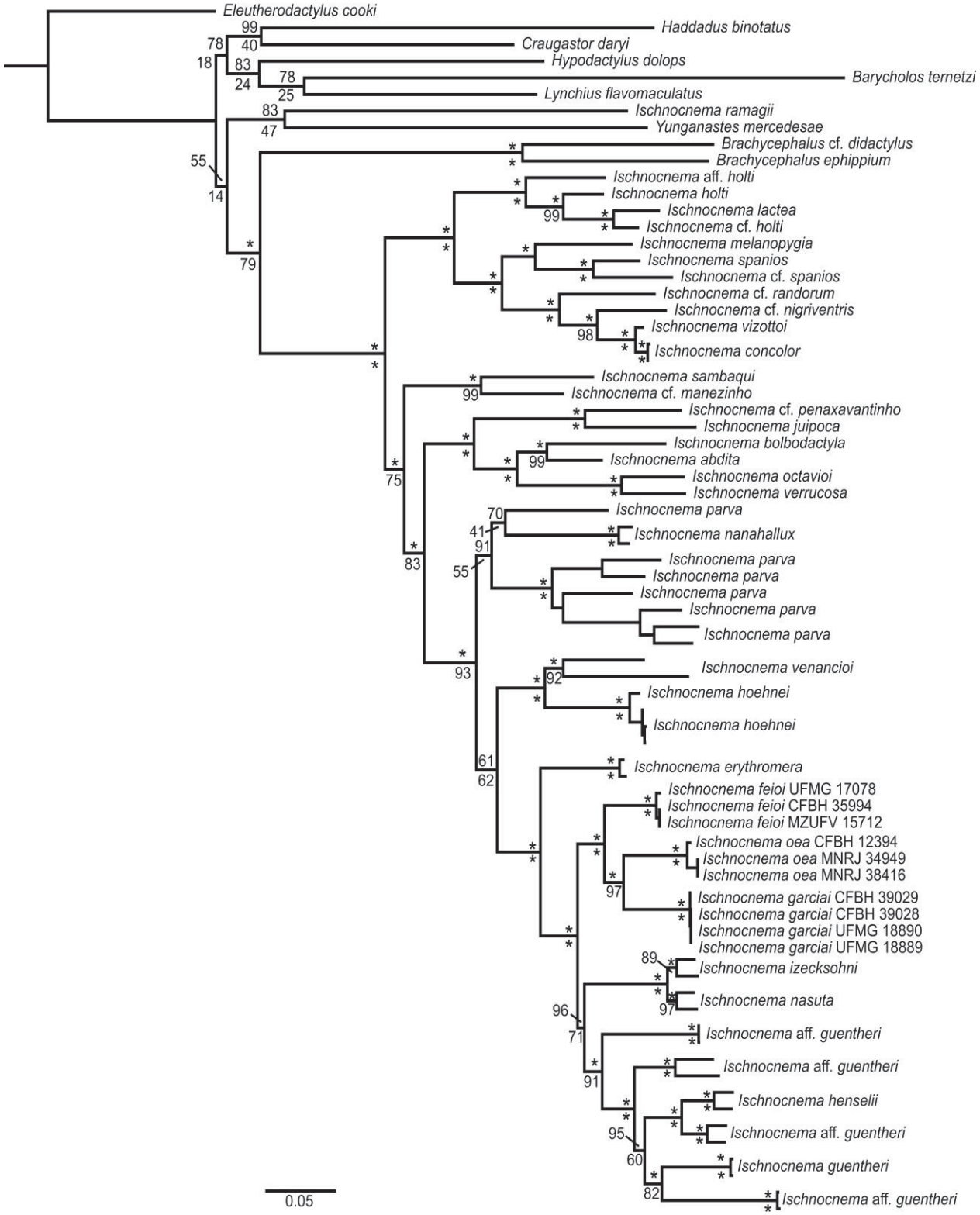
FIG. 5.— Dorsal and ventral views of the holotype of *Ischnocnema oea* (MNRJ 1244). Scale bar = 5 mm.

FIG. 6.— Geographic distribution of *Ischnocnema oea*, *I. feioi*, and *I. garciai*. Solid symbols represent type localities of each species. Area above 500 and 1000 m shaded gray.

FIG. 7.— Holotype of *Ischnocnema feioi*, CFBH 35994: (A) dorsal and (B) lateral views of the head, (C) ventral view of the left hand, and (D) ventral view of the left foot. Scale bar = 5 mm.

FIG. 8.— Holotype of *Ischnocnema garciai*, CFBH 39028: (A) dorsal and (B) lateral views of the head, (C) ventral view of the left hand, and (D) ventral view of the left foot. Scale bar = 5 mm.

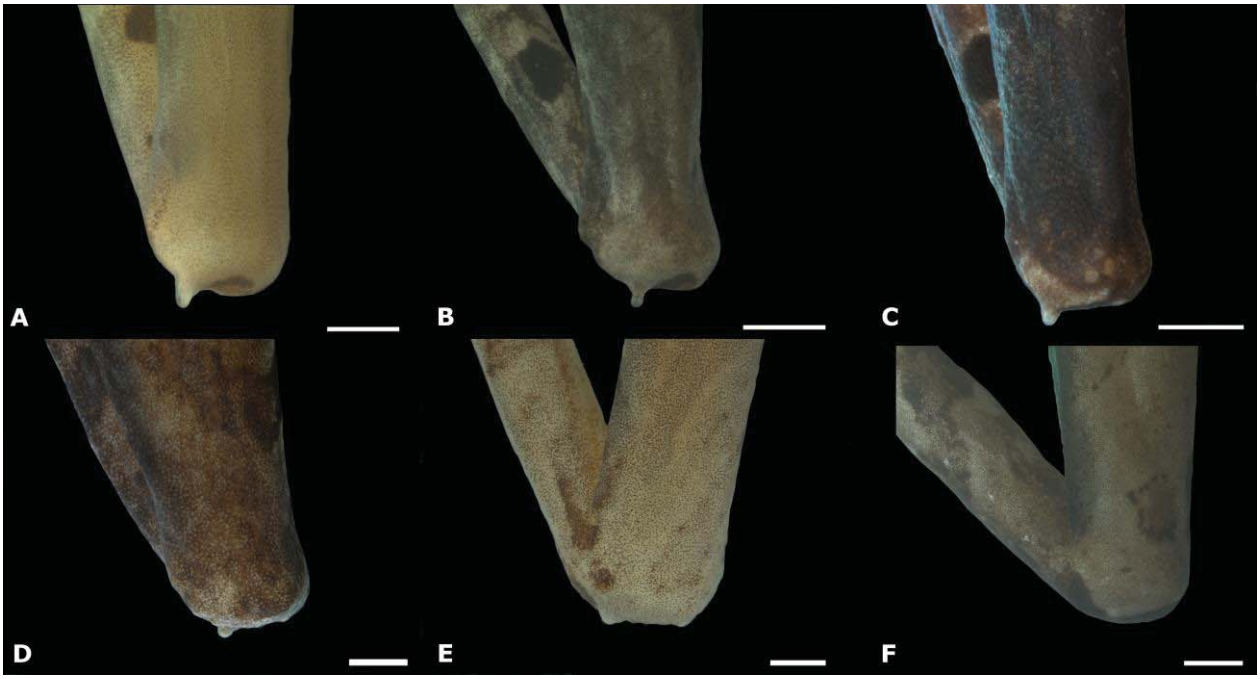
1128 FIG. 1.



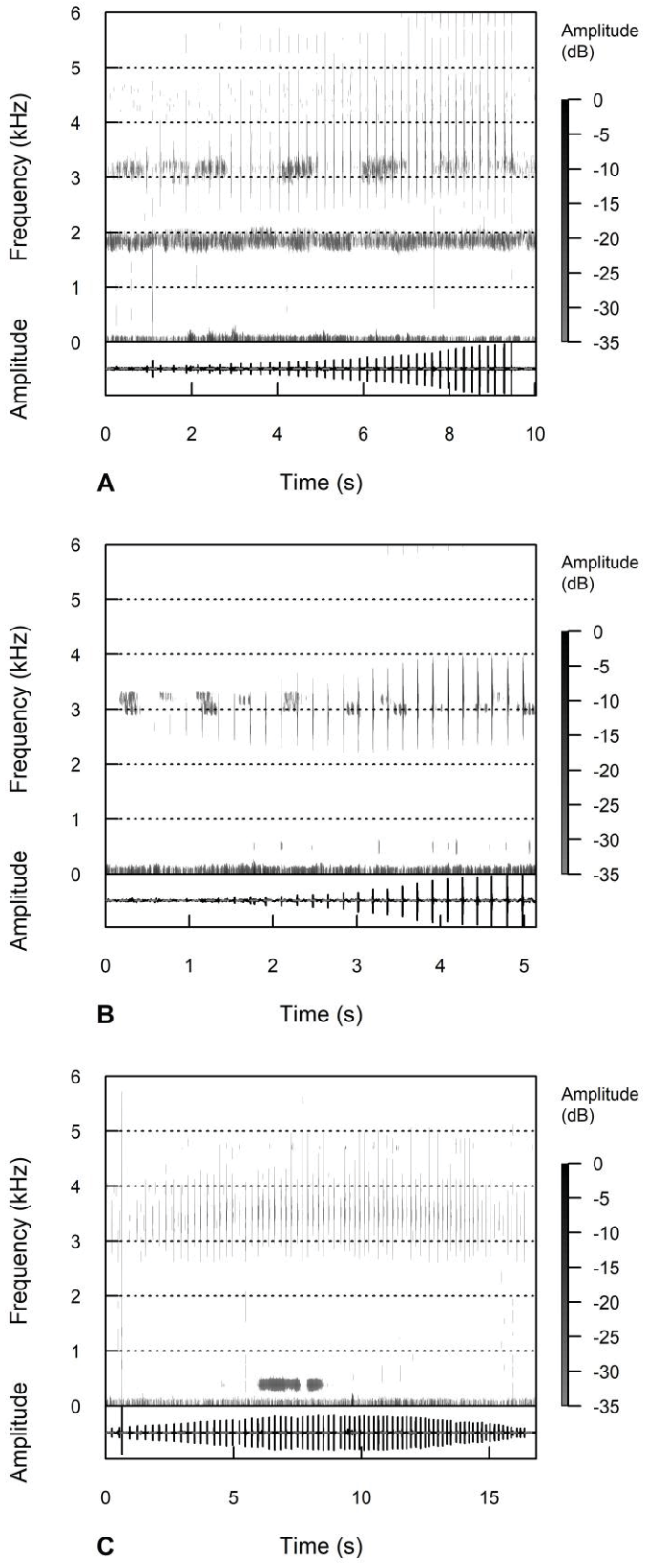
1129

1130

FIG. 2.

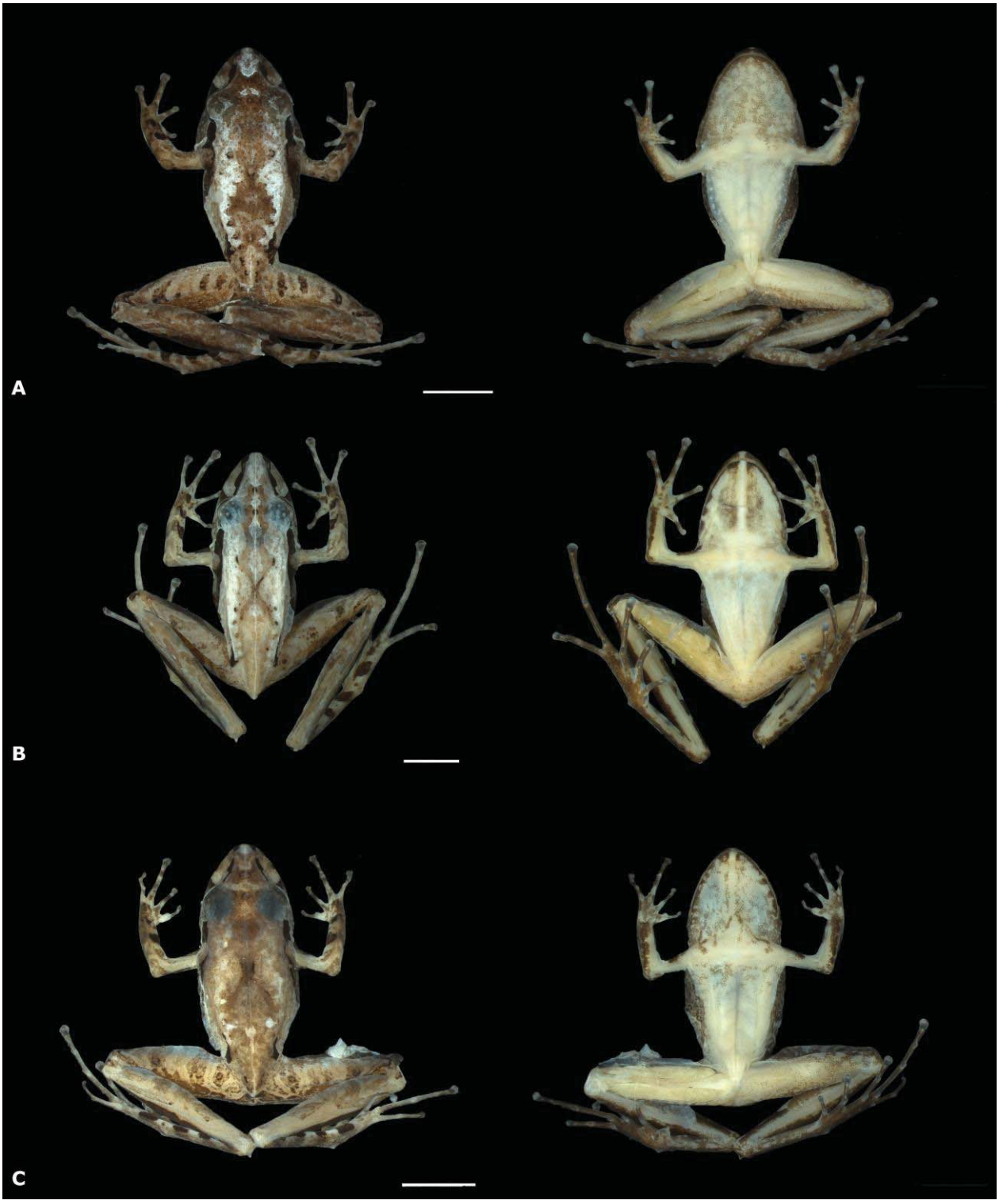


1134 FIG. 3.



1135

1136 FIG. 4.



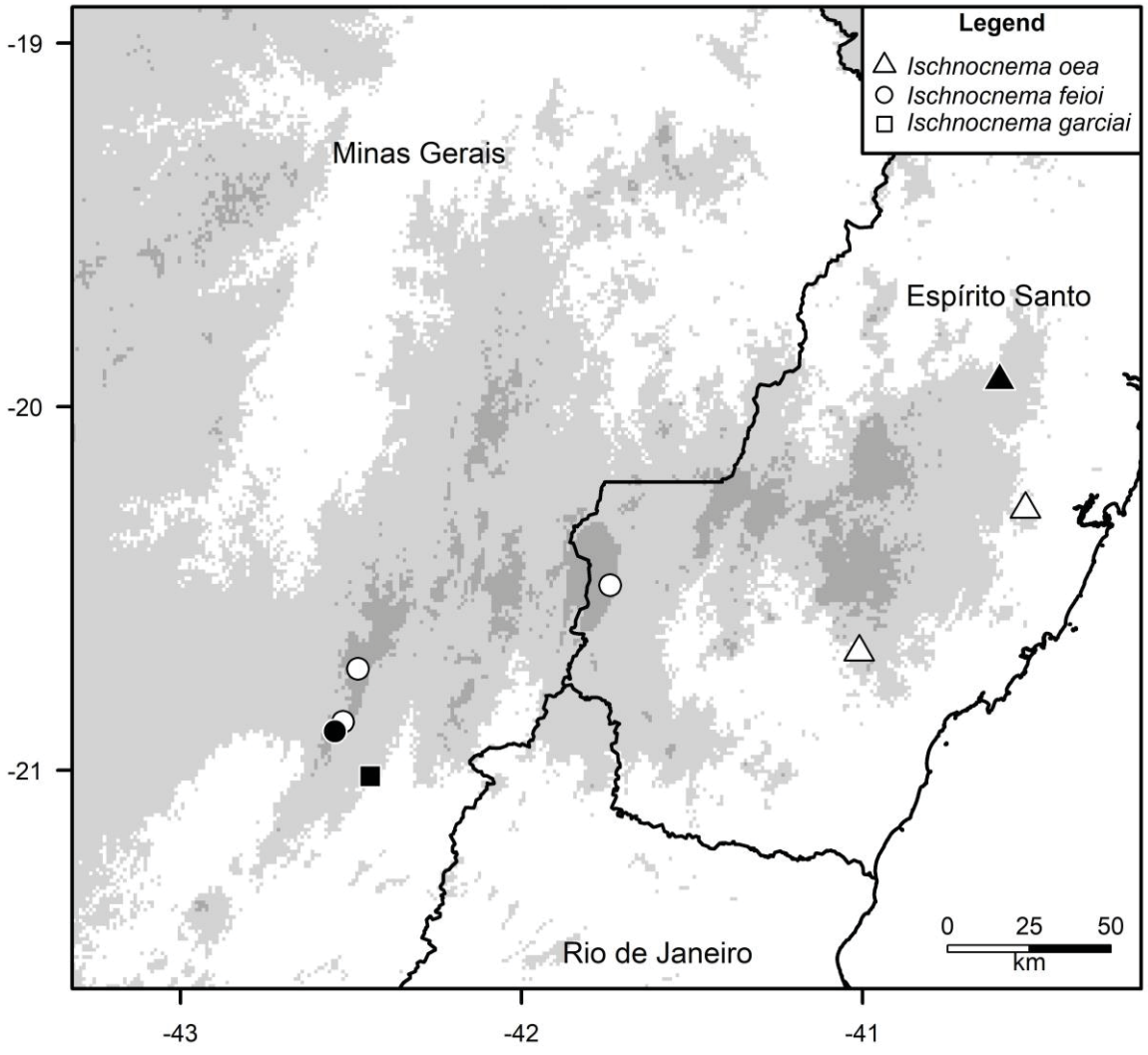
1137

1138

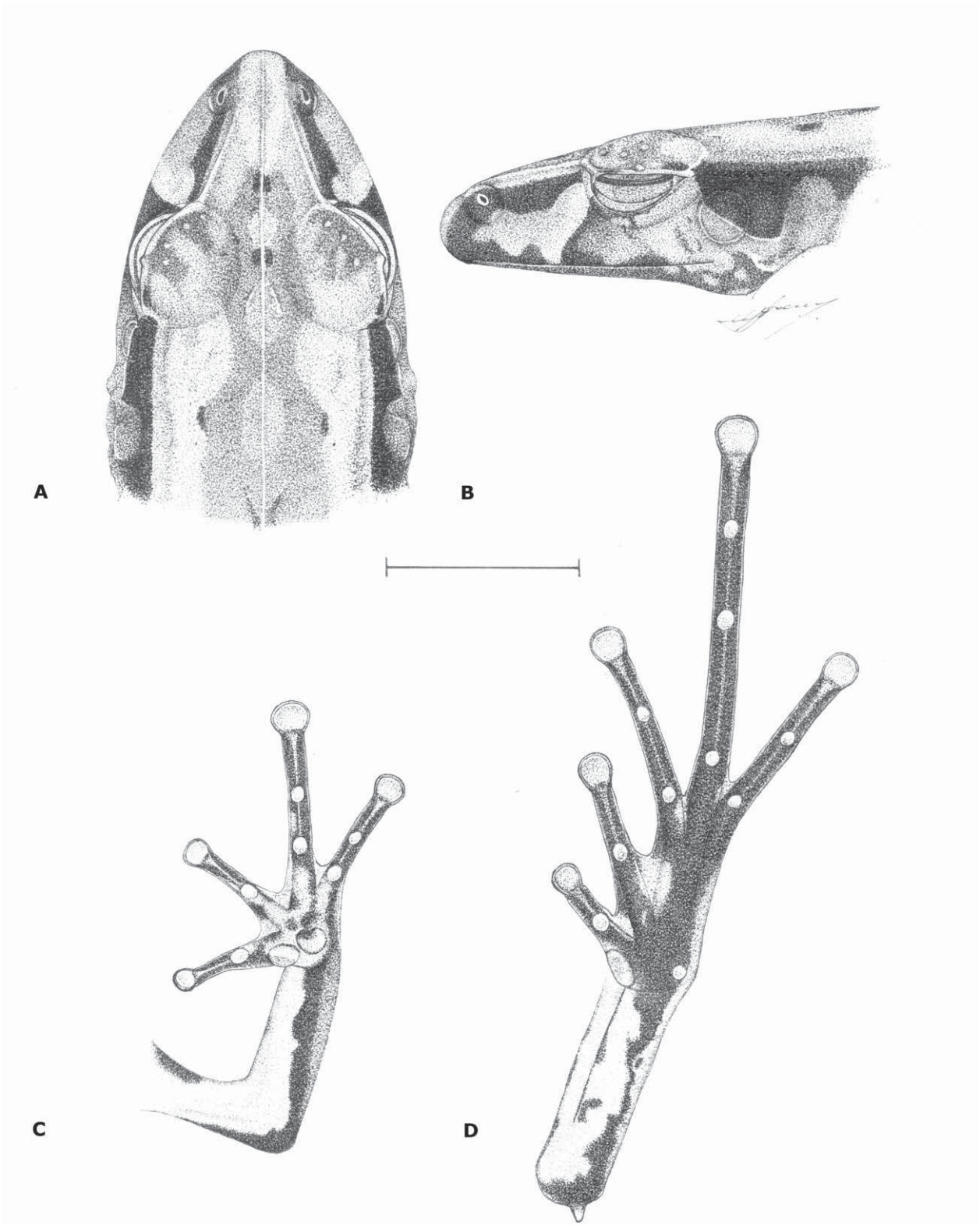
FIG. 5.



FIG. 6.

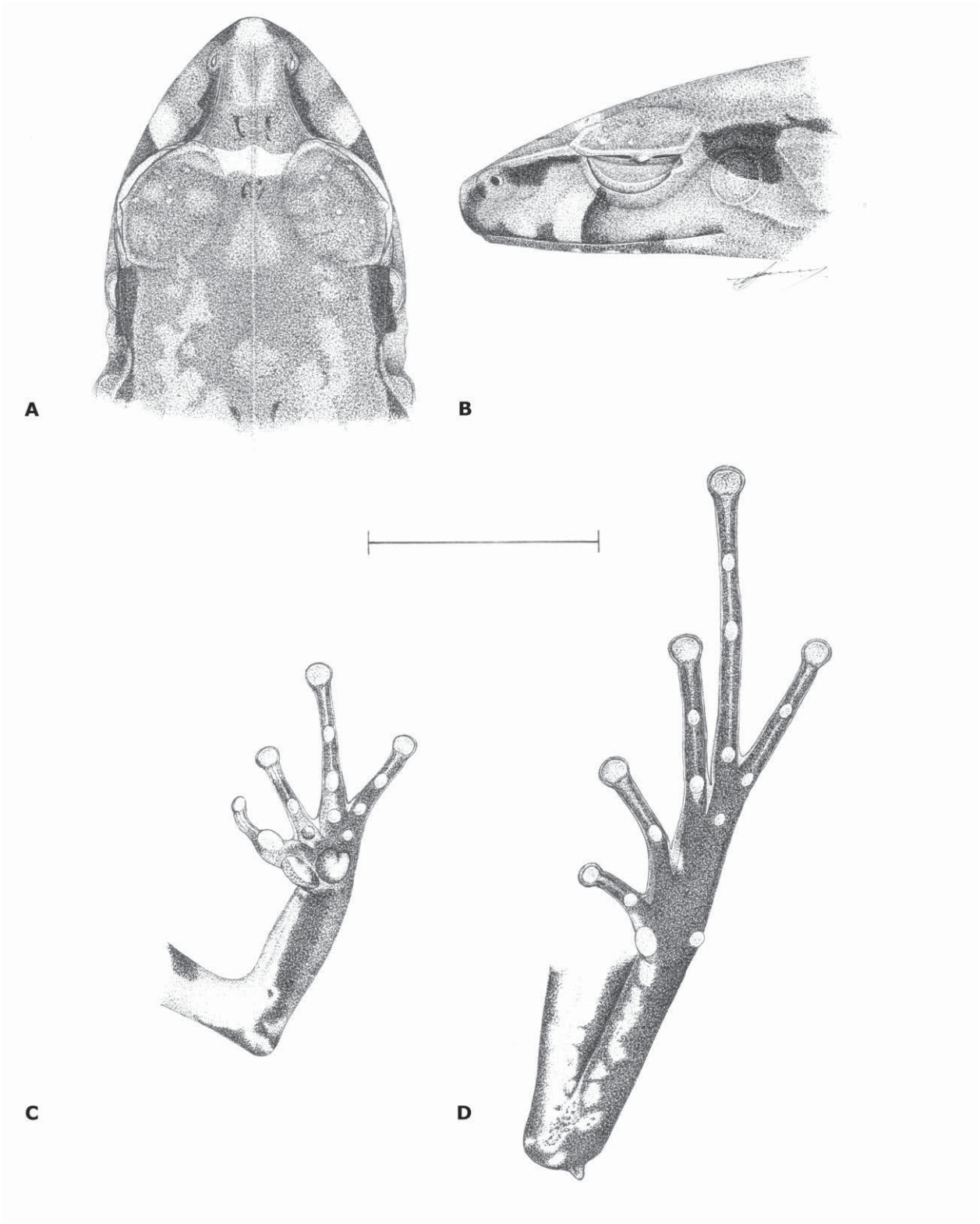

Legend
Ischnocnema oea
Ischnocnema feioi
Ischnocnema garciai
Minas Gerais
Espírito Santo
Rio de Janeiro
0 25 50
km
-19
-20
-21
-43
-42
-41

1145 FIG. 7.



1146
1147

1148 FIG. 8.



1149

Molecular phylogeny of *Ischnocnema* (Anura: Brachycephalidae) with the redefinition of its series and the description of two new species[†]

Pedro P. G. Taucce[a]*, Clarissa Canedo[b,f], Júlia Soares Parreiras[c], Leandro O. Drummond[d], Paulo Nogueira-Costa[e,f], Célio F. B. Haddad[a]

[a]*Instituto de Biociências, UNESP – Univ Estadual Paulista, Câmpus Rio Claro, Departamento de Zoologia and Aquaculture Center (CAUNESP), Cx. Postal 199, 13506-569, Rio Claro, SP, Brazil*

[b]*Instituto de Biologia Roberto Alcântara Gomes, UERJ – Universidade do Estado do Rio de Janeiro, Departamento de Zoologia, Laboratório de Diversidade e Evolução de Anfíbios, Rua São Francisco Xavier, 524, Maracanã, 20550-013, Rio de Janeiro, RJ, Brazil*

[c]*Instituto de Ciências Biológicas, UFMG – Universidade Federal de Minas Gerais, Departamento de Zoologia, Laboratório de Herpetologia, Avenida Antônio Carlos, 6627, Pampulha, 31270-910, Belo Horizonte, MG, Brazil*

[d]*Universidade Federal do Rio de Janeiro (UFRJ), Departamento de Ecologia, Laboratório de Vertebrados. Cx. Postal 68020, Ilha do Fundão. CEP 21941-901, Rio de Janeiro, RJ, Brazil.*

[e] *Universidade do Estado do Rio de Janeiro, Departamento de Ecologia, Laboratório de Ecologia de Vertebrados, Rua São Francisco Xavier, 524, Maracanã, Rio de Janeiro, RJ, Brazil.*

[f]*Universidade Federal do Rio de Janeiro, Museu Nacional, Departamento de Vertebrados, Quinta da Boa Vista, s/n, 20940-040, Rio de Janeiro, RJ, Brazil.*

** Corresponding author: pedrotaucce@gmail.com*

[†]Capítulo submetido para o periódico *Molecular Phylogenetics and Evolution*

ABSTRACT

We present a new phylogenetic hypothesis for *Ischnocnema*, a Neotropical brachycephaloid genus of ground-dwelling direct-developing frogs. We performed Bayesian inference, maximum likelihood, and maximum parsimony analyses using two nuclear (RAG1 and Tyr) and three mitochondrial genes (12S rRNA, tRNA-Val, and 16S rRNA) in a matrix comprising 28 of the 35 described species (80%). We recover *I. nanahallux* outside the *I. parva* series, and it is now unassigned to any species series, as are *I. manezinho* and *I. sambaqui*. We propose the *I. venancioi* species series to allocate *I. venancioi*, *I. hoehnei*, and two new species described herein (*Ischnocnema parnaso* sp. nov. and *Ischnocnema colibri* sp. nov.). Furthermore, we designate a lectotype for *I. venancioi*. The nuptial pad present in males is an important character in the genus and having a large, conspicuous, and glandular-appearing nuptial pad seems to be a putative synapomorphy for the clade composed of the *I. parva, I. guentheri*, and the newly proposed *I. venancioi* series.

Keywords: Amphibia, Bioacoustics, Brachycephaloidea, Systematics, Taxonomy, Terrarana

1. Introduction

The Neotropical genus *Ischnocnema* Reinhardt and Lütken, 1862, is a group of ground-dwelling frogs belonging to Brachycephaloidea Günther, 1858, a superfamily of direct-developing frogs (*i.e.*, they do not pass through a larval phase during their development). It currently comprises 35 species (Frost, 2018) divided into four series distributed throughout South and Southeast Brazil and adjacent Argentina, mainly in the Atlantic Forest domain: *I. guentheri, I. lactea, I. parva,* and *I. verrucosa* (Canedo and Haddad, 2012; Padial et al., 2014). Not long ago *Ischnocnema* was considered a junior synonym of *Eleutherodactylus* Duméril & Bibron, 1841 (Caramaschi and Canedo, 2006), but the taxonomic status of the genus and its species has changed a lot over time.

Lynch (1976) divided the South American *Eleutherodactylus* into ten groups, based on morphological characters. Four of these groups contained species from the Atlantic Forest: the *E. binotatus* group, which included *E. binotatus* (Spix, 1824), *E. gualteri* B. Lutz, 1974, *E. guentheri* (Steindachner, 1864), *E. nasutus* (A. Lutz, 1925), *E. octavioi* Bokermann, 1965, and *E. plicifer* (Boulenger, 1888); the *E. lacteus* group, which included *E. bolbodactylus* (A. Lutz, 1925), *E. lacteus* (Miranda-Ribeiro, 1923), *E. nigriventris* (A. Lutz, 1925), and *E. venancioi* B. Lutz, 1958; the *E. parvus* group, which included *E. parvus* (Girard, 1853) and *E. pusillus* Bokermann, 1967; and finally the *E. ramagii* group, which included *E. paulodutrai* Bokermann, 1975 “1974” and *E. ramagii* (Boulenger, 1888).

Heyer (1984) created the *E. guentheri* cluster to allocate part of the *E. binotatus* group and three new species he described at the time. The cluster contained *E. epipedus* Heyer, 1984, *E. erythromerus,* Heyer, 1984, *E. gualteri*, *E. guentheri*, *E. nasutus,* and *E. oeus* Heyer, 1984.

Further, Lynch and Duellman (1997) created the *E. binotatus* series to allocate the four Atlantic Forest groups from Lynch (1976). To the *E. binotatus* group (*sensu* Heyer, 1984) the authors added *E. heterodactylus* (Miranda-Ribeiro, 1937), *E. hoehnei* B. Lutz, 1958, *E. izecksohni* Caramaschi and Kisteumacher, 1989 "1988", and *E. juipoca* Sazima and Cardoso, 1978. From the *E. lacteus* group, the authors removed *E. venancioi* and included *E. holti* Cochran, 1948, while the *E. parvus* and *E. ramagii* groups remained the same. The authors also assigned *E. randorum* Heyer, 1985; *E. spanios* Heyer, 1985; *E. venancioi*; and *E. vinhai* Bokermann, 1975 "1974" to the *E. binotatus* series, despite not having been assigned to any group.

Until recently, the genus *Ischnocnema* comprised only one member from the Atlantic Forest, *I. verrucosa* (Reinhardt and Lütken, 1862 "1861"), while the other six species were from the Andes and their vicinities (Padial et al., 2005). Caramaschi and Canedo (2006), based on osteological features observed in *I. verrucosa* (type species of the genus), placed *Ischnocnema* under the synonymy of *Eleutherodactylus* (where most current brachycephaloid frogs were placed at the time) and resurrected *Oreobates* Jiménez de la Espada, 1872, to allocate the five Andean species. Heinicke et al. (2007) then resurrected *Ischnocnema* to allocate the *Eleutherodactylus* from the Brazilian Atlantic Forest, with the exception of the former *E. binotatus* and *E. plicifer*, currently placed in the genus *Haddadus* Hedges, Duellman and Heinicke, 2008. Hedges et al. (2008) presented a phylogenetic hypothesis and proposed a new classification for New World direct-developing frogs, a clade they called Terrarana (currently the family Brachycephaloidea). Although only a few *Ischnocnema* species were present in their phylogenetic hypothesis (five of 29 species at the time), they divided the genus into five species series based on morphology and previous taxonomic proposals: *I. guentheri, I. lactea, I. parva, I. ramagii,* and *I. verrucosa*. The *I. guentheri* series contained the

96 species from Heyer (1984) plus *I. henselii* (Peters, 1870), which was resurrected from
97 the synonymy of *I. guentheri* by Kwet and Solé (2005), and *I. hoehnei*, *I. octavioi*, *I.*
98 *izecksohni*, and *I. vinhai*. The *I. lactea* series contained the species from the *E. lacteus*
99 group from Lynch and Duellman (1997) plus *I. bilineata* Bokermann, 1975 "1974", *I.*
100 *gehrti* (Miranda-Ribeiro, 1926), *I. manezinho* (Garcia, 1996), *I. paranaensis* (Langone
101 and Segalla, 1996), *I. randorum*, *I. sambaqui* (Castanho and Haddad, 2000), *I. spanios*,
102 and *I. venancioi*. The *I. parva* and *I. ramagii* series had the same content as the *E.*
103 *parvus* and *E. ramagii* groups of Lynch and Duellman (1997), respectively. Hedges et
104 al. (2008) also created the *I. verrucosa* series to allocate *I. verrucosa* and *I. juipoca*.
105 Canedo et al. (2010) described *I. surda* Canedo, Pimenta, Leite and Caramaschi,
106 2010, and placed it in the *I. verrucosa* series. They also took *I. octavioi* out of the *I.*
107 *guentheri* series and placed it, together with *I. penaxavantinho* Giaretta, Toffoli and
108 Oliveira, 2007, in the *I. verrucosa* series based on morphological characters. Canedo
109 and Haddad (2012) proposed a new classification for the superfamily
110 Brachycephaloidea based on the greatest sample effort of *Ischnocnema* in a
111 phylogenetic study until then, with about 80% of its described species. Among their
112 most important findings was that the *I. ramagii* series and *I. vinhai* actually belonged to
113 *Pristimantis* Jiménez de la Espada, 1870 and that *I. bilineata* was part of a distinct
114 family of Brachycephaloidea, Craugastoridae Hedges, Duellman and Heinicke, 2008.
115 Because they could not precisely identify the generic relationships of the latter, they
116 placed it as *incertae sedis* within the subfamily Holoadeninae Hedges, Duellman and
117 Heinicke, 2008. They also changed the content of all remaining *Ischnocnema* species
118 series (except for *I. parva*), with most of the changes occurring in the *I. lactea* series.
119 *Ischnocnema abdita* Canedo and Pimenta, 2010 (placed in the *I. lactea* series based on
120 morphology in the original description) and *I. bolbodactyla* went to the *I. verrucosa*

series, and *I. venancioi* went to the *I. guentheri* series. Additionally, Canedo and Haddad (2012) unassigned *I. manezinho* and *I. sambaqui* to the *I. lactea* series, and did not place them in any other series because of divergences in the phylogenetic position of the clade composed of these species among their phylogenetic analyses. The recently described *I. concolor* Targino, Costa and Carvalho-e-Silva, 2009, *I. melanopygia* Targino, Costa and Carvalho-e-Silva, 2009, and *I. vizzotoi* Martins and Haddad, 2010, had their taxonomic position confirmed within the *I. lactea* series. Later, the *I. parva* series gained a third member with the description of *I. nanahallux* Brusquetti, Thomé, Canedo, Condez and Haddad, 2013. Brusquetti et al. (2013) made a phylogenetic hypothesis including only five species of *Ischnocnema* and one *Brachycephalus* Fitzinger, 1826, where *I. nanahallux* was the sister species of *I. parva.* Despite the innumerous morphological similarities between *I. nanahallux* and the other members of the *I. parva* series, Taucce et al. (2018) tested its phylogenetic position in a more robust matrix, including all species of *Ischnocnema* with available genetic data at the time, and recovered it within the *I. parva* series with very low support. They argued that this lack of support was probably because they only had about 500 bp available for *I. nanahallux,* while their final alignment had more than 3500 bp. The authors also described *I. feioi* Taucce, Canedo and Haddad, 2018, and *I. garciai* Taucce, Canedo and Haddad, 2018, and placed them within the *I. guentheri* series.

Recent fieldwork and museum visits allowed us to discover new populations of *Ischnocnema* morphologically similar to *I. hoehnei* and *I. venancioi*, in the Brazilian states of Rio de Janeiro and Espírito Santo. Our main goals with this paper are to: (1) construct a robust molecular phylogenetic hypothesis for *Ischnocnema* to assess mainly the phylogenetic positions of *I. nanahallux* and our new populations, and (2) evaluate, using three lines of evidence (molecular, acoustic, and morphological data), whether our

146 newly discovered populations are conspecifics to *I. hoehnei* and *I. venancioi* or distinct
147 evolving lineages deserving a name.
148
149 2. Material and Methods
150
151 *2.1. Taxon and gene sampling*
152
153 We compiled a molecular dataset with an ingroup composed of all available
154 *Ischnocnema* species in GenBank (all terminals and respective accession numbers,
155 including those sequences produced during this work, are listed in Appendix A). We
156 also included specimens from three putative new species related to *I. venancioi* and *I.*
157 *hoehnei*: one from the municipality of Cachoeiras de Macacu, one from the high
158 grasslands of the Serra dos Órgãos National Park (PARNASO), both from the state of
159 Rio de Janeiro, and one from the municipality of Santa Teresa, state of Espírito Santo.
160 As an outgroup we used six *Brachycephalus* species, to represent the other lineage
161 within the family Brachycephalidae, and one species from each of the following
162 brachycephaloid genera: *Bryophryne* Hedges, Duellman and Heinicke, 2008;
163 *Craugastor* Cope, 1862; *Eleutherodactylus*; *Haddadus*; *Hypodactylus* Hedges,
164 Duellman and Heinicke, 2008; *Lynchius* Hedges, Duellman and Heinicke, 2008;
165 *Pristimantis*; and *Yunganastes* Padial, Castroviejo-Fisher, Köhler, Domic and De la
166 Riva, 2007.
167 We chose the mitochondrial 12S rRNA, tRNA Val, and partial sequence of 16S
168 rRNA genes, and partial sequences of the nuclear genes tyrosinase precursor (Tyr) and
169 recombination activation gene 1 (RAG1), because they have been successfully used in

most of the systematic studies of the Brachycephaloidea (*e.g.* Hedges et al. 2008; Canedo and Haddad, 2012; Padial et al. 2014).

2.2. Laboratory procedures

We extracted whole DNA from 100% ethanol-preserved muscle tissue using an ammonium acetate precipitation method (adapted by Lyra et al., 2017 from Maniatis et al., 1982) and then carried out PCR amplifications using Taq DNA Polymerase Master Mix (Ampliqon S/A, Denmark) and Axygen Maxygene thermocyclers. The standard PCR program for the mitochondrial markers follows Taucce et al. (2018). For the nuclear markers we used a nested-PCR program consisting of a first PCR reaction using the most external primers (Table 1). We then took 1 μL of the reaction product, added the most internal primers, and did a second PCR reaction. The first reaction consisted of a 3-min initial denaturing step at 95°C, followed by 20 cycles of 20 s at 95°C, 20 s at 52°C, and 45 s at 68°C, followed by a final extension step of 3 min at 68°C. The second reaction consisted of a 3-min initial denaturing step at 95°C, followed by 40 cycles of 20 s at 95°C, 20 s at 53°C, and 45 s at 68°C, followed by a final extension step of 3 min at 68°C. We purified PCR products following Lyra et al. (2017), which were sequenced in both directions, with a BigDye Terminator Cycle Sequencing Kit (version 3.0, Applied Biosystems) in an ABI 3730 automated DNA sequencer (Applied Biosystems) at Macrogen Inc. (Seoul, South Korea).

2.3. Molecular analyses

2.3.1. Alignment, partition schemes, and nucleotide substitution model selection

We performed alignment using MAFFT v7.130b (Katoh and Standley, 2013). For the nuclear gene fragments, we used the G-INS-i algorithm, which assumes the entire region can be aligned. For the mitochondrial gene fragments we used the E-INS-i algorithm, which is adapted for sequences with conserved domains and rich in gaps.

We conducted an *a priori* partition scheme with the three mitochondrial gene fragments and each codon position of the nuclear fragments as separate partitions. Then we made a search for the best partition scheme and best fitting nuclear models using PartitionFinder 2.1.1 (Lanfear et al., 2017) under the Corrected Akaike Information Criterion (AICc; Hurvich and Tsai, 1989). PartitionFinder uses maximum likelihood software to conduct part of the analyses and we chose PhyML 3.0 (Guindon et al., 2010) for this purpose.

2.3.2. Phylogenetic analyses and genetic distances

We conducted tree searches using three optimality criteria: Bayesian inference, maximum likelihood, and maximum parsimony. We computed Bayesian inference analysis in MrBayes 3.2.6 (Ronquist et al., 2012) using two independent runs of 1.0 x 10^7 generations, starting with random trees and four Markov chains (one cold), sampled every 1000 generations. We discarded 25% of generations and trees as burnin and performed the run with unlinked character state frequencies, substitution rates of the GTR model, gamma shape parameters, and proportion of invariable sites between partitions. We used the standard deviation of split frequencies (< 0.01), Estimated Sample Size (ESS > 100), and Potential Scale Reduction Factor (PSRF; Gelman and Rubin, 1992; should approach 1.0 as runs converge) to assess run convergence. We

computed maximum likelihood analysis in RAxML v. 8.2.10 (Stamatakis, 2014), searching the most likely tree 100 times and conducting 1000 non-parametric bootstrap replicates. We used the software TNT v. 1.5 (Goloboff and Catalano, 2016) treating gaps as missing data to construct the maximum parsimony hypothesis. The search for the most parsimonious tree was made using 50 RAS + TBR holding 100 trees per replicate and the resulting trees were used to construct a strict consensus tree. Parsimony Jackknife absolute frequencies were estimated on the consensus tree using 50 RAS + TBR and holding 10 trees per replicate for a total of 1000 replicates. The command *ttags* was used to save a SVG version of the tree. We used *Eleutherodactylus* as the root for all analyses and we drew the Bayesian inference tree using FigTree 1.4.2 (Rambaut, 2014).

We used the mitochondrial 16S rRNA fragment limited by the primers 16SAR and 16SBR (ca. 600 bp; Palumbi et al., 1991) to calculate genetic distances among *Ischnocnema hoehnei*, *I. venancioi*, and our newly discovered populations. We estimated the uncorrected pairwise distances utilizing R platform version 3.3.3 (R Core Team, 2017) with the packages APE version 5.0 (Paradis et al., 2004) and SPIDER version 1.4-2 (Brown et al., 2012).

2.4. Morphological analyses

We took the following measurements to the nearest 0.1 mm with a Mitutoyo® digital caliper under a stereomicroscope: snout-vent length (SVL), head length (from the tip of the snout to the angle of the jaw), head width (between the angles of the jaws), forearm length (from the elbow to the wrist), hand length (from the wrist to the tip of the third finger), thigh length (from the middle of the cloacal opening to the outer edge

of the knee), tibia length (from the outer edge of the knee to the outer edge of the heel), tarsal length (from the outer edge of the heel to the inner metatarsal tubercle), and foot length (from the proximal border of the inner metatarsal tubercle to the tip of the fourth toe). We also took eye diameter (between anterior and posterior margins of the eye), tympanum diameter (between anterior and posterior margins of the tympanum), eye-nostril distance (from the anterior margin of the eye to the posterior margin of the nostril), internarial distance (between the two medial margins of the nostrils), eye-to-eye distance (between the anterior margins of the eyes), third finger disk length (maximum width of disk on third finger), and fourth toe disk length (maximum width of disk on fourth toe) with an ocular micrometer coupled to a stereomicroscope. Sex was determined by the observation of nuptial pads and vocal slits in males and direct observation of the gonads of female specimens. Morphological nomenclature follows previous literature on Brachycephaloidea (Heyer, 1984; Heyer et al., 1990; Hedges et al., 2008; Duellman and Lehr, 2009). Museum acronyms follow Sabaj (2016) and a full list of specimens examined is given in Appendix B.

2.5. Call analyses

We recorded advertisement calls using a Marantz PMD 661 or a Tascam DR-40, coupled to a Sennheiser K6/ME66 unidirectional microphone. Recordings were carried out at 44.1 kHz with a 16 bit sampling size. Oliveira et al. (2008) described the call of *Ischnocnema hoehnei* and the analyzed call was kindly made available by one of the authors (Giaretta, A. A.), which we reanalyzed and redescribed it to facilitate comparisons.

To analyze the recordings we used the software Raven pro 1.5 (Bioacoustics Research Program, 2011). Spectrograms were produced using a window size of 512 samples, 75% overlap, hop size of 128 samples, Discrete Fourier Transform (DFT) of 1024 samples, and window type Hann. Resolution, contrast, and brightness were program default. We obtained spectrogram and oscillogram figures using tuneR version 1.3.2 (Ligges et al., 2013) and seewave version 2.0.5 (Sueur et al., 2008) packages of R platform version 3.3.3 (R Core Team, 2017). Spectrogram figures were produced with a window length of 512 samples, 75% overlap, hop size of 128 samples, and window name Hanning. Call recordings of Pedro P. G. Taucce (PPGT 009–014) and Leandro O. Drummond (LOD 001–005) are deposited in the CFBH collection. Voucher specimens are housed at CFBH and MNRJ. We list full information for the recordings in Appendix C.

We measured the following call parameters: call duration (Köhler et al., 2017), call rise time (Hepp and Canedo, 2013), dominant frequency (Köhler et al., 2017), notes per call, note (repetition) rate (total number of notes minus one, divided by the time between the beginning of the first note to the beginning of the last note; modified from the call rate parameter of Cocroft and Ryan, 1995), and note (repetition) rate acceleration (Gehara et al., 2013). Call and note concepts follow Köhler et al. (2017).

3. Results

3.1. Molecular analyses

3.1.1. Alignment, partition schemes, and nucleotide substitution model selection

294 We obtained a final alignment of 3800 base pairs (bp). Mitochondrial 12S
295 rRNA, tRNAVal, and 16S rRNA had 1029, 76, and 1528 bp respectively; nuclear
296 RAG1 and Tyr had 636 and 531 bp, respectively. Some species had one or two codon
297 insertion-deletions in RAG1 and we moved them to maintain the reading frame when
298 necessary. The best fitting partition scheme resulted in seven partitions, which are
299 shown together with the respective best fitting nucleotide substitution model in Table 2.
300 Although we used the seven partition schemes for the maximum likelihood analysis, we
301 used the General Time Reversible model with γ–distribution for all of them because
302 RAxML does not support applying different models to different partitions.
303
304 *3.1.2. Phylogenetic analyses and genetic distances*
305
306 The maximum likelihood and Bayesian inference analyses resulted in similar
307 topologies (Fig. 1) and Bayesian inference runs converged for all parameters we
308 checked (see session 2.3.2). The maximum parsimony tree also resulted in an overall
309 similar topology, but with some important differences (Fig. S1). From now on we will
310 give support in the following order, inside parentheses, when we talk about a clade:
311 Bayesian inference posterior probability, maximum likelihood bootstrap, and maximum
312 parsimony jackknife. The three topologies recovered the family Brachycephalidae (1.0,
313 93, and 71) and both genera *Brachycephalus* (1.0, 100, and 100) and *Ischnocnema* (1.0,
314 100, and 100) as monophyletic with high support, as well as the *I. lactea* (1.0, 100, and
315 100) and the *I. guentheri* series (0.98, 78, and 76). Within the *I. guentheri* series, the
316 three analyses recovered *I. venancioi*, *I. hoehnei*, and our putative species in a fully-
317 supported clade (1.0, 100, and 100), separated from a clade composed of the remaining
318 species of the *I. guentheri* series (1.0, 100, and 100). The *I. verrucosa* series was also

recovered as monophyletic, but it was poorly supported in the maximum parsimony topology (1.0, 99, and 58). The phylogenetic placement of the clade composed of *I.* cf. *manezinho* and *I. sambaqui* (1.0, 100, and 99) was not congruent among the three analyses. This clade was the sister group of all *Ischnocnema* except for the *I. lactea* series in the Bayesian inference and the maximum likelihood analyses (1.0 and 88); while in the maximum parsimony tree this clade was the sister of all *Ischnocnema* except for the *I. lactea* and *I. verrucosa* series, but with very low support (41). None of the analyses recovered the *I. parva* series as monophyletic. The recently described *I. nanahallux* was sister (1.0, 100, and 89) to a clade composed of the remaining members of the *I. parva* series and the members of the *I. guentheri* series (1.0, 100, and 77), with high support in the three topologies.

The uncorrected pairwise distance among *Ischnocnema venancioi*, *I. hoehnei,* and our putative species ranged from 7.3% (population from Cachoeiras de Macacu and population from Santa Teresa) to 14.9% (population from Cachoeiras de Macacu and population from the highland grasslands of PARNASO). The uncorrected pairwise distance within species ranged from 0.0% (*I. venancioi* and the population from Santa Teresa) to 2.2% (within *I. hoehnei*). Distances between and within species are summarized in Table 3.

3.2. Morphological analyses

Both external morphology and morphometric characters were important for the recognition of *Ischnocnema hoehnei*, *I. venancioi*, and our putative species. However, because only one specimen from the population from Cachoeiras de Macacu was available for us to examine, we preferred to exclude it from our morphometric analysis.

Two characters distinguish both our putative species from the other species from the *I. guentheri* series: Finger I smaller than Finger II (Finger I approximately the same size as Finger II in other species) and disks of fingers III and IV large and truncated (smaller and usually rounded in other species; Fig. 2). The SVL (Table 4; Fig. 3), the pattern of the posterior surface of the thigh (Fig. 4), the relative size of Finger I compared to Finger II, and the ratios foot length/SVL, tibia length/SVL, and fourth toe disk width/third finger disk width were important for differentiating *I. venancioi*, *I. hoehnei*, and the populations from Santa Teresa and the high-elevation grasslands of PARNASO. We give detailed information about the diagnostic characters and other morphological traits in the Taxonomic Accounts section.

3.3. Call analyses

We analyzed 30 advertisement calls from 12 individuals. We had calls available for *Ischnocnema hoehnei* and for the putative species from Santa Teresa and the high-elevation grasslands of the PARNASO. The advertisement calls are emitted sporadically as groups of short notes, without regular intervals between calls. The first notes have low energy, with notes increasing in energy gradually until an energy peak is reached (Fig. 5A–C). All analyzed advertisement calls are different from each other, and they are distinguished mainly by the dominant frequency, note (repetition) rate, and notes per call (Table 5). We also analyzed 19 territorial calls from two individuals from the population of Santa Teresa. The territorial and advertisement calls share a similar structure, but the first has a shorter call duration and its notes increase in energy more sharply than in the latter (Fig. 5D; Table 5).

369 *3.4. Taxonomic accounts*

370

371 The *Ischnocnema parva* series, as it is presently known (Brusquetti *et al.,* 2013;
372 followed by Padial *et al.,* 2014), comprises *I. parva*, *I. pusilla,* and *I. nanahallux*. In our
373 three phylogenetic analyses the *I. parva* series is recovered as polyphyletic (Figs. 1 and
374 S1), with *I. nanahallux* as the sister group of the *I. parva* and *I. guentheri* series. So, to
375 avoid non-monophyletic groupings, we propose the removal of *I. nanahallux* from the *I.*
376 *parva* series.
377 *Ischnocnema venancioi* and *I. hoehnei* are currently in the *I. guentheri* series
378 (Canedo and Haddad, 2012; Padial *et al.,* 2014; Taucce *et al.,* 2018). We recovered
379 these and the other related species in a fully supported clade (1.0, 100, and 100), sister
380 to all the remaining members of the *I. guentheri* series. Our results show that the
381 members of the *I. venancioi* clade, besides being molecularly different, are also
382 phenotypically distinguishable from all other currently recognized *Ischnocnema* species
383 series. For this reason, we propose the *Ischnocnema venancioi* species series to include
384 the members of this clade. We also redefine the *I. guentheri* series to fit this new
385 arrangement.
386 Finally, based on the molecular, acoustic, and morphological evidences
387 presented here, we consider *Ischnocnema venancioi*, *I. hoehnei*, and the two populations
388 from the high-elevation grasslands of the PARNASO and Santa Teresa as distinct
389 evolving lineages. We also have strong molecular evidence that the population from
390 Cachoeiras de Macacu is a distinct evolving lineage. However, because we are using an
391 integrative approach and we have only one specimen from this population without an
392 advertisement call, we will not describe it as new species. So, herein we redescribe *I.*
393 *venancioi*, *I. hoehnei*, and, since there is no available name for the populations from

Santa Teresa and from the high-elevation grasslands of PARNASO, we describe them as two new species.

3.4.1. ***Ischnocnema guentheri*** *species series*

Diagnosis: The *Ischnocnema guentheri* series is distinguished from all other *Ischnocnema* species series by the following combination of characters: (1) Finger I approximately the same size as Finger II; (2) tips of fingers II–IV expanded, discs of fingers III and IV medium-sized and usually rounded (Fig. 2C and D); (3) long legs, tibia length > 60% of SVL; (4) one large, conspicuous, glandular-appearing nuptial pad on Finger I; (5) dorsum smooth or finely tuberculate.

Content: The taxon contains 10 species: *Ischnocnema epipeda* (Heyer, 1984); *I. erythromera* (Heyer, 1984); *I. feioi* Taucce, Canedo and Haddad, 2018; *I. garciai* Taucce, Canedo and Haddad, 2018; *I. gualteri* (B. Lutz, 1974); *I. guentheri* (Steindachner, 1867); *I. henselii* (Peters, 1870); *I. izecksohni* (Caramaschi and Kisteumacher, 1989 “1988”); *I. nasuta* (A. Lutz, 1925); and *I. oea* (Heyer, 1984).

Distribution: The taxon is distributed throughout the Atlantic Forest in Southeast and South Brazil, in the states of Rio Grande do Sul, Santa Catarina, Paraná, São Paulo, Rio de Janeiro, Minas Gerais, and Espírito Santo. *Ischnocnema henselii* reaches the province of Misiones, northern Argentina.

Remarks: *Ischnocnema epipeda* and *I. gualteri* have yet to be phylogenetically tested, but we agree with previous authors (Canedo and Haddad, 2012; Taucce *et al.*, 2018) and

maintain these two species in the *I. guentheri* series based on external morphology. The last collection of these species dates from the late 1970's (Heyer, 1984), so there is no available material for DNA extraction. We went to the type localities of both *I. gualteri* (Granja Comari, municipality of Teresópolis, state of Rio de Janeiro) and *I. epipeda* (Santa Teresa, state of Espírito Santo), but we did not succeed in finding them. Efforts towards finding both species are of paramount importance to understand the phylogenetic relationships within the *I. guentheri* series.

3.4.2. ***Ischnocnema venancioi*** *species series, new taxon*

Diagnosis: The *Ischnocnema venancioi* series is distinguished from all other *Ischnocnema* species series by the following combination of characters: (1) Finger I smaller than Finger II; (2) tips of fingers II–IV expanded, discs of fingers III and IV large and truncated (Figs. 2A and B); (3) one large, conspicuous, glandular-appearing nuptial pad on Finger I; (4) dark-brown to black mask-like stripe starting at the tip of the snout or the nostril, contouring the *canthus rostralis*, passing through the eye (better seen in life, color fades in preservative, Fig. 6), contouring the dorsal portion of the tympanum, and finishing near arm insertion; (5) dorsum smooth or finely tuberculate.

Content: The taxon contains four species: *Ischnocnema venancioi* (Lutz, 1958), *Ischnocnema hoehnei* (Lutz, 1958), *Ischnocnema parnaso* sp. nov., and *Ischnocnema colibri* sp. nov.

Distribution: The taxon is distributed in the mountainous lands of Serra do Mar mountain range of the states of São Paulo and Rio de Janeiro and in the north portion of

444 the Serra da Mantiqueira mountain range in the state of Espírito Santo, all in Southeast
445 Brazil, from 800 m to almost 2200 m of elevation (Fig. 6).
446
447 *Remarks*: Bertha Lutz (1958) had already noted that the species of this series were
448 related, and described *Ischnocnema venancioi* and *I. hoehnei* in the same paper. All
449 subsequent phylogenetic hypotheses including both species have recovered them as
450 sister taxa (Canedo and Haddad, 2012; Taucce *et al.,* 2018). The two species were
451 previously placed in the *I. guentheri* series (Canedo and Haddad, 2012, Padial *et al.,*
452 2014, Taucce *et al.,* 2018), and despite the two series being closely related and are
453 always recovered as sister taxa (Canedo and Haddad, 2012; Taucce *et al.,* 2018, this
454 study), the previously proposed morphological diagnosis for the *I. guentheri* series,
455 including the *I. venancioi* series members, is no longer applicable for species of both
456 series together. We recovered the *I. venancioi* series as a fully-supported clade in our
457 three analyses and our data show that these species share some morphological features
458 distinguishing them from all other *Ischnocnema* species series. For these reasons we
459 decided to create the *I. venancioi* series.
460
461 *3.4.2.1.* ***Ischnocnema venancioi*** *(B. Lutz, 1958)*
462
463 Redescription (Figs. 2B, 3A, 4A, B, 5A, B, and 8)
464 *Eleutherodactylus venancioi* B. Lutz, 1958
465 *Eleutherodatylus (Eleutherodactylus) venancioi* – Lynch and Duellman, 1997
466 *Ischnocnema venancioi* – Heinicke, Duellman and Hedges, 2007
467

Lectotype: MNRJ 53573, adult male, designated herein, Serra dos Órgãos National Park (PARNASO), municipality of Teresópolis, state of Rio de Janeiro, Brazil, collected by Bertha Lutz in February 1956.

Paralectotypes: MNRJ 35185–35187, adult males collected in the municipality of Teresópolis, state of Rio de Janeiro, Brazil, by B. Lutz and J. Venancio in November 1944. MNRJ 53565–53566, poorly preserved, sex undetermined, collected in the municipality of Teresópolis, state of Rio de Janeiro, Brazil, by B. Lutz on 21 October 1952. MNRJ 53572, 53574–53580, 53582–53589, adult males and MNRJ 53581, poorly preserved, sex undetermined, collected with the holotype. MNRJ 53597, adult male, and MNRJ 53598, juvenile, collected in the municipality of Teresópolis, state of Rio de Janeiro, Brazil, by B. Lutz and J. Venancio in July 1943. MNRJ 53599–53600, poorly preserved, sex undetermined, collected at PARNASO, municipality of Teresópolis, state of Rio de Janeiro, Brazil, by B. Lutz and J. Venancio on 20 October 1946. MNRJ 56191–53194, adult males collected at PARNASO, municipality of Teresópolis, state of Rio de Janeiro, Brazil, by B. Lutz on 23–26 November 1956. MNRJ 56213, adult male, and MNRJ 56214, juvenile, collected at PARNASO, municipality of Teresópolis, state of Rio de Janeiro, Brazil, by B. Lutz and J. Venancio on 1–10 December 1944.

Diagnosis: In the *Ischnocnema venancioi* series by phylogenetic placement (Fig. 1) and the following combination of characters: (1) Finger I smaller than Finger II; (2) tips of fingers expanded, discs of fingers III and IV large and truncated (Fig. 2B); (3) one large, conspicuous, glandular-appearing nuptial pad on Finger I; (4) black mask-like stripe starting at the tip of the snout or the nostril, contouring the *canthus rostralis*, passing

493 through the eye (better seen in life, color fades in preservative, Fig. 5), contouring the
494 dorsal portion of the tympanum, and finishing near arm insertion; (5) dorsum smooth or
495 finely tuberculate.

496 *Ischnocnema venancioi* is distinguished from all other species of the *I. venancioi*
497 series by the following combination of characters: (1) small size (SVL in males 15.7–
498 22.3 mm, n = 31; female 24.1 mm, n = 1); (2) in preservative, posterior face of the thigh
499 with cream oval spots surrounded by a dark-brown background or with slim dark-brown
500 bars on a cream background (Fig. 2 A, B; cream spots and background yellow to orange
501 in life); (3) Finger I much smaller than Finger II (Finger I half to two thirds the size of
502 Finger II, not reaching the base of its disk); (4) foot small (foot length/SVL 0.40–0.54);
503 (5) tibia small; (tibia length/SVL = 0.48–0.60); (6) fourth toe disk small (fourth toe disk
504 width/third finger disk width = 0.53–0.93).
505
506 *Description of lectotype*: Small size (SVL 17.4 mm). Head longer than wide; head
507 length 46% of SVL, head width 37% of SVL; snout sub-elliptical in dorsal view,
508 acuminate in lateral view; nostril rounded, oriented laterally, located near the tip of the
509 snout; *canthus rostralis* slightly distinct, straight; loreal region slightly concave;
510 postrictal tubercles absent; eye protuberant, oriented laterally; eye diameter 31% of head
511 length; palpebral tubercles absent; tympanum distinct, rounded; tympanic membrane
512 undifferentiated; annulus present, visible externally; tympanum diameter 34% of eye
513 diameter; supratympanic fold absent; vocal slits present; vocal sac not apparent; tongue
514 elliptical, without posterior notch; choanae rounded; dentigerous processes of the vomer
515 located posteromedially to choanae, triangle-shaped, medially separated by a gap
516 approximately the width of one dentigerous process; vomerine teeth present.

Forelimb slender; palmar tubercle indistinct; thenar tubercle indistinct; single glandular-appearing nuptial pad, extending dorsally from the distal to the proximal portion of metacarpus on Finger I; palm smooth; supernumerary tubercles absent; single subarticular tubercles prominent, rounded, large; fingers slender, without fringes; tip of Finger I slightly expanded; tips of fingers II– IV fairly expanded, truncated, with a V-shaped median slit in dorsal view; fourth toe disk small, width 56% of third finger disk; Finger I approximately two thirds the size of Finger II; finger lengths I < II < IV < III.

Hindlimb slender; shank longer than thigh; tibia length 57% of SVL, thigh length 51% of SVL; calcar tubercle absent; tarsal folds absent; foot small, length 45% of SVL; inner metatarsal tubercle elliptical, much larger than rounded outer metatarsal tubercle; sole of foot smooth; supernumerary tubercles absent; single subarticular tubercles present, large, prominent, rounded; toes long, slender, without fringes; tip of Toe I slightly expanded; tips of toes II–V fairly expanded, truncated, with a V-shaped median slit in dorsal view; toe lengths I < II < V < III < IV.

Dorsal skin smooth, with a few sparse tubercles; vertebral line from behind the eyes to vent; venter smooth; discoidal and thoracic folds absent.

Coloration of lectotype in preservative: The specimen is rather faded so the dorsal pattern is unclear. Dorsum yellowish-brown; one large brown heart-shaped spot starting just posterior to eyes and reaching level of the top of tympanum; two brown dots at the level of arm insertion; one brown transverse narrow band at the level of the sacral vertebra; head yellowish-brown, with one brown spot on the dorsal surface just anterior to eyes; loreal region with brown mask-like stripe from the tip of the nose to near the arm insertion; forelimb yellowish-brown; hindlimb yellowish-brown; posterior surface

of the thigh with cream-colored oval spots surrounded by a brown background; venter and gular region cream-colored, with sparse brown dots.

Measurements of lectotype (in millimeters): SVL 17.4, head length 8.0, head width 6.5, eye diameter 2.5, tympanum diameter 0.9, eye-nostril distance 1.5, internarial distance 1.8, eye-to-eye distance 2.8, forearm length 3.8, hand length 4.2, third finger disk length 0.9, thigh length 8.8, tibia length 10.0, tarsal length 5.9, foot length 7.9, and fourth toe disk length 0.5.

Variation: Additional referred specimens are listed in Appendix B. Nostril opening can also be elliptical, as can also be the tympanum. Tongue is elliptical, ovoid, or rounded. Finger I is half to two-thirds as large as Finger II. Some specimens have palpebral tubercles. Palmar and thenar tubercles are sometimes slightly distinct, the former heart-shaped and the latter elliptical, both the same size. Posterior surface of the thigh in preservative with cream-colored spots over a brown background or brown bars over a cream-colored background (Fig. 4A, B; cream-colored portions yellow to orange in life, Fig. 5A, B). Dorsum can also be finely tuberculate. Lutz (1958) stated, and we confirm, that *Ischnocnema venacioi* has three dorsal patterns: one with “longitudinal bands of diverse tones” (Fig. 3A; Figs. 1, 3, and 6 in B. Lutz [1958]); the “tapestry-like” pattern, with “intrincate figures, centered around the narrow light vertebral line” (Fig. 5B; Figs. 2, 4, and 5 in B. Lutz [1958]); and no distinct pattern (Fig. 5A). Sometimes the nuptial pad is difficult to see because it is exactly the same color as the skin. Female specimen (SVL 24.1 mm, n = 1) is much larger than male specimens (SVL 15.7–22.3 mm, n = 31). Variation in SVL and body proportions is given in Table 4. In life the iris is bicolored, with a lighter superior half with shades going from metallic blue to light

566 brown, and a darker lower half usually of a dark brown shade similar to that of the
567 canthal stripe.
568
569 *Advertisement call*: Not formally described. In the original description (B. Lutz, 1958)
570 the sound is described as a *"crrr crrr*", which makes sense when you listen to the calls
571 of the other species in the *I. venancioi* series (described below).
572
573 *Comparison with other species*: Finger I smaller than Finger II distinguishes
574 *Ischnocnema venancioi* from members of the *I. guentheri, I. parva*, and *I verrucosa*
575 series and from *I. manezinho* (Finger I approximately the same size as Finger II in these
576 species; Garcia, 1996; Hedges et al., 2008). Expanded tips of fingers II–IV and large
577 truncated discs of fingers III and IV distinguish *I. venancioi* from members of the *I.*
578 *parva* series, *I. nanahallux* (tips of fingers not expanded in these species; Hedges et al.,
579 2008, Brusquetti et al., 2013), and members of the *I. verrucosa* series (disks small or
580 moderately-sized in these species; Hedges et al., 2008, Canedo et al., 2012). The large,
581 conspicuous, glandular-appearing nuptial pad differentiates *I. venancioi* from *I.*
582 *manezinho*, *I. sambaqui*, *I. nanahallux*, and the members of the *I. lactea* series (minute
583 nuptial pad in *I. randorum*; translucent in *I.* nigriventris and *I. vizottoi*; reduced to some
584 white granules in *I. holti*; absent in *I.* manezinho, *I. sambaqui, I. nanahallux, I.*
585 *melanopygia* and *I. spanios*; unknown in other species; Heyer, 1985; Hedges et al.,
586 2008; Targino and Carvalho-e-Silva, 2008; Berneck et al., 2013) and *I. verrucosa* series
587 (except for *I. surda*; faint, translucent nuptial pad in *I. karst* [Canedo, Targino, Leite and
588 Haddad, 2012]; absent in other species; Hedges et al., 2008; Canedo et al. 2010, 2012).
589 The mask-like stripe starting at the tip of the snout or the nostril, contouring the *canthus*
590 *rostralis*, passing through the eye, contouring the dorsal portion of the tympanum, and

591 finishing near arm insertion distinguishes *I. venancioi* from *I. manezinho, I. sambaqui*,
592 and the members of the *I. guentheri*, *I. lactea,* and *I. verrucosa* series (mask-like stripe
593 usually absent in these species; when present it does not pass through the eye). The
594 smooth or finely tuberculate dorsum distinguishes *I. venancioi* from *I. sambaqui* (rugose
595 in *I. sambaqui*; Castanho and Haddad, 2000) and from the members of the *I. verrocusa*
596 series (tuberculate in these species; Hedges at al., 2008, Canedo et al., 2010, 2012).
597 *Ischnocnema venancioi* (SVL of males 15.7–22.3 mm, female 24.1 mm) differs
598 from all other species of the *I. venancioi* series by its smaller size (SVL of males of
599 other species of the *I. venancioi* species series 22.9–34.8 mm; of females 31.1–42.7
600 mm), by the posterior surface of the thigh with cream-colored ovoid spots surrounded
601 by a dark-brown background or with dark-brown slim bar on a cream-colored
602 background in preservative (cream-colored spots and background yellow to orange in
603 life; posterior surface of the thigh mottled in other species of the *I. venancioi* species
604 series), and by Finger I being much smaller than Finger II (Finger I reaching
605 approximately the base of the disk of Finger II in other species of the *I. venancioi*
606 species series).
607 By its smaller foot, *I. venancioi* (foot length/SVL = 0.40–0.54) differs from *I.*
608 *hoehnei* (foot length/SVL = 0.67–0.70) and from *I. parnaso* sp. nov. (foot length/SVL =
609 0.55–0.63). By its smaller tibia, *I. venancioi* (tibia/SVL = 0.48–0.60) differs from *I.*
610 *hoehnei* (tibia/SVL = 0.67–0.73) and by the smaller fourth toe disk, *I. venancioi* (fourth
611 toe disk length/third finger disk length = 0.53–0.93) differs from *I. parnaso* sp. nov.
612 (fourth toe disk length/third finger disk length = 1.00–1.09).
613

Geographic distribution: *Ischnocnema venancioi* is currently known from the highlands above 800 m of the Serra dos Órgãos mountain range in the state of Rio de Janeiro, in the municipalities of Teresópolis and Nova Friburgo.

Natural history notes: The species is usually found in association with bromeliad plants (B. Lutz, 1958, this study). Individuals start calling at dusk while perched on the leaves of ground bromeliads or other low vegetation (B. Lutz, 1958).

Remarks: In the original description of *Eleutherodactylus venancioi* (= *Ischnocnema venancioi*), Bertha Lutz (1958) included in the "Type locality and types" section (*Localidade tipo e tipos* section in the part in Portuguese) "6 female cotypes, 60 paratypes, males or not sexed" but did not designate a holotype or give museum numbers. Based on the article 72.1.1 of the International Code of Zoological Nomenclature, we consider all 66 specimens as the type series, because the author referred to all of them as types (B. Lutz 1958). Additionally, separating the specimens in "cotypes" and "paratypes" is not a situation provided by article 72.4.6, so we consider all 66 specimens as syntypes. We found 33 specimens at the Museu Nacional, Rio de Janeiro, Brazil, collected before 1958 (the year of the species description), and since Bertha Lutz worked at the Museu Nacional, and all the specimens were collected by her, we assume that these were part of the specimens she used to describe *E. venancioi*. Most specimens are well-preserved and bear all the diagnostic characters we used to identify the species. So, among these well-preserved specimens, we hereby designate the MNRJ 53573 as the lectotype of *Eleutherodactylus venancioi*. All other specimens (partially listed above) are paralectotypes.

Frost (2017) mentions that the species is known from the coastal mountains of Rio de Janeiro and São Paulo, Brazil, but we are not aware of *I. venancioi* occurring in any locality outside the state of Rio de Janeiro.

3.4.2.2. ***Ischnocnema hoehnei*** *(B. Lutz, 1958)*

Redescription (Figs. 2A, 3D, 4C, 5C, and 9)

Eleutherodactylus hoehnei B. Lutz, 1958

Eleutherodatylus (Eleutherodactylus) hoehnei – Lynch and Duellman, 1997

Ischnocnema hoehnei – Heinicke, Duellman and Hedges, 2007

Holotype: AL-MN 2525, adult female collected at Reserva Biológica do Alto da Serra de Paranapiacaba (RBASP, formerly Estação Biológica do Alto da Serra), Paranapiacaba, municipality of Santo André, state of São Paulo, Brazil, by F. C. Hoehne in April 1934.

Paratypes: AL-MN 2526 (collected with the holotype; not examined), AL-MN 3376 (cleared for osteological studies according to the original publication; not examined), MZUSP 10201–10206, 10177–10178, 11000, 11064 (not examined).

Diagnosis: In the *Ischnocnema venancioi* series by phylogenetic placement (Fig. 1) and the following combination of characters: (1) Finger I smaller than Finger II; (2) tips of fingers expanded, discs of fingers III and IV large and truncated (Fig. 2A); (3) one large, conspicuous, glandular-appearing nuptial pad on Finger I; (4) black mask-like stripe starting at the tip of the snout or the nostril, contouring the *canthus rostralis*,

passing through the eye (better seen in life, Fig. 5), contouring the dorsal portion of the tympanum, and finishing near arm insertion; (5) dorsum smooth or finely tuberculate. *Ischnocnema hoehnei* is distinguished from all other species of the *I. venancioi* series by the following combination of characters: (1) large size (SVL of males 30.6–34.8 mm, n = 3; female 42.7 mm, n = 1); (2) foot large (foot length/SVL 0.67–0.70); (3) tibia large (tibia length/SVL = 0.67–0.73); (4) posterior face of thigh mottled, forming small irregular spots in some specimens (Fig. 2C); (5) Finger I slightly smaller than Finger II (tip of Finger I reaching the base of the disk of Finger II approximately); (6) fourth toe disk small (fourth toe disk width/third finger disk width = 0.93–0.96); (7) low advertisement call frequency (1.90 kHz); (8) advertisement call with a high number of notes (59); (9) medium note (repetition) rate (35.85 notes per second).

Redescription of holotype: large size (42.7 mm), head longer than wide; head length 43% of SVL; head width 36% of SVL; snout sub-elliptical in dorsal view, acuminate in lateral view; nostril elliptical, oriented laterally, located near tip of snout; *canthus rostralis* distinct, straight; loreal region slightly concave; postrictal tubercles absent; eye protuberant, oriented laterally; eye diameter 34% of head length; one palpebral tubercle; tympanum distinct, rounded; tympanic membrane undifferentiated; annulus present, visible externally; tympanum diameter 38% of eye diameter; supratympanic fold absent; tongue large, ovoid, without posterior notch; choanae rounded; dentigerous processes of the vomer located posteriormedialy to choanae, triangle-shaped, medially separated by a gap approximately the width of one dentigerous process; vomerine teeth present.

Forelimb slender; palmar tubercle slightly distinct, heart-shaped; thenar tubercle elliptical, less than half the size of palmar tubercle; palm smooth; three slightly distinct supernumerary tubercles; single subarticular tubercles prominent, rounded, large;

fingers slender, without fringes; tip of Finger I slightly expanded; tips of fingers II– IV fairly expanded, truncated, with a V-shaped median slit in dorsal view; fourth toe disk small; fourth toe disk width 93% of third finger disk; Finger I slightly smaller than Finger II, its length reaching the base of Finger II disk; finger lengths I < II < IV < III.

Hindlimb slender; shank longer than thigh; tibia length 73% of SVL; thigh length 59% of SVL; posteroventral surface of the thighs areolate; calcar tubercle small; tarsal folds absent; foot large; foot length 67% of SVL; inner metatarsal tubercle elliptical, much larger than outer metatarsal tubercle, rounded; sole of foot smooth; a few small supernumerary tubercles; single subarticular tubercles present, large, prominent, rounded; toes long, slender, with discrete fringes; tip of Toe I slightly expanded; tips of toes II–V fairly expanded, truncated, with a V-shaped median slit in dorsal view; toe lengths I < II < V < III < IV.

Dorsal skin smooth, with a few sparse tubercles; vertebral line from just anterior to eyes extending almost to vent; venter finely tuberculate; discoidal and thoracic folds present.

Coloration of holotype in preservative: The specimen is somewhat faded. Dorsum with shades of beige and brown, with a broad brown band of irregular width starting posterior to the eyes and finishing at the vent, narrowing three times throughout its length, and irregularly spaced brown dots; loreal region with brown mask-like stripe from the tip of the nose to near arm insertion; forelimb beige; hindlimb striped beige and faded brown dorsally; cream-colored ventrally; posterior surface of the thighs beige; venter beige.

Measurements of holotype (in millimeters): SVL 42.7, head length 18.5, head width 15.2, eye diameter 6.3, tympanum diameter 2.4, eye-nostril distance 3.6, internarial distance 5.2, eye-to-eye distance 7.3, forearm length 9.5, hand length 13.2, third finger disk length 2.4, thigh length 25.1, tibia length 31.0, tarsal length 14.6, foot length 28.8, and fourth toe disk length 2.2.

Variation: Additional referred specimens are listed in Appendix B. Dorsum can be finely tuberculate, mask-like stripe can reach beyond the insertion of the arms, and tongue is elliptical in some specimens. Fingers of other specimens bear discrete fringes and the dorsal pattern is variable (see B. Lutz, 1958 for illustrations). Vocal sac in males is single, subgular, and slightly expanded externally, vocal slits present and nuptial pad single, apparently-glandular, same color as the hand. Female specimen (SVL 42.7 mm, n = 1) is much larger than male specimens (SVL 30.6–34.8 mm, n = 3). Variation in SVL and body proportions is given in Table 4.

Advertisement call: Only one advertisement call was available for our analysis. The call consists of several short notes emitted in regular intervals. The call begins with low energy notes, which increase in energy over time, until reaching a peak almost at the end of the call. The last note has notably less energy than the penultimate note (Fig. 7A). Call duration 1.65 s, call rise time 96%, dominant frequency 1.90 kHz, 59 notes per call, note (repetition) rate 35.85 notes per second, and note (repetition) rate acceleration -20%.

Comparison with other species: Finger I smaller than Finger II distinguishes *Ischnocnema hoehnei* from members of the *I. guentheri, I. parva*, and *I verrucosa* series

and from *I. manezinho* (Finger I approximately the same size as Finger II in these species; Garcia, 1996; Hedges et al., 2008). Expanded tips of fingers II–IV and large truncated discs of fingers III and IV distinguish *I. hoehnei* from members of the *I. parva* series, *I. nanahallux* (tips of fingers not expanded in these species; Hedges et al., 2008, Brusquetti et al., 2013), and members of the *I. verrucosa* series (disks small or moderately-sized in these species; Hedges et al., 2008, Canedo et al., 2012). The large, conspicuous, glandular-appearing nuptial pad differentiates *I. hoehnei* from *I. manezinho*, *I. sambaqui*, *I. nanahallux*, and the members of the *I. lactea* (minute nuptial pad in *I. randorum;* translucent in *I.* nigriventris and *I. vizottoi*; reduced to some white granules in *I. holti*; absent in *I. melanopygia* and *I. spanios*; unknown in other species; Heyer, 1985; Hedges et al., 2008; Targino and Carvalho-e-Silva, 2008; Berneck et al., 2013) and *I. verrucosa* series (except for *I. surda*; faint, translucent nuptial pad in *I. karst*; absent in other species; Hedges et al., 2008; Canedo et al., 2010, 2012). The mask-like stripe starting at the tip of the snout or the nostril, contouring the *canthus rostralis*, passing through the eye, contouring the dorsal portion of the tympanum, and finishing near arm insertion distinguishes *I. hoehnei* from *I. manezinho, I. sambaqui*, and the members of the *I. guentheri*, *I. lactea,* and *I. verrucosa* series (mask-like stripe usually absent in these species; when present it does not pass through the eye). The smooth or finely tuberculate dorsum distinguishes *I. hoehnei* from *I. sambaqui* (rugose; Castanho and Haddad, 2000) and from the members of the *I. verrocusa* series (tuberculate in these species; Hedges at al., 2008, Canedo et al., 2010, 2012).

By its large size (SVL of males 30.6–34.8 mm, n = 3; female 42.7 mm, n = 1), large foot (foot length/SVL 0.67–0.70), and large shank (tibia length/SVL 0.67–0.73), *Ischnocnema hoehnei* differs from all other species of the *I. venancioi* species series (combined SVL of males 15.7–30.3 mm, n = 41; females 24.1–38.0 mm, n = 5).

762 The mottled posterior surface of the thigh, forming small irregular cream-
763 colored spots in some specimens, of *I. hoehnei* distinguishes it from *I. venancioi*
764 (posterior surface of the thigh with cream-colored oval spots surrounded by a dark-
765 brown background or with dark-brown slim bars on a clear background; cream-colored
766 spots and background yellow to orange in life), *I. parnaso* sp. nov. (posterior surface of
767 the thigh with cream-colored large irregular-shaped spots surrounded by a mottled
768 background), and *I. colibri* sp. nov. (posterior surface of the thigh mottled, interleaved
769 with cream-colored bars, forming a striped pattern, or with large irregular-shaped
770 cream-colored spots surrounded by a mottled background). Having Finger I slightly
771 smaller than the Finger II, reaching approximately the base of Finger II, distinguishes *I.*
772 *hoehnei* from *I. venancioi* (Finger I much smaller than Finger II, not reaching the base
773 of Finger II) and by having the fourth toe disk small (fourth toe disk width/third finger
774 disk width = 0.93–0.96) differentiates *I. hoehnei* from *I. parnaso* sp. nov. (fourth toe
775 disk width/third finger disk width = 1.00–1.09).
776 *Ischnocnema hoehnei* differs from *I. parnaso* sp. nov. and *I. colibri* sp. nov. by
777 the lower frequency of its advertisement call (1.90 kHz in *I. hoehnei*; 2.34–2.84 kHz in
778 the two new species), by the higher number of notes per call (59 in *I. hoehnei*; 18–53 in
779 the two new species), and by the intermediate note (repetition) rate (35.85 notes per
780 second in *I. hoehnei*; 41.30–44.82 notes per second in *I. colibri* sp. nov. and 16.55–
781 21.17 notes per second in *I. parnaso* sp. nov.).
782
783 *Natural history notes*: The natural history and habits of *I. hoehnei* are poorly known.
784 Specimens are usually found perched on ground bromeliads or other ground plants
785 (Heyer *et al.,* 1990; Malagoli, L. R. personal communication). The species is commonly

found in open areas inside forests, such as clearings or stream margins (B. Lutz, 1958; Heyer *et al.,* 1990; Oliveira *et al.,* 2008).

Geographic distribution: *Ischnocnema hoehnei* is currently known from the highlands (above 800 m of elevation) of Serra do Mar mountain range in the state of São Paulo, Brazil, from the municipalities of Santo André, Itanhaém, Salesópolis, Pilar do Sul, and São Miguel Arcanjo.

Remarks: Heyer *et al.* (1990) mentioned one male (SVL = 22.0 mm) and one female (SVL = 29.4 mm) specimen from Boracéia, municipality of Salesópolis. They stated that the male specimen lacked vocal slits and nuptial pads. All male specimens that we analyzed had both these characters and our smallest specimen had an SVL of 30.6 mm, much larger than the male from Boracéia. The authors mentioned some diagnostic characters of *Ischnocnema hoehnei*, like the mask-like stripe, the large foot, and the large shank. We did not examine these specimens but we believe they are indeed *I. hoehnei* and the male specimen lacked vocal slits and nuptial pads because it was a subadult. Hedges *et al.* (2008) also mentioned that *I. hoehnei* lacks nuptial pads, probably following Heyer *et al.* (1990).

As noted by B. Lutz (1958) in the original description, the large size and the color pattern (including the mask-like stripe) of *I. hoehnei* is superficially similar to that of *Haddadus binotatus* (Spix, 1824). However, the two species have notable differences. *Haddadus binotatus* has a series of longitudinal glandular ridges in the dorsum and Finger I is much larger than Finger II (dorsum lacking glandular ridges and Finger I slightly smaller than Finger II in *I. hoehnei*). Males of *H. binotatus* lack nuptial pads on Finger I (nuptial pads present in males of *I. hoehnei*).

811

812 *3.4.2.3.* ***Ischnocnema parnaso*** *sp. nov.*

813

814 (Figs. 3C, 4D, 5D, and 10)

815

816 *Holotype:* CFBH 41812, adult male collected at Pedra do Sino, Serra dos Órgãos
817 National Park (PARNASO), municipality of Guapimirim, state of Rio de Janeiro, Brazil
818 (22°27'42"S, 43°01'50"W, 2180 m of elevation), by Drummond, L. O. and Nogueira-
819 Costa, P. on December 20 2015.

820

821 *Paratypes*: CFBH 41813, adult male, MNRJ 91759, adult female, both collected with
822 the holotype. MNRJ 91756–91758, adult males collected at Pedra da Baleia,
823 PARNASO, municipality of Guapimirim, state of Rio de Janeiro, Brazil (22°27'40"S,
824 43°01'38"W, 2142 m of elevation), by Drummond, L. O. and Nogueira-Costa, P. on
825 December 21 2015.

826

827 *Diagnosis*: In the *Ischnocnema venancioi* series by phylogenetic placement (Fig. 1) and
828 the following combination of characters: (1) Finger I smaller than Finger II; (2) tips of
829 fingers expanded, discs of fingers III and IV large and truncated; (3) one large,
830 conspicuous, glandular-appearing nuptial pad on Finger I; (4) black mask-like stripe
831 starting at the tip of the snout or the nostril, contouring the *canthus rostralis*, passing
832 through the eye, contouring the dorsal portion of the tympanum, and finishing near arm
833 insertion; (5) dorsum smooth. *Ischnocnema parnaso* sp. nov. is distinguished from all
834 other species of the *I. venancioi* series by the following combination of characters: (1)
835 medium-size (SVL of males 27.1–30.3 mm, n = 5; female 38.0 mm, n = 1); (2) medium-

836 size foot (foot length/SVL 0.55–0.63); (3) small tibia (tibia length/SVL = 0.55–0.59);
837 (4) posterior surface of the thigh with large irregular-shaped cream-colored spots
838 surrounded by a mottled background; (5) Finger I slightly smaller than Finger II (tip of
839 Finger I reaching the base of Finger II approximately); (6) fourth toe disk large (fourth
840 toe disk width/third finger disk width = 1.00–1.09); (7) high advertisement call
841 frequency (2.34–2.67 kHz); (8) advertisement call with low number of notes (18–29);
842 (9) low note (repetition) rate (16.55–21.17 notes per second).
843
844 *Description of holotype*: Medium-size (SVL = 29.1 mm). Head longer than wide; head
845 length 39% of the SVL, head width 35% of the SVL; snout sub-elliptical in dorsal view,
846 acuminate in lateral view; nostril rounded, oriented laterally, located near the tip of
847 snout; *canthus rostralis* slightly distinct, straight; loreal region slightly concave;
848 postrictal tubercles absent; eye protuberant, oriented laterally; eye diameter 31% of head
849 length; palpebral tubercles absent; tympanum distinct, rounded; tympanic membrane
850 undifferentiated; annulus present, visible externally; tympanum diameter 43% of eye
851 diameter; supratympanic fold absent; vocal slits present; vocal sac slightly distinct, one
852 visible fold parallel to left side of the jaw; tongue large, elliptical, without posterior
853 notch; choanae rounded; dentigerous processes of the vomer located posteromedially to
854 choanae, triangle-shaped, medially separated by a gap approximately the same size as
855 one dentigerous process; vomerine teeth present.
856 Forelimb slender; palmar tubercle barely distinct, heart-shaped, its diameter
857 approximately equal that of the thenar tubercle; thenar tubercle barely distinct, elliptical;
858 single glandular-appearing nuptial pad, extending dorsally from the distal to the
859 proximal portion of metacarpus on Finger I, the same color as the surrounding skin;
860 palm smooth; supernumerary tubercles absent; single subarticular tubercles prominent,

rounded, large; fingers slender, without fringes; tip of Finger I not expanded; tip of Finger II slightly expanded; tips of fingers III and IV fairly expanded, truncated, with a V-shaped median slit in dorsal view; Finger I slightly smaller than Finger II, its length reaching the base of Finger II disk; finger lengths I < II < IV < III.

Hindlimb slender; shank longer than thigh; tibia length 58% of SVL; thigh length 55% of SVL; calcar tubercle absent; tarsal folds absent; foot medium-size; foot length 60 % of SVL; inner metatarsal tubercle elliptical, twice as big as outer metatarsal tubercle; outer metatarsal tubercle rounded; sole of foot smooth; supernumerary tubercles absent; single subarticular tubercles present, large, prominent, rounded; toes long, slender, without fringes; tip of Toe I slightly expanded; tips of toes II–V fairly expanded, truncated, with a V-shaped median slit in dorsal view; toe lengths I < II < V< III< IV.

Dorsal skin smooth; vertebral line absent; venter smooth; discoidal and thoracic folds absent.

Coloration of holotype: Background cream-colored; dorsum with several sparse dark-brown dots; loreal region with dark-brown mask-like stripe from the tip of the snout to near the arm insertion; dark-brown dots forming a blotch on the dorsal part of the head, between the eyes; forelimb cream-colored, with several dark-brown dots larger than those of the dorsum over the dorsal surfaces of the arm, forearm, and hand; ventral surfaces of the arm, forearm, and hand with more sparse dark-brown dots; hindlimb cream-colored, with several dark-brown dots larger than those of the dorsum and smaller than those of the forelimb over dorsal and ventral surfaces of the thigh, tibia, and dorsal surface of the foot; dark-brown dots less sparse on the sole of the foot; posterior surface of the thigh with cream-colored irregular spots surrounded by dark-

brown mottled background; venter cream-colored with a few dark-brown dots on the chest; gular region cream-colored; jaw bordered by concentrated small dark-brown dots forming a thin line.

Measurements of holotype (in millimeters): SVL 29.1, head length 11.3, head width 10.2, eye diameter 3.5, tympanum diameter 1.5, eye-nostril distance 2.5, internarial distance 2.8, eye-to-eye distance 5.0, forearm length 5.5, hand length 8.6, third finger disk length 1.4, thigh length 15.9, tibia length 17.0, tarsal length 8.0, foot length 17.6, and fourth toe disk length 1.5.

Variation: Tongue is rounded, elongated, or triangular and choanae is elliptical in some specimens. Postrictal tubercle is present in female specimen. Thoracic fold is present in some specimens. Sometimes the nuptial pad is difficult to see because it is exactly the same color as the surrounding skin. Female specimen (SVL 38.0 mm, n = 1) is much larger than male specimens (SVL 27.1–30.3 mm, n = 5). Variation in SVL and body proportions is given in Table 4.

Etymology: The name "PARNASO" is the abbreviation for Parque Nacional da Serra dos Órgãos (Serra dos Órgãos National Park), type locality of the species. The park was created on November 30, 1939, and it is the third oldest park in Brazil, housing astonishing biodiversity. It is also the type locality of several anurans and one of the most important Atlantic Forest conservation units in Brazil. The name is used here as a noun in apposition.

910 *Advertisement call*: The advertisement call (19 calls of five males; Table 6; Fig. 7B) is
911 emitted sporadically and is composed of 18 to 29 notes ($\bar{X}$ = 25.00 ± 3.04) emitted at
912 regular intervals. The call begins with low energy notes, which increase in energy over
913 time, until reaching a peak almost at the end of the call. The last note usually has
914 notably less energy than the penultimate note. The call rise time is 42–92% ($\bar{X}$ = 66.06 ±
915 15.34) and the dominant frequency 2.34–2.67 kHz ($\bar{X}$ = 2.46 ± 0.09). The advertisement
916 call lasts 1.00 to 1.50 s ($\bar{X}$ = 1.25 ± 0.12) and the note (repetition) rate is 16.55–21.17
917 notes per second ($\bar{X}$ = 19.58 ± 1.32). The note rate decelerates at the end of the call,
918 with a note rate acceleration of -36–-11% ($\bar{X}$ = -22.98 ± 5.99).
919
920 *Comparison with other species*: Finger I smaller than Finger II distinguishes
921 *Ischnocnema parnaso* sp. nov. from members of the *I. guentheri, I. parva*, and *I*
922 *verrucosa* series and from *I. manezinho* (Finger I approximately the same size as Finger
923 II in these species; Garcia, 1996; Hedges et al., 2008). Expanded tips of fingers II–IV
924 and large truncated discs of fingers III and IV distinguish *I. parnaso* sp. nov. from
925 members of the *I. parva* series, *I. nanahallux* (tips of fingers not expanded in these
926 species; Hedges et al., 2008, Brusquetti et al., 2013), and members of the *I. verrucosa*
927 series (disks small or moderately-sized in these species; Hedges et al., 2008, Canedo et
928 al., 2012). The large, conspicuous, glandular-appearing nuptial pad differentiates *I.*
929 *parnaso* sp. nov. from *I. manezinho*, *I. sambaqui*, *I. nanahallux*, and the members of the
930 *I. lactea* (minute nuptial pad in *I. randorum;* translucent in *I.* nigriventris and *I. vizottoi*;
931 reduced to some white granules in *I. holti*; absent in *I. melanopygia* and *I. spanios*;
932 unknown in other species; Heyer, 1985; Hedges et al., 2008; Targino and Carvalho-e-
933 Silva, 2008; Berneck et al., 2013) and *I. verrucosa* series (except for *I. surda*; faint,
934 translucent nuptial pad in *I. karst*; absent in other species; Hedges et al., 2008; Canedo

et al., 2010, 2012). The mask-like stripe starting at the tip of the snout or the nostril, contouring the *canthus rostralis*, passing through the eye, contouring the dorsal portion of the tympanum and reaching near arm insertion distinguishes *I. parnaso* sp. nov. from *I. manezinho, I. sambaqui*, and the members of the *I. guentheri*, *I. lactea,* and *I. verrucosa* series (mask-like stripe usually absent in these species; when present it does not pass through the eye). The smooth or finely tuberculate dorsum distinguishes *I. parnaso* sp. nov. from *I. sambaqui* (rugose; Castanho and Haddad, 2000) and from the members of the *I. verrocusa* series (tuberculate in these species; Hedges at al. 2008, Canedo et al. 2010, 2012).

Ischnocnema parnaso sp. nov. differs from all other species of the *I. venancioi* series by its large fourth toe disk (fourth toe disk width/third finger disk width = 1.00–1.09 in the new species; 0.53–0.96 in other species). Also, *I. parnaso* sp. nov. (SVL of males 27.1–30.3 mm, n = 5; female 38.0 mm) is smaller than *I. hoehnei* (SVL of males 30.6–34.8 mm, n = 3; female 42.7 mm, n = 1) and larger than *I. venancioi* (SVL of males 15.7–22.3 mm, n = 31; female 24.1 mm, n = 1) and *I. colibri* sp.nov. (SVL of males 22.9–25.2 mm, n = 5; SVL of females 31.1–34.6 mm, n = 3); and has a smaller foot (foot length/SVL 0.55–0.63) than *I. hoehnei* (foot length/SVL 0.67–0.70) and a larger foot than *I. venancioi* (foot length/SVL 0.40–0.54).

The posterior surface of the thigh with cream-colored large irregular-shaped spots surrounded by a mottled background distinguishes *I. parnaso* sp. nov. from *I. hoehnei* (posterior surface of the thigh mottled, forming small irregular cream-colored spots in some specimens) and *I. venancioi* (posterior surface of the thigh with cream-colored oval spots surrounded by a dark-brown background or with dark-brown slim bars on a clear background; spots and background yellow to orange in life). The small tibia (tibia length/SVL 0.55–0.59) differentiates *I. parnaso* sp. nov. from *I. hoehnei*

960 (tibia length/SVL 0.67–0.73) and having Finger I slightly smaller than Finger II (Finger
961 I tip reaching the base of the disk of the Finger II) differentiates the new species from *I.*
962 *venancioi* (Finger I much smaller than Finger II; its size half to two thirds the size of
963 Finger II).

964 *Ischnocnema parnaso* sp. nov. differs from *I. hoehnei* and *I. colibri* sp. nov. by
965 the lower note (repetition) rate (16.55–21.17 notes per second in the new species;
966 35.78–44.82 notes per second in other species) and the lower number of notes per call
967 (18–29 in the new species; 40–59 in other species). Additionally, the higher frequency
968 of advertisement call (2.34–2.67 kHz) distinguishes *I. parnaso* sp. nov. from *I. hoehnei*
969 (1.90 kHz).

970

971 *Natural history notes:* This species was found exclusively associated with high-
972 elevation grasslands (*Campos de Altitude*), an open phytophysiognomy found on the
973 granitic soils of the higher elevations of mountainous regions of Atlantic Forest. At the
974 time of collection, we observed a high abundance of individuals calling at the type
975 locality and its immediate surroundings. The species was active at dusk and night and
976 males were observed calling perched on low vegetation, mainly grasses (*e.g. Cortaderia*
977 *modesta*). The female was observed on rocky soil.

978

979 *Geographic distribution*: The species is currently known only from the surroundings of
980 Pedra do Sino (type locality) and Pedra da Baleia, in grasslands located above 2000 m
981 of elevation at the PARNASO, in the municipality of Guapimirim, state of Rio de
982 Janeiro, Brazil.

983

Remarks: The phylogenetic placement of *Ischnocnema parnaso* sp. nov. within the *I. venancioi* series is uncertain. It is the sister group of all other members of the *I. venancioi* series in the Bayesian inference analysis (posterior probability of the whole clade 1.0 and of the immediately less inclusive clade 0.71) and the sister species of *I. hoehnei* in the maximum likelihood and the maximum parsimony analyses (40 and 58% bootstrap and jackknife, respectively). Future studies with more data are paramount for understanding the phylogenetic placement of *I. parnaso* sp. nov.

3.4.2.4. ***Ischnocnema colibri*** *sp. nov.*

(Figs. 3B, 4E, 5E, and 11)

Holotype: CFBH 41810, adult male collected at Augusto Ruschi Biological Reserve, municipality of Santa Teresa, state of Espírito Santo, Brazil (19°54’25”S, 40°33’09”W, 803 m), by Taucce, P. P. G. and Parreiras, J. S. on January 21 2017.

Paratypes: CFBH 41809, adult male collected at Augusto Ruschi Biological Reserve, municipality of Santa Teresa, state of Espírito Santo, Brazil (19°54’25”S, 40°33’09”W, 803 m), by Taucce, P. P. G. and Parreiras, J. S. on January 20 2017. CFBH 41811, adult male, collected with holotype. MBML 10568–10569, adult males collected in the municipality of Santa Teresa, state of Espírito Santo, Brazil, by Ferreira, R. B., Ferreira, F. C. L. and Zandomenico, C. Z. on December 12 2012. MBML 10570–10571, adult females collected in the municipality of Santa Teresa, state of Espírito Santo, Brazil, by Ferreira, R. B., Ferreira, F. C. L. and Zandomenico, C. Z. on July 1 2013. MBML 10572, adult female collected near Augusto Ruschi Biological Reserve, municipality of

1009 Santa Teresa, state of Espírito Santo, Brazil, by Ferreira, R. B., Ferreira, F. C. L. and
1010 Zandomenico, C. Z. on October 30 2015.
1011
1012 *Diagnosis*: In the *Ischnocnema venancioi* series by phylogenetic placement (Fig. 1) and
1013 the following combination of characters: (1) Finger I smaller than Finger II; (2) tips of
1014 fingers expanded, discs of fingers III and IV large and truncated; (3) one large,
1015 conspicuous, glandular-appearing nuptial pad on Finger I; (4) dark-brown mask-like
1016 stripe starting at the tip of the snout or the nostril, contouring the *canthus rostralis*,
1017 passing through the eye, contouring the dorsal portion of the tympanum, and finishing
1018 near arm insertion; (5) dorsum smooth or finely tuberculate. *Ischnocnema colibri* sp.
1019 nov. is distinguished from all other species of the *I. venancioi* series by the following
1020 combination of characters: (1) medium-size (SVL of males 22.9–25.2 mm, n = 5;
1021 females 31.1–34.6 mm, n = 3); (2) foot medium-size (foot length/SVL 0.52–0.60); (3)
1022 tibia medium-size (tibia length/SVL = 0.56–0.62); (4) posterior surface of the thigh
1023 mottled, interleaved with cream-colored bars, forming a striped pattern, or with cream-
1024 colored large irregular-shaped spots surrounded by a mottled background ; (5) Finger I
1025 slightly smaller than Finger II (tip of Finger I reaching the base of Finger II
1026 approximately); (6) small fourth toe disk (fourth toe disk width/third finger disk width =
1027 0.73–0.96); (7) high advertisement call frequency (2.67–2.84 kHz); (8) advertisement
1028 call with medium number of notes (40–53); (9) high note (repetition) rate (41.30–44.82
1029 notes per second).
1030
1031 *Description of holotype*: Medium-size (23.3 mm). Head longer than wide; head length
1032 39% of SVL; head width 32% of SVL; snout sub-elliptical in dorsal view, acuminate in
1033 lateral view; nostril ovoid, oriented laterally, located near the tip of the snout; canthus

rostralis slightly distinct, straight; loreal region slightly concave; eye protuberant, oriented laterally; eye diameter 32% of the head length; upper eyelid with a few diminutive tubercles; tympanum distinct, rounded; tympanic membrane undifferentiated; annulus present, visible externally; tympanum diameter 38% of eye diameter; supratympanic fold absent; vocal slits present; vocal sac slightly distinct, one visible fold parallel to each side of the jaw; tongue large, elliptical, without posterior notch; choanae elliptical; dentigerous processes of the vomer located posteromedially to choanae, triangle-shaped, medially separated by a gap approximately the width of one dentigerous process; vomerine teeth present, five on the right side and five on the left side.

Forelimb slender; palmar tubercle barely distinct, heart-shaped, its diameter approximately equal that of thenar tubercle; thenar tubercle elliptical, distinct; glandular-appearing nuptial pad, extending dorsally from the distal to the proximal portion of metacarpus on Finger I, distinct; palm smooth; five supernumerary tubercles present; single subarticular tubercles prominent, rounded, large; fingers slender, without fringes; tip of Finger I not expanded; tip of Finger II slightly expanded; tips of fingers III and IV fairly expanded, truncated, with a V-shaped median slit in dorsal view; Finger I slightly smaller than Finger II, its length reaching the base of Finger II disk; finger lengths I < II < IV < III.

Hindlimb slender; shank longer than thigh; tibia length 56% of SVL; thigh length 52% of SVL; calcar tubercle absent; tarsal folds absent; foot medium-size; foot length 53% of SVL; inner metatarsal tubercle elliptical, twice as large as outer metatarsal tubercle, rounded; sole of foot smooth; four supernumerary tubercles present; single subarticular tubercles present, large, prominent, rounded; toes long, slender,

without fringes; tip of Toe I slightly expanded; tips of toes II–V fairly expanded, truncated, with a V-shaped median slit in dorsal view; toe lengths I < II < VI< III < IV.

Dorsal skin finely tuberculate; vertebral line absent; venter smooth; discoidal and thoracic folds present.

Coloration of holotype: Background cream-colored; dorsum with several dark-brown dots, some of them forming blotches with no defined pattern, with an x-like mark starting near the pectoral girdle and ending on the sacral vertebrae; loreal region with dark-brown mask-like stripe from the tip of the snout to near the arm insertion; dark-brown dots forming a blotch on the dorsal part of the head between the eyes; forelimb cream-colored; several dark-brown dots forming irregular blotches on the dorsal surfaces of the arm, forearm, dorsal, and ventral surfaces of the hand; hindlimb cream-colored, with several dark-brown dots forming a striped pattern on its dorsal surface and on the posterior surface of the thigh; ventral surface of the thigh and shank with small sparse dark-brown dots; ventral surface of the tarsus and sole of the foot with plenty of small dark-brown dots; venter cream-colored, with very sparse small dark-brown dots; gular region cream-colored, with sparse dark-brown dots; jaw bordered by concentrated small dark-brown dots.

Measurements of holotype (in millimeters): SVL 23.3, head length 9.5, head width 7.7, eye diameter 2.9, tympanum diameter 1.1, eye-nostril distance 2.5, internarial distance 2.2, eye-to-eye distance 4.5, forearm length 4.9, hand length 7.4, third finger disk length 1.2, thigh length 12.1, tibia length 13.5, tarsal length 6.6, foot length 12.3, and fourth toe disk length 1.1.

Variation: Tongue may also be rounded or lanceolate. Tip of Finger I can be slightly expanded. A thick vertebral line is present in one of the female specimens. Dorsal skin can also be smooth. There are two kinds of dorsal patterns: one with an x-like mark on the back (like the holotype, Fig. 3B) and one with several small dark-brown dots, often forming rounded blotches, on a cream-colored background. The posterior surface of the thigh is mottled interleaved with cream-colored bars, forming a striped pattern (like the holotype) or with cream-colored large irregular-shaped spots surrounded by a mottled background. Female specimens are much larger than male specimens (SVL 31.1–34.6 mm, n = 3; 22.9–25.2 mm, n = 5, respectively). Variation in SVL and body proportions is given in Table 4.

Etymology: "Colibri" means hummingbird and is originally an Arawak (native people who lived on Haiti and other Caribbean islands) word. The word was adopted by many other languages, including Portuguese. The name is an allusion to the type locality of the new species, the municipality of Santa Teresa, which is known as "doce terra dos colibris" (sweet land of the hummingbirds). Santa Teresa is known as sweet land of the hummingbirds not only because of their abundance in the city, but also because of the Brazilian ornithologist Augusto Ruschi, who lived in Santa Teresa and dedicated his scientific life to the study of these little Neotropical birds. The name is used here as a noun in apposition.

Advertisement call: The advertisement call (ten calls of six males; Table 7; Fig. 7C) is emitted sporadically and is composed of 40 to 53 notes ($\bar{X}$ = 48.40 ± 3.86) emitted at regular intervals. The call begins with low energy notes, which increase in energy over time, until reaching a peak almost at the end of the call. Usually, the last two to five

notes have notably less energy than the one before and a decrease of energy is notable at the end of the call. The call rise time is 53–89% ($\bar{X}$ = 65.52 ± 12.34) and the dominant frequency is 2.67–2.84 kHz ($\bar{X}$ = 2.76 ± 0.05). Call duration is 0.90 to 1.20 s ($\bar{X}$ = 1.11 ± 0.09) and the note (repetition) rate is 41.30–44.82 notes per second ($\bar{X}$ = 43.54 ± 1.48). The note rate either accelerates or decelerates at the end of the call, and the note rate acceleration is -15–33% ($\bar{X}$ = 4.19 ± 13.70).

Territorial call: The territorial call (19 calls of two males; Table 7; Fig. 7D) has a similar structure to the advertisement call, but only the last note has notably less energy than the note before. In some calls the energy difference between the last and the penultimate note was not striking. The call rise time is 5–92% ($\bar{X}$ = 66.21 ± 28.35) and the dominant frequency is 2.63–2.89 kHz ($\bar{X}$ = 2.75 ± 0.09). Call duration is 0.17 to 0.51 s ($\bar{X}$ = 0.23 ± 0.11) and the note (repetition) rate is 44.44–48.78 notes per second ($\bar{X}$ = 46.35 ± 1.24). The note rate either accelerates or decelerates at the end of the call, and the note rate acceleration is -19–2% ($\bar{X}$ = -6.92 ± 7.46).

Comparison with other species: Finger I smaller than Finger II distinguishes *Ischnocnema colibri* sp. nov. from members of the *I. guentheri, I. parva*, and *I verrucosa* series and from *I. manezinho* (Finger I approximately the same size as Finger II in these species; Garcia, 1996; Hedges et al., 2008). Expanded tips of fingers II–IV and large truncated discs of fingers III and IV distinguish *I. colibri* sp. nov. from members of the *I. parva* series, *I. nanahallux* (tips of fingers not expanded in these species; Hedges et al., 2008, Brusquetti et al., 2013), and members of the *I. verrucosa* series (disks small or moderate sized in these species; Hedges et al., 2008, Canedo et al., 2012). The large, conspicuous, glandular-appearing nuptial pad differentiates *I. colibri* sp. nov. from *I. manezinho*, *I. sambaqui*, *I. nanahallux*, and the members of the *I. lactea*

(minute nuptial pad in *I. randorum;* translucent in *I.* nigriventris and *I. vizottoi*; reduced to some white granules in *I. holti* absent in *I. melanopygia* and *I. spanios;* unknown in other species; Heyer, 1985; Hedges et al., 2008; Targino and Carvalho-e-Silva, 2008; Berneck et al., 2013) and *I. verrucosa* series (except for *I. surda*; faint, translucent nuptial pad in *I. karst*; absent in other species; Hedges et al., 2008; Canedo et al., 2010, 2012). The mask-like stripe starting at the tip of the snout or the nostril, contouring the *canthus rostralis*, passing through the eye, contouring the dorsal portion of the tympanum and reaching the arm insertion distinguishes *I. colibri* sp. nov. from *I. manezinho, I. sambaqui*, and the members of the *I. guentheri*, *I. lactea,* and *I. verrucosa* series (mask-like stripe usually absent in these species; when present it does not pass through the eye). The smooth or finely tuberculate dorsum distinguishes *I. colibri* sp. nov. from *I. sambaqui* (rugose; Castanho and Haddad, 2000) and from the members of the *I. verrocusa* series (tuberculate in these species; Hedges at al., 2008, Canedo et al., 2010, 2012).

Its larger size distinguishes *Ischnocnema colibri* sp. nov. (SVL of males 22.9–25.2 mm, n = 5; females 31.1–34.6 mm) from *I. venancioi* (SVL of males 15.7–22.3 mm, n = 31; female 24.1 mm, n = 1) and its smaller size distinguishes it from *I. hoehnei* (SVL of males 30.6–34.8 mm, n = 3; female 42.7 mm, n = 1) and *I. parnaso* sp. nov. (SVL of males 27.1–30.3 mm, n = 5; female 38.0 mm, n = 1). The medium-size foot and the small tibia (foot length/SVL = 0.52–0.60; tibia length/SVL = 0.56–0.62) differentiate *I. colibri* sp. nov. from *I. hoehnei* (foot length/SVL = 0.67–0.70; tibia length/SVL = 0.67–0.73). The mottled posterior surface of the thigh interleaved with cream-colored bars forming a striped pattern, or with cream-colored large irregular-shaped spots surrounded by a mottled background, differentiate *I. colibri* sp. nov. from *I. hoehnei* (posterior surface of the thigh mottled, forming small irregular spots in some

specimens, spots cream-colored in life) and *I. venancioi* (posterior surface of thigh with cream-colored oval spots surrounded by a dark-brown background or with dark-brown slim bars on a cream-colored background; spots and background yellow to orange in life). The small fourth toe disk (fourth toe disk width/ third finger disk width = 0.73–0.96) differentiates *I. colibri* sp. nov. from *I. parnaso* sp. nov. (fourth toe disk large; fourth toe disk width/third finger disk width = 1.00–1.09) and Finger I slightly smaller than Finger II (Finger I tip reaching the base of the disk of the Finger II) distinguishes *Ischnocnema colibri* sp. nov. from *I. venancioi* (Finger I much smaller than Finger II; its size half to two thirds the size of Finger II).

The lower number of notes and higher dominant frequency of its advertisement call (40–53 notes per call; 2.67–2.84 kHz), differentiates *I. colibri* sp. nov. from *I. hoehnei* (59 notes per call; 1.90 kHz), and its higher number of notes in the advertisement call (40–53 notes per call) differentiates it from *I. parnaso* sp. nov. (18–29 notes per call). The higher note (repetition) rate differentiates *I. colibri* sp. nov. (41.30–44.82 notes per second) from *I. parnaso* sp. nov (16.55–21.17 notes per second) and *I. hoehnei* (35.85 notes per second).

Natural history notes: We found the species calling perched on leaves of ferns about 1.5–2.0 m in height. One male starts calling, followed by the other males. The following males start calling just before the previous male finishes his call, making a small overlap between the beginning and the end of the two calls. Some males also called alone, but we commonly heard two and three males calling together. The territorial call was not overlaid.

Geographic distribution: The species is currently known only from the municipality of Santa Teresa, state of Espírito Santo, Brazil.

Remarks: *Ischnocnema colibri* sp. nov. is the sister species of *Ischnocnema* sp. from the municipality of Cachoeiras de Macacu, state of Rio de Janeiro. We have only one specimen from Cachoeiras de Macacu, and despite its overall morphological resemblance to *I. colibri* sp. nov., we do not consider them conspecifics because it has a rounded snout in profile in dorsal view (acuminate in *I. colibri* sp. nov.) and the two species are genetically very distant (pairwise distance = 7.3% in partial 16S; Table 3). More specimens including molecular and acoustic data are paramount for the understanding of the taxonomic status of the population from Cachoeiras de Macacu.

4. Discussion

4.1. Phylogenetic relationships

Like other phylogenetic hypotheses, we recovered Brachycephalidae, *Brachycephalus*, and *Ischnocnema* as monophyletic (Hedges et al., 2008; Pyron and Wiens, 2011; Canedo and Haddad, 2012; Padial et al., 2014; Heinicke et al., 2017; Taucce et al., 2018). Despite using less species than other studies (six versus 14; Clemente-Carvalho et al., 2011; Padial et al., 2014), we also recovered the former *Psyllopryne didactyla* Izecksohn, 1971, nested among other species of *Brachycephalus*. These phylogenetic hypotheses show similar relationships, indicating that they are consistent and that probably they will not change over time.

Within the genus *Ischnocnema*, we recovered the former *I. guentheri* series (now *I. venancioi* plus *I. guentheri* series), and the *I. lactea*, and *I. verrucosa* series as monophyletic, in accordance with previous studies (Canedo and Haddad, 2012; Taucce et al., 2018). The clade formed by *I.* cf. *manezinho* and *I. sambaqui*, currently unassigned to any species series, was also recovered by us and by previous phylogenetic hypotheses, confirming a strong relationship between these two species. However, the relationships between the two species and other species of *Ischnocnema* are uncertain. Canedo and Haddad (2012) and Taucce et al. (2018) recovered them as the sister group of the clade composed of the *I. verrucosa*, *I. parva*, and *I. guentheri* series in their Bayesian inference and maximum likelihood analyses, the same relationship we found herein. Canedo and Haddad (2012) also presented a parsimony tree, in which they recover the *I. manezinho* clade as the sister group of the *I. lactea* series. Our parsimony tree shows a third phylogenetic position for the clade as sister of all *Ischnocnema* species except for the members of the *I. lactea* and the *I. verrucosa* series (Fig. S1).

The phylogenetic position of *I. nanahallux,* outside the *I. parva* series, is unprecedented. Taucce et al. (2018) were the first to test the phylogenetic position of *I. nanahallux* with a robust matrix including more than one species of all *Ischnocnema* species series, and they recovered it inside a poorly supported *I. parva* series clade (0.91 and 55 of Bayesian inference posterior probability and maximum likelihood bootstrap, respectively). The only genetic information available for *I. nanahallux* at the time was partial 16S tRNA on GenBank. Now we have more genetic information for the species (partial 12S, more parts of 16S, RAG1, and Tyr) and its position as the sister group of the *I. parva, I. venancioi*, and *I. guentheri* series was well-supported in all phylogenetic analyses we performed (see results; Figs. 1 and S1).

4.2. Systematics within ***Ischnocnema***

We increased the number of species of *Ischnocnema* to 37, with the description of two new species, and also raised the number of species series to five, with the proposition of the *I. venancioi* series. We created a new species series because the previous diagnostic morphological characters proposed for the *I. guentheri* series, including the *I. venancioi* series (see Hedges et al. 2008 and Taucce et al. 2018), no longer apply. It is also a monophyletic and fully supported grouping in our three phylogenetic analyses, which bears unique morphological diagnostic features (see section 3.5.1).

Three species are currently unassigned to any species series: *I. manezinho*, *I. nanahallux*, and *I. sambaqui*. *Ischnocnema manezinho* and *I. sambaqui* were previously assigned to the *I. lactea* series (Hedges et al., 2008) due to morphological characters. Subsequently, Canedo and Haddad (2012) left these species unassigned to any species series due to molecular evidence; although they formed a fully supported clade, their position within *Ishnocnema* was uncertain. Padial *et al.* (2014) did not test the phylogenetic position of these species, but agreed with Canedo and Haddad (2012). Our results also recover the two species as sister taxa with strong support but their phylogenetic position is similar in the Bayesian inference and in the maximum likelihood analyses, but different in the maximum parsimony analysis. *Ischnocnema manezinho* was described from Florianópolis Island, Southern Brazil, but the sequence available for the species is from the municipality of São Bento do Sul, on the continent more than 150 km from the type locality. Despite strong evidence for the monophyly of *I. manezinho* and *I. sambaqui* and that they are not nested within any other species series, we find it more prudent to keep these species unassigned to species series until

1256 the phylogenetic position of *I. manezinho* from the type locality (Córrego Grande
1257 region, municipality of Florianópolis; Garcia, 1996) is tested.
1258 *Ischnocnema nanahallux* was assigned to the *I. parva* species series at the time
1259 of its description based mainly on its morphological similarities, but also by
1260 phylogenetic placement (Brusquetti at al., 2013). The author's matrix included only five
1261 more *Ischnocnema* species (one species for each series except for the *I. guentheri* series,
1262 for which two were included) and *Brachycephalus didactylus*, but several *I. parva*
1263 specimens. Our results show a surprising phylogenetic position for *I. nanahallux*, as the
1264 sister group of the clade composed of the *I.parva*, *I. guentheri*, and *I. venancioi* series
1265 with strong support (Figs. 1 and S1). Because of the similar morphology between the
1266 members of the *I. parva* series and *I. nanahallux,* and because there are still several
1267 specimens with similar morphology in museum collections from places with DNA data
1268 not yet available, such as the states of Espírito Santo and Minas Gerais, Southeast Brazil
1269 (Taucce, P. P. G., unpublished data), we have chosen to take *I. nanahallux* out of the *I.*
1270 *parva* series and not create a species series for the single species until there is more
1271 genetic data available.
1272
1273 *4.3. The nuptial pad*
1274
1275 Most anurans have sexually dimorphic structures, such as vocal sacs, vocal slits,
1276 and nuptial pads. These pads, present in male specimens, are glandular, keratinized,
1277 sometimes spiny structures typically on the first finger (Thomas et al., 1993; Luna et al.,
1278 2012). In the genus *Ischnocnema*, this character is an apparently-glandular structure
1279 present on Finger I. Some species lack the pad, yet for others its presence is unknown. It
1280 can be large and conspicuous, like in the members of the *I. parva, I. guentheri,* and *I.*

venancioi series, and also *I. surda* (member of the *I. verrucosa* series; Canedo et al., 2010; Brusquetti et al., 2013; Taucce et al., 2018; this study); minute, like in *I. randorum* (Heyer, 1985); faint and translucent, like in *I. karst, I. nigriventris*, and *I. vizottoi* (Martins and Haddad, 2010; Canedo et al., 2012; Berneck et al., 2013); and even reduced to some white granules as in *I. holti* (Targino and Carvalho-e-Silva, 2008). The nuptial pad is absent in the remaining species of the *I. verrucosa* series (Hedges at al. 2008), in *I. melanopygia* and *I. spanios,* from the *I. lactea* series (Heyer, 1985; Targino et al., 2009), in *I. manezinho* (Garcia, 1996), in *I. nanahallux* (Brusquetti et al. 2013), and in *I. sambaqui* (Castanho and Haddad, 2000).

Taucce et al. (2018) also recovered a close relationship between the *I. parva* and the *I. guentheri* (including the *I. venancioi* series) species series. The authors also noted that the presence of a large, conspicuous, glandular-appearing nuptial pad on Finger I is a morphological feature that reinforces this close relationship, despite its absence in *I. nanahallux*. According to our results, the presence of a large, conspicuous, glandular-appearing nuptial pad is a putative synapomorphy of the clade composed of the *I. parva*, *I. guentheri*, and *I. venancioi* series, which now does not include *I. nanahallux*. Outside this clade, this kind of nuptial pad is only present in *I. surda* (Canedo et al. 2010). This species was placed in the *I. verrucosa* series with its original description, but its phylogenetic position has never been tested. Due to the morphological variation of the nuptial pad in *Ischnocnema*, studies concerning morphological, histological, and chemical aspects of the pads are paramount to understanding the evolution of this character. It is also important to include more *Ischnocnema* species (like *I. surda* and *I. karst*) in future phylogenetic studies to learn the phylogenetic distribution of this character.

5. Conclusions

Our results demonstrate the monophyly of Brachycephalidae, *Brachycephalus*, and *Ischnocnema* with strong support. These relationships are recurrent in the literature and we think they are unlikely to change over time. The relationships within *Ischnocnema* are still weakly supported and controversial in some parts of the tree, and it is paramount to add more species and/or more genes to future analyses. The nuptial pad seems to be an important character in *Ischnocnema* and future studies concerning morphological, histological, and chemical aspects of the pads allied with a strong phylogenetic hypothesis are necessary to understand the evolution of this character. The new *I. venancioi* series is a fully-supported clade with several diagnostic morphological characters and its relationships with the *I. parva* and the *I. guentheri* series are molecularly well-supported. A large, conspicuous, glandular-appearing nuptial pad is a putative synapomorphy for the clade formed by these species series. We raised the number of *Ischnocnema* species to 37 with the desctiption of *I. parnaso* sp. nov. and *I. colibri* sp. nov. About 40% of these species were described over the past ten years, showing that there remains much taxonomic work to do for the genus.

Acknowledgments

We thank H. Q. Boudet, T. S. Soares (MBML), J. P. Pombal Jr (MNRJ), and K. de Queiroz (USNM) for making available material under their care. For support at the MNRJ we thank P. Pinna and M. W. Cardoso, and at USNM we thank A. Wynn. M. L. Lyra helped with laboratory procedures. We are grateful to Centro de Estudos de Insetos Sociais (CEIS; São Paulo State University [UNESP]) for allowing us the use of the

molecular laboratory. A. A. Giaretta kindly shared call recordings and L. R. Malagoli kindly shared an *I. hoehnei* photograph. R. Collins helped with the package SPIDER. L. N. Barreto executed the drawings. E. R. Wild made English review. This research was supported by resources supplied by the Center for Scientific Computing (NCC/GridUNESP) of UNESP and Cyberinfrastructure for Phylogenetic Research (CIPRES). P. P. G. T. thanks São Paulo Research Foundation (FAPESP), grant #2014/05772-4, Conselho Nacional de Desenvolvimento Científico e Tecnológico (CNPq), and Coordenação de Aperfeiçoamento de Pessoal de Nível Superior (CAPES) for the PhD fellowship and financial support, and Instituto Chico Mendes de Conservação da Biodiversidade (ICMBio) for collection permits (#42108). C. C. thanks Fundação Carlos Chagas Filho de Amparo à Pesquisa do Estado do Rio de Janeiro (FAPERJ), grant E-26/102.818/2011, for financial support. C. F. B. H. thanks FAPESP grant #2013/50741-7, FAPESP / Fundação Grupo Boticário de Proteção à Natureza grant #2014/50342-8, and CNPq for financial support. P. N. C. thanks Fundação Carlos Chagas Filho de Amparo à Pesquisa do Estado do Rio de janeiro (FAPERJ) for post-doctoral fellowships (processes E-26/201.760/2015, E-26/201.829/2015). L. O. D Thanks Conselho Nacional de Desenvolvimento Científico e Tecnológico (CNPq) for a PhD fellowship. L. O. D and P. N. C. thank Rede BioM.A. “Inventários: Padrões de diversidade, biogeografia e endemismo de espécies de mamíferos, aves, anfíbios, drosófilas e parasitos na Mata Atlântica” for financial and structural support (CNPq—process 457524/2012-0).

Appendices A, B, and C. Supplementary material

References

Berneck, B.V.M., Targino, M., Garcia, P.C.A, 2013. Rediscovery and re-description of *Ischnocnema nigriventris* (Lutz, 1925) (Anura: Terrarana: Brachycephalidae). Zootaxa 3694, 131–142. https://doi.org/10.11646/zootaxa.3694.2.2

Bioacoustics Research Program, 2011. Raven Pro: interactive sound analysis software.

Bokermann, W.C.A., 1975 "1974". Três espécies novas de *Eleutherodactylus* do sudeste da Bahia, Brasil (Anura, Leptodactylidae). Rev. Bras. Biol. 34, 11–18.

Bokermann, W.C.A., 1967. Una nueva espécie de *Eleutherodactylus* del sudeste brasileño (Amphibia, Leptodactylidae). Neotropica 13, 1–3.

Bokermann, W.C.A., 1965. A new *Eleutherodactylus* from Southeastern Brazil. Copeia 1965, 440–441. https://doi.org/10.2307/1440993

Boulenger, G.A., 1888. V.— On some reptiles and batrachians from Iguarasse, Pernambuco. J. Nat. Hist. Ser. 6 2, 40–43. https://doi.org/10.1080/00222938809460873

Brown, S.D.J., Collins, R.A., Boyer, S., Lefort, M.C., Malumbres-Olarte, J., Vink, C.J., Cruickshank, R.H., 2012. Spider: an R package for the analysis of species identity and evolution, with particular reference to DNA barcoding. Mol. Ecol. Resour. 12, 562–565. https://doi.org/10.1111/j.1755-0998.2011.03108.x

Brusquetti, F., Thomé, M.T.C., Canedo, C., Condez, T.H., Haddad, C.F.B., 2013. A New species of *Ischnocnema parva* Species Series (Anura, Brachycephalidae) from northern state of Rio de Janeiro, Brazil. BioOne 69, 175–185. https://doi.org/10.1655/HERPETOLOGICA-D-12-00050

Canedo, C., Haddad, C.F.B., 2012. Phylogenetic relationships within anuran clade Terrarana, with emphasis on the placement of Brazilian Atlantic rainforest frogs

genus *Ischnocnema* (Anura: Brachycephalidae). Mol. Phylogenet. Evol. 65, 610–620. https://doi.org/10.1016/j.ympev.2012.07.016

Canedo, C., Pimenta, B.V.S., 2010. New species of *Ischnocnema* (Anura, Brachycephalidae) from the Atlantic rainforest of the state of Espírito Santo, Brazil. South Am. J. Herpetol. 5, 199–206. https://doi.org/10.2994/057.005.0305

Canedo, C., Pimenta, B.V.S., Leite, F.S.F., Caramaschi, U., 2010. New species of *Ischnocnema* (Anura: Brachycephalidae) from the state of Minas Gerais, Southeastern Brazil, with comments on the *I. verrucosa* Species Series. Copeia 2010, 629–634. https://doi.org/10.1643/CH-09-159

Canedo, C., Targino, M., Leite, F.S.F., Haddad, C.F.B., 2012. A new species of *Ischnocnema* (Anura) from the São Francisco Basin Karst Region, Brazil. Herpetologica 68, 393–400. https://doi.org/10.1655/HERPETOLOGICA-D-11-00065.1

Caramaschi, U., Canedo, C., 2006. Reassessment of the taxonomic status of the genera *Ischnocnema* Reinhardt and Lütken, 1862 and *Oreobates* Jiménez-de-la-Espada, 1872, with notes on the synonymy of *Leiuperus verrucosus* Reinhardt and Lütken, 1862 (Anura: Leptodactylidae). Zootaxa 1116, 43–54.

Caramaschi, U., Kisteumacher, G., 1989 “1988”. A new species of *Eleutherodactylus* (Anura : Leptodactylidae) from Minas Gerais, Southeastern Brazil. Herpetologica 44, 423–426.

Castanho, L.M., Haddad, C.F.B., 2000. New species of *Eleutherodactylus* (Amphibia : Leptodactylidae) from Guaraqueçaba, Atlantic Forest of Brazil 2000, 777–781.

Clemente-Carvalho, R.B.G., Klaczko, J., Ivan Perez, S., Alves, A.C.R., Haddad, C.F.B., Dos Reis, S.F., 2011. Molecular phylogenetic relationships and phenotypic diversity in miniaturized toadlets, genus *Brachycephalus* (Amphibia: Anura:

1405 Brachycephalidae). Mol. Phylogenet. Evol. 61, 79–89.
1406 https://doi.org/10.1016/j.ympev.2011.05.017
1407 Cochran, D.M., 1948. A new subspecies of frog from Itatiaya, Brazil. Am. Museum
1408 Novit. 1375, 1–3.
1409 Cocroft, R.B., Ryan, M. J. Patterns of advertisement call evolution in toads an dchorus
1410 frogs. Anim. Behav. 49, 283–303.
1411 Cope, E.D., 1862. On some new and little known American Anura. Proc. Acad. Nat.
1412 Sci. Philadelphia 14, 151–159+594.
1413 Duellman, W.E., Lehr, E., 2009. Terrestrial-breeding frogs (Strabomantidae) in Peru.
1414 Natur und Tier - Verlag GmbH, Münster, Germany.
1415 Dumeril, A.M.C., Bibron, G., 1841. Erpétologie générale ou histoire naturelle complète
1416 des reptiles. Tome huitième. Librarie Enclyclopedique de Roret, Paris.
1417 Fitzinger, L.J.F.J., 1826. Neue classification der reptilien nach ihren natürlichen
1418 verwandtschaften : nebst einer verwandtschafts-tafel und einem verzeichnisse der
1419 reptilien-sammlung des K. K. zoologischen museum's zu Wien, Isis Von Oken. J.
1420 G. Heubner, Wien : https://doi.org/10.5962/bhl.title.4683
1421 Frost, D.R., 2018. Amphibian Species of the World: an Online Reference [WWW
1422 Document]. Am. Museum Nat. Hist. New York, USA. URL
1423 http://research.amnh.org/herpetology/amphibia/index.html (accessed 1.15.18).
1424 Garcia, P.C.A., 1996. Nova espécie de *Eleutherodactylus* Duméril and Bibron, 1891
1425 (Amphibia, Anura, Leptodactylidae) do Estado de Santa Catarina, Brasil.
1426 Biociências 4, 57–68.
1427 Gehara, M., Canedo, C., Haddad, C.F.B., Vences, M., 2013. From widespread to
1428 microendemic: Molecular and acoustic analyses show that *Ischnocnema guentheri*

(Amphibia: Brachycephalidae) is endemic to Rio de Janeiro, Brazil. Conserv. Genet. 14, 973–982. https://doi.org/10.1007/s10592-013-0488-5

Gelman, A., Rubin, D.B., 1992. Inference from iterative simulation using multiple sequences. Stat. Sci. 7, 457–472.

Giaretta, A.A., Toffoli, D., Oliveira, L.E., 2007. A new species of *Ischnocnema* (Anura: Eleutherodactylinae) from open areas of the Cerrado Biome in southeastern Brazil. Zootaxa 51, 43–51.

Girard, C., 1853. Descriptions of new species of reptiles, collected by the U.S. Exploring Expedition, under the command of Capt. Charles Wilkes, U.S.N. Second part—including the species of batrachians, exotic to North America. Proc. Acad. Nat. Sci. Philadelphia 6, 420–424.

Goloboff, P.A., Catalano, S.A., 2016. TNT version 1.5, including a full implementation of phylogenetic morphometrics. Cladistics 32, 221–238. 10.1111/cla.12160

Guindon, S., Dufayard, J.F., Lefort, V., Anisimova, M., Hordijk, W., Gascuel, O., 2010. New algorithms and methods to estimate maximum-likelihood phylogenies: Assessing the performance of PhyML 3.0. Syst. Biol. 59, 307–321. https://doi.org/10.1093/sysbio/syq010

Hedges, S.B., Duellman, W.E., Heinicke, M.P., 2008. New World direct-developing frogs (Anura: Terrarana): molecular phylogeny, classification, biogeography, and conservation. Zootaxa 1737, 1–182.

Heinicke, M.P., Duellman, W.E., Hedges, S.B., 2007. Major Caribbean and Central American frog faunas originated by ancient oceanic dispersal. Proc. Natl. Acad. Sci. U. S. A. 104, 10092–10097. https://doi.org/10.1073/pnas.0611051104

Heinicke, M.P., Lemmon, A.R., Lemmon, E.M., McGrath, K., Hedges, S.B., 2017. Phylogenomic support for evolutionary relationships of New World direct-

developing frogs (Anura: Terraranae). Mol. Phylogenet. Evol. 118, 145–155. https://doi.org/10.1016/j.ympev.2017.09.021

Hepp, F., Canedo, C., 2013. Advertisement and aggressive calls of *Ischnocnema oea* (Heyer, 1984) (Anura, Brachycephalidae). Zootaxa 3710, 197–199. https://doi.org/10.11646/zootaxa.3710.2.6

Heyer, W.R., 1985. New species of frogs from Boracéia, São Paulo, Brazil. Proc. Biol. Soc. Washingt. 98, 657–671.

Heyer, W.R., 1984. Variation, systematics, and zoogeography of *Eleutherodactylus guentheri* and closely related species (Amphibia: Anura: Leptodactylidae). Smith Contr Zool 402, 15342. https://doi.org/10.5479/si.00810282.402

Heyer, W.R., 1984. Zoogeography of *Eleutherodactylus guentheri* and closely related species (Amphibia : Anura : Leptodactylidae). Smithson. Contrib. to Zool. 402, 1–42.

Heyer, W.R., Rand, A.S., Cruz, C.A.G. Da, Peixoto, O.L., Nelson, C.E., 1990. Frogs of Boracéia. Arq. Zool. 31, 235–410.

Hurvich, C., Tsai, C., 1989. Regression and time series model selection in small samples. Biometrika 76, 297–307. https://doi.org/10.1093/biomet/76.2.297

Izecksohn, E., 1971. Nôvo gênero e nova espécie de Brachycephalidae do Estado do Rio de Janeiro. Bol. do Mus. Nac. Nov. Série, Zool. 280, 1–12.

Jiménez de la Espada, M., 1870. Fauna neotropicalis species quaedam nondum cognitae. J. Sciências, Mathemáticas, Phys. e Naturaes 3, 57–65.

Katoh, K., Standley, D.M., 2013. MAFFT multiple sequence alignment software version 7: improvements in performance and usability. Mol. Biol. Evol. 30, 772–780. https://doi.org/10.1093/molbev/mst010

1478 Köhler, J., Jansen, M., Rodríguez, A., Kok, P.J.R., Toledo, L.F., Emmrich, M., Glaw,
1479 F., Haddad, C.F.B., Rödel, M.O., Vences, M., 2017. The use of bioacoustics in
1480 anuran taxonomy: theory, terminology, methods and recommendations for best
1481 practice, Zootaxa. https://doi.org/10.11646/zootaxa.4251.1.1
1482 Kwet, A., Solé, M., 2005. Validation of *Hylodes henselii* Peters, 1870, from Southern
1483 Brazil and description of acoustic variation in *Eleutherodactylus guentheri* (Anura:
1484 Leptodactylidae). J. Herpetol. 39, 521–532. https://doi.org/10.1670/53-04A.1
1485 Lanfear, R., Frandsen, P.B., Wright, A.M., Senfeld, T., Calcott, B., 2017. Partitionfinder
1486 2: new methods for selecting partitioned models of evolution for molecular and
1487 morphological phylogenetic analyses. Mol. Biol. Evol. 34, 772–773.
1488 https://doi.org/10.1093/molbev/msw260
1489 Langone, J.A., Segalla, M.V., 1996. Una nueva especie de *Eleutherodactylus* del Estado
1490 de Paraná, Brasil. Comun. Zool. del Mus. Hist. Nat. Montevideo 12, 1–5.
1491 Ligges, U., Krey, S., Mersman, O., Schnackenberg, S., 2013. tuneR: analysis of music.
1492 URL: http://r-forge.r-project.org/projects/tuner/.
1493 Luna, M.C., Taboada, C., Baêta, D., Faivovich, J., 2012. Structural diversity of nuptial
1494 pads in Phyllomedusinae (Amphibia: Anura: Hylidae). J. Morphol. 273, 712–724.
1495 https://doi.org/10.1002/jmor.20016
1496 Lutz, A., 1925. Batraciens du Brésil. Comptes Rendus Mémoires Hebd. des Séances la
1497 Société Biol. des ses Fil. 22, 211–214.
1498 Lutz, B., 1974. *Eleutherodactylus gualteri*, a new species from the Organ Mountains of
1499 Brazil. J. Herpetol. 8, 293–295. https://doi.org/10.2307/1562897
1500 Lutz, B., 1958. Anfíbios novos e raros das serras costeiras do Brasil: *Eleutherodactylus*
1501 *venancioi* n.sp., *E. hoehnei* n.sp., *Holoaden bradei* n.sp. e *H. lüderwaldti* Mir. Rib.,

1502 1920. Mem. Inst. Oswaldo Cruz 56, 372–389. https://doi.org/10.1590/S0074-
1503 02761958000200002
1504 Lynch, J.D., 1976. The species groups of South American frogs of the genus
1505 *Eleutherodactylus* (Leptodactylidae). Occas. Pap. Museum Nat. Hist. Univ. Kansas
1506 61, 1–24.
1507 Lynch, J.D., Duellman, W.E., 1997. Frogs of the genus *Eleutherodactylus* in western
1508 Ecuador biogeography. Spec. Publ. Nat. Hist. Museum, Univ. Kansas 23, 1–236.
1509 Lyra, M.L., Haddad, C.F.B., de Azeredo-Espin, A.M.L., 2017. Meeting the challenge of
1510 DNA barcoding Neotropical amphibians: polymerase chain reaction optimization
1511 and new COI primers. Mol. Ecol. Resour. 17, 966–980.
1512 https://doi.org/10.1111/1755-0998.12648
1513 Maniatis, T., Fritsch, E.F., Sambrook, J., 1982. Molecular cloning: a laboratory manual.
1514 Cold Spring Harbour Laboratory, New York.
1515 Martins, I.A., Haddad, C.F.B., 2010. A new species of *Ischnocnema* from highlands of
1516 the Atlantic forest, Southeastern Brazil (Terrarana, Brachycephalidae). Zootaxa 65,
1517 55–65.
1518 Miranda-Ribeiro, A., 1937. Alguns batrachios novos das colleçcões do Museo Nacional.
1519 O Campo 8, 66–69.
1520 Miranda-Ribeiro, A., 1926. Notas para servirem ao estudo dos Gymnobatrachios
1521 (Anura) brasileiros. Arq. do Mus. Nac. 27, 1–227.
1522 Miranda-Ribeiro, A., 1923. *Basanitia lactea* (Um novo batracchio das collecções do
1523 Museu Paulista). Rev. do Mus. Paul. 13, 851–852.
1524 Oliveira, L.E., Oliveira, R.M.C., Giaretta, A.A., 2008. *Ischnocnema hoehnei* (Hoehnei's
1525 Robber Frog). Advertisement call. Herpetol. Rev. 39, 207–208.

1526 Padial, J.M., Castroviejo-Fisher, S., Köhler, J., Domic, E., De la Riva, I., 2007.
1527 Systematics of the *Eleutherodactylus fraudator* species group (Anura :
1528 Brachycephalidae). Herpetol. Monogr. 21, 213–240. https://doi.org/10.1655/06-
1529 007.1
1530 Padial, J.M., Grant, T., Frost, D.R., 2014. Molecular systematics of terraranas (Anura:
1531 Brachycephaloidea) with an assessment of the effects of alignment and optimality
1532 criteria. Zootaxa 3825, 1–132. https://doi.org/10.11646/zootaxa.3825.1.1
1533 Padial, J.M., Reichle, S., Riva, I. De, Padial, J.M., Riva, I.D.E.L. a, 2005. New species
1534 of *Ischnocnema* (Anura: Leptodactylidae) from the Andes of Bolivia. J. Herpetol.
1535 39, 186–191.
1536 Palumbi, S.R., Martin, A.P., Kessing, B.D., McMillan, W.O., 1991. Detecting
1537 population structure using mitochondrial DNA, in: Hoelzel, A.R. (Ed.), Genetic
1538 ecology of whales and dolphins. International Whaling Comission, Cambridge, pp.
1539 203–215.
1540 Paradis, E., Claude, J., Strimmer, K., 2004. APE: Analyses of phylogenetics and
1541 evolution in R language. Bioinformatics 20, 289–290.
1542 https://doi.org/10.1093/bioinformatics/btg412
1543 Peters, W.C.H., 1870. Über neue Amphien (*Hemidactylus*, *Urosaura*, *Tropdolepisma,*
1544 *Geophis, Uriechis, Scaphiophis, Hoplocephalus, Rana, Entomoglossus,*
1545 *Cystignathus, Hylodes, Arthroleptis, Phyllobates, Cophomantis*) des Königlich
1546 Zoologisch Museum. Monatsberichte der Königlichen Preuss. Akad. des
1547 Wissenschaften zu Berlin 1870, 641–652.
1548 Pyron, R.A., Wiens, J.J., 2011. A large-scale phylogeny of Amphibia including over
1549 2800 species, and a revised classification of extant frogs, salamanders, and

1550 caecilians. Mol. Phylogenet. Evol. 61, 543–583.
1551 https://doi.org/10.1016/j.ympev.2011.06.012
1552 Rambaut, A., 2014. FigTree. URL: http://tree.bio.ed.ac.uk/software/figtree/
1553 R Core Team, 2017. R: A language and environment for statistical computing.
1554 Reinhardt, J.T., Lütken, C.F., 1862 “1861”. Bidrag til Kundskab om Brasiliens Padder
1555 og Krybdyr. Förste Afdeling: Padderne og Öglerne. Vidensk. Meddelelser fra
1556 Dansk Naturhistorisk Foren. i Kjøbenhavn 2, 143–242.
1557 Ronquist, F., Teslenko, M., Van Der Mark, P., Ayres, D.L., Darling, A., Höhna, S.,
1558 Larget, B., Liu, L., Suchard, M.A., Huelsenbeck, J.P., 2012. Mrbayes 3.2: Efficient
1559 bayesian phylogenetic inference and model choice across a large model space.
1560 Syst. Biol. 61, 539–542. https://doi.org/10.1093/sysbio/sys029
1561 Sabaj, M.H., 2016. Standard symbolic codes for institutional resource collections in
1562 herpetology and ichthyology: an online reference. Version 6.5 (16 August 2016).
1563 Electronically accessible at http://www.asih.org/, American Society of
1564 Ichthyologists and Herpetologists, Was 5, 802–832.
1565 Sazima, I., Cardoso, A.J., 1978. Uma espécie nova de *Eleutherodactylus* do sudeste
1566 Brasileiro (Amphibia, Anura, Leptodactylidae). Rev. Bras. Biol. 38, 921–925.
1567 Spix, J.B. von, 1824. Animalia nova sive Species novae Testudinum et Ranarum quas in
1568 itinere per Brasiliam annis MDCCCXVII–MDCCCXX jussu et auspiciis
1569 Maximiliani Josephi I. F. S. Hübschmann, München.
1570 Stamatakis, A., 2014. RAxML version 8: a tool for phylogenetic analysis and post-
1571 analysis of large phylogenies. Bioinformatics 30, 1312–1313.
1572 https://doi.org/10.1093/bioinformatics/btu033

1573 Steindachner, F., 1867. Reise der österreichischen Fregatte Novara um die Erde in den
1574 Jahren 1857, 1858, 1859 unter den Bafehlen des Commodore B. von Wüllerstorf-
1575 Urbair. Zologischer Theil. 1. Amphibien. K. K. Hof- und Staatsdruckerei, Wien.
1576 Sueur, J., Aubin, T., Simonis, C., 2008. Seewave, a free modular tool for sound analysis
1577 and synthesis. Bioacoustics 18, 213–226.
1578 https://doi.org/10.1080/09524622.2008.9753600
1579 Targino, M., Carvalho-e-Silva, S.P. de, 2008. Redescrição de *Ischnocnema holti*
1580 (Amphibia: Anura: Brachycephalidae). Rev. Bras. Zool. 25, 716–723.
1581 https://doi.org/10.1590/S0101-81752008000400017
1582 Targino, M., Costa, P.N., de Carvalho-e-Silva, S.P., 2009. Two new species of the
1583 *Ischnocnema lactea* Species Series from Itatiaia highlands, Southeastern Brazil
1584 (Amphibia, Anura, Brachycephalidae). South Am. J. Herpetol. 4, 139–150.
1585 https://doi.org/10.2994/057.004.0205
1586 Taucce, P.P.G., Canedo, C., Haddad, C.F.B., 2018. Two new species of *Ischnocnema*
1587 Reinhardt and Lütken, 1862 (Anura: Brachycephalidae) from Southeastern Brazil
1588 and their phylogenetic position within the *I. guentheri* species series. Herpetol.
1589 Monogr. 32, in press.
1590 Thomas, E.O., Tsang, L., Licht, P., 1993. Comparative histochemistry of the sexually
1591 dimorphic skin glands of anuran Aamphibians. Copeia 1993, 133.
1592 https://doi.org/10.2307/1446304
1593

Table 1

Primers used in this study.

Primer		Gene	Sequence	Reference
tRNAphe-L	F	12S	AAAGCATAACACTGAAGATGTTAAGATG	Goebel et al. (1999)
tRNAval-H	R	12S–tRNA-V	GGTGTAAGCGARAGGCTTTKGTTAAG	Goebel et al. (1999)
12SL13	F	tRNA-V–16S	TTAGAAGAGGCAAGTCGTAACATGGTA	Feller and Hedges (1998)
16STitus_1	R	16S	GGTGGCTGCTTTTAGGCC	Titus and Larson (1996)
16SL2A	F	16S	CCAAACGAGCCTAGTGATAGCTGGTT	Hedges (1994)
16S-H10	R	16S	TGCTTACGCTACCTTTGCACGGT	Hedges (1994)
16SAR	F	16S	CGCCTGTTTATCAAAAACAT	Palumbi et al. (1991)
16S-Wilk2	R	16S	GACCTGGATTACTCCGGTCTGA	Wilkinson et al. (1996)
Tyr1B[a]	F	Tyrosinase	AGGTCCTCYTRAGGAAGGAATG	Bossuyt and Milinkovitch (2000)
Tyr1E[a]	R	Tyrosinase	GAGAAGAAAGAWGCTGGGCTGAG	Bossuyt and Milinkovitch (2000)
Tyr1C[b]	F	Tyrosinase	GGCAGAGGAWCRTGCCAAGATGT	Bossuyt and Milinkovitch (2000)
Tyr1G[b]	R	Tyrosinase	TGCTGGGCRTCTCTCCARTCCCA	Bossuyt and Milinkovitch (2000)
R182[a]	F	RAG1	GCCATAACTGCTGGAGCATYAT	Heinicke et al. (2007)
R270[a]	R	RAG1	AGYAGATGTTGCCTGGGTCTTC	Heinicke et al. (2007)
RAG1FF2[b]	F	RAG1	ATGCATCRAAAATTCARCAAT	Heinicke et al. (2007)
RAG1FR2[b]	R	RAG1	CCYCCTTTRTTGATAKGGWCATA	Heinicke et al. (2007)

[a]Most external primers and [b]most internal primers

Table 2

Best partition scheme and respective best fitting molecular models.

Partition	Model
12S and tVal	GTR+Γ+I
16S	GTR+Γ+I
RAG1 1st and 2nd positions	GTR+Γ
RAG1 3rd position	K80+Γ
Tyr 1st position	GTR+Γ+I
Tyr 2nd position	HKY+ Γ+I
Tyr 3rd position	GTR+Γ

Table 3

Uncorrected pairwise genetic distances within (highlighted in gray) and among members of the *Ischnocnema venancioi* species series. Data are shown as range (mean) where appropriate. NA = not applicable.

	Uncorrected pairwise distance between species (%)				
	I. hoehnei	*I. venancioi*	*I.* sp. (Cachoeiras de Macacu)	*I. colibri* sp. nov.	*I. parnaso* sp. nov.
I. hoehnei	0.0–2.2 (1.1, n = 4)				
I. venancioi	10.8–12.1 (11.8)	0.0 (n = 2)			
I. aff. *venancioi*	13.6–13.8 (12.3)	11.4	NA (n = 1)		
I. colibri sp. nov.	12.3	10.5	7.3	0.0 (n = 3)	
I. parnaso sp. nov.	10.3–12.1 (11.4)	11.4–12.3 (11.9)	14.3–14.9 (14.6)	12.3–12.5 (12.4)	2.0 (n = 2)

1607 Table 4

1608 Snout-vent length (SVL) and body proportions of *Ischnocnema venancioi*, *I. hoehnei*, *I. parnaso* sp. nov., and *I. colibri* sp. nov. Data are given as

1609 range (mean ± standard deviation) where appropriate.

SVL and body proportions	Adult males				Adult females			
	I. venancioi (n = 31)	*I. hoehnei* (n = 3)	*I. parnaso* sp. nov. (n = 5)	*I. colibri* sp. nov. (n = 5)	*I. venancioi* (n = 1)	*I. hoehnei* (n = 1)	*I. parnaso* sp. nov. (n = 1)	*I. colibri* sp. nov. (n = 3)
SVL (mm)	15.7—22.3 (17.5±1.3)	30.6—34.8 (32.4±2.2)	27.1—30.3 (28.8±1.2)	22.9—25.2 (23.9±1.1)	24.1	42.7	38.0	31.1—34.6 (33.3±1.9)
Head length/SVL	0.37—0.47 (0.43±0.03)	0.39—0.43 (0.41±0.02)	0.39—0.40 (0.39±0.01)	0.39—0.42 (0.40±0.01)	0.40	0.43	0.39	0.41—0.43 (0.42±0.01)
Head width/SVL	0.31—0.38 (0.35±0.02)	0.33—0.36 (0.34±0.02)	0.30—0.35 (0.34±0.02)	0.32—0.35 (0.33±0.1)	0.33	0.36	0.33	0.33—0.37 (0.35±0.02)
Head width/head length	0.72—0.93 (0.81±0.05)	0.81—0.84 (0.83±0.02)	0.78—0.90 (0.86±0.05)	0.79—0.82 (0.81±0.01)	0.81	0.82	0.86	0.81—0.84 (0.83±0.02)
Eye diameter/head length	0.26—0.36 (0.32±0.02)	0.28—0.32 (0.30±0.02)	0.29—0.31 (0.31±0.01)	0.29—0.36 (0.32±0.03)	0.23	0.34	0.25	0.26—0.29 (0.27±0.01)

1610

1611 Table 4

1612 Continuation

Tympanum diameter/head length	0.09—0.17 (0.12±0.02)	0.11—0.13 (0.12±0.01)	0.10—0.13 (0.12±0.01)	0.12—0.14 (0.13±0.01)	0.09	0.13	0.11	0.11—0.13 (0.12±0.01)
Tympanum diameter/eye diameter	0.27—0.57 (0.37±0.06)	0.40—0.43 (0.41±0.01)	0.34—0.43 (0.39±0.04)	0.34—0.48 (0.41±0.05)	0.32	0.38	0.44	0.38—0.48 (0.43±0.05)
Internarial distance/head length	0.21—0.54 (0.43±0.09)	0.29—0.32 (0.30±0.02)	0.34—0.49 (0.44±0.07)	0.41—0.48 (0.46±0.03)	0.20	0.35	0.32	0.32—0.34 (0.33±0.01)
Eye-to-eye distance/head length	0.34—0.55 (0.46±0.05)	0.57—0.59 (0.58±0.01)	0.41—0.47 (0.44±0.02)	0.42—0.52 (0.47±0.04)	0.39	0.39	0.46	0.42—0.47 (0.44±0.02)
Eye-nostril distance/head length	0.14—0.29 (0.20±0.04)	0.27—0.31 (0.29±0.02)	0.19—0.30 (0.23±0.04)	0.21—0.29 (0.27±0.04)	0.23	0.34	0.22	0.29—0.31 (0.30±0.01)
Forearm length/SVL	0.16—0.24 (0.21±0.02)	0.18—0.20 (0.20±0.01)	0.17—0.20 (0.19±0.01)	0.18—0.21 (0.20±0.01)	0.22	0.22	0.19	0.20—0.23 (0.21±0.01)
Hand length/SVL	0.23—0.30 (0.26±0.02)	0.31—0.32 (0.32±0.01)	0.27—0.30 (0.29±0.01)	0.28—0.32 (0.30±0.02)	0.27	0.43	0.27	0.28—0.31 (0.29±0.01)

1613

1614 Table 4

1615 Continuation

Third finger disk width/hand length	0.12—0.24 (0.17±0.03)	0.17—0.18 (0.17±0.00)	0.15—0.16 (0.16±0.01)	0.16—0.18 (0.17±0.01)	0.20	0.18	0.16	0.16—0.19 (0.17±0.01)
Fourth toe disk width/third finger disk width	0.95—0.96 (0.96±0.00)	0.53—0.93 (0.73±0.12)	1.00—1.07 (1.04±0.04)	0.87—0.96 (0.90±0.04)	0.77	0.93	1.09	0.73—0.92 (0.84±0.09)
Thigh length/SVL	0.42—0.57 (0.48±0.04)	0.57—0.61 (0.59±0.02)	0.51—0.55 (0.53±0.01)	0.52—0.54 (0.52±0.01)	0.50	0.59	0.52	0.53—0.57 (0.55±0.02)
Tibia length/SVL	0.48—0.60 (0.55±0.03)	0.67—0.72 (0.69±0.03)	0.55—0.59 (0.58±0.02)	0.56—0.59 (0.58±0.01)	0.55	0.73	0.57	0.58—0.62 (0.61±0.02)
Tarsal length/SVL	0.26—0.36 (0.32±0.03)	0.30—0.35 (0.33±0.02)	0.26—0.30 (0.28±0.02)	0.27—0.30 (0.29±0.01)	0.29	0.34	0.32	0.29—0.31 (0.30—0.01)
Foot length/SVL	0.40—0.54 (0.46±0.04)	0.67—0.70 (0.68±0.02)	0.55—0.63 (0.59±0.03)	0.52—0.55 (0.53±0.01)	0.48	0.67	0.62	0.54—0.60 (0.57—0.03)

Table 5

Acoustic parameters comparing the advertisement calls of the members of the *Ischnocnema venancioi* species series and the territorial call of *I. colibri* sp. nov. Data are given as ranges when applicable.

Species	*I. hoehnei*	*I. parnaso* sp. nov.	*I. colibri* sp. nov.	
Type of call	Advertisement call	Advertisement call	Advertisement call	Territorial call
Call duration (s)	1.65	1–1.5	0.9—1.2	0.17—0.51
Call rise time (%)	96	42—92	53—89	5—92
Dominant frequency (kHz)	1.9	2.34—2.67	2.67—2.84	2.63—2.93
Notes per call	59	18—29	40—53	8—23
Note rate (notes/s)	35.78	16.55—21.17	41.3—44.87	45—50.25
Note (repetition) rate acceleration (%)	-1	-36– -11	-15–33	-19–2

Table 6

Acoustic parameters of the advertisement call of five recorded males of *Ischnocnema parnaso* sp. nov. Data are given as range (mean ± standard deviation) where appropriate.

Call recording	LOD 001	LOD 002	LOD 003	LOD 004	LOD 005
Number of analyzed calls	2	6	3	5	3
Call duration (s)	1.00–1.05	1.14–1.27 (1.20±0.05)	1.17–1.25 (1.22±0.05)	1.25–1.38 (1.33±0.05)	1.25–1.50 (1.40±0.13)
Call rise time (%)	42–62	44–79 (64±15)	51–92 (75±22)	57–85 (72±10)	51–83 (62±18)
Dominant frequency (kHz)	2.39	2.39–2.53 (2.48±0.04)	2.44–2.67 (2.58±0.09)	2.39–2.58 (2.45±0.08)	2.34–2.44 (2.38±0.05)
Notes per call	18.00	24.00–25.00 (24.33±0.52)	23.00–25.00 (24.33±1.15)	26.00–29.00 (28.00±1.22)	26.00–27.00 (26.67±0.58)
Note rate (notes/s)	16.55–17.58	19.06–20.43 (19.79±0.53)	19.40–19.84 (19.60±0.22)	20.59–20.88 (20.75±0.14)	17.58–21.17 (18.89±1.98)
Note repetition rate acceleration (%)	-26– -20	-24– -15 (-20±4)	-18– -11 (-16±4)	-36– -23 (-27±5)	-33– -24 (-28±4)

Table 7

Acoustic parameters of five recorded males of *Ischnocnema colibri* sp. nov. Data are given as range (mean ± standard deviation) where appropriate. AC and TC are advertisement and territorial calls, respectively.

Call recording	PPGT 009	PPGT 010	PPGT 011	PPGT 012	PPGT 013		PPGT 014	
Type of call	AC	AC	AC	AC	AC	TC	AC	TC
Number of analyzed calls	1	2	1	4	1	13	1	6
Call duration (s)	1.09	1.03–1.15	1.19	1.14–1.20 (1.18±0.03)	1.04	0.18–0.51 (0.28±0.12)	0.90	0.17–0.20 (0.17±0.01)
Call rise time (%)	89	74–84	56	53–60 (57±3)	59	5–92 (54±26)	65	67–91 (81±9)
Dominant frequency (kHz)	2.67	2.76	2.80	2.76	2.84	2.71–2.93 (2.83±0.07)	2.71	2.63–2.71 (2.68±0.04)
Notes per call	49.00	46.00–52.00	53.00	47.00–52.00 (49.50±2.08)	46.00	9.00–23.00 (13.31±5.20)	40.00	8.00–10.00 (8.33±0.82)
Note rate (notes/s)	44.87	44.75–45.22	44.61	41.30–44.60 (42.25±1.58)	44.06	45–50 (47-±2)	44.35	47.06–50.25 (48.11±1.19)
Note (repetition) rate acceleration (%)	-1	-13– -1	11	-15–33 (8±20)	5	-19– -5 (-13±5)	7	-8–2 (-1±4)

Figure 1. The 50% majority rule consensus tree from Bayesian inference analysis of concatenated mitochondrial 12S rRNA, tVal rRNA, 16S rRNA, and nuclear Recombination Activating Gene 1 (RAG1) and tyrosinase precursor (Tyr). Posterior probabilities are shown above the branches and maximum likelihood bootstrap and parsimony jackknife are shown below the branches (to the left and to the right of the bar, respectively). Asterisks (*) indicate fully supported clades and hyphens (-) indicate that the clade does not appear in the specific phylogenetic analysis.

Figure 2. Character states of the tip of Finger III in the members of the *Ischnocnema venancioi* and *I. guentheri* series: large and truncated in (A) *I. hoehnei* and (B) *I. venancioi*; rounded in (C) *I. guentheri* and (D) *I. oea*. Scale bars = 1 mm (A, C) and 0.5 mm (B, D).

Figure 3. Dorsal (above) and ventral (below) views of the members of the *Ischnocnema venancioi* series, showing the size differences among them: (A) *I. venancioi*, (B) *I. colibri* sp. nov., (C) *I. parnaso* sp. nov., and (D) *I. hoehnei.* Scale bar = 5 mm.

Figure 4. Color patterns of the posterior surface of the thigh of the members of the *Ischnocnema venancioi* series: (A) and (B) *I. venancioi*, (C) *I. hoehnei*, (D) *I. parnaso* sp. nov., and (E) *I. colibri* sp. nov. Scale bar = 1 mm (A, B) and 2 mm (C, D, E).

Figure 5. Live specimens of the *Ischnocnema venancioi* series showing the mask-like pattern and the vivid yellow on the posterior surface of the thigh of *I. venancioi*. (A) *I. venancioi* (photo by L. O. Drummond), (B) *I. venancioi* (photo by L. O. Drummond),

(C) *I. hoehnei* (photo by L. R. Malagoli), (D) *I. parnaso* sp. nov. (photo by L. O. Drummond), and (E) *I. colibri* sp. nov. (photo by C. F. B. Haddad).

Figure 6. Geographic distribution of the members of the *Ischnocnema venancioi* series. Solid symbols represent the type locality of each species. Area above 500 and 1000 m shaded gray.

Figure 7. Advertisement (A, B, and C) and territorial (D) calls of the members of the *Ischnocnema venancioi* series: (A) *I. hoehnei* (recording from A. A. Giaretta), (B) *I. parnaso* sp. nov. (LOD 003), and (C, D) *I. colibri* sp. nov. (PPGT 014).

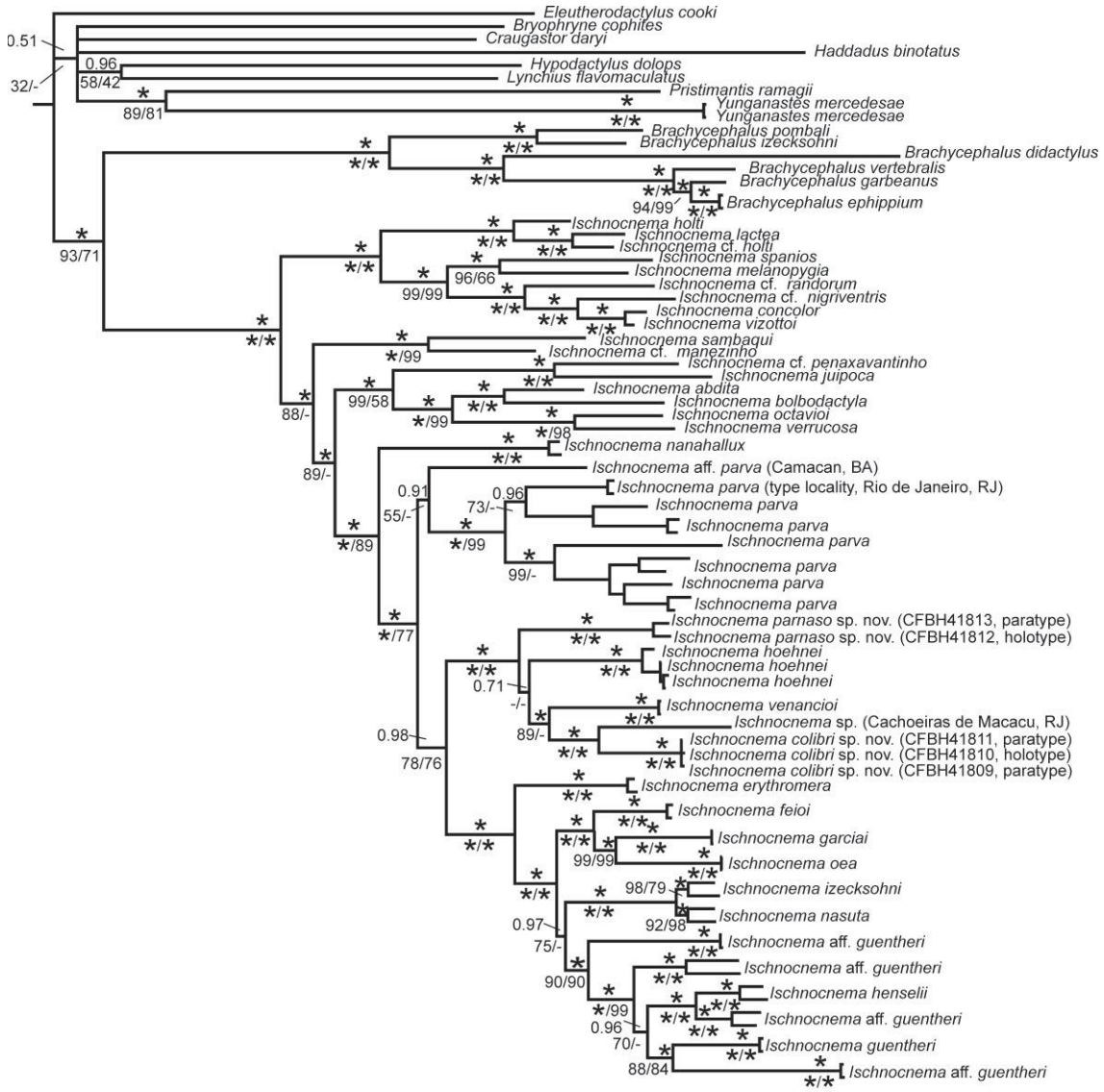
Figure 8. Clockwise, from the upper left corner: dorsal and lateral views of the head and ventral views of the left hand and left foot of the lectotype of *Ischnocnema venancioi*, MNRJ 53573. Scale bar = 5 mm.

Figure 9. Clockwise, from the upper left corner: dorsal and lateral views of the head and ventral views of the left hand and left foot of the holotype of *Ischnocnema hoehnei,* AL-MN 2525. Scale bar = 5 mm.

Figure 10. Clockwise, from the upper left corner: dorsal and lateral views of the head and ventral views of the left hand and left foot of the lectotype of *Ischnocnema parnaso* sp. nov., CFBH 40812. Scale bar = 5 mm.

Figure 11. Clockwise, from the upper left corner: dorsal and lateral views of the head and ventral views of the left hand and left foot of the lectotype of *Ischnocnema colibri* sp. nov., CFBH 40810. Scale bar = 5 mm.

1687 Fig. 1



1688

1689

Fig. 2

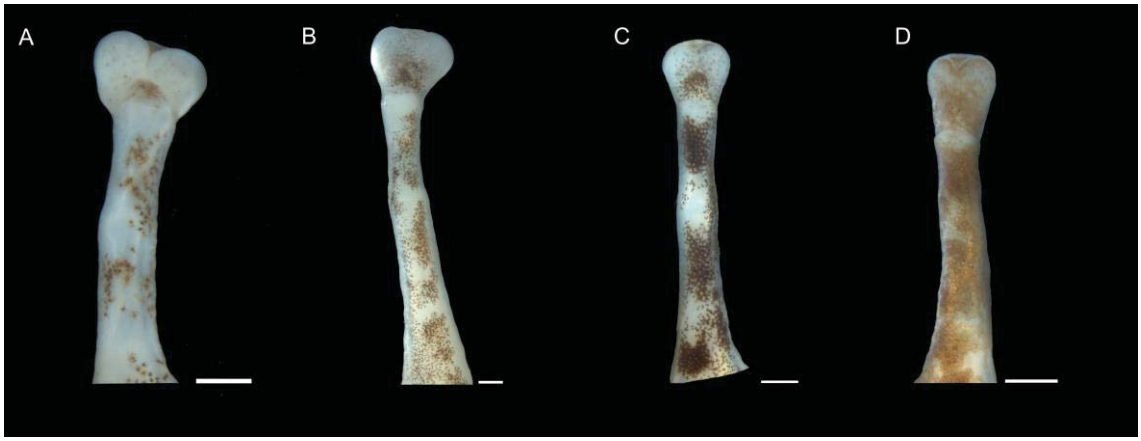


Fig. 3

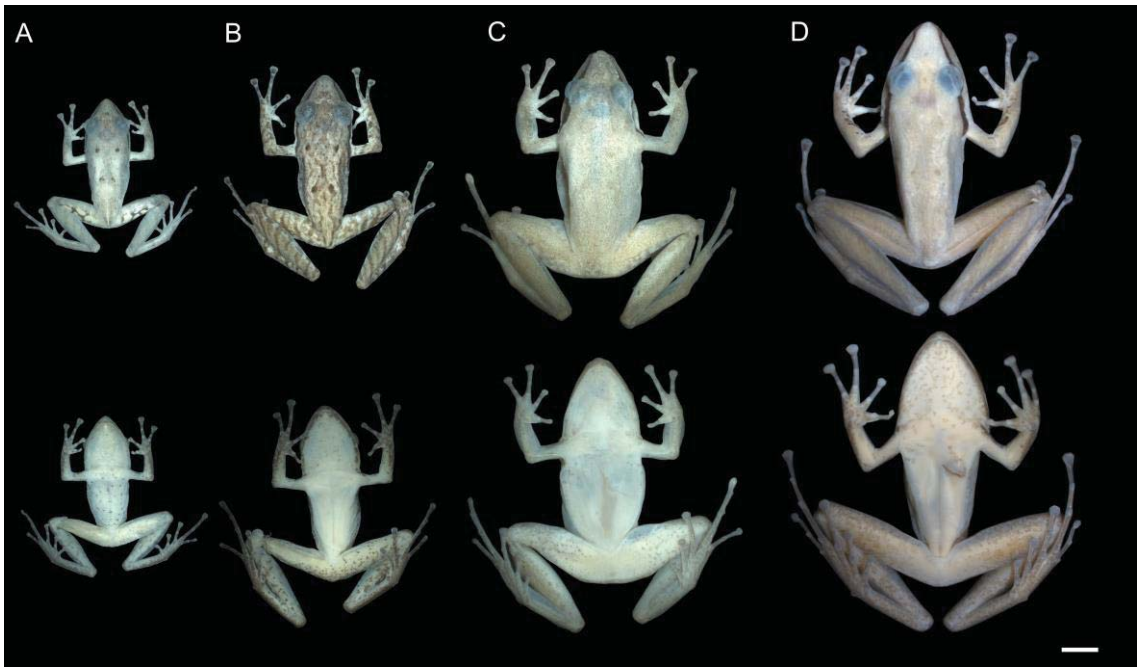


Fig. 4

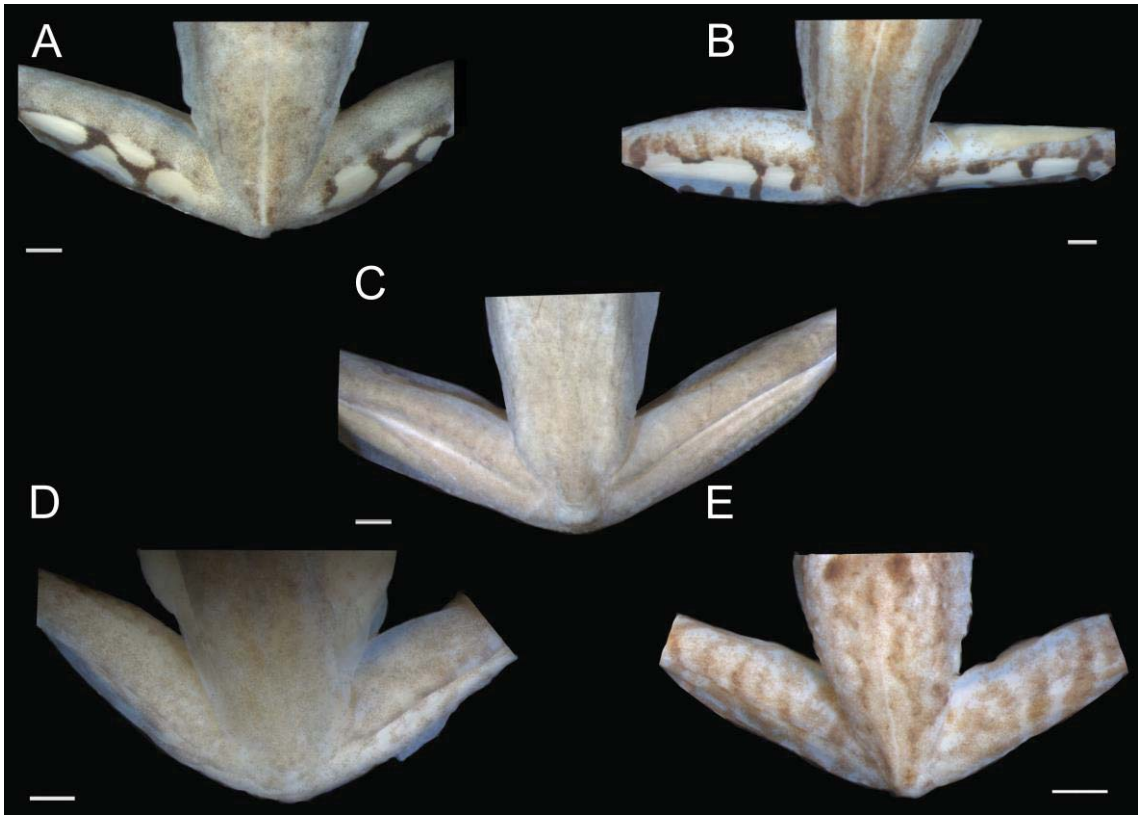
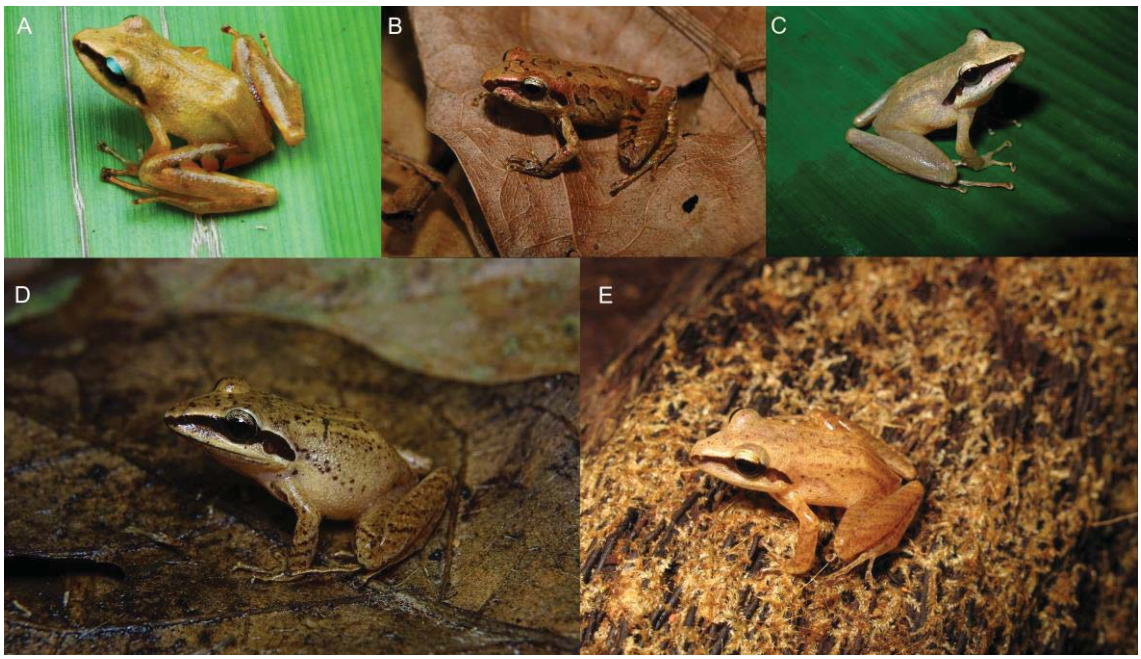
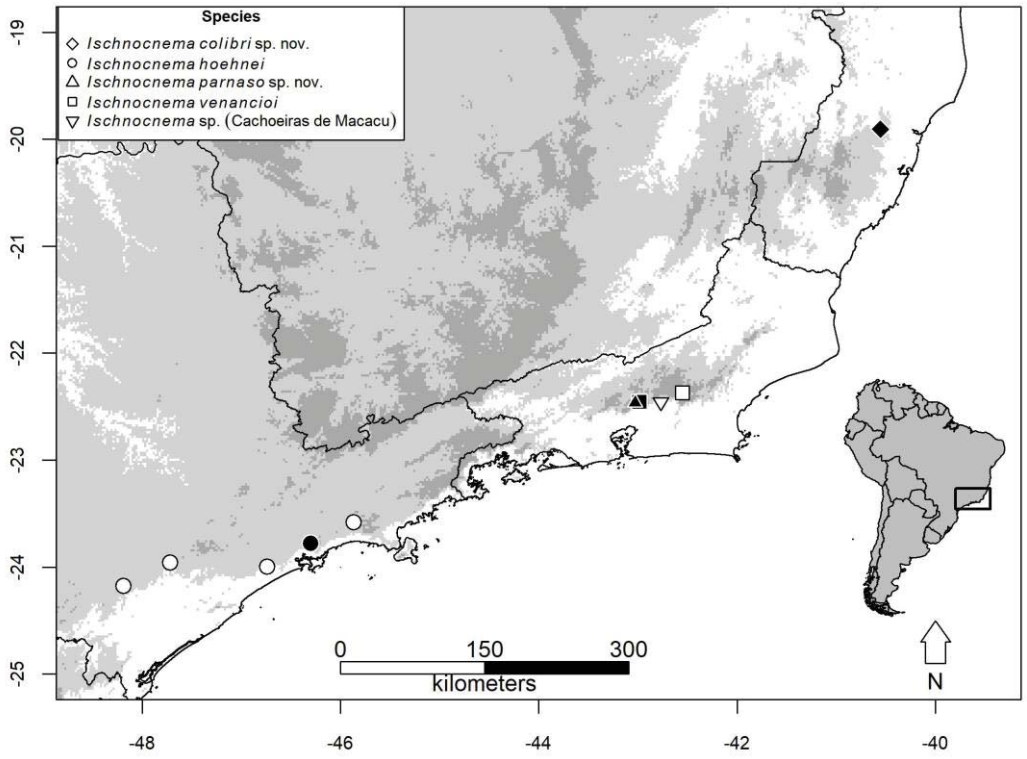


Fig. 5



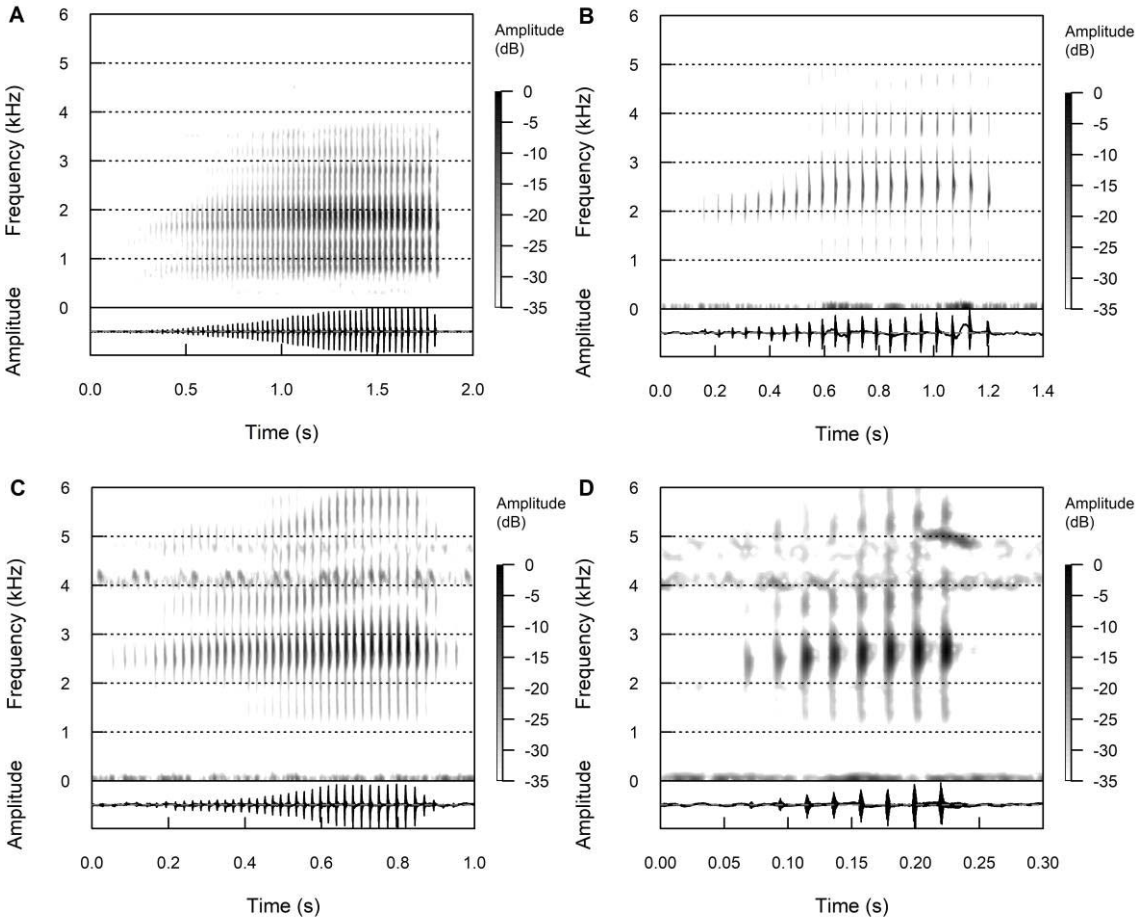
1700 Fig. 6



1701

1702

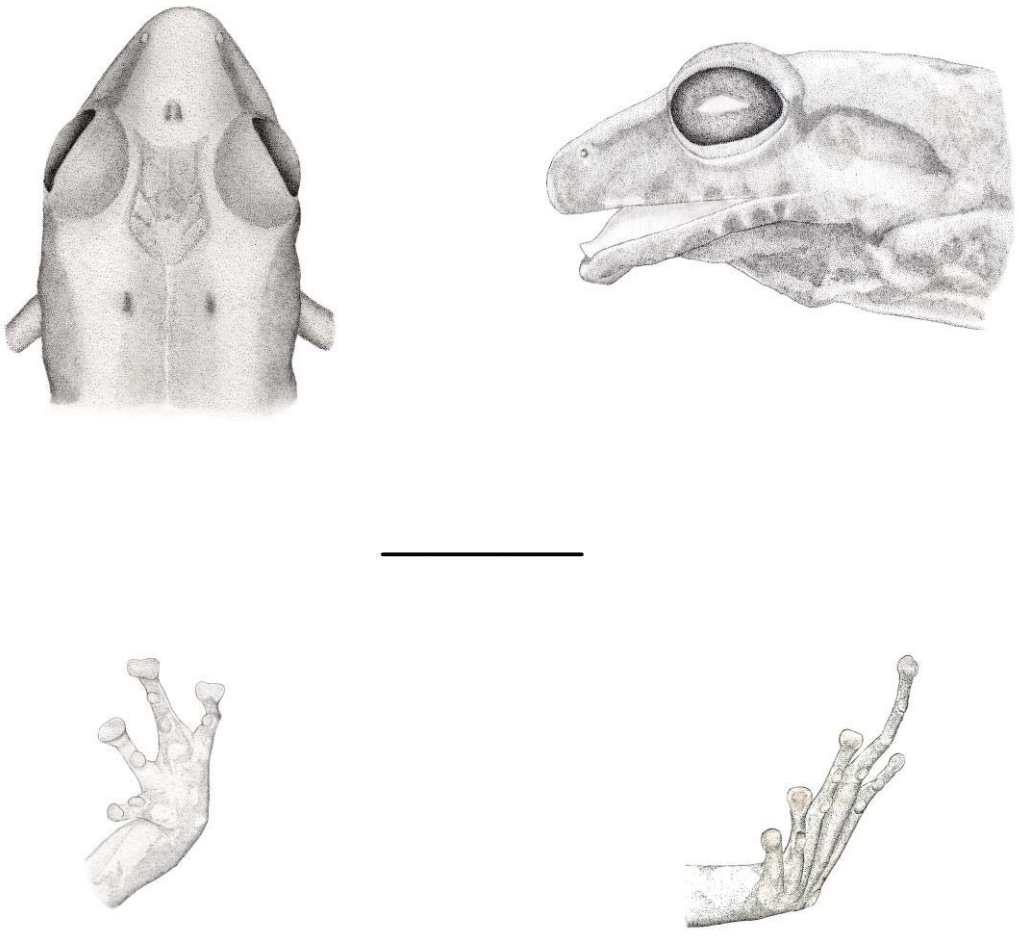
1703 Fig. 7



1704

1705

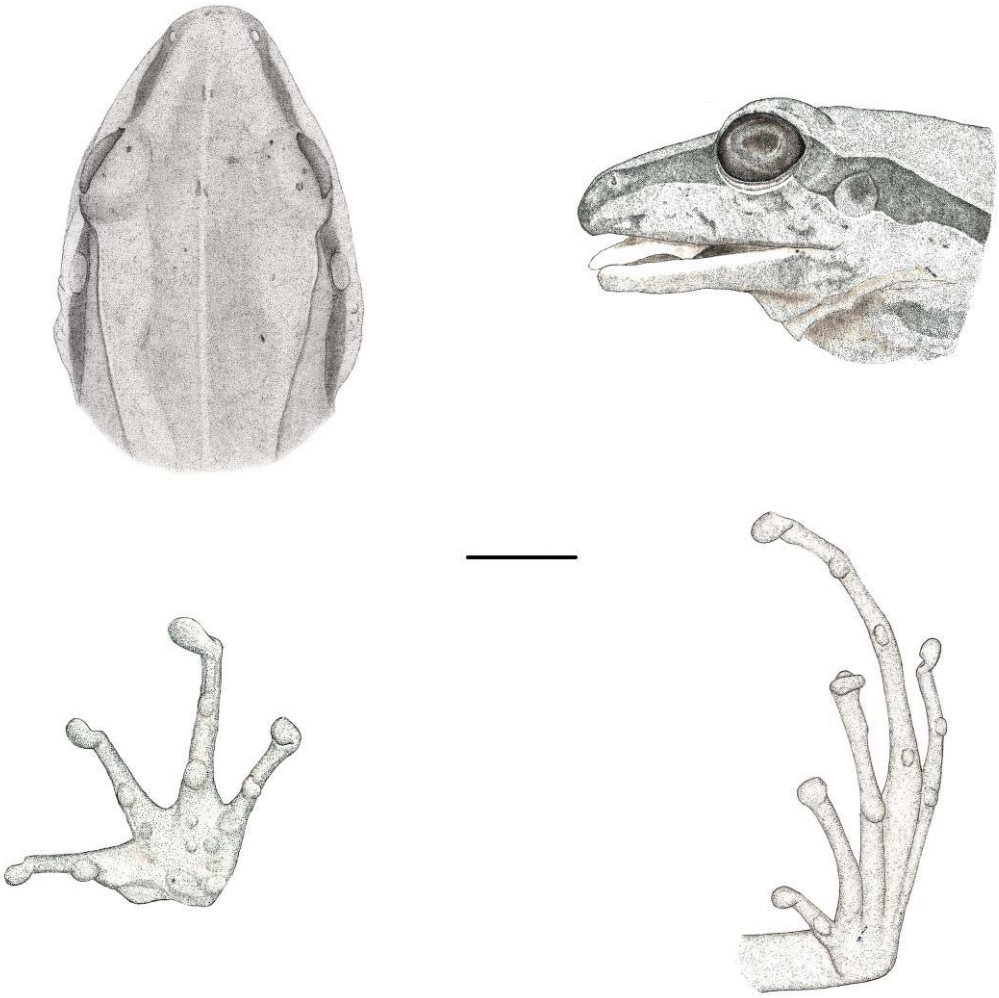
1706 Fig. 8



1707

1708

1709 Fig. 9



1710

1711

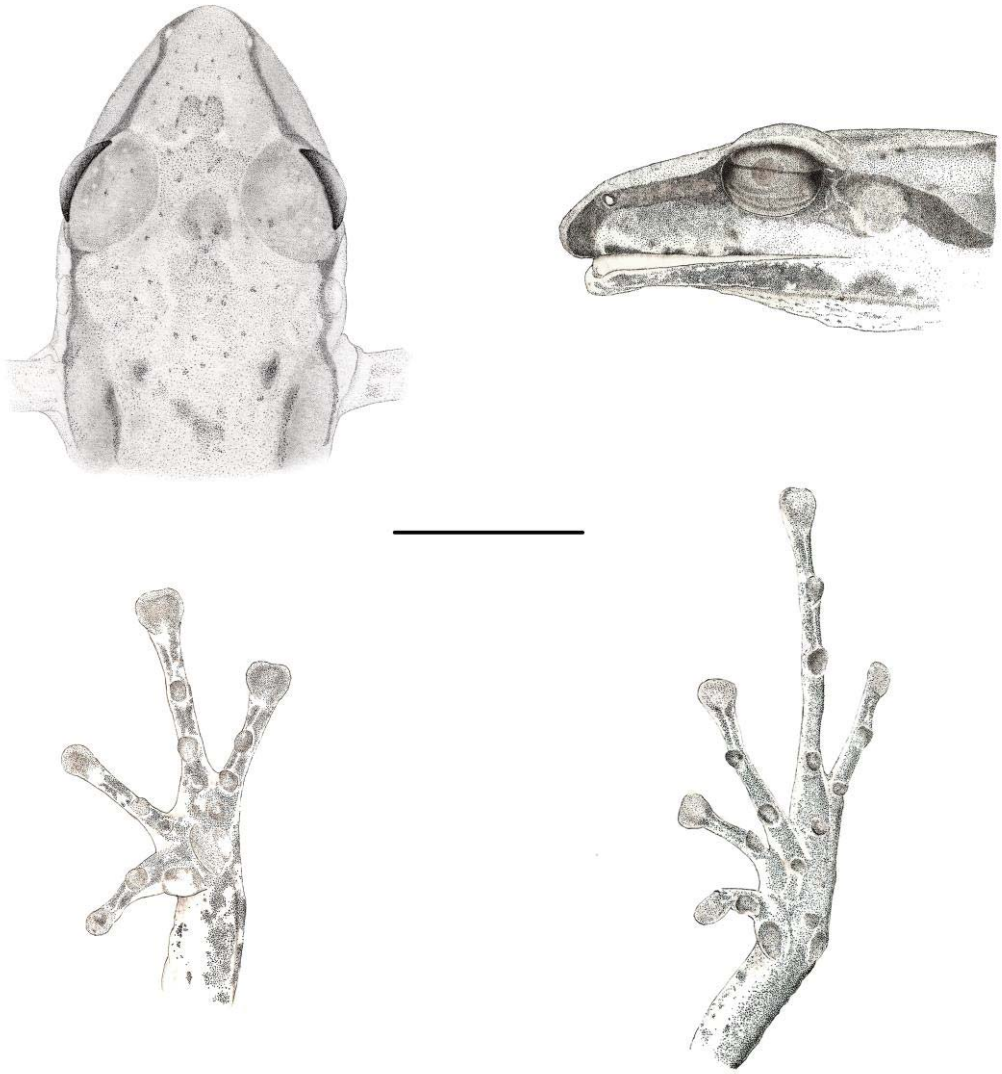
1712 Fig. 10



1713

1714

1715 Fig. 11



1716

1717

1718 Fig. S1



1719

1720 Appendix A

1721 List of terminals and accession numbers of sequences used in this paper.

Species	RAG1 GenBank ID	Tyrosinase GenBank ID	12S–tVal–16S GenBank ID
Brachycephalus cf. *didactylus*	JX267544	JX267681	JX267389, JX267467
Brachycephalus ephippium	----	DQ282917	DQ283091
Brachycephalus ephippium	HQ435721	HQ435735	HQ435679, HQ435693
Brachycephalus garbeanus	HQ435722	HQ435722	HQ435680, HQ435694
Brachycephalus izecksohni	HQ435725	HQ435739	HQ435683, HQ435696
Brachycephalus pombali	HQ435729	HQ435743	HQ435687, HQ435700
Brachycephalus vertebralis	HQ435731	HQ435745	HQ435689, HQ435702
Bryophryne cophites	EF493423	EF493508	EF493537
Craugastor daryi	EF493452	EF493480	EF493531
Eleutherodactylus cooki	EF493413	EF493455	EF493539
Haddadus binotatus	JX267547	JX267684	JX267346
Hypodactylus dolops	EF493414	EF493483	EF493394
Ischnocnema abdita	JX267551	JX267687	JX267326, JX267472
Ischnocnema bolbodactyla	JX267557	JX267692	JX267327, JX267476
Ischnocnema colibri	to be submitted	to be submitted	to be submitted
Ischnocnema colibri	to be submitted	to be submitted	to be submitted
Ischnocnema colibri	to be submitted	to be submitted	to be submitted
Ischnocnema concolor	JX267594	JX267727	JX267413, JX267366
Ischnocnema erythromera	----	JX267729	JX267340
Ischnocnema erythromera	JX267596	JX267730	JX267341
Ischnocnema feioi	MF957150	MF957160	MF957166
Ischnocnema feioi	MF957147	MF957156	MF957165
Ischnocnema garciai	MF957148	MF957158	MF957170
Ischnocnema garciai	MF957149	MF957159	MF952878, MF957163
Ischnocnema aff. *guentheri*	JX267597	JX267731	JX267339, JX267494
Ischnocnema aff. *guentheri*	JX267602	JX267737	JX267417, JX267368
Ischnocnema aff. *guentheri*	JX267605	JX267740	JX267420, JX267370
Ischnocnema aff. *guentheri*	JX267606	JX267741	JX267421, JX267371
Ischnocnema aff. *guentheri*	MF957144	MF957154	MF952879, MF952883
Ischnocnema aff. *guentheri*	MF957145	MF957155	MF952880, MF952884
Ischnocnema aff. *guentheri*	MF957141	MF957151	MF957164
Ischnocnema aff. *guentheri*	MF957143	MF957153	MF952877, MF957162, MF952881

1722

Appendix A
Continued.

Species	RAG1 GenBank ID	Tyrosinase GenBank ID	12S–tVal–16S GenBank ID
Ischnocnema guentheri	JX267611	JX267746	JX267331, JX267501, JX267502
Ischnocnema guentheri	JX267612	JX267747	JX267332, JX267503
Ischnocnema henselii	JX267563	JX267698	JX267328, JX267478
Ischnocnema henselii	JX267599	JX267734	JX267303
Ischnocnema hoehnei	----	JX267749	JX267347
Ischnocnema hoehnei	JX267614	JX267750	JX267372
Ischnocnema hoehnei	JX267615	JX267751	JX267506
Ischnocnema hoehnei	JX267616	JX267752	JX267345, JX267507
Ischnocnema cf. *holti*	JX267564	JX267699	JX267329, JX267479
Ischnocnema holti	JX267617	JX267754	JX267306
Ischnocnema izecksohni	JX267618	JX267755	JX267307
Ischnocnema izecksohni	JX267636	JX267774	JX267433, JX267375
Ischnocnema juipoca	JX267620	JX267757	JX267349
Ischnocnema lactea	JX267626	JX267763	JX267342
Ischnocnema cf. *manezinho*	JX267566	JX267701	JX267335, JX267481
Ischnocnema melanopygia	JX267634	JX267771	JX267431, JX267292
Ischnocnema nanahallux	to be submitted	to be submitted	KC569985
Ischnocnema nanahallux	to be submitted	to be submitted	KC569986
Ischnocnema nasuta	----	JX267772	JX267311
Ischnocnema nasuta	JX267637	JX267775	JX267434, JX267291, JX267520
Ischnocnema cf. *nigriventris*	JX267568	JX267704	JX267398, JX267483
Ischnocnema octavioi	JX267639	JX267777	JX267334, JX267521
Ischnocnema oea	JX267640	JX267778	JX267338
Ischnocnema oea	JX267641	JX267779	JX267313
Ischnocnema parnaso	to be submitted	to be submitted	to be submitted
Ischnocnema parnaso	to be submitted	to be submitted	to be submitted
Ischnocnema aff. *parva*	JX267656	JX267795	JX267445, JX267529
Ischnocnema parva	----	----	KY399231
Ischnocnema parva	----	KY781316	KY399230
Ischnocnema parva	JX267649	JX267787	JX267438, JX267379
Ischnocnema parva	JX267317	JX267317	JX267317
Ischnocnema parva	----	KT590282	KT590350
Ischnocnema parva	----	KT590275	KT590330
Ischnocnema parva	----	KT590316	KT590388

1727 Appendix A
1728 Continued.

Species	RAG1 GenBank ID	Tyrosinase GenBank ID	12S–tVal–16S GenBank ID
Ischnocnema parva	----	KT590297	KT590367
Ischnocnema parva	JX267648	JX267786	JX267437, JX267378
Ischnocnema parva	JX267647	JX267785	JX267436, JX267377
Ischnocnema parva	----	KT590315	KT590387
Ischnocnema cf. *penaxavantinho*	JX267574	JX267708	JX267298
Ischnocnema cf. *randorum*	JX267578	JX267799	JX267401, JX267361
Ischnocnema sambaqui	JX267661	JX267801	JX267449, JX267531
Ischnocnema spanios	JX267584	JX267717	JX267407, JX267490
Ischnocnema sp.	JX267667	JX267807	JX267454, JX267382
Ischnocnema venancioi	JX267666	JX267806	JX267321
Ischnocnema venancioi	----	----	KC468531
Ischnocnema verrucosa	JX267670	JX267810	JX267457, JX267538
Ischnocnema vizottoi	JX267672	JX267812	JX267350
Lynchius flavomaculatus	EU186745	EU186766	EU186667
Pristimantis ramagii	JX267658	JX267797	JX267318
Yunganastes mercedesae	JF809920	JF809899	JF809939
Yunganastes mercedesae	----	----	FJ539071, FJ539066

1729

1730

Appendix B

Specimens examined.

***Ischnocnema epipeda*:** BRAZIL: Espírito Santo: Santa Teresa (MNRJ 1874, USNM 200446, 235613–235620).

***Ischnocnema erythromera*:** BRAZIL: Rio de Janeiro: Santa Maria Madalena: Parque Estadual do Desengano (CFBH 28111–28115); Teresópolis (CFBH 27349, 40985).

Ischnocnema feioi: BRAZIL: Minas Gerais: Muriaé (CFBH 35994, *Ischnocnema feioi* holotype); Ervália (MZUFV 15712, *Ischnocnema feioi* paratype, 15575); Araponga (UFMG 3285, *Ischnocnema feioi* paratype). Espírito Santo: (UFMG 17078, *Ischnocnema feioi* paratype).

Ischnocnema garciai: BRAZIL: Minas Gerais: Muriaé (CFBH 39028, *Ischnocnema garciai* holotype, 39026, 39027, 39029–39033, MNRJ 90703, 90704, UFMG 18889, 18890, MZUFV 8896–8899, *Ischnocnema garciai* paratypes, 8900).

Ischnocnema gualteri: BRAZIL: Rio de Janeiro: Teresópolis (USNM 96452–96454, 208506, 208508, 208510, 208511, 208517–208519, 208527–208530).

***Ischnocnema guentheri*:** BRAZIL: Rio de Janeiro: Rio de Janeiro: Floresta da Tijuca (CFBH 26989–26994, 27440, 27442–27444, MNRJ 31666, 36483, 87540–87541, 87544–87545, 87548).

***Ischnocnema henselii*:** BRAZIL: PARANÁ: Arianópolis (CFBH 27470–27471); Piraquara (CFBH 11039–11040). SANTA CATARINA: Anitápolis (CFBH 9367–9368); São Bonifácio (CFBH 27549–27554). SÃO PAULO: São Bernardo do Campo (CFBH 12298); Tapiraí (CFBH 23298).

***Ischnocnema hoehnei*:** BRAZIL: SÃO PAULO: Itanhaém (CFBH 22139); Pilar do Sul (CFBH 8336); Salesópolis (USNM 209141); Santo André: Paranapiacaba (AL-MN 2525, *Eleutherodactylus hoehnei* holotype, CFBH 29043); São Miguel Arcanjo (CFBH 40727).

Ischnocnema izecksohni: BRAZIL: MINAS GERAIS: Aiuruoca (CFBH 36919–36920); Alto Caparaó: Parque Nacional do Caparaó (CFBH 40977–40980); Belo Horizonte (MNRJ 4217, *Eleutherodactylus izecksohni* holotype, MNRJ 4218–4219, *Eleutherodactylus izecksohni* paratypes); Conceição do Ouro (CFBH 39908–39910); Muriaé (CFBH 35990–35991, 39016, 39020–39021, 39039); Ouro Preto: Rodrigo Silva (CFBH 35793, 35796–35799).

Ischnocnema nanahallux: BRAZIL: RIO DE JANEIRO: Santa Maria Madalena: (CFBH 28085, *Ischnocnema nanahallux* holotype, 28051–28053, 28067, 28073, 28074, 28084, 28117–28119, *Ischnocnema nanahallux* paratypes).

***Ischnocnema nasuta*:** BRAZIL: RIO DE JANEIRO: Nova Friburgo (CFBH 40981–40984).

***Ischnocnema oea*:** BRAZIL: Espírito Santo: Cariacica: Reserva Biológica de Duas Bocas (CFBH 22517–22518, 22520); Santa Teresa (MNRJ 1244 *Eleutherodactylus oeus* holotype, UFMG 13735–13738, USNM 235612 *Eleutherodactylus oeus* paratype); Santa Teresa: Reserva Biológica Augusto Ruschi (CFBH 24778–24779, 30732, 40987); Santa Teresa: São Lourenço (CFBH 10815–10816, 10876–10877, 27090–27091, 37242); Vargem Alta (CFBH 25050, 27013).

Ischnocnema* sp.*: BRAZIL: Rio de Janeiro: Cachoeiras de Macacu (MNRJ 60163).

***Ischnocnema venancioi*:** BRAZIL: Rio de Janeiro: Nova Friburgo (CFBH 27435); Teresópolis (CFBH 40986, MNRJ 53573 *Eleutherodactylus venancioi* lectotype, MNRJ 35185–35187, 53565, 53566, 53572, 53574–53589, 53597–53600, 56191–56194, 56213, 56214 *Eleutherodactylus venancioi* paralectotypes, USNM 208551–208554).

Appendix C

Call records analyzed.

Call ID	Voucher	Species	Locality	Recorder
A. A. G.	Photo[a]	*Ischnocnema hoehnei*	Paranapiacaba, Santo André, Brazil	Uher 4200
LOD 001	Unvouchered[b]	*Ischnocnema parnaso*	Pedra da Baleia, Guapimirim, Rio de Janeiro, Brazil	Tascam DR-40
LOD 002	Unvouchered[b]	*Ischnocnema parnaso*	Pedra da Baleia, Guapimirim, Rio de Janeiro, Brazil	Tascam DR-40
LOD 003	Unvouchered[b]	*Ischnocnema parnaso*	Pedra do Sino, Guapimirim, Rio de Janeiro, Brazil	Tascam DR-40
LOD 004	Unvouchered[b]	*Ischnocnema parnaso*	Pedra do Sino, Guapimirim, Rio de Janeiro, Brazil	Tascam DR-40
LOD 005	Unvouchered[b]	*Ischnocnema parnaso*	Pedra do Sino, Guapimirim, Rio de Janeiro, Brazil	Tascam DR-40
PPGT 009	Unvouchered	*Ischnocnema colibri*	Reserva Biológica Augusto Ruschi, Santa Teresa, Espírito Santo, Brazil	Marantz PMD-661
PPGT 010	Unvouchered	*Ischnocnema colibri*	Reserva Biológica Augusto Ruschi, Santa Teresa, Espírito Santo, Brazil	Marantz PMD-661
PPGT 011	Unvouchered	*Ischnocnema colibri*	Reserva Biológica Augusto Ruschi, Santa Teresa, Espírito Santo, Brazil	Marantz PMD-661
PPGT 012	Unvouchered	*Ischnocnema colibri*	Reserva Biológica Augusto Ruschi, Santa Teresa, Espírito Santo, Brazil	Marantz PMD-661
PPGT 013	Unvouchered	*Ischnocnema colibri*	Reserva Biológica Augusto Ruschi, Santa Teresa, Espírito Santo, Brazil	Marantz PMD-661
PPGT 014	CFBH 40810	*Ischnocnema colibri*	Reserva Biológica Augusto Ruschi, Santa Teresa, Espírito Santo, Brazil	Marantz PMD-661

[a]AmphibiaWeb photo (CalPhotos ID: 0000 0000 0504 0973, AmphibiaWeb, 2018).

[b]The collectors recorded the males and had the calls marked for each specimen. However, this information was lost.

References

AmphibiaWeb. 2018. <https://amphibiaweb.org> University of California, Berkeley, CA, USA. Accessed 17 Jan 2018.

Species limits within the *Ischnocnema guentheri* species complex (Anura: Brachycephalidae) revealed by an integrative approach using high-throughput sequencing[†]

Pedro P. G. Taucce[a]*, Michael J. Hickerson[b], Clarissa Canedo[c], Mariana L. Lyra[a], Marcelo Gehara[d], Alan L. Lemmon[e], Emily M. Lemmon[f], Paulo C. A. Garcia[g], Miguel Vences[h], Célio F. B. Haddad[a]

[a]*Instituto de Biociências, UNESP – Univ Estadual Paulista, Câmpus Rio Claro, Departamento de Zoologia and Centro de Aquacultura (CAUNESP), Cx. Postal 199, 13506-569, Rio Claro, SP, Brazil*

[b]*Department of Biology, Marshak Science Building, City College of New York, New York, NY, USA.*

[c]*Instituto de Biologia Roberto Alcântara Gomes, UERJ – Universidade do Estado do Rio de Janeiro, Departamento de Zoologia, Rua São Francisco Xavier, 524, Maracanã, 20550-013, Rio de Janeiro, RJ, Brazil*

[d]*Department of Herpetology, American Museum of Natural History, New York, NY, USA*

[e]*Department of Scientific Computing, Florida State University, Tallahassee, Florida 32306, USA*

[f]*Department of Biological Science, Florida State University, Tallahassee, Florida 32306, USA*

[g]*Instituto de Ciências Biológicas, UFMG – Universidade Federal de Minas Gerais, Departamento de Zoologia, Laboratório de Herpetologia, Avenida Antônio Carlos, 6627, Pampulha, 31270-910, Belo Horizonte, MG, Brazil*

[†]Capítulo a ser submetido para o periódico *Molecular Phylogenetics and Evolution*

[h]*Division of Evolutionary Biology, Zoological Institute, Technical University of Braunschweig, Mendelssohnsstr. 4, 38106 Braunschweig, Germany*

** Corresponding author: pedrotaucce@gmail.com*

ABSTRACT

Despite species are one of the fundamental units of contemporary biology, there is no consensus regarding how scientists should recognize them. The recent advent of integrative taxonomy has led to an intensive discussion about how scientists should delimit species and to a renewal of taxonomy as a science. Although many studies using integrative protocols have been used in the past few years, they still need non-overlapping diagnostic characters what may be a complicated task depending on the study group. The Neotropical genus *Ischnocnema* comprises 33 species of ground-dwelling frogs with notable inter and intra-specific morphological variation, and some of them may actually be a complex of several species. Herein we apply an integrative approach with two phenotypic and one genetic lines of evidence, using 388 gene fragments, to test the hypothesis that the *I. guentheri* complex is actually composed of six species. We also use several non-Bayesian and one Bayesian species tree approaches to estimate the phylogenetic relationships within this species complex, and test them for gene-flow. We conclude thatthere are at least six morphologically crypt species within the *I. guentheri* complex. They are different from each other by acoustic and genetic characters and the level of gene flow within the species is either absent or very low. There is also a strong genetic structure among northern and southern populations of two of our candidate species. Despite not all of them have non-overlapping acoustic diagnostic characters, sister species do and we recommend careful with the taxonomic decisions regarding this species group because there is at least one available name for the species in the *I. guentheri* complex.

54 *Keywords:* Amphibia, Bioacoustics, Integrative taxonomy, Morphometry,

55 Phylogenomics.

56

1. Introduction

Species are one of the fundamental units of contemporary biology (Mayr, 1982). However, despite of its importance in biological sciences, there is no consensus regarding how scientists should recognize species and innumerous different species concepts, including some partially discordant, appeared in the literature over the years (see Mayden, 1997 and de Queiroz, 1998 for a revision). Because of that, the search for a unified species concept has been recurrent. De Queiroz (2007) proposed that existent species concepts can be unified and what they all have in common is that species are separately evolving metapopulation lineages. Nevertheless, even though we agree with a unique species concept, it is still a challenge for taxonomists to infer species boundaries, mainly in morphologically cryptic species complexes.

The recent use of the approach called integrative taxonomy (term formally introduced by Dayrat, 2005 and Will et al., 2005) has led to an intensive discussion about how scientists should delimit species (e.g. De Salle et al., 2005; Padial et al., 2010; Schlick-Steiner et al., 2010) and consequently to a renewal of taxonomy as science. Therefore, many studies have also emerged in the past few years using integrative taxonomy protocols to help delimiting species (see Pante et al., 2015 for a survey). However, operationally, describing species using this kind of protocol still requires non-overlapping diagnosable characters, which can be a complicated task depending on the study group.

The brachycephalid genus *Ischnocnema* comprises 33 species (Frost, 2018) of ground-dwelling frogs divided in the *I. guentheri*, *I. lactea*, *I. parva*, and *I. verrucosa* series (Canedo and Haddad, 2012). Ten species are presently recognized in the *I. guentheri* series, although some of them may represent morphologically cryptic species

complexes (Kwet & Solé, 2005; Gehara et al., 2013). The group presents notable morphological variation, especially with regard to color patterns (Heyer, 1984), making classic morphology-based taxonomy extremely difficult. Gehara et al. (2013) studied the whole known geographic distribution of *I. guentheri* (Steindachner, 1864) and *I. henselii* (Peters, 1870), using genetic and acoustic data to assess the limits of these species. They concluded that both species could actually be a complex of six candidate species (which will be called *I. guentheri* complex hereinafter) based on the following arguments: (1) strong deep genetic structure of the clades, (2) the clades were partly syntopic without admixture (no haplotype sharing in the only analyzed nuclear gene), and (3) advertisement call differences, non-overlapping, mainly in temporal parameters.

Understanding microevolutionary processes in a geographic context is paramount for understanding lineage and species diversification. Genetic drift and geographic isolation may induce speciation, whereas gene flow may prevent it. Natural selection can either induce or prevent the emergence of new species, depending of which type of selection dominates the system. Therefore, investigation of these processes and identification of the main forces driving or preventing speciation can help improve species delimitation.

The recent genome-scale datasets have brought a significant increase in the resolution of population scale parameters. The aim of the present study is to test the species limits among the species of the *I. guentheri* complex under an integrative approach, using high-throughput sequencing data. We construct a strong phylogenetic hypothesis for the species within the complex and test them for gene-flow. We also used previous sample efforts for acoustic data and added morphological analysis for all species.

2. Material and Methods

2.1. Taxon sampling, species hypothesis, and species recognition

We sampled all candidate species (lineages) in the *Ischnocnema guentheri* species complex based on the six candidate species from Gehara et al. (2013). Because some of them are syntopic, we included samples from localities where lineages co-occur and samples that are geographically isolated from other lineages (Fig. 1), totaling 15 terminals. Genetic materials for the high-throughput sequencing came from areas located in the following counties, all in Southern or Southeastern Brazil: Lima Duarte (Minas Gerais state), Nova Friburgo, Rio de Janeiro (both in Rio de Janeiro state), Bertioga, Cunha, Iguape, Ubatuba (all in São Paulo state), Morretes (Paraná state), São Bonifácio, and São Francisco do Sul (both in Santa Catarina state). The outgroup selection was based on previous phylogenetic studies (Canedo and Haddad, 2012; Taucce et al., 2018) and comprised three species: *I. nasuta* (Lutz, 1925), *I. oea* (Heyer, 1984), and *I. erythromera* (Heyer, 1984).

In order to correctly attribute each of our analyzed specimens to the correct candidate species, we first performed a Bayesian inference analysis with MrBayes 3.2.6 software (Ronquist et al., 2012) using a 16S rRNA combined matrix containing the sequences of Gehara et al. (2013) together with our sequences. Unvouchered advertisement calls and a few no-sequenced calling specimens were attributed to the candidate species by comparison of its calls with the call of a neighbor calling male that was sequenced and recorded. Our Bayesian tree, as well as primers, sequenced specimens, and GenBank accession numbers are given in Appendix A.

For all the analyses we used two datasets. The first one included all candidate species in the *Ischnocnema guentheri* complex (Fig. 1A, complete dataset) and the second one included all candidate species but *I.* sp. CS4 and divided *I.* sp. CS1 and *I. henselii* in southern and northern populations (Fig. 1B, north–south dataset).

2.2. Laboratory procedures

We extracted total DNA from ethanol-preserved muscle tissues using the DNeasy Qiagen® kit following manufacturer's protocols. DNA was eluted to a volume of 100 µl and quantified using a Qubit fluorometer dsDNA BR Assay Kit (Thermo Fisher Scientific Inc.). Extraction with at least 2.0 ng/µl was sent to the Center for Anchored Pylogenomics, Tallahasee, FL, USA to sequencing and initial bioinformatics analysis.

Sequencing was carried out using an Anchored Phylogenomics protocol (Lemmon et al., 2012). This method consists in designing probes that usually target single-copy, low-indel exons which are flanked by more variable introns. The resulting loci are well conserved to identify orthology, carry information beyond species level, and are variable to allow responding questions related to population genetics.

2.3. Phylogenetic analyses

2.3.1. Gene trees

We chose likelihood as the optimality criterion and used the software RAxML version 8.2.10 (Stamatakis, 2014) to infer gene trees for our resulting loci. For each

alignment RAxML searched for the most likely tree once using the GTR + Γ substitution model and then did 100 rapid bootstrap replicates.

2.3.2. Non-Bayesian species tree coalescent methods

We used four non-Bayesian coalescent methods in order to estimate our species trees. The STAR method (Liu et al., 2009) uses rooted gene trees as an input to construct a Neighbor Joining tree from a distance matrix in which the entries are twice the average ranks of coalescences in gene trees across loci. The NJst method (Liu and Yu, 2011) calculates the internode distance for each terminal pairs on gene trees to construct a distance matrix with the average internode distance for each species. Then it reconstructs a distance tree using the distance matrix. The MP-EST method (Liu et al., 2010) uses a pseudo-likelihood function to estimate the species tree given gene trees and gives the branch lengths as coalescent units. Finally, ASTRAL-III (Zhang et al., 2017) uses unrooted gene trees and finds the species tree that agrees with the largest number of quartet trees induced by the set of the gene trees. Although it is not a Bayesian analysis, ASTRAL-III gives support as local posterior probability (LPP), which is computed based on gene tree quartet frequencies (Sayyari and Mirarab, 2016). We rooted all the species trees in *Ischnocnema erythromera*, according to previous phylogenetic studies (Canedo and Haddad, 2012; Taucce et al., in press).

2.3.3. Bayesian coalescent species tree method

We used StarBEAST2 package (Ogilvie et al., 2017) from the BEAST2 software (Bouckaert et al., 2014) to estimate the species tree under a Bayesian optimality

criterion, running it for 1.0 x 10^9 generations. We used an HKY nucleotide substitution model for all genes because the model test built in BEAST2 does not work with StarBEAST2 yet (H. Ogilvie, personal communication). We used strict molecular clock and estimated clock rate (the absolute mutation rate, mutations/MY) using a narrow prior based on the mutation rates from Gehara et al. (2017) study with *Ischnocnema parva*. We kept substitution rates (relative substitution rates across partitions) fix because estimating both substitution and clock rates can make the run do not converge. We checked the run for convergence using the software Tracer 1.6 (Rambaut et al., 2013). We used Estimated Sample Size (ESS) value larger than 200 to assess run convergence.

2.4. Gene Flow Inference

We applied Generalized Phylogenetic Coalescent Sampler (G-PhoCS, Gronau et al., 2011), a Bayesian coalescent-based approach, to estimate rates of gene flow among our lineages in the two datasets. The probabilistic model of G-PhoCS uses a scaled version of migration rate, $M = m/\mu$, where m is the probability of migration from one lineage to the other and μ is the mutation rate. In order to have more tangible results we give gene flow as migrants per generation, given by $M_{AB} * \theta_B$ (McManus et al., 2015).

In G-PhoCS, gene flow is modeled using migration bands of constant migration rate throughout the history of the sampled populations. Because this approach can lead to spurious results with large number of migration bands, we first did both ways of each migration band (Figs. 2 and 3) and then we took all bands with positive gene flow and did another analysis. We considered the migration band positive to gene flow when its 95% HPD interval did not include zero. For all of the analyses we did 1.0 x 10^6

206 generations and checked convergence using ESS (> 200) on Tracer 1.6. One sample
207 control file used as an input for G-PhoCS with other parameters is shown on Appendix
208 B.
209
210 *2.5. Phenotypic analyses*
211
212 *2.5.1. Advertisement calls*
213
214 We recorded advertisement calls from each of the *Ischnocnema guentheri*
215 complex candidate species using a Marantz PMD 660, PMD 661, or a Tascam DR-40,
216 coupled to a Sennheiser K6/ME66 unidirectional microphone. We carried out
217 recordings at 44.1 kHz on a 16 bit sampling resolution. To analyze the recordings we
218 used the software Raven pro 1.4 (Bioacoustics Research Program 2011). We produced
219 spectrograms using window size of 512 samples, 75% overlap, hop size of 128 samples,
220 Discrete Fourier Transform (DFT) of 1024 samples, and window type Hann.
221 Resolution, contrast, and brightness were Raven 1.4 default. We obtained spectrogram
222 and oscillogram figures using tuneR version 1.0 (Ligges et al., 2013) and seewave
223 version 2.0.2 (Sueur et al., 2008) packages of R platform version 3.3.3 (R Core Team
224 2018). We produced spectrogram figures with window length of 512 samples, 75%
225 overlap, hop size of 128 samples, and window name Hanning. Voucher specimens are
226 housed at CFBH and UFMG (collection acronyms follow Sabaj [2016]). We also
227 reanalyzed the calls from Gehara et al. (2013) in order to enhance comparisons.
228 We measured the following call parameters: call duration (Köhler et al., 2017),
229 call rise time (Hepp and Canedo, 2013), dominant frequency (Köhler et al., 2017), notes
230 per call, note (repetition) rate (total number of notes minus one divided by the time

between the beginning of the first note to the beginning of the last note, modified from call rate parameter from Cocroft and Ryan, 1995), note (repetition) rate for the first five notes (Gehara et al., 2013), note (repetition) rate for the last five notes (Gehara et al., 2013), note (repetition) rate acceleration (note [repetition] rate of the last five notes divided by the note [repetition] rate of the first five notes times 100, this subtracted by 100 results is in a given percentage; Gehara et al., 2013). Call and note concepts follow Köhler et al. (2017).

Because for various lineages call recordings were available only for a single temperature (*Ischnocnema guentheri* and *I.* sp. CS2), or without temperature data (*I.* sp. CS1), a temperature correction by using regression residuals was not possible. We therefore assumed that temperature-dependence of call variables would be similar in all species, and chose one lineage (*I.* sp. CS4) for which recordings were available for 16°C, 18°C, 19°C, 21°C, and 22°C, and numerous variables showed a convincing trend of linear temperature-dependence without many outliers. For this lineage, we calculated regressions of each call variable against temperature and used the calculated slope (in percent of original call duration, obtained by log-transforming the original call variable data) to normalize all call recordings of all species for which recording temperature was available. We normalized call recordings to 19°C which was the temperature for which the majority of call recordings of other species was available, thus minimizing the assumptions and the corrections applied.

2.5.2. Morphology

In order to enhance comparisons, we only measured adult males. We took the following measurements to the nearest 0.1 mm with a Mitutoyo® digital caliper under a

stereomicroscope: snout-vent length (SVL), head length (HL), head width (HW), forearm length (FAL), hand length (HAL), thigh length (THL), tibia length (TL), tarsal length (TAL), foot length (FL), eye diameter (ED), tympanum diameter (TD), eye to nostril distance (END), internarial distance (IND), distance between the anterior margins of the eyes (AMD), maximum width of disk on third finger (3FD), and maximum width of disk on fourth toe (4TD). SVL, HL, HW, FAL, TL, FL, ED, TD, END, and IND follow Duellman (1970); 3FD and 4TD follow Heyer (1984); HAL, THL, and TAL follow Heyer et al. (1990); and AMD follows Garcia et al. (2003). We determined sex by the observation of secondary sexual characters of male specimens (presence of nuptial pads and vocal slits) and by direct observation of the gonads or eggs visibility through the belly wall in females. Morphological nomenclature follows previous literature on Brachycephaloidea (Heyer 1984; Heyer et al., 1990; Hedges et al., 2008; Duellman and Lehr, 2009). Museum acronyms follow Sabaj (2016) and a full list of specimens examined is given in Appendix C.

2.5.3. Principal components analyses (PCAs)

To visualize variation in bioacoustics and morphometric traits amongst the six candidate species of the *I. guentheri* complex, we performed a Principal Components Analysis (PCA). For bioacoustics variables, we used both raw and temperature-corrected acoustic datasets. We excluded the call rise time parameter in the acoustic PCAs because this variable showed no significant variation among any species in exploratory tests. We also excluded note (repetition) rate acceleration because it is directly correlated with note (repetition) rate of the first five notes and note (repetition) rate of the last five notes. Because the units in the acoustic dataset differ amongst the

281 variables, thus hampering parameter estimates, we $\log_{10}$-transformed all acoustic
282 variables.
283 Because some morphometric variables lack statistical independence relative to
284 SVL, we used, instead, the residuals stemming from linear models between SVL and
285 each of the variables. We then tested the normality of the residual using the Shapiro-
286 Wilk test of normality (Shapiro and Wilk, 1965). To avoid model overfitting, we
287 performed a progressive elimination of morphometric variables based on their adjusted
288 coefficient of correlation with SVL. Our final dataset in the morphometric PCAs
289 consisted of 85 observations, SVL and the residuals of the nine variables that showed
290 the lowest correlations with SVL.
291 We focused our interpretations in the first three components of the PCAs,
292 because, in all cases, there was a negligible increase in constrained variation by adding a
293 fourth component. We performed the PCAs, linear models, and normality tests in R
294 Statistical Environment (R Core Team, 2018). We visualized the PCAs using the R
295 packages ggbiplot (Vu, 2011), ggConvexHull, and factoextra (Kassambara and Mundt,
296 2017).
297
298 **3. Results**
299
300 *3.1. Species Tree Analyses*
301
302 *3.1.1. Non-Bayesian coalescent methods*
303
304 We used all 388 gene trees inferred using RAxML as an input to the ASTRAL-
305 III, STAR, MP-EST, and NJst software packages. The analyses of the two datasets

306 resulted in identical topologies using all four methods (Fig. 4). All branches were well-
307 supported in all methods, most of them fully supported. The branch including
308 *Ischnocnema guentheri*, *I.* sp. CS2, and *I.* sp. CS3, despite well-supported (bootstrap
309 support higher than 87% and LPP higher than 0.98), was not fully supported in the
310 topologies resulted from STAR, MP-EST, and NJst methods.
311
312 *3.1.2. Bayesian coalescent method*
313
314 StarBEAST 2 package infers gene trees and species tree simultaneously and
315 needs all species to be present on each gene tree. Because of this we used 331 genes on
316 the complete dataset and 365 on the north–south dataset. All parameters in both
317 analyses had ESS value higher than 200. The topologies in both analyses were different
318 regarding the position of *Ischnocnema* sp. CS3. In the complete analysis *I.* sp. CS3 was
319 the sister species of *I. guentheri* and *I* sp. CS2, whereas in the partial dataset analysis *I.*
320 sp. CS3 was the sister species of the northern and southern populations of *I.* sp. CS1 and
321 *I. henselii* (Fig. 5). In both analyses all the clades were fully supported, except for the
322 most inclusive clades with *I.* sp. CS3 (Fig. 5A, B, posterior probability of 0.96 and 0.64,
323 respectively). The uncertainty regarding the position of this species is shown by the red
324 line in figure 5C, D.
325
326 *3.2. Gene Flow Inference*
327
328 On the complete analysis of gene flow, only one migration band was positive, so
329 we did not repeat the run (Fig. 6). The phylogenetic position of *Ischnocnema* CS3 was
330 uncertain both in the complete and in the north-south datasets (see previous session) and

we used both topologies as input for G-PhoCS (Fig 5). We will call topology A when *Ischnocnema* sp. CS3 groups with *I.* sp. CS1 and *I. henselii* (Fig. 6, left) and topology B when *I.* sp. CS3 groups with *I.* sp. CS2 and *I. guentheri* (Fig. 6, right).

Both topologies A and B lead G-PhoCS to the same positive migration bands (Fig. 6). On the complete analysis, the migration band was from *Ischnocnema* sp. CS1 to *I.* sp. CS3 and there were 0.002–0.049 (0.023 ± 0.000) and 0.001–0.038 (0.017 ± 0.000) migrants per generation on topologies A and B, respectively. On the north–south analysis we had two migration bands. The first one was from *I.* sp. CS3 to the ancestral population of *I.* sp. CS1 south and north populations and it had 0.036–0.200 (0.106 ± 0.000) and 0.061–0.292 (0.162 ± 0.000) migrants per generation on topologies A and B, respectively. The second migration band was from the ancestral of *I. henselii* north and south populations to the ancestral of *I.* sp. CS1 north and south populations and it had 0.248–0.748 (0.464 ± 0.000) and 0.204–0.730 (0.407 ± 0.000) migrants per generation on topologies A and B, respectively.

3.3. Phenotypic analyses

3.3.1. Advertisement calls

We analyzed a total of 134 calls from 42 individuals (Table 1) raising the total amount of acoustic data in about 180% compared to the most comprehensive previous study (Gehara et al., 2013; 48 calls from 15 individuals). *Ischnocnema* sp. CS2, *I. guentheri*, and *I. henselii* had diagnostic acoustic characters differentiating them to every other species within the complex (Table 1, 2), both in the raw (Fig. 7) and the temperature-corrected (Fig. 8) datasets. Note (repetition) rate was the parameter that

most differentiated species pairs: 10 out of 15 in the raw and 7 out of 10 in the temperature-corrected dataset. *Ischnocnema* sp. CS1, *I.* sp. CS3, and *I.* sp. CS4 had no non-overlapping acoustic parameters differentiating them from each other. Another important finding is that the species pairs who are sister species are undoubtedly diagnosable among each other on the basis of bioacoustics (*I.* sp. CS1 and *I. henselii*; *I.* sp. CS2 and *I. guentheri*; Table 2). Despite the lack of diagnostic acoustic parameters between all species pairs, the advertisement calls show a great amount of variation (Fig. 9) and our PCA shows a tendency in grouping according to our species hypothesis in both raw and temperature corrected datasets (Figs. 10 and 11).

Our PCA with the raw dataset (Fig. 10) show a very strong tendency in grouping according to our species hypothesis already in the plot of PC1 versus PC2, where the only mixing is one individual of *Ischnocnema* sp. CS3 inside *I.* sp. CS1 polygon. However, these two species are plotted separated in the plot of PC1 versus PC3. The three first PCs explained 98.65% of the variation and note (repetition) rate to the first five notes, notes per call, and dominant frequency explained most of the variation in PC1, PC2, and PC3, respectively (Fig. 12).

The PCA with the temperature-corrected dataset (Fig. 11) also showed a very strong tendency in grouping according to our species hypothesis in the plot of PC1 versus PC2, despite the lack of *Ischnocnema* sp. CS1. *Ischnocnema* sp. CS3 and *I.* sp. CS4 only showed a clear separation in the plot pf PC2 versus PC3, despite not being totally overlapped in the other two plots. The first three PCs explained 96.93% of the variation and the parameters explaining most of the variation in each PC were the same as in the raw dataset analysis.

3.3.2. Morphology

Morphological characters were highly variable both intra and interspecifically and there was no discrete or morphometric character allowing us to distinguish between species. In our PCA the only species pairs forming non-overlapping groupings on one another were *Ischnocnema henselii* and *I.* sp. CS2, and *I. henselii* and *I.* sp. CS4 (Fig. 13), both in plot of PC1 versus PC2 and in the plot of PC2 with PC3. The three first PCs explained 83.51% of the variation and SVL, head width, and tarsal length explained most of the variation in PC1, PC2, and PC3, respectively (Fig. 12).

4. Discussion

4.1. Tree topologies

We recovered the same results both for the complete and the north-south datasets among all our non-Bayesian coalescent methods and the Bayesian coalescent method. We also recovered a similar overall topology with StarBEAST2 and the north-south dataset, the only difference was the position of *Ischnocnema* sp. CS3, sister group of the clade composed by *I.* sp. CS1 and *I. henselii* northern and southern lineages, versus *I.* sp. CS3 as the sister group of the clade composed by *I.* sp. CS2 and *I. guentheri* recovered in other analyses. There is a third phylogenetic hypothesis for the species complex, which is also similar to the ones recovered herein, and the only difference is also the position of *I.* sp. CS3, as the sister group of the clade composed by *I.* sp. CS1, *I. henselii*, *I.* sp. CS2, and *I. guentheri.* All three phylogenetic hypotheses recover *I.* sp. CS4 as the sister species of all other species within the *I. guentheri*

405 complex and also the species pairs *I.* sp. CS1 and *I. henselii*, and *I.* sp. CS2 and *I.*
406 *guentheri* as sister species.
407 Speciation events closely spaced in time, as appears to be the case of the clade
408 containing all species but *Ischnocnema* sp. CS4 (Fig. 5C, D), often have small
409 phylogenetic signal, leading to short branches whose relationships are difficult to
410 resolve (Phillipe et al., 1994). The incongruity with respect to the phylogenetic
411 relationships of *I.* sp. CS3 may be due to this rapid diversification event.
412
413 *4.2. Species limits within the* ***Ischnocnema guentheri*** *complex*
414
415 In the past few years, much evidence has lead authors to conclude that
416 *Ischnocnema guentheri* most likely is a complex of species, mainly based on
417 bioacoustical and Sanger sequencing data (Kwet and Solé, 2005; Gehara et al., 2013).
418 Herein we used three robust lines of evidence, including high-throughput sequencing,
419 and robust methods to test the hypothesis that *I. guentheri* is a species complex.
420 Our G-PhoCS analyses inferred one gene flow band from *Ischnocnema* sp. CS1
421 to *I.* sp. CS3 in the complete analysis, with a very low rate of less than one migrant per
422 generation (see section 3.2). In the north-south dataset, G-PhoCS detected two gene
423 flow bands, also with less than one migrant per generation each (see section 3.2). This
424 amount of gene flow is very low and it is not enough to homogenize the populations
425 (Slatkin and Maddison, 1989), evidencing the genetic isolation of our species pairs. In
426 this case we could also detect the isolation of northern and southern populations of *I.*
427 *henselii* and *I.* sp. CS1.
428 *Ischnocnema guentheri*, *I. henselii*, and *I.* sp. CS2 have unique acoustic
429 diagnostic characters (Table 2), and it is easy to differentiate them from each other and

430 from other species within the complex. Although *I.* sp. CS1, *I.* sp. CS2, and *I.* sp. CS3
431 have no acoustic diagnostic characters among each other, our PCAs of acoustic data
432 show a strong trend towards acoustic differentiation among these species. Also, the
433 sister species *I. henselii* and *I.* sp. CS1, and *I. guentheri* and *I.* sp. CS2 are acoustically
434 easily diagnosable from each other (Table 2).
435 Our morphological and morphometric characters were not good to differentiate
436 our putative species, because they were very variable inter and intra-specifically, and we
437 were not able to recognize each one of our species using morphology only. Although
438 morphological diagnostic characters are desirable to describe species, one does not need
439 to have two morphologically diagnosable species to describe them and some species
440 have being described based on their advertisement call differences only (Toledo et al.,
441 2007; Angulo and Reichle, 2008; Carvalho and Giaretta, 2013), including within the
442 *Ischnocnema* genus (Taucce et al., 2018). The anuran advertisement call functions in
443 mate recognition and vocal differences are important pre-zygotic isolation mechanisms
444 (Kelley et al., 2001). So, we assume that populations with different calls do not have
445 gene flow or if they have it will be very low.
446 To conclude, our species hypothesis satisfies several species concepts, including
447 those based on reproductive isolation (Mayr, 1942; Dobzansky, 1970) and
448 phylogenenetics (Kluge, 1990; Nixon and Wheeler, 1990; Grant, 2002). Our results
449 show that *Ischnocnema guentheri, I. henselii, I.* sp. CS1, *I.* sp. CS2, *I.* sp. CS3, and *I.* sp.
450 CS4 are separately evolving metapopulation lineages (*sensu* de Queiroz, 2007) and each
451 of those deserve a different names. Despite the north and southern populations of *I.*
452 *henselii* and *I.* sp. CS1 also show patterns of genetic isolation, we have no acoustic data
453 for the northern population of *I.* sp. CS1 and we have no sufficient data to assess the
454 species limits within these lineages.

455

456 *4.3. Comments about the taxonomic status of* ***Elosia divisa*** *Wandolleck, 1907 and*
457 ***Hylodes nasutus*** *Lutz, 1925*

458

459 *Elosia divisa* Wandolleck, 1907 is currently under the synonymy of *Hylodes*
460 *guentheri* Steindachner, 1864 (currently *Ischnocnema guentheri*; Cochran, 1955; Heyer,
461 1984). The type, collected by Dr. Ohaus in the municipality of Petrópolis, state of Rio
462 de Janeiro, Brazil, was destroyed together with approximately 90% of the herpetological
463 collection of the Dresden Museum of Zoology during the bombing of Dresden, on
464 February 13, 1945 and its original catalogue number was MTKD D 2041 (Wandolleck,
465 1907; Heyer, 1984; R. Ernst, personal communication). Despite the type is destroyed,
466 the excellent original description and illustrations (Wandolleck, 1907, his figs. 7, 7A, B)
467 make easy the association of the species with the *I. guentheri* series. According to the
468 original description (Wandolleck, 1907), diagnostic characters for the species series
469 were present in the holotype, such as long legs, a large nuptial pad, and the tips of the
470 fingers expanded (Taucce et al., unpublished data). Since there is no morphological
471 difference between the *I. guentheri* complex lineages, based on morphology, the name
472 *Elosia divisa* Wandolleck, 1907 could be attributed to any of our putative species of the
473 *I. guentheri* complex. However, we found only two lineages in the municipality of
474 Petrópolis, *I.* sp. CS3 and *I.* sp. CS4, and the name could be attributed to any of those.
475 The original description mentions that the specimen had a “heavily tuberculate surface”,
476 but according to our morphological analysis the degree of dorsal tuberculation was
477 highly variable intra-specifically, but *I.* sp. CS3 had, in general, a more tuberculate
478 dorsum. Also, a white stripe from the tip of the snout to the vent was present in the type
479 specimen (Wandolleck, 1907, species description, his Fig. 7A), and only *I.* sp. CS3 had

such a stripe in the specimens we analyzed (4 out of the 23 adult male specimens). Because of the confirmed destruction of the holotype (see above), we recommend the designation of a neotype for *Elosia divisa* Wandolleck, 1907, and we recommend that the neotype is taken from the *I.* sp. CS3 species. We are aware that such a decision has to be coupled with a formal description of the taxon and, since the species descriptions are not in the scope of our paper, we will not designate the neotype herein.

Hylodes nasutus Lutz, 1925 (currently *Ischnocnema nasuta*) was described from "the grounds of Hotel Lemburger" (Cochran, 1955), in the municipality of Nova Friburgo, state of Rio de Janeiro, Brazil (Lutz, 1925). The original description (Lutz, 1925) does not have any associated specimen or museum number, but the specimens USNM 96468–96470 were attributed as sintypes of *H. nasutus* after the description (Cochran, 1955; 1961). Heyer (1984) found only USNM 96468 and 96469, the former in the MNRJ collection. He stated that the description of *H. nasutus* was based in more than one specimen and until a thorough search be done in the Adolpho Lutz collection (AL-MN, today in the MNRJ), he preferred not to designate a lectotype for the species. We were able to examine the type series of *H. nasutus* at the Smithsonian Institution and also at Museu Nacional, and the type series is composed of at least eight specimens, all collected by A. Lutz on February 22, 1923: MNRJ 24023 (formerly USNM 96468), AL-MN 420–425, and USNM 96469. The specimen USNM 96470 was apparently exchanged with MNRJ (Cochran, 1961) but we did not find this specimen at MNRJ or USNM. The specimens housed at the AL-MN collection had a label note saying that they were collected at Leuenroth Hotel, not Lemberger hotel as Cochran (1955) stated. Leuenroth Hotel was a hotel in downtown Nova Friburgo and today there is a Leuenroth street where the Hotel was, as a tribute. We did not find any record about a Lemberger Hotel, so we think that it is likely that all specimens were collected at Leuenroth Hotel.

505 The most surprising finding regarding the type series of *H. nasutus* is that it is
506 composed of two species. The first one has a narrow snout in dorsal view and *canthus*
507 *rostralis* straight. It is the form historically associated with *I. nasuta* (Cochran, 1955;
508 Heyer, 1984; Caramaschi and Kisteumacher, 1989 "1988"). We collected this form at
509 the type locality and it is genetically and acoustically identical to *Eleutherodactylus*
510 *izecksohni* Caramaschi and Kisteumacher, 1989 "1988" (Taucce et al., unpublished
511 data). It is also the form we call *I. nasuta* herein because of historical reasons (see
512 Heyer, 1984). The second one has a more obtuse snout in dorsal view and convex-
513 shaped *canthus rostralis*. Despite the large size (SVL = 28 mm) it is morphologically
514 more similar to the species of the *I. guentheri* complex. Three of our putative species
515 occur in Nova Friburgo region, *I.* sp. CS2, *I.* sp. CS3, and *I.* sp. CS4, but the only
516 lineage we found calling in the urban part of the municipality was *I.* sp. CS2, and it is
517 probably the second species of the *H. nasutus* type series. Given the new facts, until a
518 lectotype is designated for *Hylodes nasutus* Lutz, 1925, the taxonomic status of this
519 species will remain unknown.
520
521 **5. Conclusions**
522
523 Our genetic analyses with 388 gene fragments show that the five putative
524 species within the *Ischnocnema guentheri* complex and also the two populations within
525 *Ischnocnema henselii* and *I.* sp. CS1 have a strong genetic structure, with no or very low
526 levels of gene-flow among them. Additionally, the phylogenetic position of *I.* sp. CS3 is
527 uncertain and it is probably because of the rapid diversification of the clade composed
528 by all species in the *I. guentheri* complex but *I.* sp. CS4. The acoustic parameters we
529 analyzed also show a strong tendency in grouping towards our species hypothesis and

three species, *I. guentheri*, *I. henselii*, and *I.* sp. CS2 have non-overlapping diagnostic acoustic parameters among each other and among the other three species, *I.* sp. CS1, *I.* sp. CS3, and *I.* sp. CS4. Because we do not have acoustic information for the northern population of *I.* sp. CS1 we did not assess the species limits between *I.* sp. CS1 and *I. henselii* northern and southern populations. Our morphological analyses showed the *I. guentheri* complex is a composed of several morphologically cryptic species, and no species has any diagnostic morphologic character. Our set of evidences show that *I. guentheri*, *I. henselii*, *I.* sp. CS1, *I.* sp. CS2, *I.* sp. CS3, and *I.* sp. CS4 are separately evolving metapopulation lineages and each of those deserve a different name. We recommend the taxonomic decisions regarding this species complex are done with caution, given that there is one or, depending on other decisions, two available names for some of the candidate species.

Acknowledgments

We thank J. P. Pombal Jr (MNRJ), P. C. A. Garcia (UFMG), and K. de Queiroz (USNM) for making available material under their care. For support at the MNRJ we thank P. Pinna and M. W. Cardoso, at UFMG we thank I. Marques, and at USNM we thank A. Wynn. We are grateful to Centro de Estudos de Insetos Sociais (CEIS; São Paulo State University [UNESP]) for allowing us the use of the molecular laboratory. G. Thom and I. Overcast helped with Bioinformatics procedures and D. M. Neves helped with R. This research was supported by resources supplied by the Center for Scientific Computing (NCC/GridUNESP) of the UNESP and Cyberinfrastructure for Phylogenetic Research (CIPRES). P. P. G. T. thanks São Paulo Research Foundation (FAPESP)/ Coordenação de Aperfeiçoamento de Pessoal de Nível Superior (CAPES) grants

#2014/05772-4 and BEPE #2016/22450-6 and for the Ph. D. fellowship and financial support and Instituto Chico Mendes de Conservação da Biodiversidade (ICMBio) for collection permits (#42108). C. C. thanks Fundação Carlos Chagas Filho de Amparo à Pesquisa do Estado do Rio de Janeiro (FAPERJ), grant E-26/102.818/2011, for financial support. C. F. B. H. thanks FAPESP grant #2013/50741-7, FAPESP / Fundação Grupo Boticário de Proteção à Natureza grant #2014/50342-8, and Conselho Nacional de Desenvolvimento Científico e Tecnológico (CNPq) for financial support.

Appendices A, B, and C. Supplementary material

References

Angulo, A., Reichle, S., 2008. Acoustic signals, species diagnosis, and species concepts: the case of a new cryptic species of *Leptodactylus* (Amphibia, Anura, Leptodactylidae) from the Chapare region, Bolivia. Zool. J. Linn. Soc. 59–77. https://doi.org/10.1111/j.1096-3642.2007.00338.x

Bioacoustics Research Program, 2011. Raven Pro: Interactive Sound Analysis Software.

Bouckaert, R., Heled, J., Kühnert, D., Vaughan, T., Wu, C.H., Xie, D., Suchard, M.A., Rambaut, A., Drummond, A.J., 2014. BEAST 2: A Software Platform for Bayesian Evolutionary Analysis. PLoS Comput. Biol. 10, 1–6. https://doi.org/10.1371/journal.pcbi.1003537

Canedo, C., Haddad, C.F.B., 2012. Phylogenetic relationships within anuran clade Terrarana, with emphasis on the placement of Brazilian Atlantic rainforest frogs genus *Ischnocnema* (Anura: Brachycephalidae). Mol. Phylogenet. Evol. 65, 610–620. https://doi.org/10.1016/j.ympev.2012.07.016

580 Caramaschi, U., Kisteumacher, G., 1989 “1988”. A New Species of *Eleutherodactylus*
581 (Anura : Leptodactylidae) From Minas Gerais, Southeastern Brazil. Herpetologica
582 44, 423–426.
583 Carvalho, T.R. de, Giaretta, A.A., 2013. Taxonomic circumscription of *Adenomera*
584 *martinezi* (Bokermann, 1956) (Anura: Leptodactylidae: Leptodactylinae) with the
585 recognition of a new cryptic taxon through a bioacoustic approach. Zootaxa 3701,
586 207–237. https://doi.org/10.11646/zootaxa.3701.2.5
587 Cochran, D.M., 1961. Type Specimens of Reptiles and Amphibians in the U.S. National
588 Museum. Bull. United States Natl. Museum 220, xv+289.
589 https://doi.org/10.5479/si.03629236.220
590 Cochran, D.M., 1955. Frogs of Southeastern Brazil. Bull. U.S. Natl. Museum 206, 1–
591 406.
592 Cocroft, R., Ryan, M.J., 1995. Patterns of advertisement call evolution in toads and
593 chorus frogs. Anim. Behav. 49, 283–303. https://doi.org/10.1006/anbe.1995.0043
594 Dayrat, B., 2005. Towards integrative taxonomy. Biol. J. Linn. Soc. 85, 407–415.
595 https://doi.org/10.1111/j.1095-8312.2005.00503.x
596 de Queiroz, K., 2007. Species concepts and species delimitation. Syst. Biol. 56, 879–
597 886. https://doi.org/10.1080/10635150701701083
598 De Salle, R., Egan, M.G., Siddall, M., 2005. The unholy trinity: taxonomy, species
599 delimitation and DNA barcoding. Philos. Trans. R. Soc. Lond. B. Biol. Sci. 360,
600 1905–16. https://doi.org/10.1098/rstb.2005.1722
601 Dobzhansky, T., 1970. Genetics of the evolutionary process. Columbia University
602 Press, New York.
603 Duellman, W.E., 1970. The Hylid of Middle America. Monogr. Mus. Nat. Hist. Univ.
604 Kans.1–2: 1–753.

605 Duellman, W.E., Lehr, E., 2009. Terrestrial-Breeding Frogs (Strabomantidae) in Peru.
606 Natur und Tier - Verlag GmbH, Münster, Germany.
607 Frost, D.R., 2018. Amphibian Species of the World: an Online Reference. Am. Museum
608 Nat. Hist. New York, USA. URL
609 http://research.amnh.org/herpetology/amphibia/index.html (accessed 2.04.18).
610 Garcia, P.C.A., Vinciprova, G., Haddad, C.F.B., 2003. The taxonomic status of *Hyla*
611 *pulchella joaquini* (Anura: Hylidae) with description of its tadpole and
612 vocalization. Herpetologica 59, 350–363. https://doi.org/10.1655/01-54
613 Gehara, M., Barth, A., Oliveira, E.F. de, Costa, M.A., Haddad, C.F.B., Vences, M.,
614 2017. Model-based analyses reveal insular population diversification and cryptic
615 frog species in the *Ischnocnema parva* complex in the Atlantic forest of Brazil.
616 Mol. Phylogenet. Evol. 112, 68–78. https://doi.org/10.1016/j.ympev.2017.04.007
617 Gehara, M., Canedo, C., Haddad, C.F.B., Vences, M., 2013. From widespread to
618 microendemic: Molecular and acoustic analyses show that *Ischnocnema guentheri*
619 (Amphibia: Brachycephalidae) is endemic to Rio de Janeiro, Brazil. Conserv.
620 Genet. 14, 973–982. https://doi.org/10.1007/s10592-013-0488-5
621 Grant, T., 2002. Testing Methods: The Evaluation of Discovery Operations in
622 Evolutionary Biology. Cladistics 18, 94–111. https://doi.org/10.1111/j.1096-
623 0031.2002.tb00142.x
624 Gronau, I., Hubisz, M.J., Gulko, B., Danko, C.G., Siepel, A., 2011. Bayesian inference
625 of ancient human demography from individual genome sequences. Nat. Genet. 43,
626 1031–1035. https://doi.org/10.1038/ng.937
627 Hedges, S.B., Duellman, W.E., Heinicke, M.P., 2008. New World direct-developing
628 frogs (Anura: Terrarana): Molecular phylogeny, classification, biogeography, and
629 conservation. Zootaxa 1737, 1–182.

630 Hepp, F., Canedo, C., 2013. Advertisement and aggressive calls of *Ischnocnema oea*
631 (Heyer, 1984) (Anura, Brachycephalidae). Zootaxa 3710, 197–199.
632 https://doi.org/10.11646/zootaxa.3710.2.6
633 Heyer, W.R., 1984. Variation, systematics, and zoogeography of Eleutherodactylus
634 guentheri and closely related species (Amphibia: Anura: Leptodactylidae). Smith
635 Contr Zool 402, 15342. https://doi.org/10.5479/si.00810282.402
636 Heyer, W.R., Rand, A.S., Cruz, C.A.G. Da, Peixoto, O.L., Nelson, C.E., 1990. Frogs of
637 Boraceia. Arq. Zool. 31, 235–410.
638 Kassambara, A., Mundt, F., 2017. factoextra: Extract and visualize the results of
639 multivariate data analyses.
640 Kelley, D.B., Tobias, M.L., 2001. Producing and perceiving frog songs: dissecting the
641 neural bases for vocal behaviors in *Xenopus laevis*, in: Ryan, M.J. (Ed.), Anuran
642 Communication. Smithsonian Institution Press, Washington, pp. 156–166.
643 Kluge, A.G., 1990. Species as historical individuals. Biol. Philos. 5, 417–431.
644 https://doi.org/10.1007/BF02207380
645 Köhler, J., Jansen, M., Rodríguez, A., Kok, P.J.R., Toledo, L.F., Emmrich, M., Glaw,
646 F., Haddad, C.F.B., Rödel, M.O., Vences, M., 2017. The use of bioacoustics in
647 anuran taxonomy: Theory, terminology, methods and recommendations for best
648 practice, Zootaxa. https://doi.org/10.11646/zootaxa.4251.1.1
649 Kwet, A., Solé, M., 2005. Validation of *Hylodes henselii* Peters, 1870, from Southern
650 Brazil and description of acoustic variation in *Eleutherodactylus guentheri* (Anura:
651 Leptodactylidae). J. Herpetol. 39, 521–532. https://doi.org/10.1670/53-04A.1
652 Lemmon, A.R., Emme, S.A., Lemmon, E.M., 2012. Anchored hybrid enrichment for
653 massively high-throughput phylogenomics. Syst. Biol. 61, 727–744.
654 https://doi.org/10.1093/sysbio/sys049

655 Ligges, U., Krey, S., Mersman, O., Schnackenberg, S., 2013. tuneR: Analysis of music.
656 Liu, L., Yu, L., 2011. Estimating species trees from unrooted gene trees. Syst. Biol. 60,
657 661–667. https://doi.org/10.1093/sysbio/syr027
658 Liu, L., Yu, L., Edwards, S. V, 2010. A for estimating species trees under thmaximum
659 pseudo-likelihood approach e coalescent model. BMC Evol. Biol. 10, 302.
660 https://doi.org/10.1186/1471-2148-10-302
661 Liu, L., Yu, L., Pearl, D.K., Edwards, S. V., 2009. Estimating species phylogenies using
662 coalescence times among sequences. Syst. Biol. 58, 468–477.
663 https://doi.org/10.1093/sysbio/syp031
664 Lutz, A., 1925. Batraciens du Brésil. Comptes Rendus Mémoires Hebd. des Séances la
665 Société Biol. des ses Fil. 22, 211–214.
666 Martin, C.A., 2017. ggConvexHull: Add a convex hull geom to ggplot2.
667 Mayden, R.L., 1997. A hierarchy of species concepts: The denouement in the saga of
668 the species problem, in: Claridge, M.F., Dawah, H.A., Wilson, M.R. (Eds.),
669 Species: The Units of Biodiversity. Chapman and Hall, London, pp. 381–424.
670 Mayr, E., 1982. The Growth of Biological Thought: Diversity, Evolution, and
671 Inheritance. Belknap Press of Harvard University Press, Cambridge,
672 Massachusetts.
673 Mayr, E., 1942. Systematics and the origin of species. Columbia University Press, New
674 York.
675 McManus, K.F., Kelley, J.L., Song, S., Veeramah, K.R., Woerner, A.E., Stevison, L.S.,
676 Ryder, O.A., Project, G.A.G., Kidd, J.M., Wall, J.D., Bustamante, C.D., Hammer,
677 M.F., 2015. Inference of gorilla demographic and selective history from whole-
678 genome sequence data. Mol. Biol. Evol. 32, 600–612.
679 https://doi.org/10.1093/molbev/msu394

680 Nixon, K.C., Wheeler, Q.D., 1990. An amplification of the phylogenetic species
681 concept. Cladistics 6, 211–223. https://doi.org/10.1111/j.1096-
682 0031.1990.tb00541.x
683 Ogilvie, H.A., Bouckaert, R.R., Drummond, A.J., 2017. StarBEAST2 brings faster
684 species tree inference and accurate estimates of substitution rates. Mol. Biol. Evol.
685 34, 2101–2114. https://doi.org/10.1093/molbev/msx126
686 Padial, J.M., Miralles, A., De la Riva, I., Vences, M., 2010. The integrative future of
687 taxonomy. Front. Zool. 7, 16. https://doi.org/10.1186/1742-9994-7-16
688 Pante, E., Schoelinck, C., Puillandre, N., 2015. From integrative taxonomy to species
689 description: One step beyond. Syst. Biol. 64, 152–160.
690 https://doi.org/10.1093/sysbio/syu083
691 Peters, W.C.H., 1870. Über neue Amphien (*Hemidactylus*, *Urosaura*, *Tropdolepisma,*
692 *Geophis, Uriechis, Scaphiophis, Hoplocephalus, Rana, Entomoglossus,*
693 *Cystignathus, Hylodes, Arthroleptis, Phyllobates, Cophomantis*) des Königlich
694 Zoologisch Museum. Monatsberichte der Königlichen Preuss. Akad. des
695 Wissenschaften zu Berlin 1870, 641–652.
696 Phillipe, H., Chenuil, A., Adoutte, A., 1994. Can the Cambrian explosion be inferred
697 through molecular phylogeny? Dev. Suppl. 1994, 15–25.
698 R Core Team, 2018. R: A language and environment for statistical computing.
699 Rambaut, A., Suchard, M.A., Drummond, A.J., 2013. Tracer version 1.6.
700 Ronquist, F., Teslenko, M., Van Der Mark, P., Ayres, D.L., Darling, A., Höhna, S.,
701 Larget, B., Liu, L., Suchard, M.A., Huelsenbeck, J.P., 2012. Mrbayes 3.2: Efficient
702 bayesian phylogenetic inference and model choice across a large model space.
703 Syst. Biol. 61, 539–542. https://doi.org/10.1093/sysbio/sys029

704 Sabaj, M.H., 2016. Standard Symbolic Codes for Institutional Resource Collections in
705 Herpetology and Ichthyology: an Online Reference. Version 6.5 (16 August 2016).
706 Electronically accessible at http://www.asih.org/, American Society of
707 Ichthyologists and Herpetologists, Was 5, 802–832. https://doi.org/Available at:
708 http://www.asih.org/resources. Archived by WebCite at
709 http://www.webcitation.org/6lkBdh0EO on 3 November 2016.
710 Sayyari, E., Mirarab, S., 2016. Fast coalescent-based computation of local branch
711 support from quartet frequencies. Mol. Biol. Evol. 33, 1654–1668.
712 https://doi.org/10.1093/molbev/msw079
713 Schlick-Steiner, B.C., Steiner, F.M., Seifert, B., Stauffer, C., Christian, E., Crozier,
714 R.H., 2010. integrative taxonomy: A multisource approach to exploring
715 biodiversity. Annu. Rev. Entomol. 55, 421–438. https://doi.org/10.1146/annurev-
716 ento-112408-085432
717 Shapiro, S.S., Wilk, M.B., 1965. An analysis of variance test for normality (complete
718 samples). Biometrika 52, 591. https://doi.org/10.2307/2333709
719 Slatkin, M., Maddison, W.P., 1989. A cladistic measure of gene flow inferred from the
720 phylogenies of alleles. Genetics 123, 603–613.
721 Stamatakis, A., 2014. RAxML version 8: a tool for phylogenetic analysis and post-
722 analysis of large phylogenies. Bioinformatics 30, 1312–1313.
723 https://doi.org/10.1093/bioinformatics/btu033
724 Steindachner, F., 1864. Batrachologische Mittheilungen. Verhandlungen des Zool.
725 Vereins Wien 14, 239–288.
726 Sueur, J., Aubin, T., Simonis, C., 2008. Seewave , a free modular tool for sound
727 analysis and synthesis. Bioacoustics 18, 213–226.
728 https://doi.org/10.1080/09524622.2008.9753600

729 Toledo, L.F., Garcia, P.C.A., Lingnau, R., Haddad, C.F.B., 2007. A new species of
730 *Sphaenorhynchus* (Anura; Hylidae) from Brazil. Zootaxa 68, 57–68.
731 https://doi.org/10.1163/156853804322992788
732 Vu, V.Q., 2011. ggbiplot: A ggplot2 based biplot.
733 Wandolleck, B., 1907. Einige neue und weniger bekannte Batrachier von Brazilien.
734 Abhandlungen und Berichte des Zool. und Anthropol. Museums zu Dresden 11, 1–
735 15.
736 Will, K.W., Mishler, B.D., Wheeler, Q.D., 2005. The Perils of DNA Barcoding and the
737 Need for Integrative Taxonomy. Syst. Biol. 54, 844–851.
738 https://doi.org/10.1080/10635150500354878
739 Zhang, C., Sayyari, E., Mirarab, S., 2017. Comparative Genomics, in: Meidanis, J.,
740 Nakhleh, L. (Eds.), Comparative Genomics, Lecture Notes in Computer Science.
741 Springer International Publishing, Cham, pp. 53–75. https://doi.org/10.1007/978-3-
742 319-67979-2

743 Table 1. Advertisement call parameters range of *Ischnocnema guentheri*, *I. henselii*, and the four candidate species.

Species	Number of analyzed individuals (calls)	Call duration (s)	Call rise time (%)	Dominant frequency (kHz)	Notes per call	Note (repetition) rate (notes/s)	Note (repetition) rate to the first five notes (notes/s)	Note (repetition) rate to the last five notes (notes/s)	Note (repetition) rate acceleration (%)
Ischnocnema sp. CS1	4 (15)	0.48–1.95	81–100	2.15–2.89	6–28	8.86–13.95	8.60–14.04	8.95–13.89	-3–30
Ischnocnema sp. CS2	5 (20)	1.79–9.32	22–100	2.41–2.91	56–218	21.13–30.99	6.05–25.97	22.60–30.53	12–289
Ischnocnema sp. CS3	14 (42)	1.45–13.94	79–100	2.20–3.28	20–71	4.43–13.10	2.99–13.89	0.82–12.90	-90–152
Ischnocnema sp. CS4	6 (30)	1.04–11.18	67–100	2.02–3.06	21–135	11.56–20.77	5.73–21.39	10.75–20.51	-23–107
Ischnocnema guentheri	6 (12)	26.82–43.21	85–100	2.91–3.28	71–142	2.20–3.32	1.74–3.07	2.71–4.55	44–112
Ischnocnema henselii	7 (15)	12.80–20.98	68–99	2.80–3.19	103–190	6.16–10.43	3.61–7.12	7.43–13.20	56–207

744 Table 2. Temperature corrected (up right) and raw (down left) diagnostic acoustic
745 parameters among the species pairs within the *Ischnocnema guentheri* complex. CD =
746 call duration, CRT = call rise time, DF = dominant frequency, NPC = notes per call,
747 NRA = note (repetition) rate acceleration, NRF = note (repetition) rate to the first five
748 notes, NRL = note (repetition) rate to the last five notes, N. A. = not applicable.

	Ischnocnema sp. (CS1)	*Ischnocnema* sp. (CS2)	*Ischnocnema* sp. (CS3)	*Ischnocnema* sp. (CS4)	*Ischnocnema guentheri*	*Ischnocnema henselii*
Ischnocnema sp. (CS1)		N.A.	N.A.	N.A.	N.A.	N.A.
Ischnocnema sp. (CS2)	NPC, NRR, NRL		NPC, NRR, NRL	NPC, NRR, NRL	CD, DF, NPC, NRR, NRF, NRL	CD, NRR, NRF, NRL
Ischnocnema sp. (CS3)	------	NRR, NRL		------	CD, NPC, NRR, NRF	NPC, NRL
Ischnocnema sp. (CS4)	------	NRR, NRL	------		CD, NRR, NRF, NRL, CRT	CD, NRF, NRA
Ischnocnema guentheri	CD, DF, NPC, NRR, NRF, NRL, NRA	CD, DF, NRR, NRF, NRL	CD, NPC, NRR, NRF	CD, NRR, NRF, NRL		CD, NRR, NRF, NRL, NRA
Ischnocnema henselii	CD, NPC, NRF, NRA	CD, NRR, NRF, NRL	NPC	CD, NRR	CD, NRR, NRF, NRL	

749

Figure 1. Sampled specimens of the *Ischnocnema guentheri* complex. (A) Complete and (B) north–south datasets. Areas above 500 and 1000 m of elevation are shaded gray.

Figure 2. Migration bands of the complete dataset tested on the Generalized Phylogenetic Coalescent Sampler (G-PhoCS). 1 = *Ischnocnema* sp. CS1, 2 = *I.* sp. CS2, 3 = *I.* sp. CS3, 4 = *I.* sp. CS4, g = *I. guentheri*, and h = *I. henselii*.

Figure 3. Migration bands of the north–south dataset tested on the Generalized Phylogenetic Coalescent Sampler (G-PhoCS). 1n = *Ischnocnema* sp. CS1 north, 1s = *I.* sp. CS1 south, 2= *I.* sp. CS2, 3 = *I.* sp. CS3, g = *I. guentheri*, hn = *I. henselii* north, and hs = *I. henselii* south.

Figure 4. Species tree topologies for *Ischnocnema guentheri* species complex inferred with several non-Bayesian coalescent based methods. (A) Complete dataset, clockwise: ASTRAL-III, STAR, MP-EST, and NJst. (B) Northern-southern dataset, clockwise: ASTRAL-III, STAR, MP-EST, and NJst. Numbers are bootstrap supports, except for ASTRAL-III, which gives support as local posterior probability.

Figure 5. Species tree topologies for *Ischnocnema guentheri* species complex inferred using StarBEAST 2 software package under Bayesian optimality criterion. Maximum clade credibility tree of (A) complete and (B) north–south datasets. Set of all species trees minus 10 percent burnin of (C) complete and (D) north–south datasets. The most common topology is drawn in blue and the second most common one is drawn in red, showing the uncertainty of the position of *Ischnocnema* sp. CS3 in both analyses.

Figure 6. Positive migration bands for *Ischnocnema guentheri* complex inferred by Generalized Phylogenetic Coalescent Sampler (G-PhoCS). (A) Complete and (B) north–south datasets. Both topologies A (left) and B (right) represented. HEN = *Ischnocnema henselii*, GUE = *I. guentheri*, and CS1–CS4 = *I.* sp. CS1–CS4. Lineages beginning with "anc" are ancestral lineages and root is the ancestral lineage of the whole tree.

Figure 7. Boxplots showing full range of variation of the eight measured acoustic parameters in the six putative species within the *Ischnocnema guentheri* complex. Sister species share the same color. 1–4 = *I.* sp. CS1–CS4, g = *I. guentheri*, and h = *I. henselii*.

Figure 8. Boxplots showing full range of variation of the eight measured acoustic parameters in the five putative species within the *Ischnocnema guentheri* complex available in the temperature corrected dataset. Sister species share the same color. 1–4 = *I.* sp. CS1–CS4, g = *I. guentheri*, and h = *I. henselii*.

Figure 9. Spectrogram (above) and oscillogram (bellow) of the six putative species within the *Ischnocnema guentheri* complex. (A–D) *I.* sp. CS1–CS4, (E) *I. guentheri*, and (F) *I. henselii*.

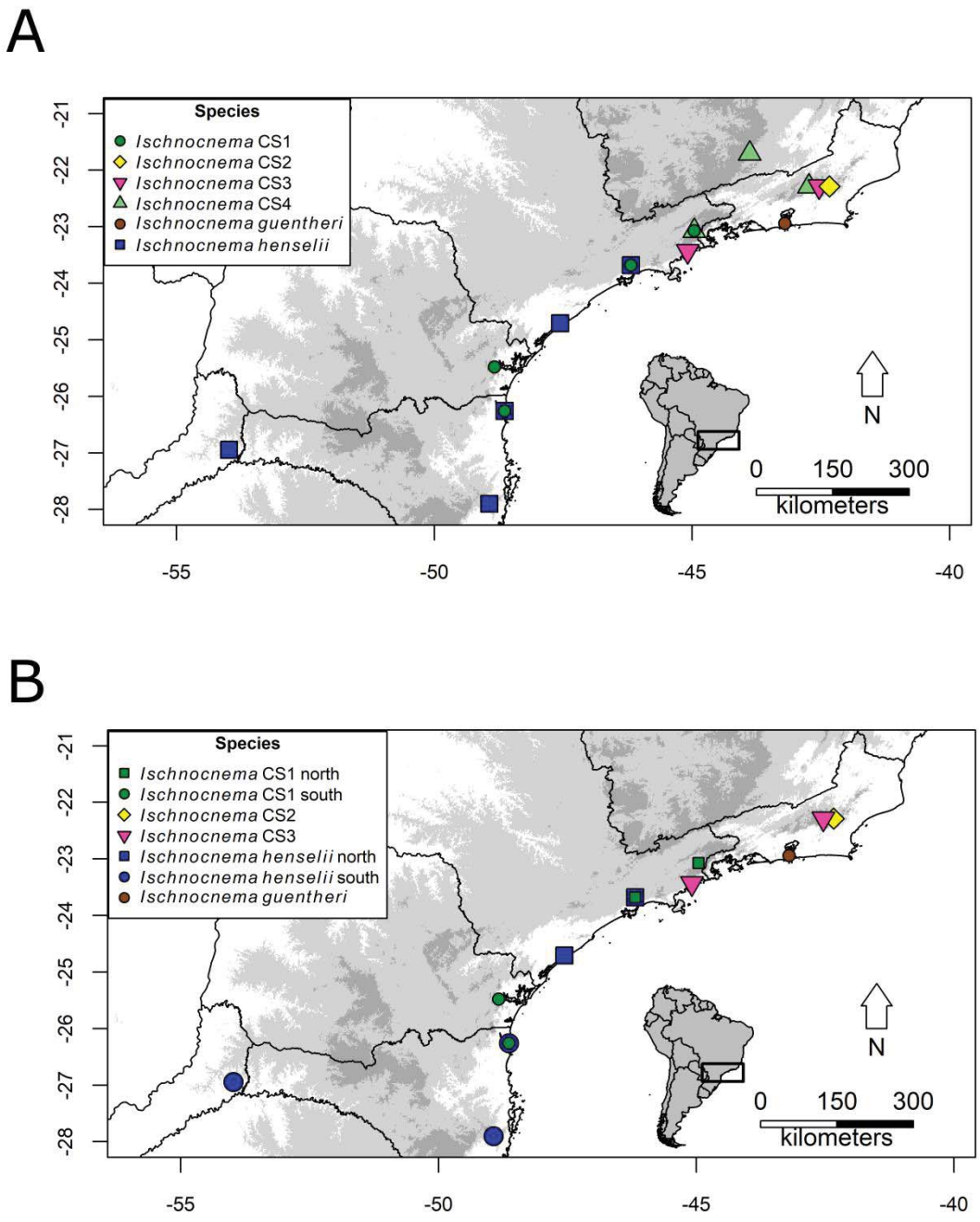
Figure 10. Principal Component Analysis of the advertisement call parameters of the six putative species within the *Ischnocnema guentheri* complex showing the three principal components explaining most of the variation.

Figure 10. Principal Component Analysis of the advertisement call parameters of the five putative species within the *Ischnocnema guentheri* complex available in the temperature-corrected dataset showing the three principal components explaining most of the variation.

Figure 11. Histograms showing the amount of contribution, in percentage, of each variable of the Principal Component Analyses of both raw and temperature-corrected acoustic and also morphometric datasets in the three principal components explaining most of the variation. The red dashed line shows the expected average contribution. CD = call duration, DF = dominant frequency, NPC = notes per call, NRA = note (repetition) rate acceleration, NRF = note (repetition) rate to the first five notes, NRL = note (repetition) rate to the last five notes. Other abbreviations are in the text.

Figure 12. Principal Component Analysis of the morphometric measurements of the six putative species within the *Ischnocnema guentheri* complex showing the three principal components explaining most of the variation.

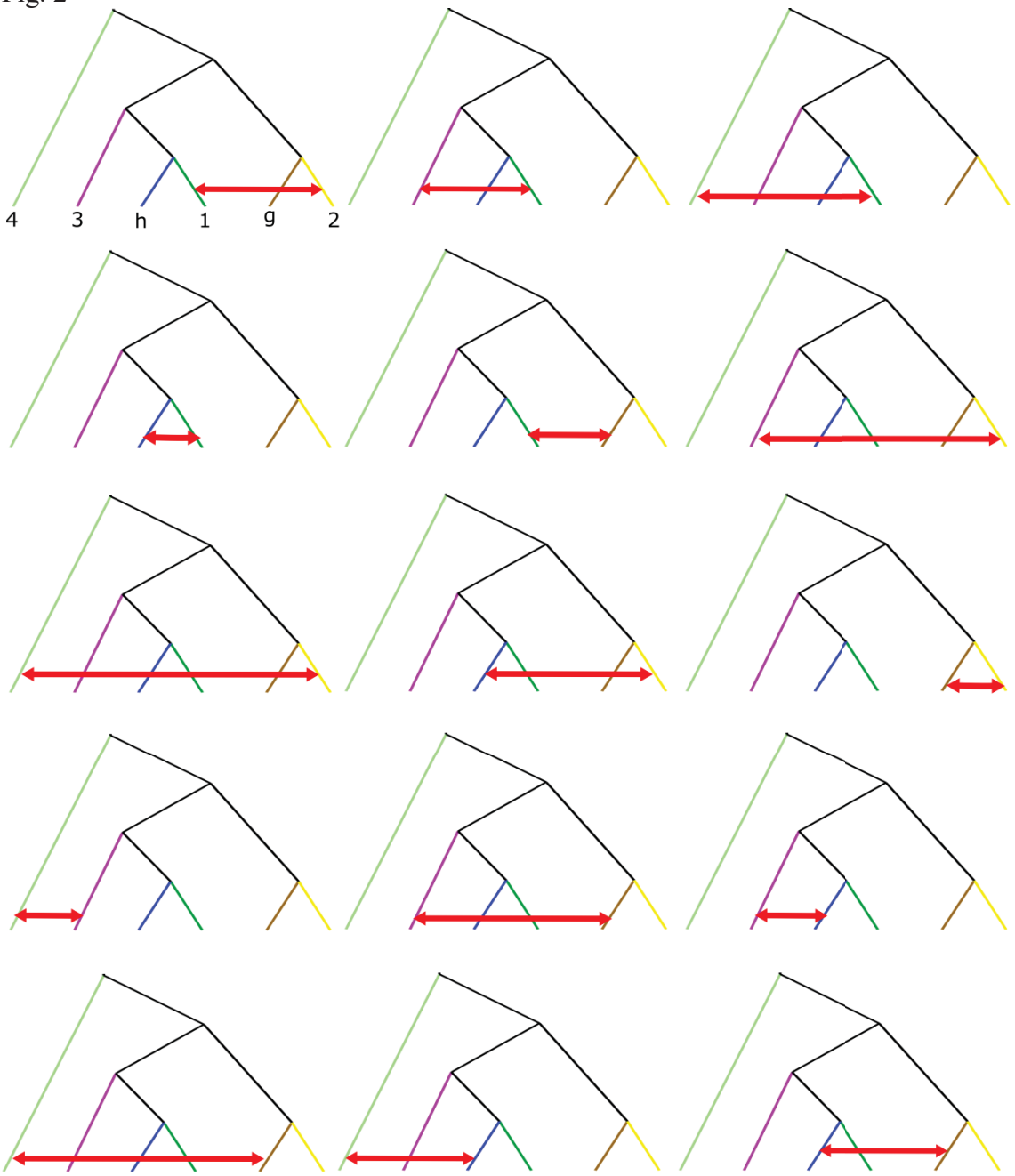
816 Fig 1.



817

818

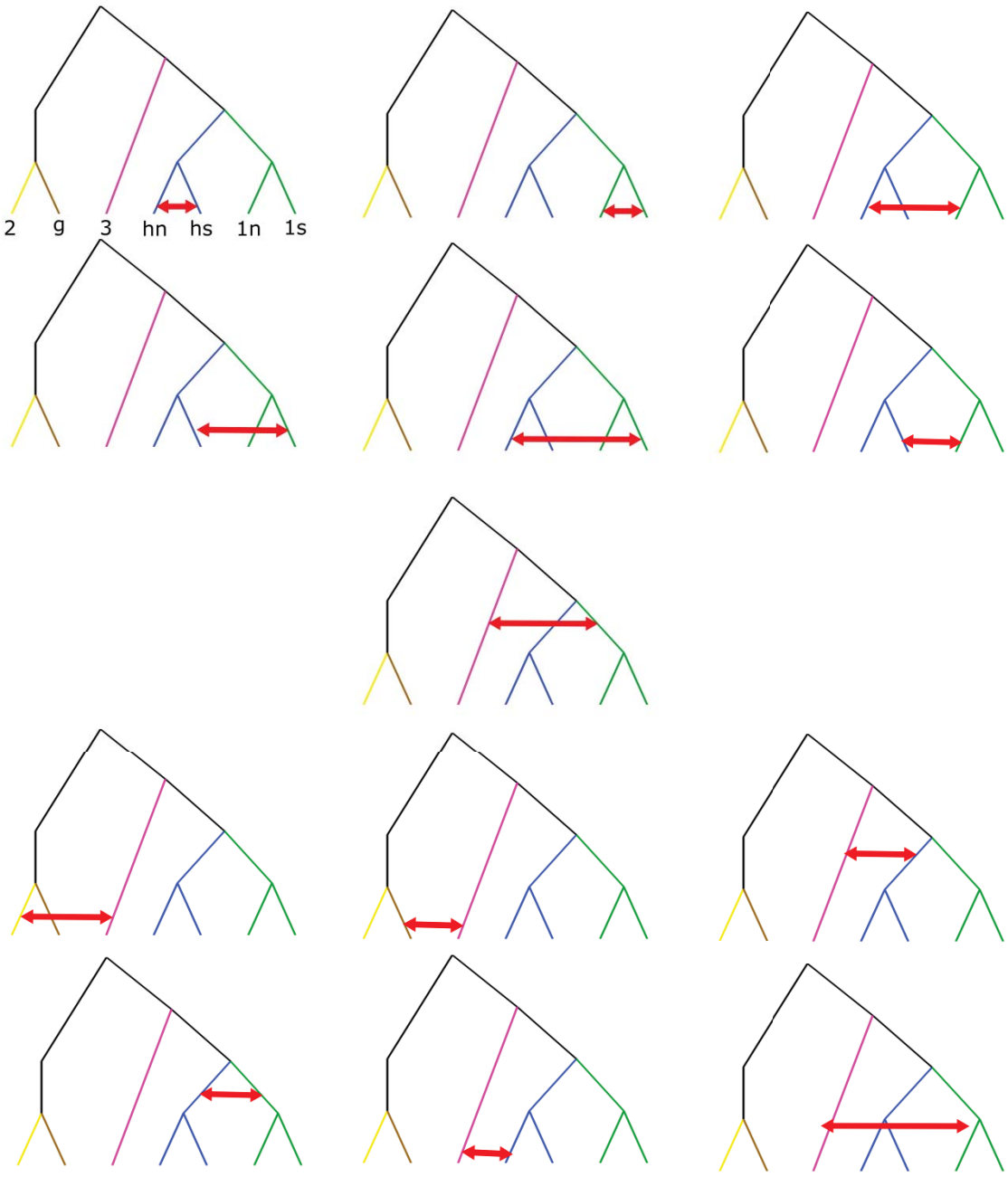
819 Fig. 2



820

821

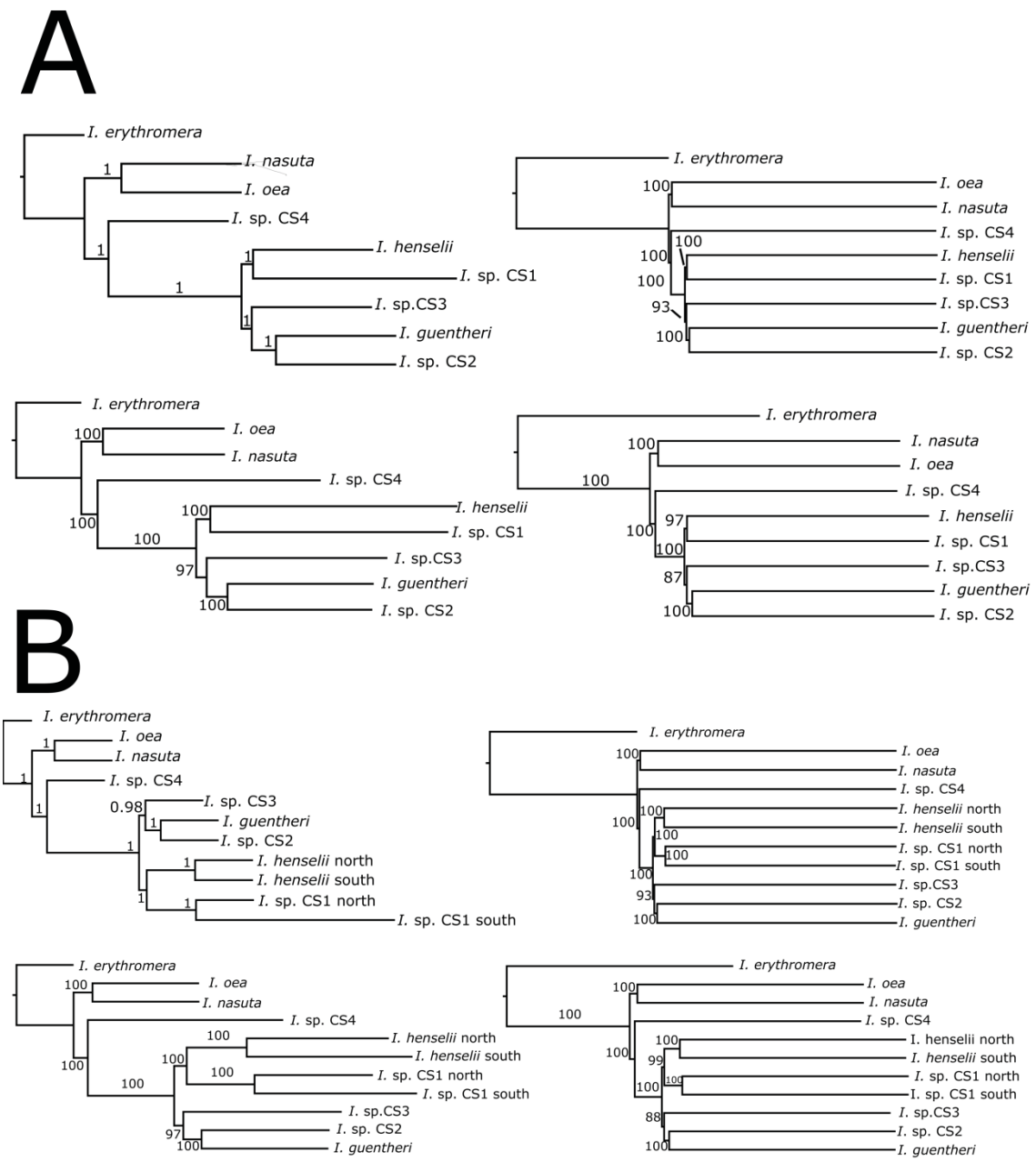
822 Fig. 3



823

824

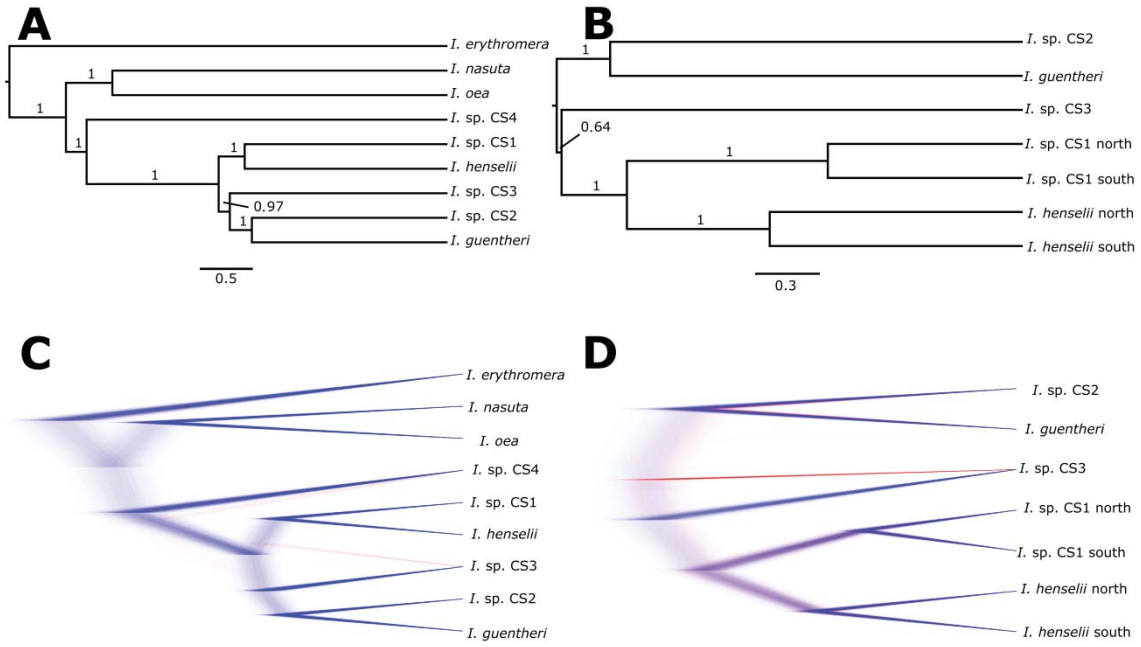
825 Fig. 4



826

827

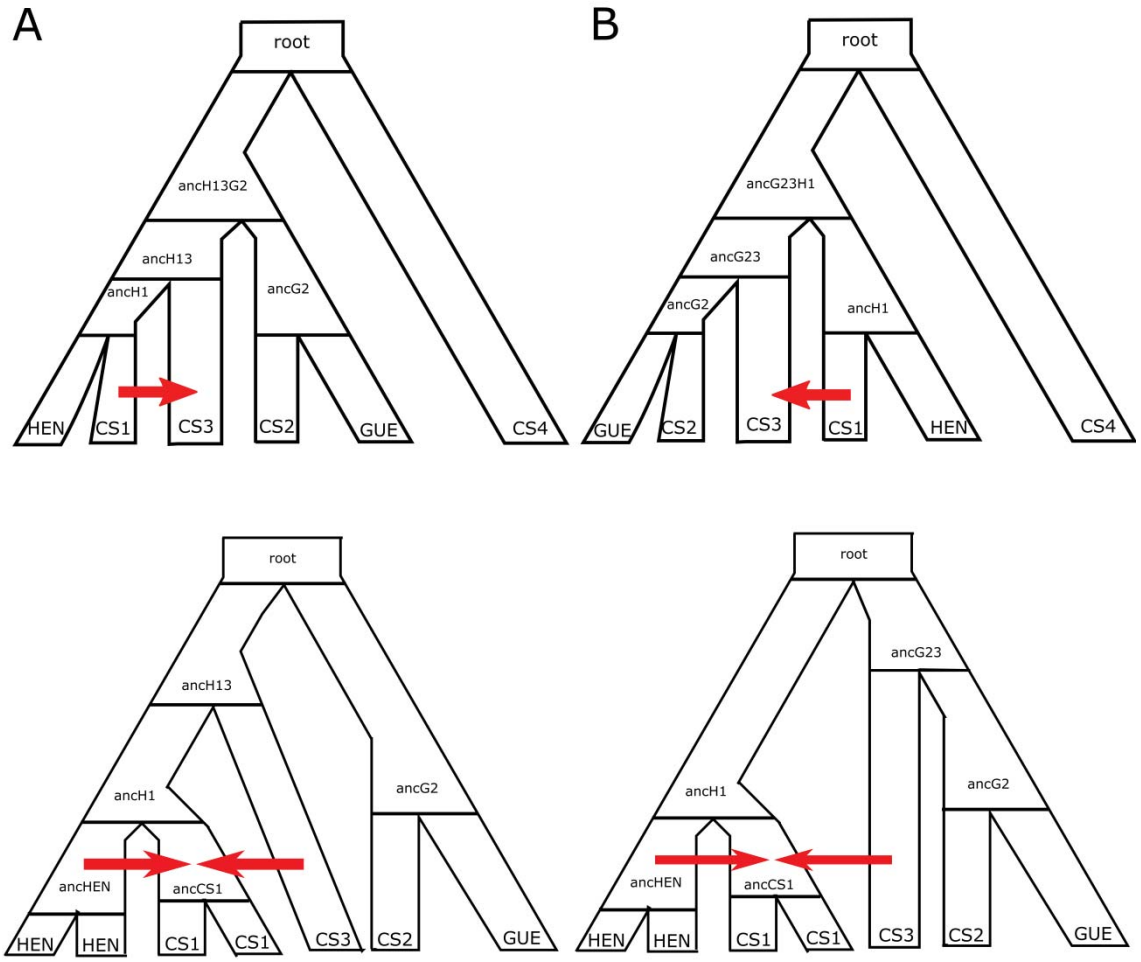
828 Fig. 5



829

830

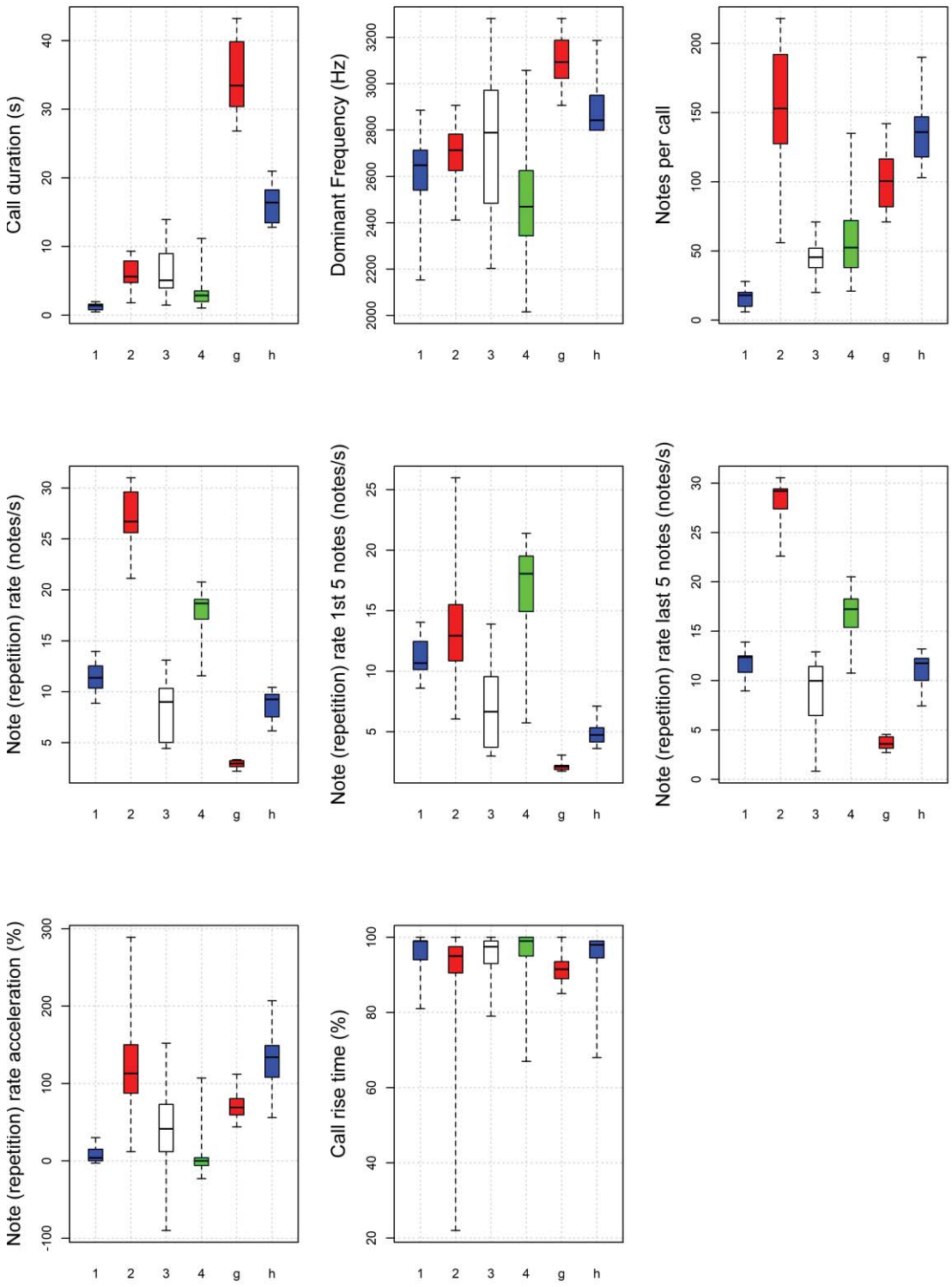
831 Fig. 6



832

833

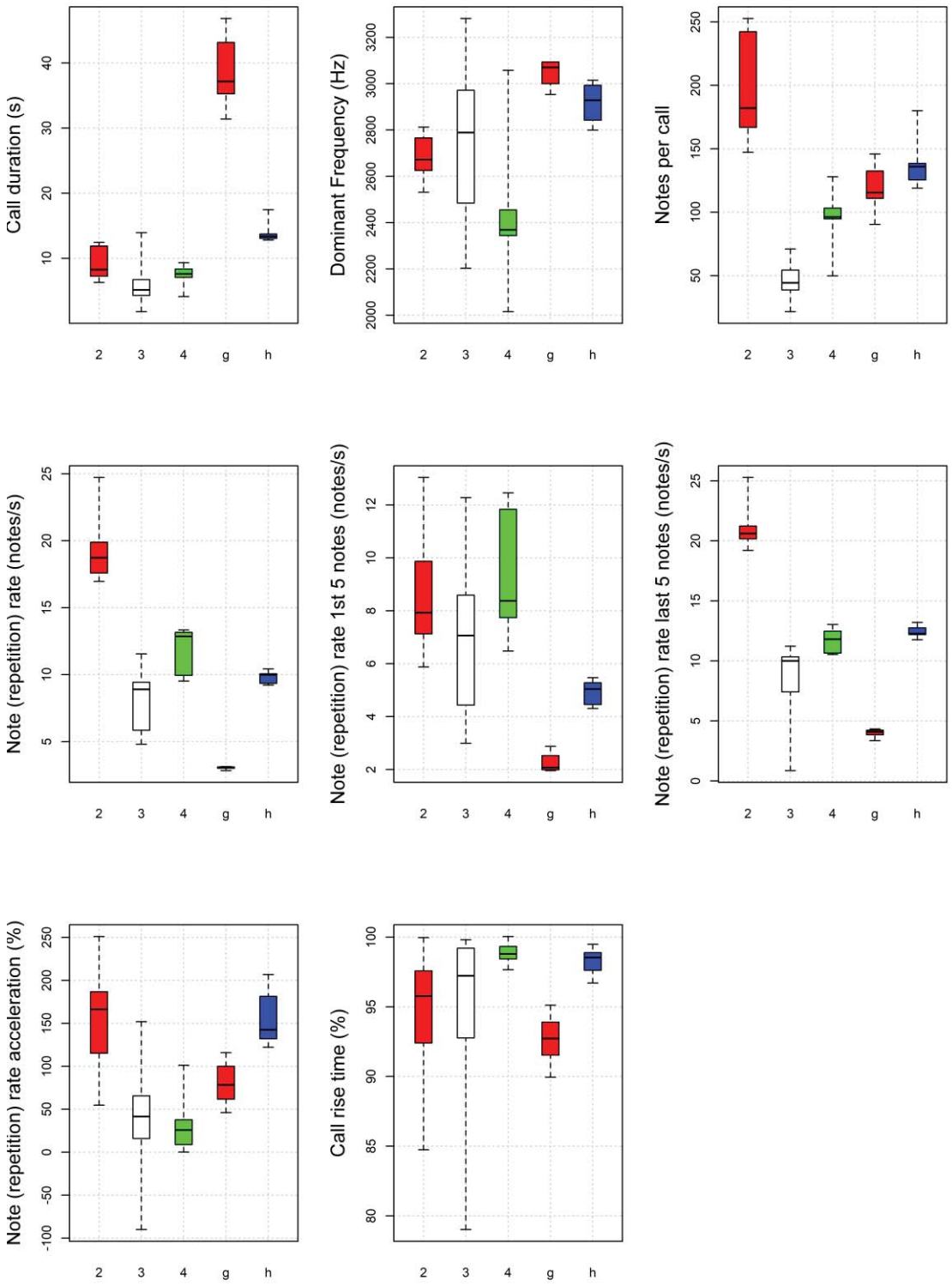
834 Fig. 7



835

836

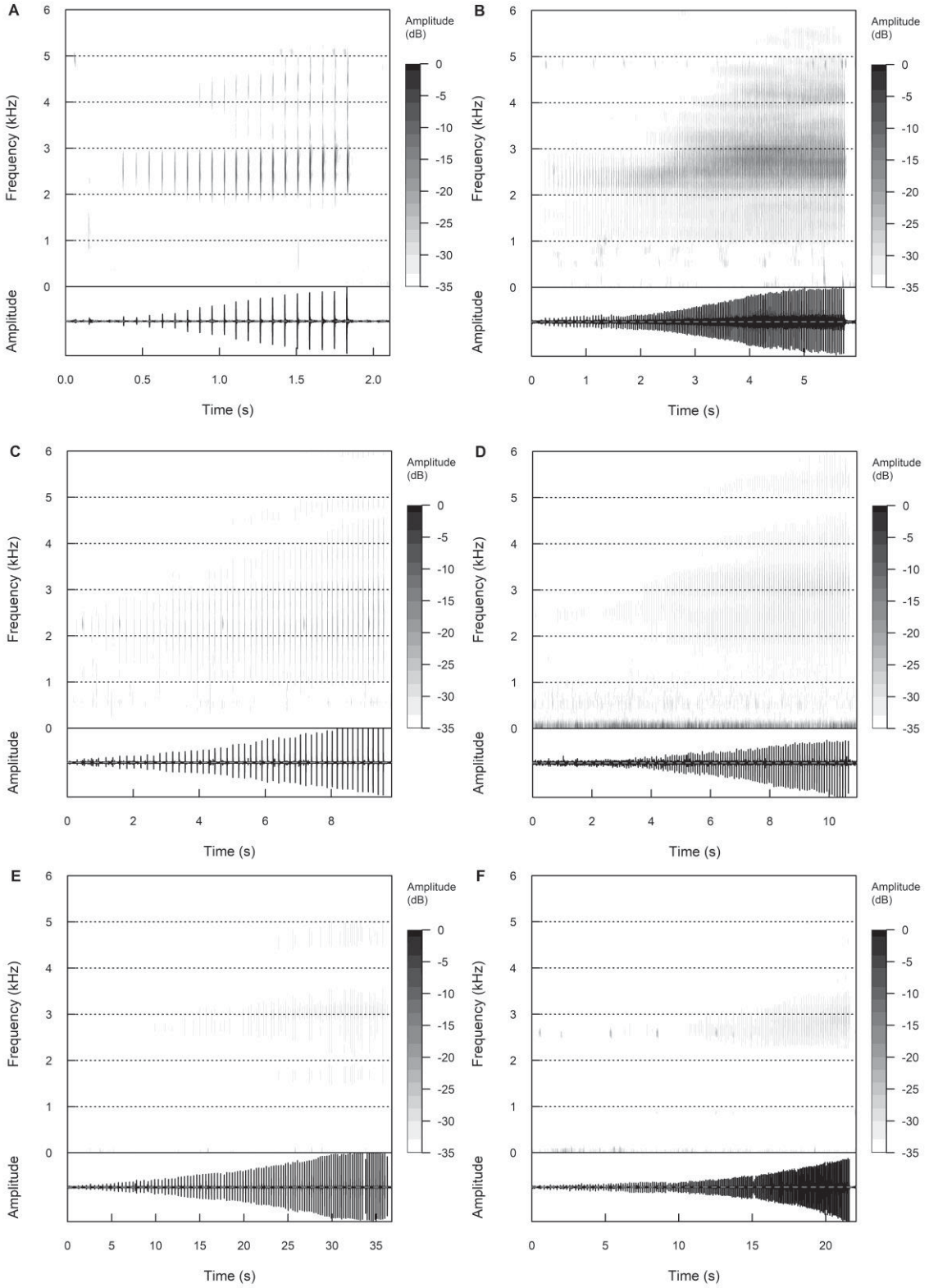
837 Fig. 8



838

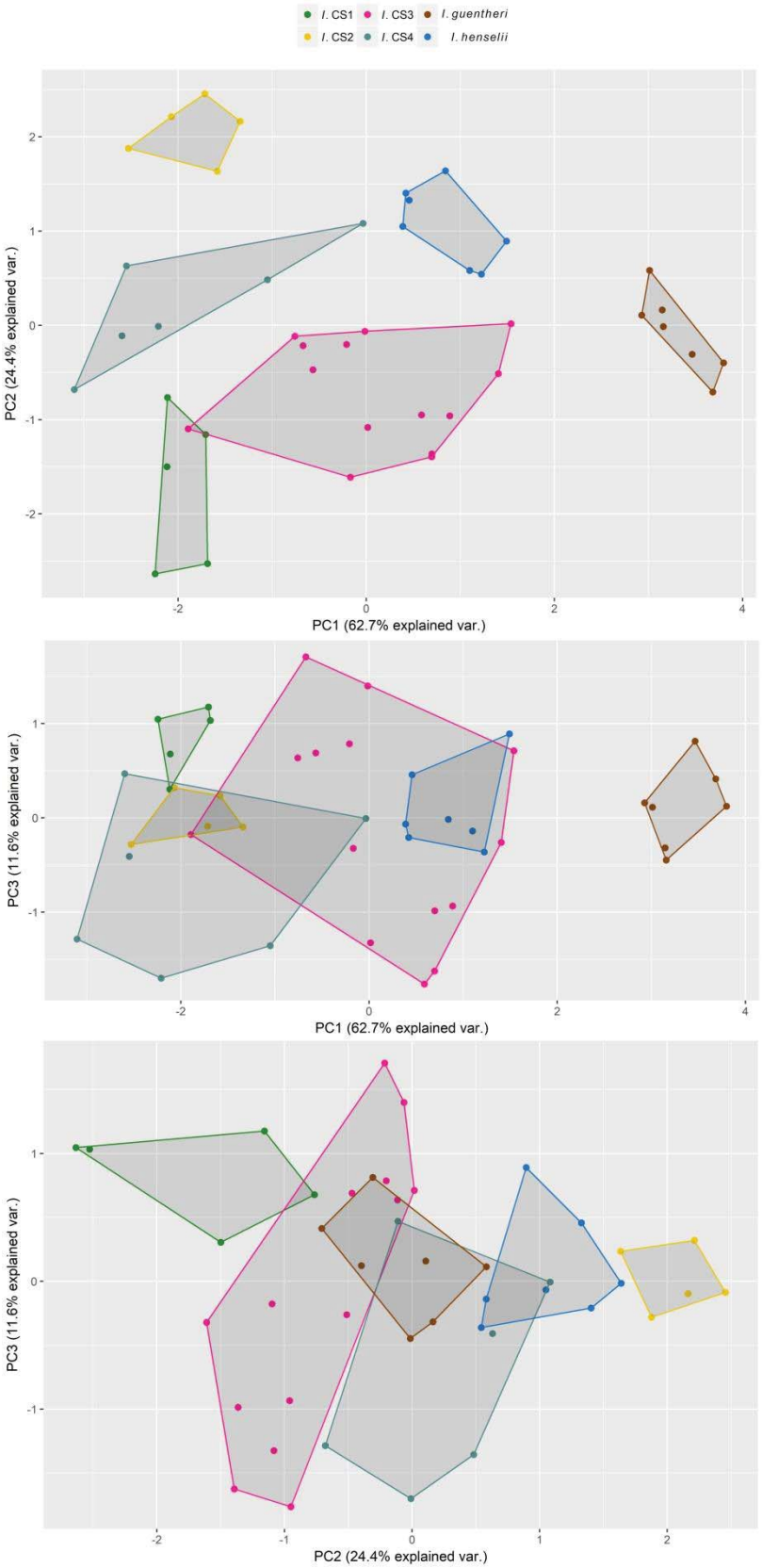
839

840 Fig. 9



841
842

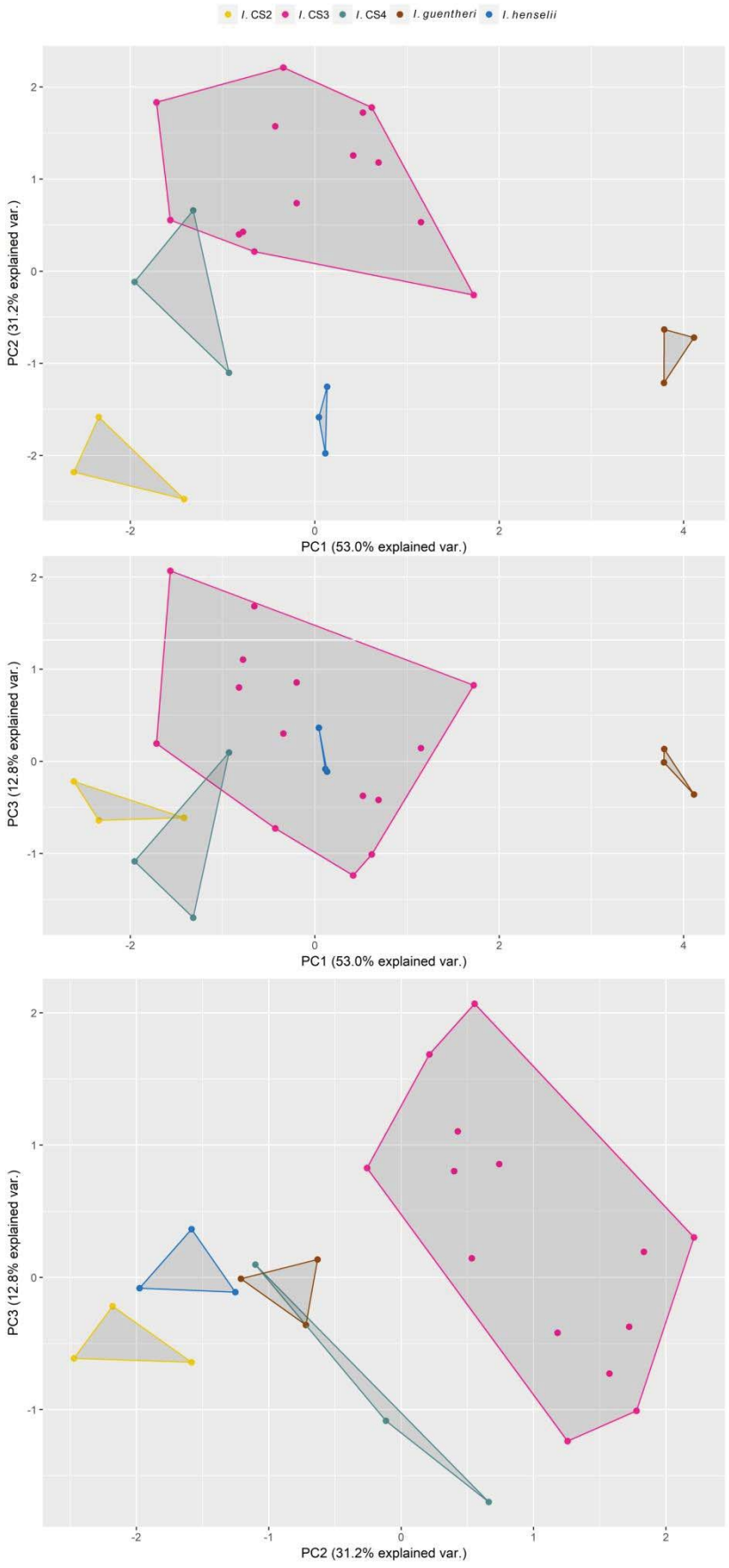
843 Fig. 10



844

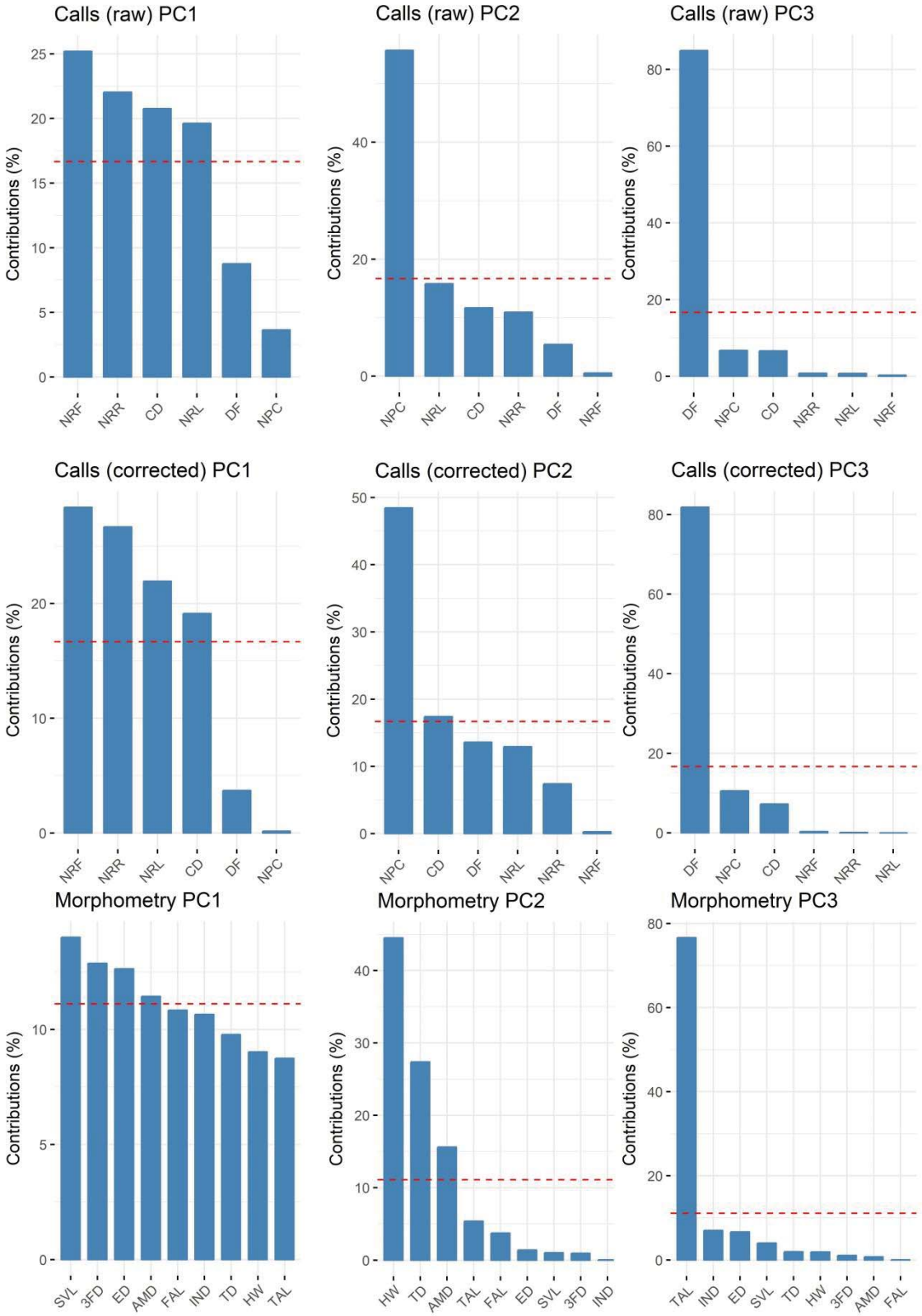
845

846 Fig. 11



847

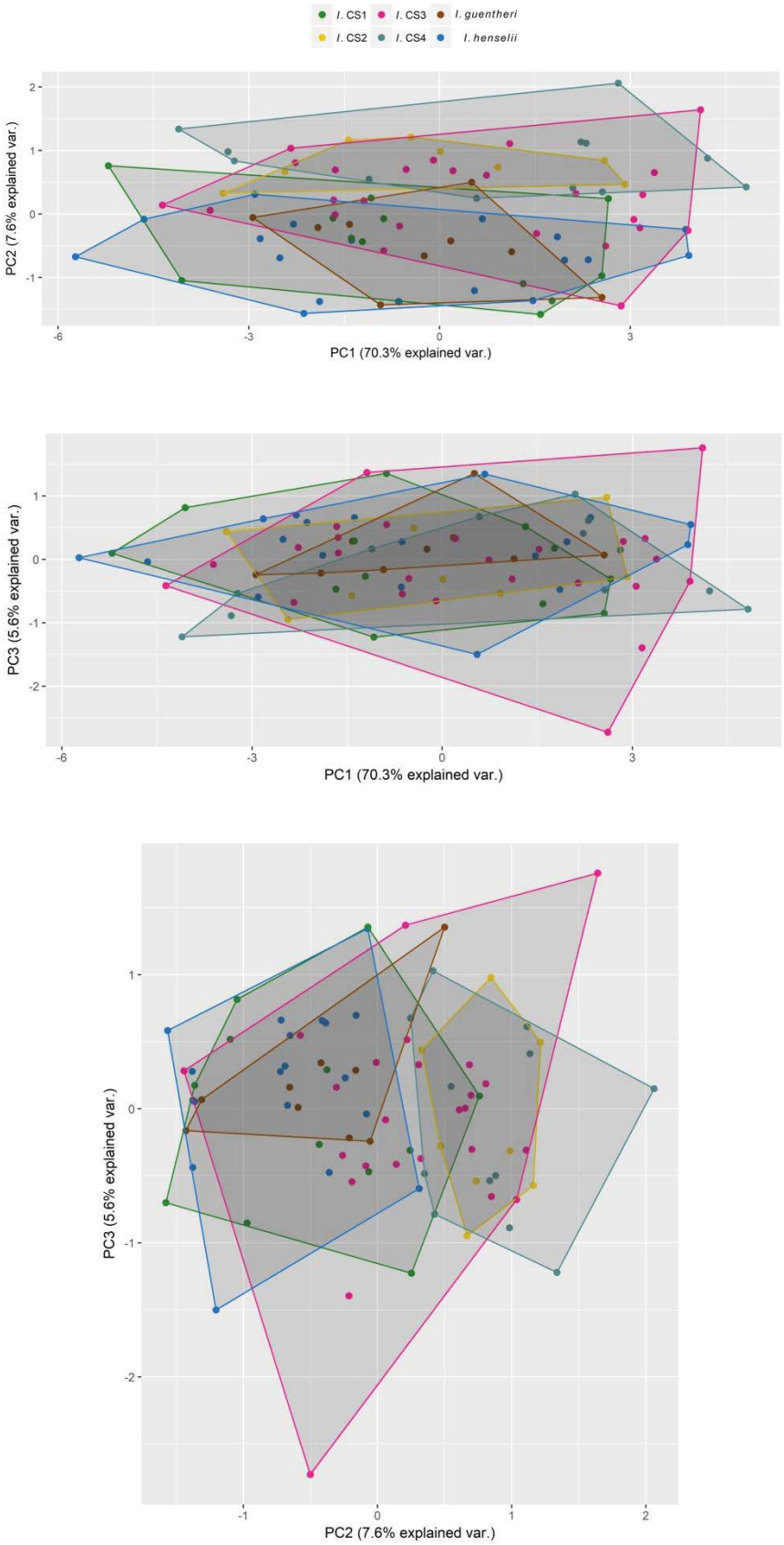
848 Fig. 12



849

850

851 Fig. 13



852

853 Appendix A

854 Table S1. Species and GenBank accession number of specimens used on our 16S rDNA

855 tree. Collection acronyms follow Sabaj (2016).

Species	Voucher#	GenBank ID	Species	Voucher#	GenBank ID
I. sp. CS1	*	KC468462.1	*I.* sp. CS4	CFBH 6493	KC468490.1
I. sp. CS1	*	KC468464.1	*I.* sp. CS4	*	KC468506.1
I. sp. CS1	*	KC468502.1	*I.* sp. CS4	*	KC468507.1
I. sp. CS1	CFBH 7718	KC468419.1	*I.* sp. CS4	*	KC468509.1
I. sp. CS1	*	KC468503.1	*I.* sp. CS4	*	KC468510.1
I. sp. CS1	LRM 945	to be submitted	*I.* sp. CS4	*	KC468512.1
I. sp. CS1	CFBH 16196	KC468518.1	*I.* sp. CS4	*	KC468513.1
I. sp. CS1	CFBH 15035	KC468495.1	*I.* sp. CS4	*	KC468514.1
I. sp. CS1	CFBH 15034	KC468494.1	*I.* sp. CS4	*	KC468515.1
I. sp. CS1	CFBH 15042	KC468499.1	*I.* sp. CS4	CFBH 12180	KC468473.1
I. sp. CS1	CFBH 41853	to be submitted	*I.* sp. CS4	*	KC468463.1
I. sp. CS1	CFBH 42298	to be submitted	*I.* sp. CS4	*	KC468511.1
I. sp. CS1	CFBH 42300	to be submitted	*I.* sp. CS4	LRM 937	to be submitted
I. sp. CS1	CFBH 23222	KC468400.1	*I.* sp. CS4	*	KC468505.1
I. sp. CS1	CFBH 27496	KC468435.1	*I.* sp. CS4	*	KC468508.1
I. sp. CS1	CFBH 27522	KC468436.1	*I.* sp. CS4	CFBH 6482	KC468489.1
I. sp. CS1	CFBH 27525	KC468439.1	*I.* sp. CS4	MNRJ 55570	KC468383.1
I. sp. CS1	CFBH 27523	KC468437.1	*I.* sp. CS4	MNRJ 55571	KC468384.1
I. sp. CS1	CFBH 27524	KC468438.1	*I.* sp. CS4	CFBH 9575	KC468452.1
I. sp. CS1	CFBH 27526	KC468440.1	*I.* sp. CS4	CFBH 9575	KC468453.1
I. sp. CS1	MCP 8167	KC468530.1	*I.* sp. CS4	UFMG 13363	to be submitted
I. sp. CS1	CFBH 27494	KC468434.1	*I.* sp. CS4	UFMG 13365	to be submitted
I. sp. CS1	CFBH 39282	to be submitted	*I. guentheri*	CFBH 26988	KC468402.1
I. sp. CS1	CFBH 25851	KC468390.1	*I. guentheri*	CFBH 26989	KC468403.1
I. sp. CS2	UFMG 13906	to be submitted	*I. guentheri*	CFBH 26990	KC468404.1

856

857 Table S1. Cont.

Species	Voucher#	GenBank ID	Species	Voucher#	GenBank ID
I. sp. CS2	UFMG 13905	to be submitted	*I. guentheri*	CFBH 26991	KC468405.1
I. sp. CS2	UFMG 13907	to be submitted	*I. guentheri*	CFBH 26992	KC468406.1
I. sp. CS2	UFMG 13908	to be submitted	*I. guentheri*	CFBH 27440	KC468428.1
I. sp. CS2	CFBH 27318	KC468408.1	*I. guentheri*	CFBH 27442	KC468429.1
I. sp. CS2	CFBH 27319	KC468409.1	*I. guentheri*	CFBH 27443	KC468430.1
I. sp. CS2	CFBH 27320	KC468410.1	*I. guentheri*	CFBH 27444	KC468431.1
I. sp. CS2	CFBH 27321	KC468411.1	*I. henselii*	CFBH 41854	to be submitted
I. sp. CS2	CFBH 27322	KC468412.1	*I. henselii*	****	KC468470.1
I. sp. CS2	CFBH 27324	KC468414.1	*I. henselii*	****	KC468471.1
I. sp. CS2	CFBH 27356	KC468415.1	*I. henselii*	*	KC468482.1
I. sp. CS2	CFBH 27357	KC468416.1	*I. henselii*	CFBH 39255	to be submitted
I. sp. CS2	CFBH 27359	KC468417.1	*I. henselii*	CFBH 26694	KC468398.1
I. sp. CS2	CFBH 27323	KC468413.1	*I. henselii*	CFBH 26695	KC468399.1
I. sp. CS2	PPGT 620	to be submitted	*I. henselii*	****	KC468465.1
I. sp. CS2	PPGT 621	to be submitted	*I. henselii*	****	KC468466.1
I. sp. CS2	PPGT 623	to be submitted	*I. henselii*	****	KC468467.1
I. sp. CS2	PPGT 624	to be submitted	*I. henselii*	****	KC468475.1
I. sp. CS2	CFBH 27434	KC468427.1	*I. henselii*	CFBH 17651	KC468516.1
I. sp. CS3	CFBH 11350	KC468487.1	*I. henselii*	CFBH 12298	KC468476.1
I. sp. CS3	*	KC468532.1	*I. henselii*	CFBH 12299	KC468477.1
I. sp. CS3	CFBH 11554	KC468491.1	*I. henselii*	CFBH 12301	KC468479.1
I. sp. CS3	CFBH 12252	KC468485.1	*I. henselii*	****	KC468468.1
I. sp. CS3	CFBH 9230	KC468449.1	*I. henselii*	****	KC468469.1
I. sp. CS3	CFBH 9236	KC468450.1	*I. henselii*	****	KC468478.1
I. sp. CS3	**	KC468484.1	*I. henselii*	*	KC468480.1
I. sp. CS3	CFBH 12263	KC468483.1	*I. henselii*	*	KC468481.1
I. sp. CS3	CFBH 15036	KC468497.1	*I. henselii*	CFBH 13525	KC468520.1
I. sp. CS3	CFBH 15044	KC468498.1	*I. henselii*	CFBH 13527	KC468521.1

858

859 Table S1. Cont.

Species	Voucher#	GenBank ID	Species	Voucher#	GenBank ID
I. sp. CS3	CFBH 15033	KC468493.1	*I. henselii*	*	KC468522.1
I. sp. CS3	CFBH 15045	KC468501.1	*I. henselii*	CFBH 35837	to be submitted
I. sp. CS3	CFBH 15040	KC468496.1	*I. henselii*	CFBH 42295	to be submitted
I. sp. CS3	CFBH 15038	KC468500.1	*I. henselii*	CFBH 27549	KC468441.1
I. sp. CS3	CFBH 27428	KC468422.1	*I. henselii*	CFBH 27550	KC468442.1
I. sp. CS3	CFBH 27431	KC468424.1	*I. henselii*	CFBH 27551	KC468443.1
I. sp. CS3	CFBH 27432	KC468425.1	*I. henselii*	CFBH 27552	KC468444.1
I. sp. CS3	CFBH 27433	KC468426.1	*I. henselii*	CFBH 27553	KC468445.1
I. sp. CS3	CFBH 27427	KC468421.1	*I. henselii*	CFBH 27554	KC468446.1
I. sp. CS3	CFBH 27430	KC468423.1	*I. henselii*	CFBH 8497	KC468448.1
I. sp. CS3	CFBH 27426	KC468420.1	*I. henselii*	CFBH 9368	KC468451.1
I. sp. CS3	CFBH 27407	KC468418.1	*I. henselii*	UFSC 2934	KC468459.1
I. sp. CS3	PPGT 631	to be submitted	*I. henselii*	MCP 10700	KC468525.1
I. sp. CS3	PPGT 634	to be submitted	*I. henselii*	MCP 10702	KC468526.1
I. sp. CS3	PPGT 635	to be submitted	*I. henselii*	MCP 10703	KC468527.1
I. sp. CS3	MNRJ 57640	KC468385.1	*I. henselii*	MCP 10704	KC468528.1
I. sp. CS3	CFBH 13931	KC468488.1	*I. henselii*	MCP 10762	KC468529.1
I. sp. CS3	*	KC468458.1	*I. henselii*	*	KC468472.1
I. sp. CS3	***	KC468407.1	*I. henselii*	CFBH 39280	to be submitted
I. sp. CS3	CFBH 24772	KC468391.1	*I. henselii*	CFBH 39281	to be submitted
I. sp. CS3	CFBH 24773	KC468392.1	*I. henselii*	CFBH 11040	KC468460.1
I. sp. CS3	CFBH 24774	KC468394.1	*I. henselii*	CFBH 27470	KC468432.1
I. sp. CS3	CFBH 24771	KC468393.1	*I. henselii*	CFBH 27471	KC468433.1
I. sp. CS3	PPGT 626	to be submitted	*I. henselii*	MLPDB 8704	KC468447.1
I. sp. CS3	PPGT 630	to be submitted	*I. henselii*	MCP 10561	KC468523.1
I. sp. CS3	PPGT 628	to be submitted	*I. henselii*	MCP 10565	KC468524.1
I. sp. CS4	CFBH 24141	KC468388.1	*I. henselii*	CFBH 11655	KC468461.1
I. sp. CS4	CFBH 7201	KC468519.1	*I. henselii*	CFBH 13473	KC468486.1

860

861 Table S1. Cont.

Species	Voucher#	GenBank ID	Species	Voucher#	GenBank ID
I. sp. CS4	CFBH 24143	KC468387.1	*I. henselii*	CFBH 23298	KC468386.1
I. sp. CS4	CFBH 6725	KC468504.1	*I. henselii*	CFBH 26686	KC468397.1
I. sp. CS4	*	KC468456.1	*I. henselii*	CFBH 26871	KC468401.1
I. sp. CS4	CFBH 16236	KC468517.1	*I. henselii*	*	KC468492.1
I. sp. CS4	CFBH 9891	KC468457.1	*I. erythromera*	MNRJ 44562	JX267341.1
I. sp. CS4	CFBH 9892	KC468454.1	*I. erythromera*	MNRJ 51868	JX267340.1
I. sp. CS4	CFBH 9917	KC468455.1	*I. nasuta*	CFBH 25439	KC468389.1
I. sp. CS4	CFBH 24769	KC468395.1	*I. nasuta*	CFBH 24782	JX267520.1
I. sp. CS4	CFBH 24770	KC468396.1	*I. izecksohni*	UFMG 7503	JX267510.1
I. sp. CS4	PPGT 648	to be submitted	*I. oea*	MNRJ 34949	JX267338.1
I. sp. CS4	PPGT 647	to be submitted	*I. oea*	MNRJ 38416	JX267313.1
I. sp. CS4	PPGT 622	to be submitted			

862 *Tissues from which we were not able to trace the vouchers.

863 **Whole specimen used as tissue sample

864 ***Specimen housed at UFJF collection, number untraceable

865 ****Specimen housed at MZUSP collection, number untraceable

866

867 Table S2. Primers used in this study

Primer		Gene	Sequence	Reference
16SAR	F	16S	CGCCTGTTTATCAAAAACAT	Palumbi et al. (1991)
16S-Wilk2	R	16S	GACCTGGATTACTCCGGTCTGA	Wilkinson et al. (1996)
16SBR	R	16S	GACCTGGATTACTCCGGTCTGA	Palumbi et al. (1991)

868

869

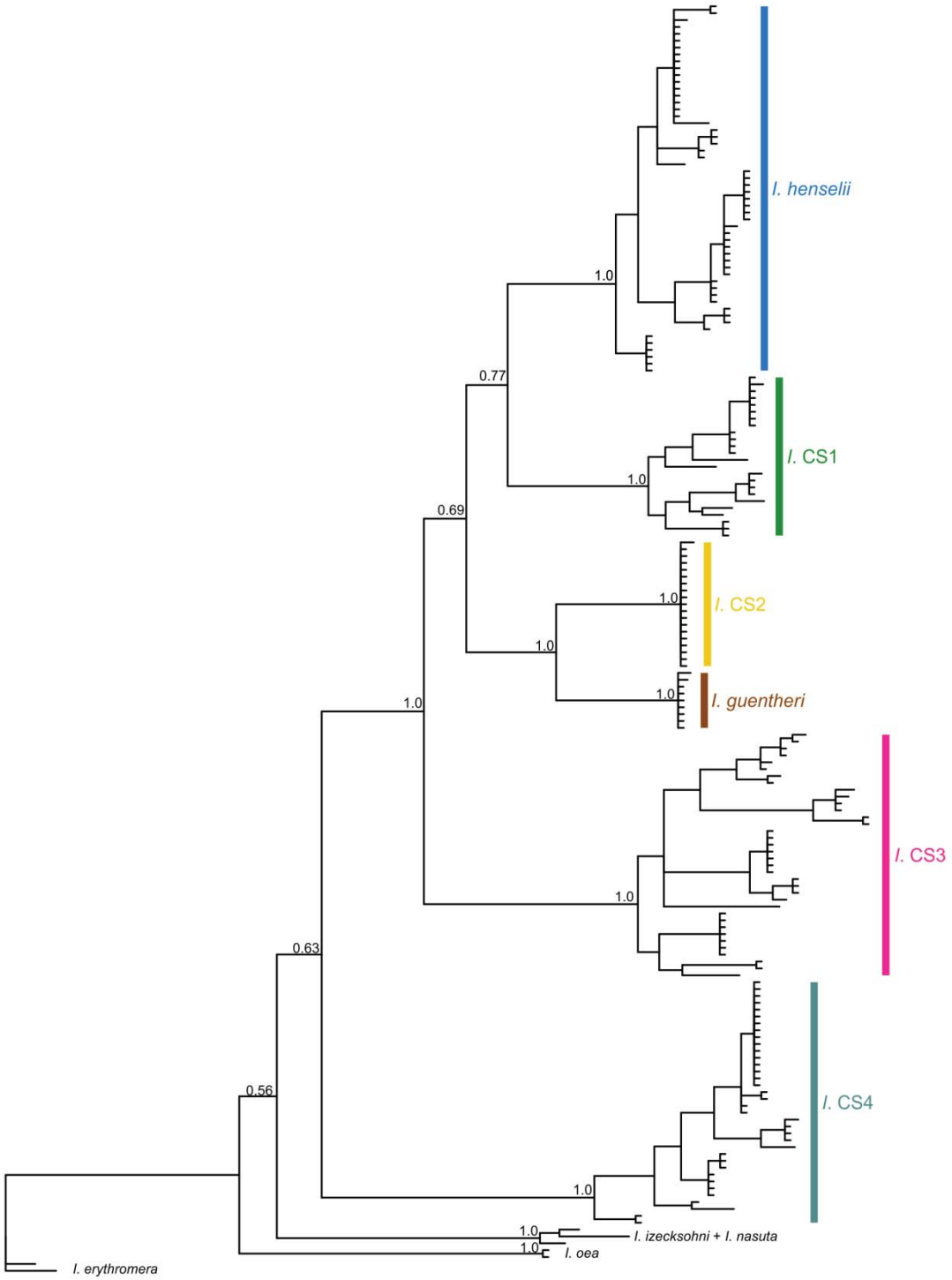


Fig S1. The 50% majority rule consensus tree from Bayesian inference analysis of 16S rRNA, inferred under the GTR + Γ + I model. Numbers above branches show posterior probabilities.

Appendix B

G–PhoCS input control file

```
GENERAL-INFO-START

        seq-file                        ingroup.gph
        trace-file                      cs1cs2-mcmc-trace.log
        mcmc-iterations                 1000000
        iterations-per-log              100
        logs-per-line                   100
        mcmc-sample-skip                10

        find-finetunes                  TRUE

        tau-theta-alpha                 1.0
        tau-theta-beta                  10000.0

        mig-rate-alpha                  0.002
        mig-rate-beta                   0.00001

        locus-mut-rate                  CONST

GENERAL-INFO-END

CURRENT-POPS-START

        POP-START
                name            CS1
                samples         BB454_CS1_seq1 h BB454_CS1_seq2 h
BB479_CS1_seq1 h BB479_CS1_seq2 h DB952_CS1_seq1 h DB952_CS1_seq2 h
LRM945_CS1_seq1 h LRM945_CS1_seq2 h
        POP-END

        POP-START
                name            CS2
                samples         PPGT620_CS2_seq1 h PPGT620_CS2_seq2 h
        POP-END

        POP-START
                name            CS3
                samples         CH451_CS3_seq1 h CH451_CS3_seq2 h
CFBH27433_CS3_seq1 h CFBH27433_CS3_seq2 h
        POP-END

        POP-START
                name            CS4
                samples         LRM937_CS4_seq1 h LRM937_CS4_seq2 h
PCAG1763_CS4_seq1 h PCAG1763_CS4_seq2 h PPGT622_CS4_seq1 h
PPGT622_CS4_seq2 h
        POP-END

        POP-START
                name            HEN
                samples         BB455_henselii_seq1 h
BB455_henselii_seq2 h CC226_henselii_seq1 h CC226_henselii_seq2 h
DB949_henselii_seq1 h DB949_henselii_seq2 h PPGT456_henselii_seq1 h
PPGT456_henselii_seq2 h CFBH27554_henselii_seq1 h
CFBH27554_henselii_seq2 h
        POP-END
```

```
934         POP-START
935                 name            GUE
936                 samples         CFBH27440_guentheri_seq1 h
937   CFBH27440 guentheri seq2 h
938         POP-END
939
940   CURRENT-POPS-END
941
942   ANCESTRAL-POPS-START
943
944         POP-START
945                 name    ancH1
946                 children        CS1     HEN
947         POP-END
948
949         POP-START
950                 name    ancG2
951                 children        CS2     GUE
952         POP-END
953
954         POP-START
955                 name    ancG23
956                 children        CS3     ancG2
957         POP-END
958
959         POP-START
960                 name            ancH1G23
961                 children        ancH1   ancG23
962         POP-END
963
964         POP-START
965                 name            root
966                 children        ancH1G23        CS4
967         POP-END
968
969   ANCESTRAL-POPS-END
970
971   MIG-BANDS-START
972
973   BAND-START
974           source                  CS1
975           target                  CS2
976   BAND-END
977
978   BAND-START
979           source                  CS2
980           target                  CS1
981   BAND-END
982
983   MIG-BANDS-END
984
985
```

986
987 Appendix C

988 Specimens examined

989

990 ***Ischnocnema* sp. CS1:** BRAZIL: PARANÁ: Morretes (CFBH 42298, 42300). SANTA
991 CATARINA: Blumenau (CFBH 27522–27526); Guaramirim (CFBH 27494, 27496). SÃO
992 PAULO: Ilhabela (CFBH 15034, 15042); São Luiz do Paraitinga (CFBH 7718).

993

994 ***Ischnocnema* sp. CS2:** BRAZIL: RIO DE JANEIRO: Nova Friburgo: Estrada Velha para
995 Lumiar (PPGT 620–621, 624); Nova Friburgo (CFBH 27434); Santa Maria Madalena:
996 Parque Estadual do Desengano (CFBH 27319, 27321, 27357, 27359, 27434).

997

998 ***Ischnocnema* sp. CS3:** BRAZIL: RIO DE JANEIRO: Cachoeiras de Macacu (27407);
999 Nova Friburgo (CFBH 27407, 27427, 27428, 27430, 27431, 27433); Teresópolis:
1000 Parque Nacional da Serra dos Órgãos (PPGT 626–630); Teresópolis: Parque Estadual
1001 dos Três Picos, Núcleo Vale da Revolta (CFBH 24772–24774, PPGT 631, 634–636).
1002 SÃO PAULO: Cubatão (CFBH 11350); Ilhabela (CFBH 15033, 15036, 15038, 15040,
1003 15044, 15045).

1004

1005 ***Ischnocnema* sp. CS4:** BRAZIL: MINAS GERAIS: Camanducaia (CFBH 6724); Lima
1006 Duarte: Parque Estadual do Ibitipoca (UFMG 13363, 13365). RIO DE JANEIRO: Nova
1007 Friburgo: Estrada Velha para Lumiar (PPGT 622); Petrópolis: Parque Nacional da Serra
1008 dos Órgãos (PPGT 647–649). SÃO PAULO: Campos do Jordão: parque Estadual dos
1009 Mananciais de Campos do Jordão (CFBH 9917, 24143); Jundiaí: Serra do Japí: (CFBH
1010 9575); Santo Antônio do Pinhal (CFBH 7201); São Paulo: Parque Estadual da Serra do
1011 Mar, Núcleo Caraguatatuba (CFBH 12180).

***Ischnocnema guentheri*:** BRAZIL: Rio de Janeiro: Rio de Janeiro: Floresta da Tijuca (CFBH 26989–26994, 27440, 27442–27444).

***Ischnocnema henselii*:** BRAZIL: Paraná: Arianópolis (CFBH 27470–27471); Piraquara (CFBH 11039–11040). Santa Catarina: Anitápolis (CFBH 9367–9368); São Bonifácio (CFBH 27549–27554). São Paulo: Miracatu (CFBH 35837); São Bernardo do Campo (CFBH 12298); São Paulo: Parque Estadual da Serra do Mar, Núcleo Curucutu (CFBH38048–38050, 38054); Tapiraí (CFBH 23298).

Ischnocnema nasuta: BRAZIL: Rio de Janeiro: Nova Friburgo: Hotel Leuenroth (Al-MN 420–425, MNRJ 24023 [former USNM 96468], USNM 96469, syntypes of *Hylodes nasutus*); Nova Friburgo (CFBH 40981–40984).

The mitochondrial genomes of five frog species of the Neotropical genus *Ischnocnema* (Anura: Brachycephaloidea: Brachycephalidae)*

Pedro P. G. Taucce[a], Michael J. Hickerson[b], Clarissa Canedo[c], Célio F. B. Haddad[a], Alan, L. Lemmon[d], Emily M. Lemmon[e], Miguel Vences[f], Mariana Lyra[a]

[a]*Department of Zoology and Aquaculture Center (CAUNESP), Biosciences Institute, São Paulo State University – UNESP, Rio Claro, SP, Brazil;* [b]*Department of Biology, Marshak Science Building, City College of New York, New York, NY, USA;* [c]*Department of Zoology, Instituto de Biologia Roberto Alcântara Gomes, Rio de Janeiro State University – UERJ, Rio de Janeiro, RJ, Brazil;* [d]*Department of Scientific Computing, Florida State University, Tallahassee, FL, USA;* [e]*Department of Biological Science, Florida State Univresity, Tallahasee, FL, USA;* [f]*Zoological Institute, Technical University of Braunschweig, Braunschweig, Germany*

Pedro P. G. Taucce: pedrotaucce@gmal.com; Department of Zoology and Aquaculture Center (CAUNESP), Biosciences Institute, São Paulo State University – UNESP, Cx. Postal 199, 13506-569, Rio Claro, SP, Brazil

*Capítulo a ser submetido para o periódico *Mitochondrial DNA part B: Resources*

The mitochondrial genomes of five frog species of the Neotropical genus *Ischnocnema* (Anura: Brachycephaloidea: Brachycephalidae)

We present nearly complete mitogenomes for five species of *Ischnocnema,* all within the *I. guentheri* series: *I. erythromera, I. guentheri, I. henselii, I. nasuta*, and *I. oea*. We assembled mitogenomes from anchored hybrid enrichment data using *Eleutherodactylus atkinsi* as initial seed. We recovered the 13 protein-coding genes, 22 tRNA genes, and two rRNA genes for almost all species and the order of genes agrees with most previously sequenced anurans. We provide a phylogenetic tree with four outgroups, which is consistent with previous phylogenetic hypotheses, with *I. erythromera* as the sister group of the remaining species of the *I. guentheri* series.

Keywords: Amphibia; Brazil; *Ischnocnema guentheri* series; mitogenomes; Terrarana

The Neotropical genus *Ischnocnema* Reinhardt and Lütken, 1862 comprises 33 species (Frost 2018) of leaf-litter dwelling frogs divided into four species series and two species unassigned to any series (Canedo and Haddad 2012; Padial et al. 2014). Within them, the *I. guentheri* series comprises ten species distributed all over the southern and central portions of the Atlantic Forest, throughout seven Brazilian states and the Argentinean province of Misiones (Frost 2018). The series has a challenging taxonomy, with notable intra and inter-specific morphological variation (Heyer 1984), and some of its members may actually represent complexes of morphologically cryptic species (Gehara et al. 2013). Herein we provide nearly complete metagenome sequences for half (five) of the currently recognized species of the *I. guentheri* series, assembled from anchored hybrid enrichment data: *I. erythromera* (Heyer, 1984), *I. guentheri* (Steindachner 1864), *I. nasuta* (Lutz, 1925), *I. oea* (Heyer, 1984) (one specimen each), and *I. henselii* (Peters, 1870) (five specimens). Voucher specimens and tissue samples are housed in the CFBH

or LGE collections and acronyms follow Sabaj (2016).

We extracted total DNA from ethanol-preserved muscle or liver tissues using the DNeasy Qiagen® kit following manufacturer's protocols. DNA was eluted to a volume of 100 µl and quantified using a Qubit fluorometer dsDNA BR Assay Kit (Thermo Fisher Scientific Inc). Extractions were sent to the *Center for Anchored Pylogenomics*, Tallahasee, FL, USA to be sequenced with a method for anchored hybrid enrichment analysis (Lemmon et al. 2012). Equal quantities of indexed samples were pooled and enrichments performed with probes designed for anchored loci from Amniotes (Prum et al. 2015; Ruane et al. 2015; Tucker et al. 2016). Sequencing was carried out on an Illumina HiSeq2500 sequencer. For mitochondrial genomes assemblies, each lane of raw sequence reads was first concatenated per sample and quality-trimmed using Trimmomatic (Bolger et al. 2014), and then we used MITObim v1.9 (Hahn et al. 2013) using as reference the mitogenome of *Eleutherodactylus atkinsi* (GenBank number: JX564864). Assemblies were checked by mapping the trimmed reads to the final fasta file with Geneious v6 (Kearse et al. 2012) and scanned by eye to confirm appropriate mapping. Regions with very low coverage (less than 3 reads) were manually edited to unknown nucleotides ('N'). The preliminary annotation of final mitochondrial genomes was carried out by MITOS (Bernt et al. 2013), available for online use at http://mitos.bioinf.uni-leipzig.de/, and verified by alignment with published Brachycephaloidea mitogenomes. The protein-coding regions were checked to confirm no indels or stop codons were present. The new mitogenomes have been deposited in GenBank under accession numbers xxx-xxx.We recovered the 13 protein-coding genes and two rRNA genes for all species and almost all 22 tRNA genes. The order of genes agrees with most previously sequenced Neobatrachia.

For phylogenetic inferences, *Ischnocnema* sequences were aligned to published complete or near complete genomes of four outgroups (Table 1) using the software MAFFT v.7 (Katoh and Standley 2013). To avoid ambiguous alignments, we used only protein-coding and rRNA genes in the analyzes. Search for the best partition scheme and best fitting nuclear substitution models was performed by PartitionFinder 2.1.1 (Lanfear et al. 2017). Phylogenetic analyzes were performed under Bayesian inference (BI), maximum likelihood (ML), and maximum parsimony (MP) optimality criterions with the software MrBayes 3.2.6 (Ronquist et al. 2012), RAxML 8.2.11 (Stamatakis 2014), and TNT 1.5 (Goloboff and Catalano 2016) respectively. The best partition scheme with respective best-fitting substitution models and details on each phylogenetic analysis are given in Supplemental online Material I.

The three phylogenetic analyzes are congruent and show all *Ischnocnema* species as a fully-supported clade, sister group of *Eleutherodactylus atkins,* this relationship highly-supported (Fig. 1). The two species of *Pristimantis* Jiménez de la Espada, 1870 also appear as a fully-supported clade. *Ischnocnema erythromera* is the sister species of all other *Ischnocnema* in our tree and *I. guentheri* and *I. henselii*, as well as *I. nasuta* and *I. oea*, appear as sister species. The only clade not highly-supported in our phylogeny was *I. nasuta* + *I. oea,* but only in the ML analysis (65% of bootstrap replicates). These results are congruent with the previous phylogenetic hypothesis encompassing all these *Ischnocnema* species (Canedo and Haddad 2012). The mitogenomes assembled here provide important information regarding the relationships within the *I. guentheri* species series and their genomic evolution.

Disclosure statement

The authors report no conflict of interest.

Acknowledgments

We thank Center for Scientific Computing (NCC/GridUNESP) of the UNESP and Cyberinfrastructure for Phylogenetic Research (CIPRES) for computer resources; Centro de Estudos de Insetos Sociais (CEIS; São Paulo State University [UNESP]) for allowing us the use of the molecular laboratory. A. Brunetti, C. Cassini, T. Silva Soares, D. Baêta, A. F. Sabbag, and J. S. Parreiras gave field assistance.

Funding

This work was supported by São Paulo Research Foundation (FAPESP) grants #2013/50741-7, #2014/05772-4 (together with Coordenação de Aperfeiçoamento de Pessoal de Nível Superior [CAPES]), and BEPE #2016/22450-6, and by Conselho Nacional e Desenvolvimento Científico e Tecnológico (CNPq) grant 302518/2013-4.

References

Bernt M, Donath A, Jühling F, Externbrink F, Florentz C, Fritzsch G, et al. 2013. MITOS: Improved *de novo* metazoan mitochondrial genome annotation. Mol. Phylogen. Evol. 69(2): 313–319.

Bolger AM, Lohse M, Usadel B (2014) Trimmomatic: a flexible trimmer for Illumina sequence data. Bioinformatics 30:2114–2120. doi:10.1093/bioinformatics/btu170.

Canedo C, Haddad CFB. 2012. Phylogenetic relationships within anuran clade Terrarana, with emphasis on the placement of Brazilian Atlantic rainforest frogs genus Ischnocnema (Anura: Brachycephalidae). Mol. Phylogenet. Evol. 65:610–620. doi:10.1016/j.ympev.2012.07.016.

Frost DR. 2018. Amphibian species of the world: an online reference. Am. Museum Nat. Hist. New York, USA. [accessed 2018 Mar 8]. http://research.amnh.org/herpetology/amphibia/index.html.

Gehara M, Canedo C, Haddad CFB, Vences M. 2013. From widespread to microendemic: molecular and acoustic analyses show that *Ischnocnema guentheri* (Amphibia: Brachycephalidae) is endemic to Rio de Janeiro, Brazil. Conserv. Genet. 14:973–982. doi:10.1007/s10592-013-0488-5.

122 Goloboff PA, Catalano SA. 2016. TNT version 1.5, including a full implementation of
123 phylogenetic morphometrics. Cladistics 32:221–238. doi:10.1111/cla.12160.
124 Hahn C, Bachmann L, Chevreux B. 2013. Reconstructing mitochondrial genomes
125 directly from genomic next-generation sequencing reads—a baiting and iterative
126 mapping approach. Nucl. Acids Res. 41:e129. doi:10.1093/nar/gkt371.
127 Heyer WR. 1984. Variation, systematics, and zoogeography of *Eleutherodactylus*
128 *guentheri* and closely related species (Amphibia: Anura: Leptodactylidae).
129 Smith. Contr. Zool. 402:15342. doi:10.5479/si.00810282.402.
130 Jiménez de la Espada M. 1870. Fauna neotropicalis species quaedam nondum cognitae.
131 J. Sciências, Mathemáticas, Phys. e Naturaes 3:57–65.
132 Katoh K, Standley DM. 2013. MAFFT multiple sequence alignment software version 7:
133 Improvements in performance and usability. Mol. Biol. Evol. 30:772–780.
134 doi:10.1093/molbev/mst010.
135 Kearse M, Moir R, Wilson A, Stones-Havas S, Cheung M, Sturrock S, Buxton S,
136 Cooper A, Markowitz S, Duran C, et al. 2012. Geneious Basic: an integrated and
137 extendable desktop software platform for the organization and analysis of
138 sequence data. Bioinformatics 28:1647–1649.
139 Lanfear R, Frandsen PB, Wright AM, Senfeld T, Calcott B. 2017. Partitionfinder 2: new
140 methods for selecting partitioned models of evolution for molecular and
141 morphological phylogenetic analyses. Mol. Biol. Evol. 34:772–773.
142 doi:10.1093/molbev/msw260.
143 Lemmon AR, Emme SA, Lemmon EM. 2012. Anchored hybrid enrichment for
144 massively high-throughput phylogenomics. Syst. Biol. 61:727–744.
145 doi:10.1093/sysbio/sys049.
146 Lutz A. 1925. Batraciens du Brésil. Comptes Rendus Mémoires Hebd. des Séances la
147 Société Biol. des ses Fil. 22:211–214.
148 Padial JM, Grant T, Frost DR. 2014. Molecular systematics of terraranas (Anura:
149 Brachycephaloidea) with an assessment of the effects of alignment and
150 optimality criteria. Zootaxa 3825:1. doi:10.11646/zootaxa.3825.1.1.
151 Peters WCH. 1870. Über neue Amphien (*Hemidactylus*, *Urosaura*, *Tropdolepisma,*
152 *Geophis, Uriechis, Scaphiophis, Hoplocephalus, Rana, Entomoglossus,*
153 *Cystignathus, Hylodes, Arthroleptis, Phyllobates, Cophomantis*) des Königlich
154 Zoologisch Museum. Monatsberichte der Königlichen Preuss. Akad. des
155 Wissenschaften zu Berlin 1870:641–652.

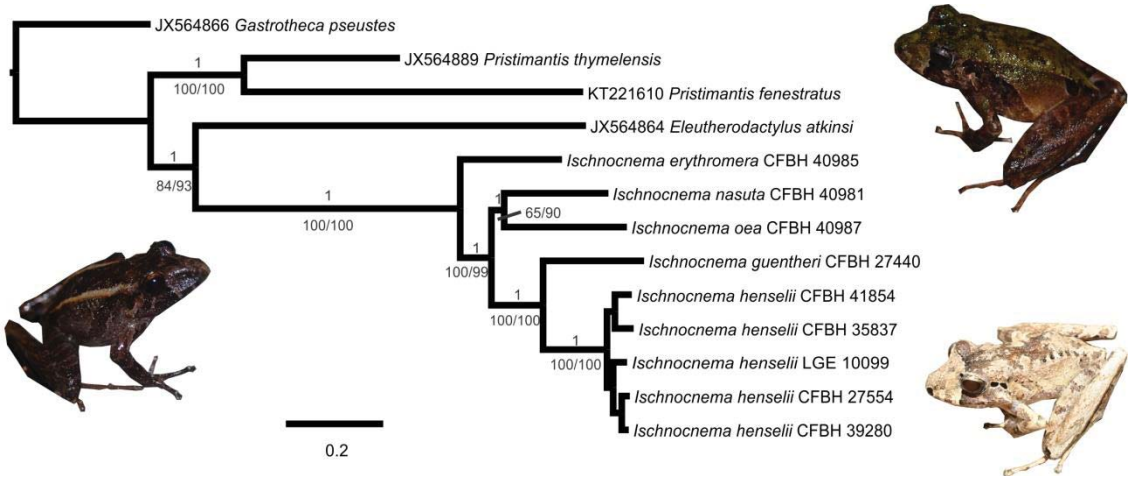
156 Prum RO, Berv JS, Dornburg A, Field DJ, Townsend JP, Lemmon EM, Lemmon AR.
157 2015. A comprehensive phylogeny of birds (Aves) using targeted next-
158 generation DNA sequencing. Nature 526:569–573. doi:10.1038/nature15697.
159 Reinhardt JT, Lütken CF. 1862 "1861". Bidrag til Kundskab om Brasiliens Padder og
160 Krybdyr. Förste Afdeling: Padderne og Öglerne. Vidensk. Meddelelser fra
161 Dansk Naturhistorisk Foren. i Kjøbenhavn 2:143–242.
162 Ronquist F, Teslenko M, Van Der Mark P, Ayres DL, Darling A, Höhna S, Larget B,
163 Liu L, Suchard MA, Huelsenbeck JP. 2012. Mrbayes 3.2: Efficient Bayesian
164 phylogenetic inference and model choice across a large model space. Syst. Biol.
165 61:539–542. doi:10.1093/sysbio/sys029.
166 Ruane S, Raxworthy CJ, Lemmon AR, Lemmon EM, Burbrink FT. 2015. Comparing
167 species tree estimation with large anchored phylogenomic and small Sanger-
168 sequenced molecular datasets: An empirical study on Malagasy
169 pseudoxyrhophiine snakes. BMC Evol. Biol. 15:1–14. doi:10.1186/s12862-015-
170 0503-1.
171 Sabaj MH. 2016. Standard symbolic codes for institutional resource collections in
172 herpetology and ichthyology: an online reference. Version 6.5 (16 August 2016).
173 Electronically accessible at http://www.asih.org/, American Society of
174 Ichthyologists and Herpetologists, Was. 5:802–832. doi:Available at:
175 http://www.asih.org/resources. Archived by WebCite at
176 http://www.webcitation.org/6lkBdh0EO on 3 November 2016.
177 Stamatakis A. 2014. RAxML version 8: a tool for phylogenetic analysis and post-
178 analysis of large phylogenies. Bioinformatics 30:1312–1313.
179 doi:10.1093/bioinformatics/btu033.
180 Steindachner F. 1864. Batrachologische Mittheilungen. Verhandlungen des Zool.
181 Vereins Wien 14:239–288.
182 Tucker DB, Colli GR, Giugliano LG, Hedges SB, Hendry CR, Lemmon EM, Lemmon
183 AR, Sites JW, Pyron RA. 2016. Methodological congruence in phylogenomic
184 analyses with morphological support for teiid lizards (Sauria: Teiidae). Mol.
185 Phylogenet. Evol. 103:75–84. doi:10.1016/j.ympev.2016.07.002.
186
187

188 Table 1. GenBank accession numbers, collection numbers, local of collection, and
189 geospatial coordinates of specimens of the *Ischnocnema* species sequenced.

Species	GB accession number	Voucher	Local of collection	Coordinates (decimal degrees)
I. erythromera	To be submitted	CFBH 40985	Teresópolis, RJ, Brazil	-22.45386, -42.99235
I. guentheri	To be submitted	CFBH 27440	Rio de Janeiro, RJ, Brazil	-22.96192, -43.28912
I. henselii	To be submitted	CFBH41854	Bertioga, SP, Brazil	-23.73123, -46.17280
I. henselii	To be submitted	CFBH 35837	Miracatu, SP, Brazil	-24.28223, -47.46796
I. henselii	To be submitted	CFBH 27554	São Bonifácio, SC, Brazil	-27.87721, -48.94057
I. henselii	To be submitted	CFBH 39280	São Francisco do Sul, SC, Brazil	-26.22797, -48.68011
I. henselii	To be submitted	LGE 10099	San Pedro, Misiones, Argentina	-26.90000, -53.86667
I. nasuta	To be submitted	CFBH 40981	Nova Friburgo, RJ, Brazil	-22.28923, -42.67095
I. oea	To be submitted	CFBH 40987	Santa Teresa, ES, Brazil	-19.90706, -40.54034

190

191



192

193 Figure 1. The 50% majority rule consensus tree from Bayesian inference analysis of
194 mitogenomic sequences of *Ischnocnema* and four outgroups. Numbers above branches
195 are posterior probabilities and numbers below branches are maximum likelihood
196 bootstrap replicates (left) and maximum parsimony jackknife replicates (right). No
197 support below species level is shown. Pictures show *Ischnocnema nasuta* (left), *I.*
198 *erythromera* (above, right), and *I. henselii* (below, right).

199

Suplemental Online Material

Phylogenetic Analyses

Bayesian inference

Bayesian inference analysis was performed in MrBayes 3.2.6 (Ronquist et al. 2012) using two independent runs of 1.0 x 10^7 generations, starting with random trees and four Markov chains (one cold), sampled every 1000 generations. Twenty-five percent of generations and trees were discarded as burnin and the analysis was performed with unlinked character state frequencies, substitution rates of GTR model, gamma shape parameters, and proportion of invariable sites between partitions. Runs were considered convergent if standard deviation of split frequencies was lower than 0.01 and Estimated Sample Size (ESS) was higher than 100. The best partition scheme and respective best fitting substitution models are shown in Table S1.

Maximum likelihood

Maximum likelihood analysis was computed in RAxML v. 8.2.11 (Stamatakis 2014), searching the most likely tree 100 times and conducting 1000 non-parametric bootstrap replicates. The best partition scheme is shown in Table S1. Because RAxML does not apply different models for different partitions, the run was performed with the GTR + Γ model for all partitions.

Maximum parsimony

Maximum parsimony analysis was performed in the software TNT v. 1.5 (Goloboff and Catalano 2016) treating gaps as missing. The low number of terminals (13 in total) allowed us to search for the most parsimonious tree using the implicit enumeration (*ienum* command) algorithm, which is not heuristic and guarantees the result to be optimal. Implicit enumeration was also used to estimate 1000 replicates of parsimony

224 Jackknife absolute frequencies.

225 Table S1. Best partition scheme and respective best fitting nucleotide substitution
226 models.

Partition	Number of sites	Model
12S	972	GTR + Γ + I
16S	1664	GTR + Γ + I
ND1, ND3, and CytB 1st positions	801	GTR + Γ + I
ND1, ND3, CytB, and COIII 2nd positions	1061	GTR + Γ
ND1, ND3, CytB, COIII, and ND4L 3rd positions	1157	GTR + Γ + I
ND2, ND5 1st positions, and ATP8 2nd position	1004	GTR + Γ + I
ND2, ND5, and ATP6 2nd positions	1165	GTR + Γ
ND2, ND4, and ND5 3rd positions	1390	GTR + Γ + I
COI 1st position	514	SYM + Γ + I
COI 2nd position	514	GTR + I
COI and COII 3rd positions	738	GTR + Γ + I
COII and COIII 1st positions	486	SYM + Γ + I
COII, ND4, and ND4L 2nd positions	775	GTR + I
ATP8 1st position	65	GTR + Γ
ATP6 and ATP 8 3rd positions	293	GTR + Γ + I
ATP6, ND4, and ND4L 1st positions	779	GTR + Γ + I
ND6 1st position	173	GTR + Γ + I
ND6 2nd position	173	GTR + Γ
ND6 3rd position	173	GTR + Γ + I

227

228 ## References

229 Goloboff PA, Catalano SA. 2016. TNT version 1.5, including a full implementation of
230 phylogenetic morphometrics. Cladistics 32:221–238. doi:10.1111/cla.12160.
231 Ronquist F, Teslenko M, Van Der Mark P, Ayres DL, Darling A, Höhna S, Larget B,
232 Liu L, Suchard MA, Huelsenbeck JP. 2012. Mrbayes 3.2: Efficient Bayesian
233 phylogenetic inference and model choice across a large model space. Syst. Biol.
234 61:539–542. doi:10.1093/sysbio/sys029.
235 Stamatakis A. 2014. RAxML version 8: a tool for phylogenetic analysis and post-
236 analysis of large phylogenies. Bioinformatics 30:1312–1313.
237 doi:10.1093/bioinformatics/btu033.

CONCLUSÕES GERAIS

- A série de *Ischnocnema guentheri* possui um clado que contém *I. oea* e duas novas espécies. Uma das novas espécies, *I. garciai,* é morfologicamente indistinguível de *I. oea* mas possui algumas características acústicas diagnósticas. Já *I. feioi* possui as características acústicas com algum nível de sobreposição com relação às de *I. oea*, mas sua morfologia difere bastante. O apêndice calcâneo mais alto que largo é uma sinapomorfia putativa para o grupo natural que corresponde às três espécies e o calo nupcial dos membros da série de *I. guentheri* parece possuir importantes características morfológicas que explicam a relação próxima entre esta série e a série de *I. parva.*
- A família Brachycephalidae e os gêneros *Brachycephalus* e *Ischnocnema* são arranjos monofiléticos e possuem alto suporte. Estes relacionamentos são recorrentes na literatura e é provável que se mantenham estáveis em análises futuras. Apesar do monofiletismo de *Ischnocnema* e de algumas de suas séries de espécies, alguns relacionamentos dentro do gênero são pouco suportados e outros se mostram instáveis quando analisados sob critérios de otimização distintos. Para que esses relacionamentos possam ser mais bem entendidos, é essencial que espécies cujas posições filogenéticas ainda não foram testadas, bem como novos marcadores moleculares, sejam adicionados à matriz.
- *Ischnocnema nanahallux* se mostrou fora da série de *I. parva*, como espécie irmã dos membros das séries de *I. guentheri*, *I. parva* e *I. venancioi*. Embora este relacionamento contrarie o senso comum devido a semelhança morfológica geral entre *I. nanahallux* e os membros da série de *I. parva*, o calo nupcial grande, conspícuo e glandular parece ser uma sinapomorfia do clado composto pelas séries de *I. guentheri, I. venancioi* e *I. parva*, estando ausente em *I. nanahallux.* A recém-proposta série de *I. venancioi* conta com a espécie que dá nome à série, *I. hoehnei* e pelo menos mais duas novas espécies.
- Nossa análise com 388 fragmentos de genes mostrou que as seis espécies do complexo de *Ischnocnema guentheri* e também as populações do norte e do sul dentro de *I. henselii* e *I.* sp. CS1 possuem uma estruturação genética bastante forte, além de quase não possuírem fluxo gênico entre as linhagens. Mesmo uma análise tão robusta e com tantos marcadores moleculares não foi capaz de posicionar uma das espécies candidatas de maneira definitiva e a posição filogenética de *I.* sp. CS3 ainda é incerta. Isso pode ter ocorrido devido à rápida diversificação de algumas espécies dentro do complexo de *I. guentheri*. A morfologia não se mostrou eficaz na separação das linhagens, mas características bioacústicas foram capazes de separar as espécies putativas do complexo de *I. guentheri*. Apesar de nem todas as espécies possuírem características acústicas

diagnósticas que as separem de todas as outras espécies sem sobreposição, as espécies irmãs são acusticamente diagnosticáveis. Os resultados acústicos e genéticos indicam que cada uma das seis espécies putativas no complexo é uma linhagem que evolui separadamente. Porém, recomenda-se cautela acerca das decisões taxonômicas a serem tomadas, pois há nomes disponíveis (um ou dois, dependendo da decisão tomada) para algumas das espécies candidatas.

- Os genomas mitocondriais de *Ischnocnema erythromera, I. guentheri*, *I. henselii*, *I. nasuta* e *I. oea* estão de acordo com os mitogenomas encontrados para a maioria dos Neobatrachia sequenciados até agora. Além disso, as relações filogenéticas recuperadas a partir desses dados são consistentes com hipóteses filogenéticas anteriores, com *I. erythromera* como grupo irmão do clado composto pelas outras espécies e *I. guentheri* intimamente relacionada a *I. henselii*.